JYU DISSERTATIONS 647

Jonni Lohi

Higher Order Approximations in Discrete Exterior Calculus

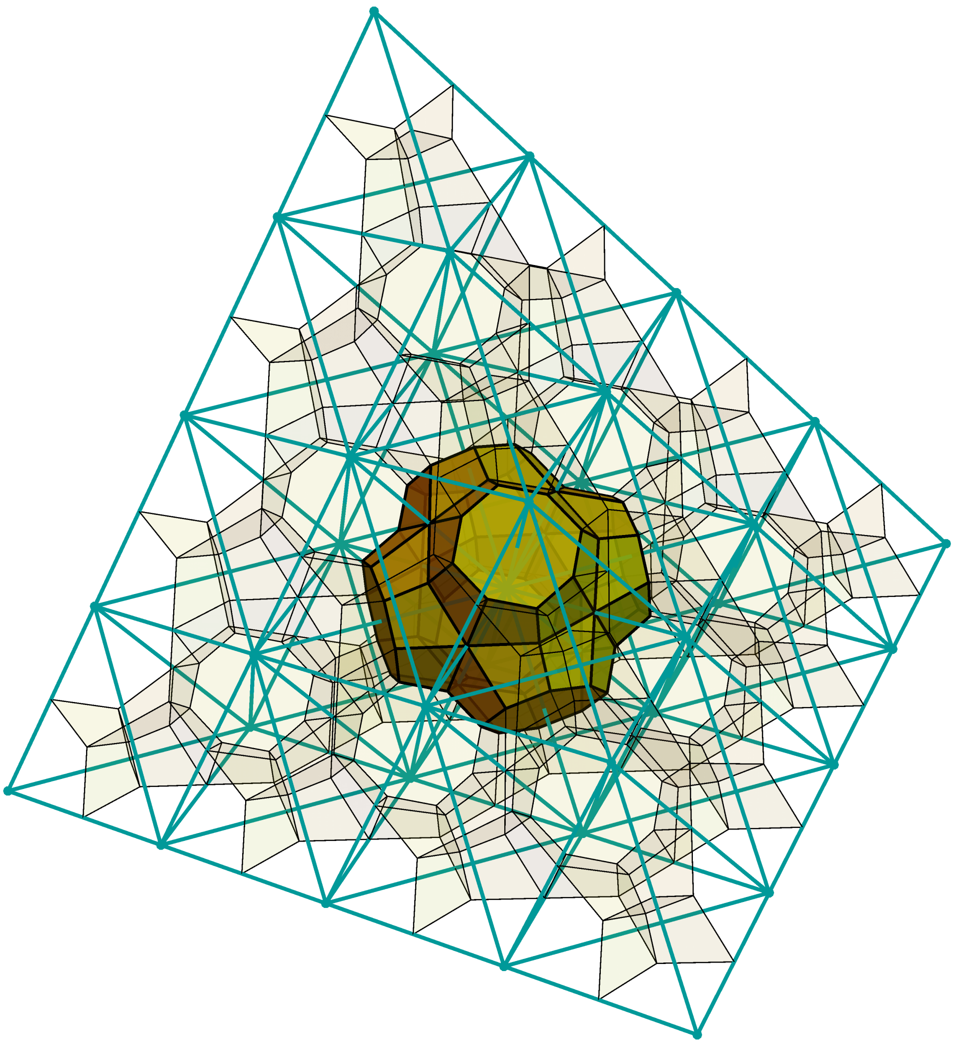

UNIVERSITY OF JYVÄSKYLÄ
FACULTY OF INFORMATION TECHNOLOGY

JYU DISSERTATIONS 647

Jonni Lohi

Higher Order Approximations in Discrete Exterior Calculus

Esitetään Jyväskylän yliopiston informaatioteknologian tiedekunnan suostumuksella
julkisesti tarkastettavaksi Agoran auditoriossa 3
kesäkuun 9. päivänä 2023 kello 12.

Academic dissertation to be publicly discussed, by permission of
the Faculty of Information Technology of the University of Jyväskylä,
in building Agora, auditorium 3, on June 9, 2023, at 12 o'clock.

JYVÄSKYLÄN YLIOPISTO
UNIVERSITY OF JYVÄSKYLÄ

JYVÄSKYLÄ 2023

Editors
Marja-Leena Rantalainen
Faculty of Information Technology, University of Jyväskylä
Päivi Vuorio
Open Science Centre, University of Jyväskylä

ISBN 978-951-39-9613-0 (PDF)
URN:ISBN:978-951-39-9613-0
ISSN 2489-9003

Permanent link to this publication: http://urn.fi/URN:ISBN:978-951-39-9613-0

ABSTRACT

Lohi, Jonni
Higher order approximations in discrete exterior calculus
Jyväskylä: University of Jyväskylä, 2023, 69 p. (+included articles)
(JYU Dissertations
ISSN 2489-9003; 647)
ISBN 978-951-39-9613-0 (PDF)

The theory of discrete exterior calculus provides tools for imitating exterior calculus in finite-dimensional cochain spaces, inducing numerical methods for problems presented in terms of differential forms. Methods based on discrete exterior calculus share the property that the coboundary operator discretises the exterior derivative exactly, in the sense that Stokes' theorem is automatically preserved in the finite-dimensional setting. Another benefit is that the dependence on metric is identifiable and restricts to the Hodge star operator and its discretisation. Although the importance of the discrete Hodge operator has been acknowledged, extending the framework of discrete exterior calculus to higher order methods has previously been an open problem. In this thesis, we extend the theory to accommodate higher order approximations. The key point is to create the mesh such that cochains can be interpolated with higher order interpolants. This can be accomplished with our systematic interpolation framework on simplicial and cubical meshes. We divide the cells of the mesh into smaller cells that can be used to define the interpolants and their degrees of freedom. When a mesh containing these small cells is used to apply discrete exterior calculus, cochains can be interpolated with higher order accuracy. This interpolation framework admits a systematic implementation covering arbitrary orders with the same code. It can also be used to define higher order discrete Hodge operators in a natural manner. These operators are, in a sense, exact for all elements in the finite-dimensional space of interpolants. The tools developed in this work enable higher order schemes based on discrete exterior calculus; we demonstrate this with elliptic and hyperbolic boundary value problems. Convergence properties are studied both theoretically and through numerical examples.

Keywords: cochains, differential forms, discrete exterior calculus, discrete Hodge operators, higher order approximations, interpolation, second order boundary value problems

TIIVISTELMÄ (ABSTRACT IN FINNISH)

Lohi, Jonni
Korkeamman asteen approksimaatiot differentiaalimuodoille
Jyväskylä: University of Jyväskylä, 2023, 69 s. (+artikkelit)
(JYU Dissertations
ISSN 2489-9003; 647)
ISBN 978-951-39-9613-0 (PDF)

Diskreetti ulkoinen laskenta (engl. *discrete exterior calculus*, DEC) mahdollistaa differentiaalimuotojen approksimoinnin numeerisiin menetelmiin soveltuvissa äärellisulotteisissa avaruuksissa. DEC-pohjaisten menetelmien etuna on ulkoderivaatan diskreetti vastine, joka perustuu Stokesin lauseeseen eikä aiheuta lainkaan virhettä. Lisäksi metrisen tensorin valinnasta riippuvat ja riippumattomat diskretoinnin osat ovat selvästi eriteltävissä. Vaikka oleellisten operaattorien merkitys on ymmärretty, diskreettiin ulkoiseen laskentaan pohjautuvat menetelmät on aiemmin mielletty alimman asteen menetelmiksi. Tässä väitöskirjassa teoriaa kehitetään kattamaan korkeamman asteen approksimaatioita. Keskeisintä on verkon muodostaminen korkeamman asteen interpolointiin soveltuvalla tavalla. Tätä varten esitetään systemaattinen strategia simplekseillä ja hyperkuutioilla. Solut jaetaan pienempiin soluihin, joita voidaan käyttää interpolanttien ja näiden vapausasteiden määrittelemiseen. Kun verkko sisältää nämä pienemmät solut, korkeamman asteen interpoloinnista tulee mahdollista. Interpolointistrategialle saadaan systemaattinen toteutus, joka kattaa kaikenasteiset approksimaatiot samalla koodilla. Lisäksi se tarjoaa luonnollisen tavan johtaa diskreettejä Hodge-operaattoreja. Väitöstutkimuksessa kehitettyjen työkalujen ansiosta reuna-arvotehtäville saadaan DEC-pohjaisia korkeamman asteen menetelmiä; tätä demonstroidaan elliptisten ja hyperbolisten tehtävien yhteydessä. Menetelmien suppenemista tarkastellaan sekä teoreettisesti että numeerisin testiesimerkein.

Avainsanat: differentiaalimuodot, diskreetti ulkoinen laskenta, interpolointi, korkeamman asteen approksimaatiot, numeerinen analyysi, toisen kertaluvun reuna-arvotehtävät

Author	Jonni Lohi Faculty of Information Technology University of Jyväskylä Finland
Supervisors	Professor Lauri Kettunen Faculty of Information Technology University of Jyväskylä Finland
	Professor Tuomo Rossi Faculty of Information Technology University of Jyväskylä Finland
Reviewers	Professor Snorre H. Christiansen Department of Mathematics University of Oslo Norway
	Associate Professor P. Robert Kotiuga College of Engineering Boston University United States
Opponent	Professor Anil N. Hirani Department of Mathematics University of Illinois Urbana–Champaign United States

ACKNOWLEDGEMENTS

I thank my supervisors for introducing me to the research topic and for believing in me during this challenging project. Besides Lauri and Tuomo, this includes Jukka Räbinä, who supervised my research in the early stages and helped me to use his code library. Jukka's implementation of discrete exterior calculus contains several classes that have been useful to me.

I appreciate the funding provided by the Faculty of Information Technology and thank all colleagues who have helped me in any way. I am grateful to the organisers of the courses I have attended — not only in our faculty, but also in the Department of Mathematics and Statistics. It is fortunate that both units are located on the same campus.

Last but not least, I would like to thank my parents, my stepmother, and my girlfriend for being there and caring.

INDEX OF NOTATION

$\Lambda^p(V)$	p-vectors of V, 14
$\Lambda^p(V)^*$	p-covectors of V, 15
$\wedge$	exterior product, 15, 19
$\langle \omega, \alpha \rangle$	product of a p-covector ω and a p-vector α, 15
$\alpha \cdot \beta$	inner product of p-vectors α and β, 16
$\lvert\alpha\rvert$	norm of a p-vector α, 16
L_*, L^*	linear maps of p-vectors and p-covectors induced by L, 16
$\star$	Hodge star operator, 17, 19
$\mathrm{vect}(\sigma)$	p-vector of an oriented p-cell σ, 17
$F^p(\Omega)$	differential p-forms in Ω, 18
$f^*\omega$	pullback of a p-form ω by f, 18
$\omega\vert_\sigma$	trace of a p-form ω on σ, 19
d	exterior derivative and the coboundary operator, 20, 24
$\Theta(\sigma)$	fullness of a p-cell σ, 22
$\lvert\sigma\rvert$	p-dimensional volume of a p-cell σ, 22
$S^p(K)$	set of p-cells in K, 22
$C_p(K)$	p-chains of K, 22
$C_p^*(K)$	p-cochains of K, 23
$F^p(K)$	differential p-forms in K, 23
d_σ^τ	incidence number relating a p-cell σ and a $(p+1)$-cell τ, 23
∂	boundary map, 23
δ_{ij}	Kronecker delta, 23
$\mathcal{C}$	de Rham map, 24
$\tilde{K}$	dual mesh of K, 24
$*$	discrete Hodge operator, 26
$I^p(K)$	finite-dimensional subspace of $F^p(K)$, 33
$\square^n$	unit n-cube $[0,1]^n$, 34
$S_k^p(K)$	set of kth order small p-cells of K, 34
K_k	refined mesh containing elements of $S_k^p(K)$ as cells, 34
$W_k^p(K)$	kth order Whitney p-forms of K, 36
$Q_k^p(K)$	kth order cubical p-forms of K, 36
$\mathfrak{I}$	interpolation operator from $C_p^*(K_k)$ to $I^p(K)$, 36
$\mathcal{C}_k$	de Rham map of K_k, 36

LIST OF FIGURES

FIGURE 1	The basic idea of discretisation methods.	13
FIGURE 2	A mesh K on the top and a dual mesh $\tilde{K}$ on the bottom.	25
FIGURE 3	A primal mesh in blue and dual cells in black.	26
FIGURE 4	Small cells of orders 2–4 in three dimensions.	35
FIGURE 5	Triangular meshes whose triangles flatten without limit.	41
FIGURE 6	An example of a mesh that is structural in the time direction.	48
FIGURE 7	The first two of the four meshes used in Example 3.	49
FIGURE 8	Illustration of the results displayed in Table 2.	50
FIGURE 9	Illustration of the results displayed in Table 6.	52

LIST OF TABLES

TABLE 1	Information about the four meshes used in Example 3.	49
TABLE 2	H^1 norms of the error in Example 3.	50
TABLE 3	Values of $\|L^{-1}\|$ in the stability analysis of Example 3.	50
TABLE 4	Values of the parameter Δl for the meshes used in Example 4.	51
TABLE 5	Values of $\|L^{-1}\|$ in the stability analysis of Example 4.	51
TABLE 6	Maximum norms of the error in Example 4.	52

CONTENTS

ABSTRACT
TIIVISTELMÄ (ABSTRACT IN FINNISH)
ACKNOWLEDGEMENTS
INDEX OF NOTATION
LISTS OF FIGURES AND TABLES
CONTENTS
LIST OF INCLUDED ARTICLES

1 INTRODUCTION 11

2 THEORETICAL FRAMEWORK 14
2.1 Exterior calculus 14
2.1.1 Exterior algebra 14
2.1.2 Differential forms 18
2.2 Discrete exterior calculus 21
2.2.1 Chains and cochains 22
2.2.2 Discrete Hodge operators 24
2.2.3 Additional remarks 28

3 SCIENTIFIC CONTRIBUTION 29
3.1 Author's independent contribution in joint articles 32
3.2 Source code of the implementation 32

4 INTERPOLATION OF COCHAINS 33
4.1 Higher order interpolation framework 33
4.2 Systematic implementation strategy 37
4.3 Bounds for the interpolation error 40

5 HIGHER ORDER DISCRETE HODGE OPERATORS 42

6 APPLICATION TO POISSON'S AND THE WAVE EQUATION 45

7 CONCLUSIONS AND FUTURE WORK 53

YHTEENVETO (SUMMARY IN FINNISH) 55

REFERENCES 57

INCLUDED ARTICLES

LIST OF INCLUDED ARTICLES

PI Jonni Lohi and Lauri Kettunen. Whitney forms and their extensions. *Journal of Computational and Applied Mathematics*, 393:113520, 2021.

PII Jonni Lohi. Systematic implementation of higher order Whitney forms in methods based on discrete exterior calculus. *Numerical Algorithms*, 91(3):1261–1285, 2022.

PIII Jonni Lohi. New degrees of freedom for differential forms on cubical meshes. *Advances in Computational Mathematics*, Accepted for publication, 2022.

PIV Jonni Lohi, Lauri Kettunen, and Tuomo Rossi. Higher order methods based on discrete exterior calculus. *Submitted*, 2022.

1 INTRODUCTION

In three words, the topic of this thesis could be summarised “approximating differential forms”. The purpose is to provide tools for numerical approximation of differential equations, which places the thesis in the field of numerical analysis. For a proper description of the topic, a brief introduction to numerical analysis is in order.

Many real-world phenomena are modelled by partial differential equations whose exact solutions are difficult or impossible to find. In such cases, numerical approximations are typically sought with the help of computers. To solve problems with computers one must first convert them into series of computations. Moreover, the number of such computations must always be finite. This (perhaps self-evident) point is important, and the process of converting problems to a finite number of computations suitable for computers is called discretisation. The resulting discrete problem can be solved using computers, with the intention that the accuracy of the numerical approximation can be increased by increasing the size of the discrete problem (by allowing more computations).

Numerical analysis is the branch of mathematics that studies this approximation process. Key issues are the design of numerical methods and questions of convergence, e.g. required conditions under which approximate solutions converge towards the actual solution. A huge amount of research has been devoted to discretisation of partial differential equations, and this is reflected by the number of different approaches. Some examples are finite difference [126], finite element [36], finite volume [64], spectral [123], and meshfree [68] methods. This list is by no means exhaustive, and each class could be further divided into various variants. Different approaches have their own merits, and none of them can be identified as “the best” for all problems, but naturally some of them have become more popular than others.

This thesis contributes to methods based on cochains and discrete exterior calculus (DEC). These methods are applicable to problems that can be formulated using exterior calculus — the calculus of differential forms. The framework of discrete exterior calculus is designed for discretising the main parts of exterior calculus, hence the name. Differential forms are approximated using cochains, so methods based on DEC are also cochain-based methods. However, the nomenclature is not definite: methods that use tools of discrete exterior calculus go by different names, e.g. generalised finite differences [30, 32], generalised finite volume methods [78], finite integration technique [46], and Yee-like schemes [34, 35]. They are also similar to mimetic methods [20, 91] in that Stokes' theorem is mimicked in finite-dimensional cochain spaces, which enables conservation properties to be fulfilled in the discrete setting. To cope with nuances in the terminology, we give a description of the methods within the scope of this thesis at the beginning of Section 2.2.

The predominant research objective that unites the parts of this article dissertation is the extension of DEC covering higher order methods. The thesis continues previous research [109, 116, 113, 115, 114, 111, 112] on DEC at the University of Jyväskylä, but this was not the only reason why the topic was chosen. Since DEC has not received as much attention as some more popular approaches, such as finite element methods, there is more potential for scientific improvements. This is likely why extending the framework to higher order methods has previously been an open problem. What is more, there have been beliefs that methods based on DEC are limited to lowest order. Such a limitation is mentioned e.g. in [78, 55]. The following quotation from [13] could be an epigraph to this thesis:

> *"In contrast to the finite element approach, these cochain-based approaches do not naturally generalize to higher-order methods."*

The present work challenges these views. We show that higher order generalisations exist and attempt to convince the reader of their naturality.

Nevertheless, the results of this thesis do not come as a complete surprise. In [52], "higher-order analogues of the discrete theory of exterior calculus" are mentioned as a future research direction, "desirable from the point of view of computational efficiency". The benefit of higher order methods is explained by the concept of order of convergence, which can be illustrated by the following simplified example. Suppose a two-dimensional domain of interest, divided into 192 triangles of diameter h by some discretisation method (as shown in Figure 1). The method is said to provide kth order convergence if there is an upper bound of the form Ch^k (with some constant C) for the approximation error. As Figure 1 suggests, the accuracy of the discretisation can be increased by using more and smaller triangles. If we refine the triangles such that the diameter h is halved, the new bound is $C(h/2)^k = Ch^k/2^k$, which predicts that the error is divided by 2^k. For a method of order eight ($k = 8$), this means that the error is cut by a factor of 256 after just one refinement. To achieve the same improvement in accuracy with a first order method, eight such refinements would be needed, requiring over 12 million triangles! In short, higher order methods result in faster convergence.

The higher order approach of this thesis can be considered a valuable contribution to the existing theory. While this work should be regarded as basic research with no specific application in focus, it is good to be aware that applications exist. Exterior calculus has applications in different branches of physics, including electromagnetism, thermodynamics, classical and quantum mechanics, and relativity [65, 122, 41, 17, 66, 57]. Already in the 1960s, Flanders [65]

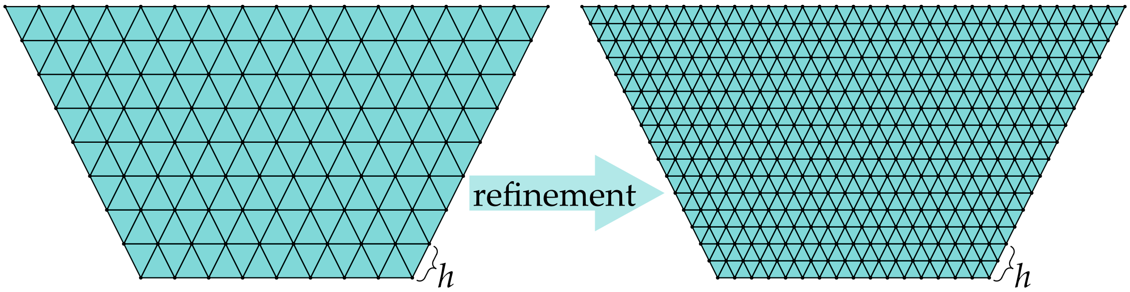

FIGURE 1 Discretisation methods typically produce approximations by dividing the domain of interest into small cells (triangles in this case), and the accuracy of the approximations can be improved by using more and smaller cells.

anticipated that “perhaps it will soon make its way into engineering”, and this prediction turned out to be correct. Indeed, there are many publications demonstrating the application of discrete exterior calculus in fields of engineering [97, 43, 106, 120, 49, 107, 82, 143, 22, 99].

The outline of this thesis is as follows. Chapter 2 presents the theoretical framework comprising exterior calculus and its discrete counterpart. This chapter reviews the existing literature, and its contents should be regarded as known. The contribution to this framework is then considered in Chapter 3, which specifies the scientific contribution of the included articles and the author’s independent contribution in joint articles. The main results are presented in Chapters 4–6, which discuss interpolation of cochains, higher order discrete Hodge operators, and the application of the framework to second order boundary value problems. We draw conclusions in Chapter 7, assessing strengths and weaknesses of the presented approach. This chapter also lists relevant issues that are left for future research and predicts the potential for further improvements.

2 THEORETICAL FRAMEWORK

In this chapter, we introduce the theoretical framework of continuous and discrete exterior calculus. The discussion reviews the known theory, but we emphasise that the work should not be considered a comprehensive survey. The main goal is to present what is required to understand the results of this article dissertation, and for this reason several simplifications are made. For more information, we provide references that can be consulted for a fuller treatment.

2.1 Exterior calculus

Exterior calculus refers to the calculus of differential forms, which are mathematical objects suitable for integration (integrands). The concept of integration requires that integrands are paired with suitable domains. In exterior calculus, the usual choice of integration domains is manifolds — locally Euclidean spaces where differential forms naturally live. However, in this thesis we assume for simplicity that our domain of interest Ω is a bounded polytope in $\mathbb{R}^n$. For those who are accustomed to manifolds, it should be visible which results generalise to manifolds and how. Besides the great book of Whitney [139], good references regarding the topics of this section are [1, 50, 90].

2.1.1 Exterior algebra

Let V be an n-dimensional real vector space. The space of *p-vectors* (i.e. multivectors of degree p [139]) is the real vector space of formal sums of the form

$$\sum_{i=1}^{m} a_i (v_{i,1} \wedge v_{i,2} \wedge \ldots \wedge v_{i,p-1} \wedge v_{i,p}), \quad a_i \in \mathbb{R},\ v_{i,j} \in V,$$

subject to the following rules:

$$
\begin{aligned}
&b\sum_{i=1}^{m} a_i(v_{i,1}\wedge v_{i,2}\wedge\ldots\wedge v_{i,p-1}\wedge v_{i,p}) = \sum_{i=1}^{m} ba_i(v_{i,1}\wedge v_{i,2}\wedge\ldots\wedge v_{i,p-1}\wedge v_{i,p}),\ b\in\mathbb{R},\\
&1(v_1\wedge\ldots\wedge v_p) = v_1\wedge\ldots\wedge v_p, \quad 0(v_1\wedge\ldots\wedge v_p) = 0,\\
&a(v_1\wedge\ldots\wedge v_p) + b(v_1\wedge\ldots\wedge v_p) = (a+b)(v_1\wedge\ldots\wedge v_p),\\
&v_1\wedge\ldots\wedge(v_i+w_i)\wedge\ldots\wedge v_p = (v_1\wedge\ldots\wedge v_i\wedge\ldots\wedge v_p) + (v_1\wedge\ldots\wedge w_i\wedge\ldots\wedge v_p),\\
&v_1\wedge\ldots\wedge(av_i)\wedge\ldots\wedge v_p = a(v_1\wedge\ldots\wedge v_i\wedge\ldots\wedge v_p),\\
&v_1\wedge\ldots\wedge v_p = 0 \text{ if } v_i = v_j \text{ for some } i\neq j.
\end{aligned}
$$

More rigorous definitions can be found in [139, 50]. Let us denote by $\Lambda^p(V)$ the vector space of p-vectors of V. When $p = 0$, these reduce to real numbers, and for $p = 1$ we get the space V.

The *exterior product* $\wedge$ takes one p-vector α and one q-vector β to produce a $(p+q)$-vector $\alpha\wedge\beta$. It can be characterised as the unique bilinear map from $\Lambda^p(V)\times\Lambda^q(V)$ to $\Lambda^{p+q}(V)$ such that

$$(v_1\wedge\ldots\wedge v_p)\wedge(w_1\wedge\ldots\wedge w_q) = v_1\wedge\ldots\wedge v_p\wedge w_1\wedge\ldots\wedge w_q.$$

For $a\in\mathbb{R}$, we define $a\wedge\alpha = \alpha\wedge a = a\alpha$. For vectors $v_1,\ldots,v_p$, the expression $v_1\wedge\ldots\wedge v_p$ in the definition of p-vectors can be considered as an exterior product; that is, $\Lambda^p(V)$ is spanned by p-vectors that are exterior products of p vectors. In addition to the rules above, the exterior product satisfies the following properties: for $\alpha\in\Lambda^p(V)$, $\beta\in\Lambda^q(V)$, and $\gamma\in\Lambda^r(V)$,

$$
\begin{aligned}
&(\alpha\wedge\beta)\wedge\gamma = \alpha\wedge(\beta\wedge\gamma),\\
&\alpha\wedge\beta = (-1)^{pq}\beta\wedge\alpha.
\end{aligned}
$$

The *exterior algebra* of V is the algebra formed by the direct sum of the spaces $\Lambda^p(V)$ for $0\le p\le n$ with the exterior product as the multiplication operation.

Multicovectors are obtained similarly as multivectors but starting with the dual space V^*. We define the space of *p-covectors* of V, denoted $\Lambda^p(V)^*$, as the space $\Lambda^p(V^*)$. As the notation suggests, $\Lambda^p(V)^*$ can be considered as the dual space of $\Lambda^p(V)$. For this we define the *product of p-covectors and p-vectors* $\langle\cdot,\cdot\rangle$ as the bilinear map $\Lambda^p(V^*)\times\Lambda^p(V)\to\mathbb{R}$ satisfying

$$\langle f_1\wedge\ldots\wedge f_p, v_1\wedge\ldots\wedge v_p\rangle = \begin{vmatrix} f_1(v_1) & \ldots & f_1(v_p)\\ \vdots & \vdots & \vdots\\ f_p(v_1) & \ldots & f_p(v_p)\end{vmatrix}$$

for $f_1,\ldots,f_p\in V^*$ and $v_1,\ldots,v_p\in V$. For $p = 0$, the operation reduces to the product of real numbers. It is shown in [139] that the product $\langle\cdot,\cdot\rangle$ is well-defined (the result is independent of how the elements of $\Lambda^p(V^*)$ and $\Lambda^p(V)$ are written) and that for each ω in the dual space of $\Lambda^p(V)$ there is exactly one $\hat{\omega}\in\Lambda^p(V^*)$ such that $\omega(\alpha) = \langle\hat{\omega},\alpha\rangle$. Hence we can identify the dual space of $\Lambda^p(V)$ with

$\Lambda^p(V^*)$, considering the product $\langle \omega, \alpha \rangle$ as the action of a p-covector ω on a p-vector α.

Let $\{v_1, \ldots, v_n\}$ be a basis for V. Then

$$\{v_{i_1} \wedge \ldots \wedge v_{i_p} \mid 1 \leq i_1 < \ldots < i_p \leq n\} \tag{1}$$

is a basis for $\Lambda^p(V)$, whose dimension is hence $n!/(p!(n-p)!)$. If $\{f_1, \ldots, f_n\}$ is the corresponding dual basis for V^*, a basis for $\Lambda^p(V)^*$ dual to (1) is given by

$$\{f_{j_1} \wedge \ldots \wedge f_{j_p} \mid 1 \leq j_1 < \ldots < j_p \leq n\}.$$

Using the dual basis, the action of a p-covector ω with components $\omega_{j_1 \ldots j_p}$ on a p-vector α with components $\alpha_{i_1 \ldots i_p}$ can be written

$$\left\langle \sum_{1 \leq j_1 < \ldots < j_p \leq n} \omega_{j_1 \ldots j_p} f_{j_1} \wedge \ldots \wedge f_{j_p}, \sum_{1 \leq i_1 < \ldots < i_p \leq n} \alpha_{i_1 \ldots i_p} v_{i_1} \wedge \ldots \wedge v_{i_p} \right\rangle = \sum_{1 \leq i_1 < \ldots < i_p \leq n} \omega_{i_1 \ldots i_p} \alpha_{i_1 \ldots i_p}.$$

If V is endowed with an inner product given by a nondegenerate symmetric bilinear form $(v_1, v_2) \mapsto v_1 \cdot v_2$, we define the *inner product of p-vectors* by requiring that

$$(v_1 \wedge \ldots \wedge v_p) \cdot (w_1 \wedge \ldots \wedge w_p) = \begin{vmatrix} v_1 \cdot w_1 & \ldots & v_1 \cdot w_p \\ \vdots & \vdots & \vdots \\ v_p \cdot w_1 & \ldots & v_p \cdot w_p \end{vmatrix}. \tag{2}$$

If the basis $\{v_1, \ldots, v_n\}$ is orthonormal, (1) yields an orthonormal basis for $\Lambda^p(V)$. We do not require that the inner product of V be positive definite, but if it is, we define the *norm of a p-vector α* by $|\alpha| = \sqrt{\alpha \cdot \alpha}$. All of this applies also to p-covectors if V^* is endowed with an inner product.

Suppose that $L : V \to W$ is a linear map from the n-dimensional vector space V to another real vector space W of dimension m, and let $L^t : W^* \to V^*$ denote its transpose, defined by $L^t g(v) = g(Lv)$. We denote by L_* and L^* the unique *linear maps of p-vectors and p-covectors induced by L* [139] satisfying

$$L_* : \Lambda^p(V) \to \Lambda^p(W), \quad L^* : \Lambda^p(W)^* \to \Lambda^p(V)^*,$$
$$L_*(v_1 \wedge \ldots \wedge v_p) = Lv_1 \wedge \ldots \wedge Lv_p, \quad v_1, \ldots, v_p \in V, \tag{3}$$
$$L^*(g_1 \wedge \ldots \wedge g_p) = L^t g_1 \wedge \ldots \wedge L^t g_p, \quad g_1, \ldots, g_p \in W^*. \tag{4}$$

By (3) and (4) we obtain at once

$$L_*(\alpha \wedge \beta) = L_*\alpha \wedge L_*\beta, \quad \alpha \in \Lambda^p(V), \beta \in \Lambda^q(V), \tag{5}$$
$$L^*(\omega \wedge \eta) = L^*\omega \wedge L^*\eta, \quad \omega \in \Lambda^p(W)^*, \eta \in \Lambda^q(W)^*. \tag{6}$$

Note that $\langle L^*\omega, \alpha \rangle = \langle \omega, L_*\alpha \rangle$ for all $\alpha \in \Lambda^p(V)$ and $\omega \in \Lambda^p(W)^*$, so L^* is the transpose of L_*.

Since $\Lambda^p(V)$ has the same dimension as $\Lambda^{n-p}(V)$, these spaces are isomorphic. If V is oriented and has an inner product, this isomorphism is canonically provided by the Hodge star operator, defined as follows. Let σ denote the n-vector such that $\sigma = v_1 \wedge \ldots \wedge v_n$ for any positively oriented orthonormal basis $(v_1, \ldots, v_n)$. The *Hodge star operator* $\star : \Lambda^p(V) \to \Lambda^{n-p}(V)$ is the unique linear map satisfying

$$\alpha \wedge (\star\beta) = (\alpha \cdot \beta)\sigma \quad \forall \alpha, \beta \in \Lambda^p(V). \tag{7}$$

The definition uses the inner product (2) and depends also on the orientation of V — the Hodge star operator changes sign if we switch to the opposite orientation. For any positively oriented orthonormal basis $(v_1, \ldots, v_n)$ and for any permutation $(i_1, \ldots, i_n)$ of $(1, \ldots, n)$, we have

$$\star(v_{i_1} \wedge \ldots \wedge v_{i_p}) = (v_{i_1} \wedge \ldots \wedge v_{i_p}) \cdot (v_{i_1} \wedge \ldots \wedge v_{i_p}) s(i_1, \ldots, i_n) v_{i_{p+1}} \wedge \ldots \wedge v_{i_n}, \tag{8}$$

where $s(i_1, \ldots, i_n) = \pm 1$ denotes the sign of the permutation and the inner product $(v_{i_1} \wedge \ldots \wedge v_{i_p}) \cdot (v_{i_1} \wedge \ldots \wedge v_{i_p}) = \pm 1$ by (2).

To see the existence of the Hodge star operator, note that using the formula (8) with any positively oriented orthonormal basis to define $\star$ in terms of the basis (1) yields a linear map satisfying (7). Moreover, it is easily checked that any two linear maps satisfying (7) must be the same. We remark that in the literature one can find different ways to define the Hodge star operator; for example, the definitions given in [65] and [50] differ slightly from ours, and in [1] it is defined only for p-covectors. We emphasise that the Hodge star is obtained in the same way for both p-vectors and p-covectors.

The purpose of the exterior algebra from our point of view is to present oriented p-dimensional volumes with p-vectors. To simplify the exposition, hereafter we take $\mathbb{R}^n$ as the space V. (We could work in an affine space and take as V the underlying vector space, endowing it with an inner product when necessary.) To each oriented p-simplex σ in $\mathbb{R}^n$ corresponds a p-vector, $\mathrm{vect}(\sigma) \in \Lambda^p(\mathbb{R}^n)$, representing the direction, volume, and orientation of σ [139]. Denoting by $x_0 \ldots x_p$ the simplex whose vertices are $x_0, \ldots, x_p \in \mathbb{R}^n$ and whose orientation is given by the ordered set $(x_1 - x_0, \ldots, x_p - x_0)$, we define the *$p$-vector of σ* as

$$\mathrm{vect}(\sigma) = \frac{1}{p!}(x_1 - x_0) \wedge \ldots \wedge (x_p - x_0). \tag{9}$$

The definition can be extended to more general oriented cells by dividing them into similarly oriented simplices and taking the sum of their p-vectors. (A cell is oriented by choosing an orientation for its plane; we discuss cells in more detail in Subsection 2.2.1.)

We say that two vectors, cells, or hyperplanes in $\mathbb{R}^n$ are parallel if the hyperplane of one of them can be moved into the hyperplane of the other by translation. For example, if v is a vector and σ is a p-simplex in $\mathbb{R}^n$, we say they are parallel if there exists a translation taking the line spanned by v into the hyperplane of σ. Suppose that P is a q-dimensional hyperplane in $\mathbb{R}^n$ (for example, the plane of a q-simplex in $\mathbb{R}^n$). We denote by $\Lambda^p(P)$ the subspace of $\Lambda^p(\mathbb{R}^n)$ that is spanned by wedge products of p vectors parallel to P. If $\alpha \in \Lambda^p(P)$, we say that α is a *p-vector in P*.

2.1.2 Differential forms

Let $\Omega \subset \mathbb{R}^n$. A *differential p-form ω in Ω* is a function whose values are p-covectors; that is, $\omega(x) \in \Lambda^p(\mathbb{R}^n)^*$ for each $x \in \Omega$. In most cases also a certain amount of smoothness is required from this function [139]; instead of going into details, we implicitly assume that forms are sufficiently smooth for our purposes. Let us denote by $F^p(\Omega)$ the real vector space of differential p-forms in Ω. Note that 0-forms are simply real-valued functions.

Differential p-forms can be integrated over oriented p-dimensional domains. For $p \geq 1$, the integral of a p-form ω over an oriented p-simplex σ is approximated by subdividing σ into similarly oriented simplices $\sigma_1, \dots, \sigma_m$ and taking the sum

$$\sum_{i=1}^{m} \langle \omega(y_i), \mathrm{vect}(\sigma_i) \rangle,$$

where y_i is the barycentre of σ_i. We define the integral $\int_\sigma \omega$ as the limit of this sum when the maximum of the diameters of the σ_i approaches zero (meaning $m \to \infty$). When ω is continuous, the limit exists and is independent of the subdivisions [139]. This definition extends immediately to oriented p-cells that can be divided into simplices. For 0-forms, note that oriented 0-cells are simply points oriented either positively or negatively. We define the integral of a 0-form ω over an oriented 0-cell σ as $\pm\omega(\sigma)$, where the sign is given by the orientation of σ. Integration can also be defined over more general domains. However, for our purposes it suffices to know how to integrate over p-cells that can be divided into p-simplices, so we do not provide more general definitions — for more information, see [139, 1].

If f is a Riemann-integrable real-valued function in an oriented p-cell σ, we denote by $\int_\sigma f = \int_\sigma f(x)dx$ the usual Riemann integral, considering σ as a subset of $\mathbb{R}^p$. The two concepts of integration are related as follows:

$$\int_\sigma \omega = \int_\sigma \langle \omega(x), \mathrm{vect}(\sigma)/|\sigma| \rangle dx,$$

where we have the integral of a p-form on the left and the Riemann integral of a function on the right. The integral of a differential form has good properties that do not hold with the usual integral. It can be defined in an affine space without metric structure, simplifies the change of variables, and enables a generalisation of integral identities from vector calculus (see (10) and (13) below).

Let $f : \Omega \to \mathbb{R}^m$ be a smooth map, and denote by $Df(x)$ its derivative at $x \in \Omega$. Since $Df(x)$ is a linear map from $\mathbb{R}^n$ to $\mathbb{R}^m$, it induces linear maps $Df(x)_* : \Lambda^p(\mathbb{R}^n) \to \Lambda^p(\mathbb{R}^m)$ and $Df(x)^* : \Lambda^p(\mathbb{R}^m)^* \to \Lambda^p(\mathbb{R}^n)^*$ by (3) and (4). If ω is a differential p-form in $f(\Omega)$, its *pullback by f*, denoted $f^*\omega$, is the p-form in Ω defined by $f^*\omega(x) = Df(x)^*\omega(f(x))$. In other words, for $x \in \Omega$ and $\alpha \in \Lambda^p(\mathbb{R}^n)$,

$$\langle f^*\omega(x), \alpha \rangle = \langle Df(x)^*\omega(f(x)), \alpha \rangle = \langle \omega(f(x)), Df(x)_*\alpha \rangle.$$

If f is a diffeomorphism onto its image and ω is an n-form in $f(\Omega)$, the pullback satisfies the transformation formula [139]

$$\int_\Omega f^*\omega = \int_{f(\Omega)} \omega. \tag{10}$$

Here Ω is assumed to be oriented, and $f(\Omega)$ is considered with the orientation induced by f.

Let $\omega \in F^p(\Omega)$ and let σ be a q-simplex in Ω. The *trace of ω on σ*, denoted $\omega|_\sigma$, is the restriction of ω to points in σ and p-vectors in the plane of σ. More precisely, $\omega|_\sigma(x)$ is defined at points $x \in \sigma$, and the value is defined by $\langle \omega|_\sigma(x), \alpha\rangle = \langle \omega(x), \alpha\rangle$ for p-vectors α in the plane of σ. While $\omega = 0$ implies $\omega|_\sigma = 0$, note that the requirement $\omega|_\sigma = 0$ is less stringent than requiring $\omega(x) = 0$ for all $x \in \sigma$. We occasionally say that $\omega = 0$ on σ if $\omega|_\sigma = 0$ (and more generally $\omega = \eta$ on σ if $\omega|_\sigma = \eta|_\sigma$).

The *exterior product of differential forms* is defined pointwise:

$$\wedge : F^p(\Omega) \times F^q(\Omega) \to F^{p+q}(\Omega), \quad (\omega \wedge \eta)(x) = \omega(x) \wedge \eta(x).$$

The properties of the exterior product that hold pointwise also extend to differential forms. In particular, (6) implies that the exterior product commutes with the pullback: $f^*(\omega \wedge \eta) = f^*(\omega) \wedge f^*(\eta)$. The same is not true with the Hodge star operator. It is also extended to differential forms pointwise, but the inner product used in the definition is allowed to vary. More precisely, we assume that we are given a metric tensor g, which is a function whose value g_x at each point $x \in \Omega$ is a nondegenerate symmetric bilinear form on the space of 1-covectors $(\mathbb{R}^n)^*$. Using (2) (with $(\mathbb{R}^n)^*$ as V), g_x induces an inner product for p-covectors. We define the *Hodge star operator for differential forms* by

$$\star\omega(x) = \star(\omega(x)),$$

where the Hodge star for p-covectors is defined by (7) using the inner product induced by g_x and the standard orientation of $\mathbb{R}^n$.

The exterior derivative d is a linear operator mapping p-forms to $(p+1)$-forms. Considering first a 0-form ω, the exterior derivative $\mathrm{d}\,\omega$ is the 1-form defined by

$$\langle \mathrm{d}\,\omega(x), v\rangle = D\omega(x)v = \sum_{i=1}^{n} \frac{\partial \omega}{\partial x_i} v_i. \tag{11}$$

Note that this is simply the directional derivative of ω at x in the direction of v. Before giving the definition for $p > 0$, we recall a standard way of presenting differential forms using coordinates. If we consider x_i as the ith coordinate function, the exterior derivatives $\mathrm{d}\,x_1, \ldots, \mathrm{d}\,x_n$ are 1-forms whose values are given by $\langle \mathrm{d}\,x_i(x), v\rangle = v_i$. In particular, the $\mathrm{d}\,x_i(x)$ yield a basis for 1-covectors. Any differential p-form ω can be written as

$$\omega(x) = \sum_{1 \le i_1 < \ldots < i_p \le n} \omega_{i_1 \ldots i_p}(x)\,\mathrm{d}\,x_{i_1} \wedge \ldots \wedge \mathrm{d}\,x_{i_p}, \tag{12}$$

where the $\omega_{i_1\ldots i_p}$ are now functions in Ω. (Since the $\mathrm{d}\,x_i$ are constant with respect to x, the argument is typically omitted; generally e.g. for $f, g \in F^0(\Omega)$ and $\omega = \mathrm{d}\,f \wedge \mathrm{d}\,g$ we would write $\omega(x) = \mathrm{d}\,f(x) \wedge \mathrm{d}\,g(x)$.) The exterior derivative of a 0-form ω has the coordinate expression

$$\mathrm{d}\,\omega = \sum_{i=1}^{n} \frac{\partial \omega}{\partial x_i}\,\mathrm{d}\,x_i.$$

We now proceed to the full definition for $p \geq 0$. The *exterior derivative* d is the unique linear operator $F^p(\Omega) \to F^{p+1}(\Omega)$ with the following properties [90]:

i) For $\omega \in F^0(\Omega)$, the exterior derivative $\mathrm{d}\,\omega$ is given by (11).
ii) For $\omega \in F^p(\Omega)$ and $\eta \in F^q(\Omega)$, $\mathrm{d}(\omega \wedge \eta) = \mathrm{d}\,\omega \wedge \eta + (-1)^p \omega \wedge \mathrm{d}\,\eta$.
iii) For $\omega \in F^p(\Omega)$, $\mathrm{d}\,\mathrm{d}\,\omega = 0$.

For a p-form presented in coordinates as in (12), the exterior derivative is hence given by

$$\mathrm{d}\left(\sum_{1 \leq i_1 < \ldots < i_p \leq n} \omega_{i_1\ldots i_p}\,\mathrm{d}\,x_{i_1} \wedge \ldots \wedge \mathrm{d}\,x_{i_p}\right) = \sum_{\substack{1 \leq i_1 < \ldots < i_p \leq n,\\ j \notin \{i_1,\ldots,i_p\}}} \frac{\partial \omega_{i_1\ldots i_p}}{\partial x_j}\,\mathrm{d}\,x_j \wedge \mathrm{d}\,x_{i_1} \wedge \ldots \wedge \mathrm{d}\,x_{i_p}.$$

The exterior derivative commutes with the trace and the pullback operations. Together with the Hodge star, it can be used to present differential operators of vector calculus, such as the gradient, curl, and divergence, in terms of differential forms. But unlike these vector calculus operators, the exterior derivative is defined for all p in n dimensions independently of metric and coordinates.

The exterior derivative satisfies Stokes' theorem, written for an oriented $(p+1)$-simplex σ and a p-form ω as

$$\int_\sigma \mathrm{d}\,\omega = \int_{\partial\sigma} \omega. \tag{13}$$

Here the boundary $\partial\sigma$ of σ means the geometrical boundary equipped with the induced orientation; this will be made more precise in the next section. Stokes' theorem can also be formulated for more general domains than simplices [1, 76]. It is a generalisation of integral identities such as the gradient theorem, Green's theorem, and the divergence theorem. As a rationale for cochain-based discretisations, Stokes' theorem is the central result in exterior calculus for our purposes.

We conclude this section by proving the following pullback inequality [139, II, 4.12], which is used in Articles PI and PIII to prove Theorem 2.

Proposition 1. *Let $f : \Omega \to \mathbb{R}^m$ be a smooth map and let ω be a p-form in $f(\Omega)$. For all x in Ω, we have*

$$|f^*\omega(x)| \leq |Df(x)|^p \cdot |\omega(f(x))|.$$

It should be noted that here the norms are defined with respect to the standard inner product in $\mathbb{R}^n$; for 1-covectors, this means that the dual basis of an orthonormal basis is orthonormal. The proof is meant to illustrate the topics of this section.

Proof. We prove a more general result: if $L : \mathbb{R}^n \to \mathbb{R}^m$ is a linear map, the induced maps L_* and L^* satisfy

$$|L_*\alpha| \leq |L|^p \cdot |\alpha| \quad \text{for all } \alpha \in \Lambda^p(\mathbb{R}^n), \tag{14}$$
$$|L^*\omega| \leq |L|^p \cdot |\omega| \quad \text{for all } \omega \in \Lambda^p(\mathbb{R}^m)^*. \tag{15}$$

The pullback inequality then follows from (15) by considering the linear map $Df(x) : \mathbb{R}^n \to \mathbb{R}^m$ at each point $x \in \Omega$.

Let $L : \mathbb{R}^n \to \mathbb{R}^m$ be linear. Using the singular value decomposition [73], we can find orthonormal bases $\{v_1, \ldots, v_n\}$ and $\{w_1, \ldots, w_m\}$ such that $Lv_i = s_i w_i$ for $1 \leq i \leq \min\{n, m\}$ and $Lv_i = 0$ for $i > \min\{n, m\}$, where the s_i are the singular values of L. (See [139] for another proof that does not use the singular value decomposition.) Let $\{f_1, \ldots, f_n\}$ and $\{g_1, \ldots, g_m\}$ be the dual bases; note that these are also orthonormal and for $1 \leq i \leq \min\{n, m\}$ we have $L^t g_i = s_i f_i$ (and $L^t g_i = 0$ for $i > \min\{n, m\}$).

Writing $\alpha \in \Lambda^p(\mathbb{R}^n)$ and $\omega \in \Lambda^p(\mathbb{R}^m)^*$ as

$$\alpha = \sum_{1 \leq i_1 < \ldots < i_p \leq n} \alpha_{i_1 \ldots i_p} v_{i_1} \wedge \ldots \wedge v_{i_p}, \quad \omega = \sum_{1 \leq i_1 < \ldots < i_p \leq m} \omega_{i_1 \ldots i_p} g_{i_1} \wedge \ldots \wedge g_{i_p},$$

we obtain

$$\begin{aligned} L_*\alpha &= \sum_{1 \leq i_1 < \ldots < i_p \leq n} \alpha_{i_1 \ldots i_p} L v_{i_1} \wedge \ldots \wedge L v_{i_p} = \sum_{1 \leq i_1 < \ldots < i_p \leq \min\{n,m\}} \alpha_{i_1 \ldots i_p} (s_{i_1} w_{i_1}) \wedge \ldots \wedge (s_{i_p} w_{i_p}) \\ &= \sum_{1 \leq i_1 < \ldots < i_p \leq \min\{n,m\}} \alpha_{i_1 \ldots i_p} \cdot s_{i_1} \cdot \ldots \cdot s_{i_p} w_{i_1} \wedge \ldots \wedge w_{i_p}, \end{aligned}$$

and since $|L|$ is equal to the largest singular value,

$$|L_*\alpha|^2 = \sum_{1 \leq i_1 < \ldots < i_p \leq \min\{n,m\}} (\alpha_{i_1 \ldots i_p} \cdot s_{i_1} \cdot \ldots \cdot s_{i_p})^2 \leq \sum_{1 \leq i_1 < \ldots < i_p \leq \min\{n,m\}} \alpha^2_{i_1 \ldots i_p} \cdot |L|^{2p} \leq |L|^{2p} \cdot |\alpha|^2.$$

Similarly we obtain $|L^*\omega|^2 \leq |L|^{2p} \cdot |\omega|^2$, and hence (14) and (15) follow. □

2.2 Discrete exterior calculus

Discrete exterior calculus enables discretisation of the continuous theory presented in the previous section. In this thesis, methods based on discrete exterior calculus are characterised by the following properties.

I) The continuous problem is formulated in terms of differential forms, using the exterior derivative and the Hodge star operator to present the differential operators involved.
II) Differential forms are approximated with cochains on a mesh, whose coboundary operator discretises the exterior derivative, fulfilling a discrete counterpart of Stokes' theorem.

III) The Hodge star operator is discretised using a dual mesh and a discrete Hodge operator, which maps primal p-cochains (on n-dimensional mesh) to dual $(n-p)$-cochains.

In particular, we view discrete exterior calculus as a framework for discretising continuous exterior calculus. This viewpoint is termed "the discretized version" in the book of Grady and Polimeni [74], which presents an alternative, inherently discrete viewpoint with no reference to any continuous space. We emphasise that the nomenclature is not definite in the literature, and the above characterisation is selected to clarify the scope of this thesis.

This section is divided into two parts. In Subsection 2.2.1, we present chains and cochains and the coboundary operator as a discrete counterpart of the exterior derivative. This part is not exclusive to our approach; there are related methods that are based on property II) in the above characterisation. It is the discrete Hodge operator — property III) — that separates discrete exterior calculus from related approaches that handle the Hodge star operator differently. This is considered in Subsection 2.2.2.

2.2.1 Chains and cochains

As usual, we start by dividing the domain Ω into a finite number of cells. In this thesis, cells are (convex and bounded) polytopes in $\mathbb{R}^n$, and their faces are defined like those of polytopes (see [38]). The dimension of a cell is the dimension of its plane, and cells or faces of dimension p are called p-cells or p-faces for short. The usual name "vertices" refers to 0-faces, and 1-faces are called "edges". We define the *fullness of a p-cell σ* as $\Theta(\sigma) = |\sigma| / \operatorname{diam}(\sigma)^p$, where diam stands for diameter and $|\sigma| = |\operatorname{vect}(\sigma)|$ denotes the *p-dimensional volume of σ*.

Let K be a finite set of oriented cells. We say that K is a mesh in Ω if

i) each face of every cell in K is also in K,
ii) the intersection of any two cells in K is either empty or a common face of theirs, and
iii) the union of all the cells in K is Ω.

The mesh is simplicial if all the cells are simplices. Similarly, we say that the mesh is cubical if all its cells are parallelotopes. Two examples of simplicial meshes were already encountered in Figure 1 in the introduction. Assuming a mesh K in Ω is given, we denote by $S^p(K)$ the set of p-cells in K.

The space of *p-chains of K* [139] is the real vector space of formal sums of the form

$$\sum_{i=1}^{m} a_i\sigma_i, \quad a_i \in \mathbb{R},\ \sigma_i \in S^p(K),$$

where m equals the number of elements in $S^p(K)$. As usual, two formal sums are added by adding the corresponding coefficients, and multiplication by a real number amounts to multiplying each coefficient. We may write σ instead of $a_i\sigma$

if $a_i = 1$ and omit the term $a_i\sigma$ altogether if $a_i = 0$. Hence any p-cell $\sigma \in S^p(K)$ can be considered as a chain. Let us denote by $C_p(K)$ the space of p-chains of K. Note that the elements of $S^p(K)$ constitute a canonical basis for $C_p(K)$, and if we assume the p-cells $\sigma_1, \ldots, \sigma_m$ are listed in a fixed order, p-chains can be presented as vectors (in $\mathbb{R}^m$) with the coefficients a_i as components.

Negative coefficients in chains indicate a change of orientation so that $-\sigma$ is meant to present σ with the opposite orientation. With this interpretation, p-chains become suitable domains of integration. Let ω be a differential p-form in Ω. We define the integral of ω over p-chains by

$$\int_{\sum_{i=1}^m a_i\sigma_i} \omega = \sum_{i=1}^m a_i \int_{\sigma_i} \omega,$$

where $\int_{\sigma_i} \omega$ is the integral of ω over the p-cell σ_i. From the definition of $\int_{\sigma_i} \omega$ (given in the previous section) it follows that the integral changes sign if the orientation of σ_i is reversed, and hence integration of ω yields a well-defined (linear) operation on $C_p(K)$.

Integration over p-cells of K does not require that $\omega \in F^p(\Omega)$: it suffices that the trace $\omega|_\sigma$ is well-defined on each p-cell σ. We use the name *differential p-forms in K* for forms that have this property; more precisely, a p-form in K is a set of p-forms ω_σ in the cells σ of K such that $\omega_\sigma|_\tau = \omega_\tau$ if τ is a face of σ [139]. We denote by $F^p(K)$ the space of differential p-forms in K. Since the exterior derivative and the trace commute, we have $\mathrm{d}\, F^p(K) \subset F^{p+1}(K)$, but the Hodge star of a p-form in K is not necessarily in $F^{n-p}(K)$.

Suppose an oriented p-cell σ is a p-face of an oriented $(p+1)$-cell τ. We say that σ is equipped with the induced orientation if its orientation agrees with that of τ (in the sense of [139]). This defines the *incidence number* d_σ^τ [132] by

$$\mathrm{d}_\sigma^\tau = \begin{cases} 1 & \text{if } \sigma \text{ is a } p\text{-face of } \tau \text{ equipped with the induced orientation,} \\ -1 & \text{if } \sigma \text{ is a } p\text{-face of } \tau \text{ equipped with the opposite orientation,} \\ 0 & \text{if } \sigma \text{ is not a } p\text{-face of } \tau. \end{cases}$$

The (geometrical) boundary $\partial\tau$ of a $(p+1)$-cell τ is the p-chain

$$\partial\tau = \sum_\sigma \mathrm{d}_\sigma^\tau\, \sigma,$$

where the sum is taken over the p-faces of τ. In other words, the boundary of τ consists of its p-faces equipped with the induced orientations. The *boundary map* $\partial : C_{p+1}(K) \to C_p(K)$ is obtained by linear extension.

The space of *p-cochains of K* is dual space of $C_p(K)$, denoted by $C_p^*(K)$. Consider $\sigma_i \in S^p(K)$ as a basis element of $C_p(K)$. It is customary to denote the corresponding element of the dual basis of $C_p^*(K)$ by the same symbol; that is, σ_i denotes also the cochain such that $\sigma_i(\sigma_j) = \delta_{ij}$ for $\sigma_j \in S^p(K)$. (In this thesis δ_{ij} is the *Kronecker delta*, which equals 1 if $i = j$ and 0 otherwise.) With this notation, also p-cochains can be considered as formal sums (or as vectors if the p-cells are ordered). Despite the notation, we treat chains and cochains as separate objects.

(Some authors [132, 108] take a step further and formulate the theory using chains only.) We will typically denote general chains and cochains by labels $c \in C_p(K)$, $X \in C^*_p(K)$. The *coboundary operator* $\mathrm{d} : C^*_p(K) \to C^*_{p+1}(K)$ is the transpose of ∂, defined by $\mathrm{d}\, X(c) = X(\partial c)$. By convention, we use the same notation d as for the exterior derivative of forms; this will be justified in what follows.

Since integration of $\omega \in F^p(K)$ produces a linear operation on $C_p(K)$, we have the *de Rham map* $\mathcal{C} : F^p(K) \to C^*_p(K)$ defined by $\mathcal{C}\omega(c) = \int_c \omega$. The cochain $\mathcal{C}\omega$ is considered a discrete counterpart (or approximation) of ω. Regarded as a vector, $\mathcal{C}\omega$ has as components the integrals of ω over p-cells of K — these are the degrees of freedom in discrete exterior calculus. The infinite-dimensional space of p-forms is approximated with the finite-dimensional space of p-cochains, and the accuracy of the approximation can be increased by increasing the number of cells in the mesh (and hence the number of degrees of freedom).

It is remarkable that the coboundary operator discretises the exterior derivative exactly, in the sense that $\mathrm{d}\,\mathcal{C}\omega = \mathcal{C}\,\mathrm{d}\,\omega$ for all $\omega \in F^p(K)$. This justifies the same notation; in fact, in the literature cochains are sometimes called "discrete differential forms" and the coboundary operator "the discrete exterior derivative" [53]. Stokes' theorem is automatically preserved in the discrete setting by the definition $\mathrm{d}\, X(c) = X(\partial c)$. The exact nature of the coboundary operator enables conservation of physical quantities (such as energy), which is an important asset of DEC-based methods. The incidence matrix is the matrix representation of the coboundary operator, also denoted by d. Its elements are the incidence numbers: $\mathrm{d}_{ij} = \mathrm{d}^{\tau_i}_{\sigma_j}$, where $\tau_i \in S^{p+1}(K)$ and $\sigma_j \in S^p(K)$. The expression $\mathrm{d}\, X$ is hence meaningful also when cochains are considered as vectors.

2.2.2 Discrete Hodge operators

In discrete exterior calculus, the Hodge star operator is handled using a dual mesh. We say that a set $\tilde{K}$ of oriented cells is a *dual mesh of K* if it satisfies properties (ii) and (iii) of the definition of mesh along with the following conditions:

a) each face of every cell in $\tilde{K}$ is either in $\tilde{K}$ or on the boundary of Ω,
b) to each $\sigma \in S^p(K)$ corresponds a unique $(n-p)$ cell $\tilde{\sigma}$ in $\tilde{K}$, called the dual of σ,
c) each cell in $\tilde{K}$ is the dual of exactly one cell in K,
d) $\sigma \in S^p(K)$ is a face of $\tau \in S^q(K)$ if and only if $\tilde{\tau}$ is a face of $\tilde{\sigma}$, and
e) for each $\sigma \in S^p(K)$, the intersection $\sigma \cap \tilde{\sigma}$ is a point and σ intersects no other $(n-p)$ cell in $\tilde{K}$.

A basic example of a dual mesh (shown in Figure 2) is the Voronoi dual (also known as the circumcentric dual), obtained from the Voronoi diagram of a Delaunay triangulation [16]. Conditions b) and c) imply a one-to-one correspondence between p-cells of K and $(n-p)$-cells of its dual. When appropriate, we call K "the primal mesh" and its cells "primal cells" to distinguish them from their dual counterparts. We may choose the orientations of dual cells such that $\mathrm{d}^{\tilde{\sigma}}_{\tilde{\tau}} = \mathrm{d}^{\tau}_{\sigma}$.

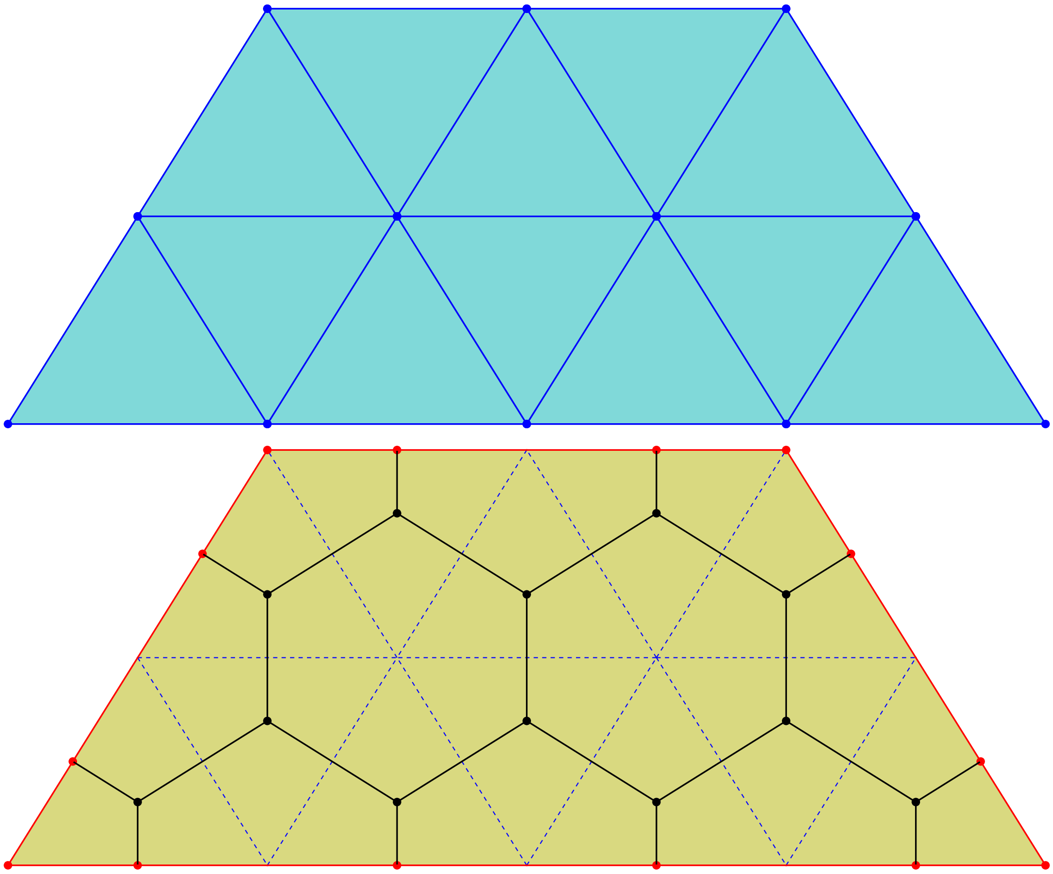

FIGURE 2 A mesh K on the top and a dual mesh $\tilde{K}$ on the bottom. Dotted blue lines represent edges of K and are not in $\tilde{K}$. Neither are the red cells on the boundary, even though they are faces of dual 2-cells.

Note that although the combinatorial structure of $\tilde{K}$ is determined by the primal mesh, locations of dual vertices may be freely chosen; hence $\tilde{K}$ is not unique.

The above description alone yields too restrictive a definition for our purposes, as the barycentric dual mesh does not comply with the requirements. To remedy this, we allow each dual p-cell $\tilde{\sigma}$, for $0 < p < n$, to be distorted and broken into pieces as follows. Choose a point x in σ, and let $\tilde{\tau}_i$ be a $(p-1)$-face of $\tilde{\sigma}$. Then the convex hull containing x and $\tilde{\tau}_i$ is a p-cell — it is one piece of the distorted dual cell. The union of these pieces (over all $(p-1)$-faces $\tilde{\tau}_i$) is considered a single cell that replaces $\tilde{\sigma}$. All dual cells that contain $\tilde{\sigma}$ as a face are also modified accordingly, so this distortion process is applied in the increasing order of dimension (first 1-cells, next 2-cells, and so on). The issue is illustrated in Figure 3. Acceptable dual meshes are those that can be obtained when this process is applied to some mesh satisfying the above conditions.

Chains $C_p(\tilde{K})$ and cochains $C_p^*(\tilde{K})$ on the dual mesh are defined in the same way as those on the primal mesh. We denote by $S^p(\tilde{K})$ the set of p-cells in $\tilde{K}$ and by $\tilde{\mathcal{C}}$ the de Rham map of the dual mesh. The boundary $\partial\tilde{\sigma}$ that is given by the map $\partial : C_{p+1}(\tilde{K}) \to C_p(\tilde{K})$ is missing those p-faces of $\tilde{\sigma}$ that are not in $\tilde{K}$, which affects dual cells touching the boundary of Ω (see condition a)). This is not an issue because these cells must be handled using boundary conditions anyway.

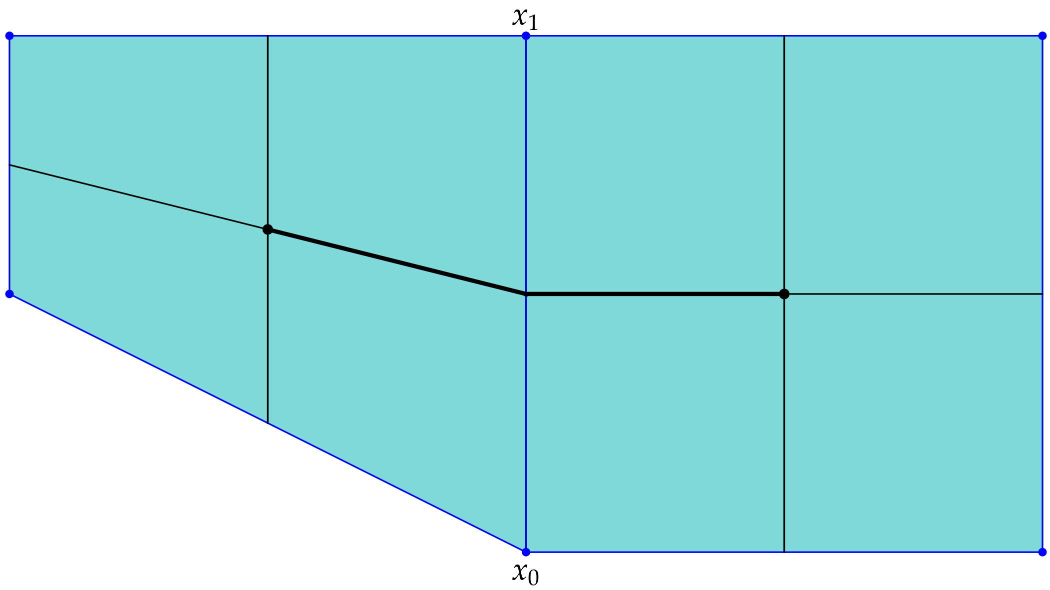

FIGURE 3 A primal mesh in blue and dual cells in black. An acceptable dual mesh is obtained when the two highlighted line segments are considered a single dual cell $\tilde{\sigma}$ of the primal 1-cell $\sigma = x_0x_1$. In this sense $\tilde{\sigma}$ is "broken".

Our choice of dual cell orientations implies that the incidence matrix of the dual mesh is the transpose of d, and hence we denote by d^t the coboundary operator of the dual mesh. For a p-form ω, we have $\mathrm{d}^t\,\tilde{\mathcal{C}}\omega(\tilde{\sigma}) = \tilde{\mathcal{C}}\,\mathrm{d}\,\omega(\tilde{\sigma})$ for all interior cells $\tilde{\sigma} \in S^{p+1}(\tilde{K})$, but $\mathrm{d}^t\,\tilde{\mathcal{C}}\omega = \tilde{\mathcal{C}}\,\mathrm{d}\,\omega$ does not hold in general unless ω has zero trace on the boundary of Ω.

The *discrete Hodge operator* $* : C^*_p(K) \to C^*_{n-p}(\tilde{K})$ is a linear map from primal p-cochains to dual $(n-p)$-cochains [2]. It is not unique, and there are different approaches to the definition, but the construction of the discrete Hodge operator is typically related to the choice of the two meshes. Unlike the coboundary operator, the discrete Hodge operator produces an additional error, in the sense that $*\,\mathcal{C}\omega = \tilde{\mathcal{C}} \star \omega$ does not hold for all $\omega \in F^p(K)$. For this reason, the discrete Hodge operator is a central issue in discrete exterior calculus. In the rest of this subsection, we review existing approaches to its construction and consider some different definitions that appear in the literature.

Orthogonal constructions [27, 32] arrange the two meshes such that each primal cell σ is orthogonal to its dual $\tilde{\sigma}$. (Orthogonality is typically interpreted with respect to the Euclidean metric, but generalisations to Lorentzian metrics [125] and nonconstant metric tensors [28, 32] exist.) As a special case we obtain the circumcentric dual mesh (shown in Figure 2), but several techniques have been devised for mesh optimisation [58, 59, 3, 101], allowing more flexibility in mesh generation. The major advantage of orthogonal constructions is that the discrete Hodge operator can be presented as a diagonal matrix. The diagonal discrete Hodge operator is defined by the relation $*\,X(\tilde{\sigma}) = (|\tilde{\sigma}|/|\sigma|)X(\sigma)$. Thanks to orthogonality, $*\,\mathcal{C}\omega = \tilde{\mathcal{C}} \star \omega$ holds for all (locally) constant p-forms $\omega \in F^p(K)$. In general, orthogonal constructions yield discrete Hodge operators with first order accuracy, but second (or third) order accuracy is achieved under (very) special conditions [121]. Besides the limitation to low orders, diagonal discrete Hodge operators have the drawback that orthogonality may be difficult to achieve.

Barycentric constructions make use of the barycentric dual mesh. It is obtained by requiring that, for each $\sigma \in S^p(K)$, the intersection $\sigma \cap \tilde{\sigma}$ is the barycentre of σ. (More generally, it could be any chosen point in σ; see [32] for more information.) One example is provided in Figure 3. In barycentric constructions, discrete Hodge operators can be defined in multiple ways. Perhaps best known is the Galerkin discrete Hodge operator on a simplicial mesh, which enables a reinterpretation of Galerkin methods as methods based on discrete exterior calculus [29, 128]. It relies on the partition of unity property of Whitney forms, which ensures $*\mathcal{C}\omega = \tilde{\mathcal{C}} \star \omega$ for constant p-forms ω (see [29] for more information). Other similar constructions exist [133, 45, 15, 47], typically based on constant local approximations. The resulting discrete Hodge operators are of lowest order. Barycentric constructions enjoy the property that the existence of a dual mesh can be guaranteed, but they do not produce diagonal discrete Hodge operators. This can be remedied with diagonal lumping [34], but then additional conditions on the mesh are again imposed.

Interpolating approaches [129, 95] are based on interpolation of cochains. These permit all kinds of dual meshes as long as suitable interpolants are available. To map a primal p-cochain with the discrete Hodge operator, we first interpolate the cochain, next apply the actual Hodge star operator to the interpolant, and finally map the resulting $(n-p)$-form with $\tilde{\mathcal{C}}$ to obtain a dual $(n-p)$-cochain. The main example in this category is the discrete Hodge operator obtained by interpolating with Whitney forms [128]. It is exact for Whitney forms in the sense that $*\mathcal{C}\omega = \tilde{\mathcal{C}} \star \omega$ for all Whitney forms ω. (More generally, the discrete Hodge operator is defined to have this property for all p-forms in the chosen space of interpolants.) The resulting Hodge matrix is sparse but not diagonal, so its inverse is generally a full matrix. A dual approach [69, 72] is to map dual $(n-p)$-cochains to primal p-cochains using interpolants on the dual mesh in a similar way and define the discrete Hodge operator as the inverse of the resulting operator. Its matrix is full but has a sparse inverse. On some occasions, this dual approach has been observed to yield better condition numbers [72, 70].

It should be mentioned that in the literature one can find discrete Hodge operators that do not fit our definition of a linear map $* : C^*_p(K) \to C^*_{n-p}(\tilde{K})$. For example, in [140, 56, 14] the discrete Hodge operator is defined as a map from $C^*_p(K)$ to $C^*_{n-p}(K)$ (using a cochain product), so only one mesh is required. Some authors define discrete Hodge operators between suitable finite-dimensional spaces of differential p-forms $\mathfrak{X}$ and $(n-p)$-forms $\mathfrak{Y}$ in a weak sense, i.e. requiring $\int_\Omega \omega \wedge *\eta = \int_\Omega \omega(x) \cdot \eta(x) dx$ for all $\omega, \eta \in \mathfrak{X}$; see e.g. [85]. These approaches do not fit into the framework of discrete exterior calculus unless the degrees of freedom for $\mathfrak{X}$ and $\mathfrak{Y}$ can be assosiated with cells on some primal–dual mesh pair; [40] serves one such special case in two dimensions.

The most general description for discrete Hodge operators is formulated in [78], enabling the interpretation of most finite element and finite volume schemes as special cases with a particular discrete Hodge operator. The definition in [78] allows a secondary mesh which is not necessarily dual to K. Discrete Hodge operators of discrete exterior calculus are obtained as its instances by using dual secondary meshes. However, the algebraic requirements stated in [78] insist that the Hodge matrices be symmetric and positive definite. The literature is not unanimous about this: the same requirement is described also e.g. in [129, 130], but symmetry is not required by several authors (see e.g. [128, 133, 33]). Bossavit [33] has commented that "whether a discrete Hodge should be symmetric is an open issue". Our definition accepts all linear maps $* : C_p^*(K) \to C_{n-p}^*(\tilde{K})$, not ruling out any particular discrete Hodge operator behorehand. In fact, in Chapter 5 we discover that even singular matrices can yield sensible discrete Hodge operators.

2.2.3 Additional remarks

We conclude Chapter 2 with some additional remarks on discrete exterior calculus. This supplementary information is not required in the subsequent chapters.

Remark 1 (On extensions of the theory). The theory of discrete exterior calculus can be extended to cover various other concepts, such as discrete versions of exterior products, Lie derivatives, and bundle-valued differential forms, but one should be aware of the complications involved; for more information, see [31, 80, 52, 89, 141, 100, 48]. Other topics omitted here include outer orientations and twisted forms [41, 25, 26], surficial domains [96, 98, 60] and unbounded domains, which can be handled with a special treatment [61, 109, 42].

Remark 2 (On implementation). Source codes implementing discrete exterior calculus are publicly available, and the framework is suitable for parallel computing [18, 109, 110, 111, 23, 88].

Remark 3 (On the literature). Considering our purely mathematical presentation, it may seem that surprisingly many references are related to the field of computational electromagnetism. This is simply because the early developments of the theory have occurred in this field. Although the relevance of exterior calculus has been acknowledged for a long time [54], the first DEC-based schemes were initially formulated in the language of vector calculus. They have been reinterpreted in terms of exterior calculus only later, after the role of differential forms increased also in numerical modelling (as advocated by Bossavit [24]). For example, covolume methods [102, 105, 104] can be reformulated in terms of differential forms [103] and interpreted as DEC-based schemes. Another example is the finite integration technique [138, 136, 46], which includes Yee's method [142] as a special case. The name "discrete exterior calculus" is widely attributed to Hirani [80], but it has appeared earlier [78] and may have a different connotation depending on the author (compare e.g. [79] with our description of DEC). Mimetic discretisations [20, 91] are closely related, but the difference is that the discrete Hodge operator, according to Bochev and Hyman [20], "is not among the discrete operations that comprise our mimetic framework" (though there are exceptions to this terminology as well [137, 19]).

3 SCIENTIFIC CONTRIBUTION

The scientific contribution of this work is established in the four included articles PI–PIV. In this chapter we introduce these articles and specify their contribution to the scientific literature. Chapters 4–6 succinctly present the key results, intended to be comprehensible without reading the included articles, but the full contribution of the thesis is best acknowledged by familiarising oneself with the whole work.

Article PI

Although differential forms can be approximated with cochains, it is apparent that cochains are different kind of objects. They cannot be evaluated at a chosen point $x \in \Omega$ to obtain p-covectors; instead, cochains produce real values on p-cells of the chosen mesh K. These values must be interpolated somehow before one can evaluate DEC-based approximations inside the cells of K. This is why interpolation of cochains is a relevant issue in discrete exterior calculus. Interpolation is performed using suitable interpolants, and the most established ones are Whitney forms on simplicial meshes. The first included article deals with Whitney forms and their extensions to higher order functions and other cell types.

The main objective of the first article is to clarify the concept and properties of Whitney forms. Although Whitney forms are a standard part of the theory, they are defined in different ways by different authors. Sometimes these definitions are equivalent and sometimes not. In addition, even though the key properties of Whitney forms are well known, there is no prior paper including proofs for all of them; the results are scattered in the literature and in some cases stated without proof. Article PI reviews different yet equivalent ways to define Whitney forms and lists all their key properties with proofs. This enables one to recognise several extensions of Whitney forms — objects that are no longer equivalent but in some sense preserve some of the properties. In Article PI we discuss some of these extensions, including higher order Whitney forms and Whitney forms on other cell types, and check which of the properties can be preserved.

Although a specialist acquainted with the topic can consider the results of

Article PI as known, it should be noted that there are technical details that have not been published before. In particular, we mention Theorems 4.9 and 5.1, on which we elaborate in Chapter 4 (see especially Section 4.3). The proof of Theorem 4.3 is original, and Proposition 4.4 has not been published before. Subsection 5.2 contains new interpretations on how the properties of Whitney forms are preserved in the higher order case. Article PI could be classified as a review paper that generates new information.

Article PII

When new higher order methods are introduced, it is typical that a theoretical description is provided for a general order k but examples are limited to low orders (say $k \leq 3$). There are even papers that focus exclusively on implementation but still carry out only a few low orders; for example, in [21] the authors present an explicit implementation strategy for higher order Whitney 1-forms, but only orders $k \leq 3$ are actually implemented. The reason is usually that a parametric implementation covering all orders with the same code is not easily achieved. Then each k has to be handled separately, and the workload typically increases heavily when k is increased, which means that only a few low orders are practically manageable. Article PII deals with the issue of systematic implementation. Its main objective is to ensure that our framework of higher order DEC can be implemented in a systematic way which covers all orders with the same code.

Article PII presents a systematic approach to the interpolation of cochains with higher order Whitney forms. The strategy is explained in Chapter 4. It is based on a refinement of a simplicial mesh that contains the small simplices of [118]. These small simplices were first used with DEC by the author in his master's thesis [92], which is summarised in [87, Sections 9–10]. However, in [92] only second order forms were implemented (in a rather ad hoc manner), and the implementation of higher orders would have been unreasonably laborous in the same way. The main contribution of Article PII is in Sections 5–6, which systematise the approach of [92] to cover arbitrary orders. In particular, Algorithms 1–3 are a significant novelty whose importance cannot be overemphasised. Without Article PII, all numerical results appearing in this thesis would be limited to low orders. We mention also Lemma B.2 in Appendix B, which generalises Proposition 3.6 of [117]. Although Article PII discusses only Whitney forms, the same ideas apply to other interpolants and enable the implementation of higher order discrete Hodge operators. All numerical results of this thesis are hence based on Article PII.

Article PIII

Higher order Whitney forms are defined on simplicial meshes, and one may wonder if our approach is limited to simplices. Article PIII shows that this is not the case, extending the framework of higher order DEC to cubical meshes. The innovation in Article PIII is that known higher order interpolants on cubical meshes can be defined using small cubes in an analogous way as higher order Whitney forms are defined using small simplices. This is established in Definitions 2.1–2.4 and Proposition 2.5. In Subsection 3.2 the small cubes are shown to yield unisolvent degrees of freedom. The result is proven for p-forms of arbitrary order in n dimensions. Article PIII also shows how the new degrees of freedom can be computed for basis functions: Subsection 3.1 provides an explicit expression. Section 4 discusses the interpolation operator and its properties. As a by-product, we obtain an easy proof for the exact sequence property of the interpolants (see Remark 4.2). Theorem 4.3 is similar to Theorem 5.1 in Article PI, but otherwise the results of Article PIII can be considered original.

We elaborate on these results regarding cubical meshes in Chapter 4. Thanks to Article PIII, it is worthwhile to first consider a general higher order interpolation strategy which is not limited to specific cell types. This enables a unified treatment of the small simplices and the small cubes, and it may be possible to include more cell types into the higher order framework in the future. Without Article PIII all results in this thesis would be limited to simplicial meshes. On some occasions Whitney forms do not provide satisfactory results (see Remark 9) but cubical meshes seem to resolve the issues. This is why Article PIII is a crucial part of the thesis.

Article PIV

The higher order interpolation strategy established in the first three articles reduces the interpolation error. As such, it does not result in higher order convergence in DEC-based methods because the error resulting from the discrete Hodge operator cannot be corrected at the interpolation stage. However, the interpolation framework enables the definition of higher order discrete Hodge operators, which is the topic of Article PIV. We show that it is possible to derive higher order methods based on discrete exterior calculus using higher order discrete Hodge operators.

Article PIV has several valuable contributions. The definition and properties of higher order discrete Hodge operators are discussed in Section 4. We review this discussion in Chapter 5. Previously few authors have considered higher order discrete Hodge operators (see Remark 8), and the topic is hence interesting as such. In Section 5 we provide a unifying approach to higher order DEC-based methods for second order boundary value problems. The novelty in this approach is that it enables the treatment of elliptic and hyperbolic problems in the same manner with different choices of metric: defining the Hodge star operator with respect to Riemannian metrics leads to elliptic problems, and hyperbolic problems are obtained with Lorentzian metrics when the cochains are considered in spacetime. Article PIV is hence a contribution also to the existing theory of spacetime formulations based on cochains [127, 67, 86, 131, 125].

Error bounds are provided for Poisson's and the wave equation in Section 6, and the numerical examples of Section 7 show that the ideas can also be implemented in practice. We summarise the approach and the results in Chapter 6, but

Article PIV can be consulted for the full treatment. Article PIV can be considered the main article of this thesis; while the first three articles prepare the necessary tools, it is this paper that brings higher order DEC-based methods to fruition.

3.1 Author's independent contribution in joint articles

The work involved in the included articles was done by the author mostly alone, but the author had discussions with his supervisors from time to time. In these discussions, the author presented recent ideas and informed how the project is progressing, and the supervisors had a chance to provide their comments and ideas that could lead to new developments. Articles PII and PIII should be considered the author's independent work. For the other two articles, the following contributions by the supervisors were deemed sufficient for coauthorship.

Article PI The topic for the article was the coauthor's idea: he suggested that there was call for a paper clarifying the definition of Whitney forms and examining the similarities and differences of different objects that go by that name. (The contents in more detail were still selected by the author.) The coauthor also helped to write about 50% of the introduction and participated in proofreading.

Article PIV The coauthors suggested the relevance of the Minkowski metric to time-dependent problems, recalling that it has been used previously in orthogonal constructions of the dual mesh; the approach of Section 5 was still the author's idea, but this guided him in the right direction. The coauthors also asked good questions about the system (5.5): is time stepping possible, and does it lead to a causal scheme? Subsections 5.2 and 5.3 should still be considered the author's work, but they were inspired by these questions. Finally, the coauthors helped to write the first paragraph of the introduction and participated in proofreading.

In other respects also these two articles can be considered the author's independent contribution.

3.2 Source code of the implementation

The tools developed in this work have been implemented in C++ programming language. The source code of the implementation is available in the repository [93], including also the numerical examples considered in the thesis. For more information, see the overview and instructions provided in [93].

4 INTERPOLATION OF COCHAINS

In discrete exterior calculus, interpolation of cochains can be considered a post-processing procedure that is not strictly mandatory. The solution in DEC-based schemes should be obtainable as a cochain using the discretisation approach presented in Section 2.2. The cochain cannot be evaluated at a chosen point $x \in \Omega$, but it approximates the integrals of the actual solution over p-cells of the chosen mesh K. If this information is satisfactory, interpolation is not required. However, it is reasonable to ask what the solution is inside the cells of K, in view of both error analysis and practical applications, and for this interpolation is necessary. Interpolation is also one approach to the construction of the discrete Hodge operator and hence a relevant issue in DEC.

This chapter combines our key results related to interpolation of cochains. The focus is especially on higher order interpolation. Interpolation of cochains with lowest order functions (such as Whitney forms and their extensions to other cell types) is well-known territory (see Article PI), but the same is not true in the higher order case. The higher order interpolation framework presented here covers simplicial and cubical meshes, but it is designed in a way that leaves open the possibility of including more cell types in the future.

4.1 Higher order interpolation framework

Interpolation is performed using suitable *interpolants*, which span finite-dimensional subspaces $I^p(K)$ of $F^p(K)$ (one for each p), and linear interpolation operators $\mathfrak{I}$ mapping p-cochains to $I^p(K)$. Since $\omega \in F^p(K)$ is discretised as the cochain $\mathcal{C}\omega$, the interpolant $\mathfrak{I}\mathcal{C}\omega \in I^p(K)$ should provide an approximation for ω, and the difference $\mathfrak{I}\mathcal{C}\omega - \omega$ can be thought of as the interpolation error. While $\mathfrak{I}\mathcal{C}\omega = \omega$ cannot hold exactly for all $\omega \in F^p(K)$, it is reasonable to require this for all $\omega \in I^p(K)$. This implies that $\mathfrak{I}$ must be surjective, and hence the dimension of $I^p(K)$ cannot exceed the dimension of the space of p-cochains. Since increasing the order of the interpolants would inevitably increase the dimension of $I^p(K)$, this has given the impression that cochain-based methods are limited to lowest order. But here comes the trick: since higher order interpolation requires more degrees of freedom, we refine the mesh K and consider the cochains on the refinement. We would like to acknowledge that the idea is not completely new; similar possibilities have been mentioned by Mattiussi [94, 95], but here the idea is developed into a proper higher order interpolation framework.

As a first step, we choose k and refine the initial mesh K to form a refined mesh K_k that contains certain small cells of order k as cells. In the following we define these small cells for simplices and cubes. The small simplices are defined in terms of barycentric coordinates. (We denote by λ_i the barycentric function corresponding to the 0-simplex x_i.) The small cubes are defined below in the unit n-cube $\square^n = [0,1]^n$, but the definition extends to a general parallelotope through the affine bijection $\phi : \square^n \to \sigma$ (see Article PIII). Both definitions use multi-index notation: for nonnegative integers i and j, we denote by $\mathcal{I}(i,j)$ the set of multi-indices with i components that sum to j and by $\mathcal{J}(i,j)$ the set of multi-indices with i components that are all less than or equal to j.

Definition 1 (Small simplices of [118]). Let $\sigma = x_0 \ldots x_n$ be an n-simplex. Each multi-index $\mathbf{k} = (k_0, \ldots, k_n) \in \mathcal{I}(n+1, k-1)$ defines a map $\mathbf{k}_\sigma : \sigma \to \sigma$ by

$$\mathbf{k}_\sigma(\lambda_0 x_0 + \ldots + \lambda_n x_n) = \frac{\lambda_0 + k_0}{k} x_0 + \ldots + \frac{\lambda_n + k_n}{k} x_n.$$

For $k \geq 1$, the set of kth order small p-simplices of σ is

$$S_k^p(\sigma) = \{\mathbf{k}_\sigma(\tau) \mid \mathbf{k} \in \mathcal{I}(n+1, k-1) \text{ and } \tau \text{ is a } p\text{-face of } \sigma\}.$$

Definition 2 (Small cubes of Article PIII). Let $\square^n$ denote the unit n-cube $[0,1]^n$. Each multi-index $\mathbf{k} = (k_1, \ldots, k_n) \in \mathcal{J}(n, k-1)$ defines a map $\mathbf{k}_{k-1} : \square^n \to \square^n$ by

$$\mathbf{k}_{k-1}(x_1, \ldots, x_n) = \frac{(k_1 + x_1, \ldots, k_n + x_n)}{k}.$$

For $k \geq 1$, the set of kth order small p-cubes of $\square^n$ is

$$S_k^p(\square^n) = \{\mathbf{k}_{k-1}(\tau) \mid \mathbf{k} \in \mathcal{J}(n, k-1) \text{ and } \tau \text{ is a } p\text{-face of } \square^n\}.$$

Examples of small simplices and small cubes are displayed in Figure 4.

We denote by $S_k^p(K)$ the set of kth order small p-cells of K; it consists of all kth order small p-cells in all cells of K. The idea is to form a refined mesh K_k containing the kth order small cells of K as cells. In the cubical case the small cells produce a subdivision of K, so K_k is uniquely defined and $S^p(K_k) = S_k^p(K)$. If K is simplicial, K_k contains also other cells, as the small simplices do not pave K. (There are holes between them when $n > 1$; see Figure 4.) Nevertheless, it is still possible to form a refinement containing $S_k^p(K)$ as cells. One way is to simply include the holes as additional cells. The holes can also be further divided into smaller cells, so K_k is not unique.

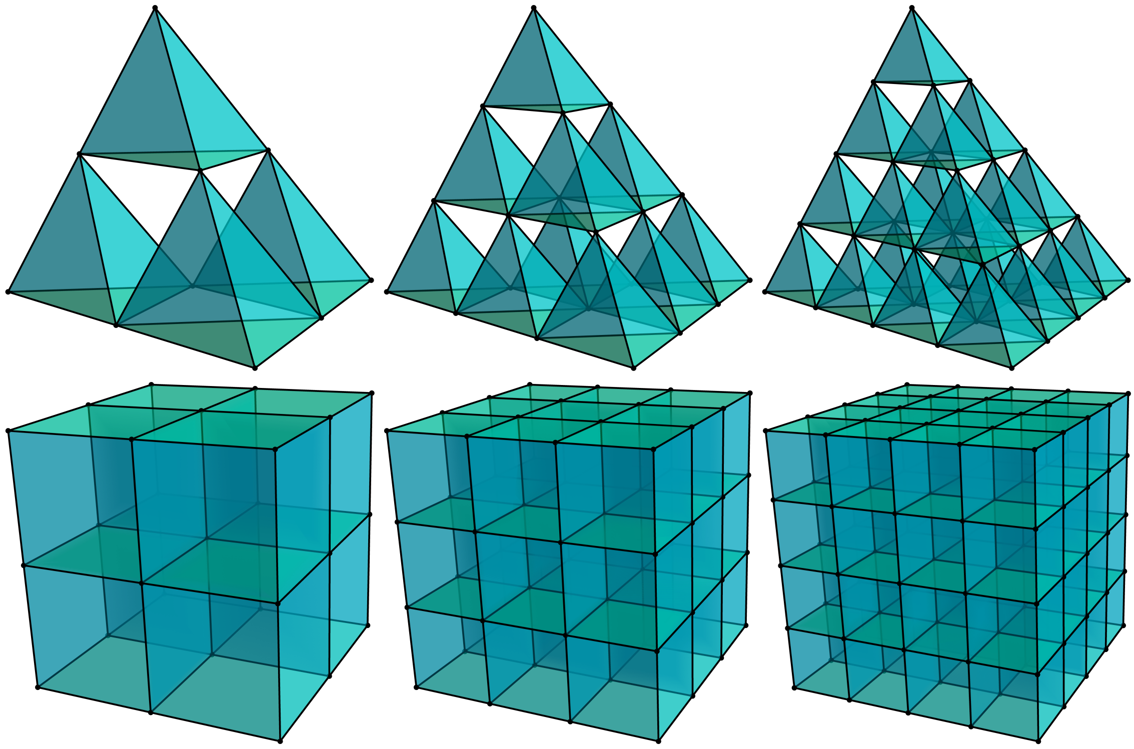

FIGURE 4 Small cells of orders 2–4 in three dimensions.

The refinement K_k can be used to apply discrete exterior calculus in the usual manner: we can consider chains $C_p(K_k)$, cochains $C_p^*(K_k)$, the dual mesh $\tilde{K}_k$, the discrete Hodge operator $* : C_p^*(K_k) \to C_{n-p}^*(\tilde{K}_k)$, and so on. The difference is that now we also have the (big) cells of K, so we can pick the interpolants with respect to the initial mesh: the interpolation operator can be defined as a map $\mathfrak{I} : C_p^*(K_k) \to I^p(K)$. This allows one to increase the dimension of $I^p(K)$ when the order k is increased. The small cells have been designed consciously to ensure that suitable higher order spaces $I^p(K)$ exist. We recall the lowest order spaces first and then extend the definitions to arbitrary order.

Definition 3 (Lowest order Whitney forms)**.** The Whitney 0-form corresponding to the 0-simplex x_i is the barycentric function $\mathcal{W}x_i = \lambda_i$. For $p > 0$, the Whitney p-form corresponding to the p-simplex $x_0 \dots x_p$ is

$$\mathcal{W}(x_0 \dots x_p) = p! \sum_{i=0}^{p} (-1)^i \lambda_i \, \mathrm{d}\,\lambda_0 \wedge \dots \wedge \widehat{\mathrm{d}\,\lambda_i} \wedge \dots \wedge \mathrm{d}\,\lambda_p,$$

where $\widehat{\quad}$ indicates a term omitted from the product.

Definition 4 (Lowest order cubical forms)**.** Let σ be a p-face of $\square^n$. Let $x_{i_1}, \dots, x_{i_p}$ be the coordinates whose plane is parallel to σ and $x_{i_{p+1}}, \dots, x_{i_n}$ the other coodinates, whose values $y_{i_{p+1}}, \dots, y_{i_n}$ are either 0 or 1 on σ. The lowest order cubical form $\mathcal{W}\sigma$ corresponding to σ is

$$\mathcal{W}\sigma = \left(\prod_{j=p+1}^{n} x_{i_j}^{y_{i_j}} (1 - x_{i_j})^{1 - y_{i_j}} \right) \mathrm{d}\,x_{i_1} \wedge \dots \wedge \mathrm{d}\,x_{i_p}.$$

Definition 5 (Higher order Whitney forms)**.** Let $\sigma = x_0 \dots x_n$ be an n-simplex, $\mathbf{k} \in \mathcal{I}(n+1, k-1)$, and τ be a p-face of σ. The kth order Whitney p-form corresponding to the small simplex $\mathbf{k}_\sigma(\tau)$ is

$$w(\mathbf{k}_\sigma(\tau)) = \left(\prod_{i=0}^{n} (\lambda_i)^{k_i}\right) \mathcal{W}\tau.$$

On a simplicial mesh K, the space of *kth order Whitney p-forms* is

$$W_k^p(K) = \operatorname{span}\{w(v) \mid v \in S_k^p(K)\}.$$

Definition 6 (Higher order cubical forms)**.** Let $\mathbf{k} \in \mathcal{J}(n, k-1)$ and τ be a p-face of $\square^n$. The kth order cubical p-form corresponding to the small cube $\mathbf{k}_{k-1}(\tau)$ is

$$w(\mathbf{k}_{k-1}(\tau)) = \left(\prod_{i=1}^{n} x_i^{k_i}(1-x_i)^{k-1-k_i}\right) \mathcal{W}\tau.$$

The space of kth order cubical p-forms in $\square^n$ is

$$Q_k^p(\square^n) = \operatorname{span}\{w(\mathbf{k}_{k-1}(\tau)) \mid \mathbf{k} \in \mathcal{J}(n, k-1) \text{ and } \tau \text{ is a } p\text{-face of } \square^n\}.$$

If K is a cubical mesh, the cubical forms corresponding to the small cubes of $\sigma \in S^n(K)$ are obtained using the affine bijection $\phi : \square^n \to \sigma$. (In more detail, $w(\phi(\mathbf{k}_{k-1}(\tau))) = (\phi^{-1})^*(w(\mathbf{k}_{k-1}(\tau)))$; see Article PIII.) This yields the space of *kth order cubical p-forms* $Q_k^p(K) = \operatorname{span}\{w(v) \mid v \in S_k^p(K)\}$. The spaces $W_k^p(K)$ and $Q_k^p(K)$ coincide with (the shape functions of) the families $\mathcal{P}_k^-\Lambda^p(K)$ and $\mathcal{Q}_k^-\Lambda^p(K)$ in finite element exterior calculus [11, 7]; a proof of the equality $W_k^p(K) = \mathcal{P}_k^-\Lambda^p(K)$ is provided in [12], and Proposition 2.5 of Article PIII shows that $Q_k^p(K) = \mathcal{Q}_k^-\Lambda^p(K)$. Many of their good properties are hence known theory. We mention in particular that also Whitney forms are affine invariant and the exterior derivative satisfies $\mathrm{d}(W_k^p(K)) \subset W_k^{p+1}(K)$ and $\mathrm{d}(Q_k^p(K)) \subset Q_k^{p+1}(K)$. The properties are discussed in more detail in Articles PI–PIII.

Now we have suitable spaces $I^p(K)$ of interpolants, and it remains to define the *interpolation operators* $\mathfrak{I} : C_p^*(K_k) \to I^p(K)$. Let $\mathcal{C}_k$ denote the de Rham map of K_k; we require $\mathfrak{I}\mathcal{C}_k\omega = \omega$ for all $\omega \in I^p(K)$. In the cubical case, this requirement actually determines the interpolation operator uniquely. This is a consequence of the following result, which shows that integration over small p-cubes of order k provides unisolvent degrees of freedom for $Q_k^p(K)$.

Theorem 1 (Theorem 3.6 of Article PIII)**.** *Let $\omega \in Q_k^p(\square^n)$. If $\int_v \omega = 0$ for all small p-cubes $v \in S_k^p(\square^n)$, then $\omega = 0$.*

The proof is given in Subsection 3.2 of Article PIII. When this result is combined with the fact that the dimensions of $Q_k^p(K)$ and $C_p^*(K_k)$ match (see Article PIII), the interpolation operator $\mathfrak{I} : C_p^*(K_k) \to Q_k^p(K)$ is uniquely defined.

Unfortunately, the same is not true for simplices. The dimensions of $W_k^p(K)$ and $C_p^*(K_k)$ are not equal, and the spanning forms corresponding to the small simplices in $S_k^p(K)$ are not even linearly independent. However, it is possible to choose a subset $\hat{S}_k^p(K)$ of $S_k^p(K)$, with cardinality equal to the dimension of $W_k^p(K)$, such that the corresponding Whitney forms provide a basis and integration over elements of $\hat{S}_k^p(K)$ yields unisolvent degrees of freedom. This possibility has previously been based on computational evidence but can be proven at least for a particular subset; see the thesis [39] for the recent state of affairs. The interpolation operator $\mathfrak{I} : C_p^*(K_k) \to W_k^p(K)$ is defined by requiring that $\int_v \mathfrak{I}X = X(v)$ for all cochains $X \in C_p^*(K_k)$ and all small simplices v in the chosen subset $\hat{S}_k^p(K)$.

Besides the property

$$\mathfrak{I}\mathcal{C}_k\omega = \omega \quad \text{for all } \omega \in I^p(K), \tag{16}$$

the interpolation operators satisfy

$$\mathcal{C}_k\mathfrak{I}X = X \quad \text{for all } X \in \mathcal{C}_k(I^p(K)), \tag{17}$$

$$\mathfrak{I}\,\mathrm{d}\,X = \mathrm{d}\,\mathfrak{I}X \quad \text{for all } X \in \mathcal{C}_k(I^p(K)). \tag{18}$$

With cubical forms $\mathcal{C}_k(I^p(K)) = C_p^*(K_k)$, so these properties hold for all cochains, but with Whitney forms this occurs only in some special cases (see Remark 4); one must accept that all features cannot be preserved in the higher order case. While (17) is a direct consequence of (16), for (18) we also need the inclusion $\mathrm{d}(I^p(K)) \subset I^{p+1}(K)$: if $X = \mathcal{C}_k\omega$, we get

$$\mathfrak{I}\,\mathrm{d}\,X = \mathfrak{I}\,\mathrm{d}\,\mathcal{C}_k\omega = \mathfrak{I}\mathcal{C}_k\,\mathrm{d}\,\omega = \mathrm{d}\,\omega = \mathrm{d}\,\mathfrak{I}\mathcal{C}_k\omega = \mathrm{d}\,\mathfrak{I}X.$$

Remark 4. In the simplicial case $\mathcal{C}_k(I^p(K)) = C_p^*(K_k)$ when $k = 1$, $p = 0$, or $n = 1$, but the properties (17)–(18) do not hold for all cochains in general. Already in the case $n = 2$, $k = 2$, and $p = 1$, neither of the properties can be fulfilled simultaneously with (16) when the small simplices are used to define degrees of freedom. However, the derivative of the interpolant can still always be computed: when $X \in C_p^*(K_k)$, we have $\mathrm{d}\,\mathfrak{I}X = \mathrm{d}\,\mathfrak{I}\mathcal{C}_k\mathfrak{I}X = \mathfrak{I}\,\mathrm{d}\,\mathcal{C}_k\mathfrak{I}X$.

Remark 5. Above we implicitly rely on a decomposition of the dual space $I^p(K)^*$, which ensures that interpolation indeed yields elements of $I^p(K)$. In short, if $\sigma \in S^q(K)$ and $X \in C_p^*(K_k)$, the trace $(\mathfrak{I}X)|_\sigma$ is uniquely determined by the values of X on those small cells that belong to σ. We return to this later.

4.2 Systematic implementation strategy

Let us next consider the implementation of the higher order interpolation framework that we have generated. For a systematic implementation strategy, it is extremely useful that the spaces of interpolants $I^p(K)$ admit geometric decompositions [12]. A thorough exposition of geometric decompositions in terms of consistent extension operators is given in [12], but without going into details, the idea can be explained in the present framework as follows.

For a q-cell σ, let us denote by $I^p(\sigma)$ the space $I^p(K)$ with K consisting of the single q-cell σ (and its faces), and define $\mathring{I}^p(\sigma)$ as the subspace

$$\mathring{I}^p(\sigma) = \{\omega \in I^p(\sigma) \mid \omega|_{\partial\omega} = 0\}.$$

A geometric decomposition expresses the space $I^p(K)$ as a direct sum

$$I^p(K) = \bigoplus_{\substack{\sigma \in S^q(K), \\ p \leq q \leq n}} E_\sigma(\mathring{I}^p(\sigma)) \tag{19}$$

using suitable extension operators E_σ, which extend p-forms defined in σ to the whole mesh. In the present framework, we need not make these extension operators explicit. The reason is that the spanning forms for $I^p(\sigma)$ are labelled with respect to the small p-cells of σ (i.e. $S_k^p(\sigma)$), which are also small p-cells of any higher dimensional cell τ containing σ as a face (i.e. $S_k^p(\sigma) \subset S_k^p(\tau)$). Hence the element $w(v) \in I^p(\sigma)$, for $v \in S_k^p(\sigma)$, extends naturally to the element $w(v) \in I^p(\tau)$ obtained when v is considered as an element of $S_k^p(\tau)$. (This results in consistent extension operators, in the sense of [12].) Hereafter we write simply $\mathring{I}^p(\sigma)$ instead of $E_\sigma(\mathring{I}^p(\sigma))$, implicitly extending the elements when appropriate.

The dual space $I^p(K)^*$ also admits a decomposition, which suits the description of the dual decomposition discussed in [12]. Let $\mathring{S}_k^p(\sigma)$ denote the subset of $S_k^p(\sigma)$ containing those small cells that are not fully contained in the boundary of σ. In our framework, the dual decomposition is simply the decomposition of $S_k^p(K)$ into the sets $\mathring{S}_k^p(\sigma)$, where σ ranges over the cells of K. As already mentioned in Remark 5, the existence of this dual decomposition is a necessity for the validity of the interpolation approach, but it is also pivotal in view of implementation. Indeed, it seems that previous implementations of higher order Whitney forms that are limited to only a few low orders have not utilised the dual decomposition to its full potential. This has been remedied in Article PII. In the following we summarise our systematic implementation strategy for the simplicial case, which is more involved; the cubical case is only simpler and can be handled with the same strategy (see Remark 6).

The first step is to choose a basis for the space $\mathring{I}^p(\sigma)$ in a generic q-cell σ, for all $p \leq q \leq n$. The idea is that then the same choice can be applied throughout the mesh, thanks to the decomposition (19). For each $\mathring{S}_k^p(\sigma)$, we select a subset $\hat{\mathring{S}}_k^p(\sigma)$ with cardinality equal to the dimension of $\mathring{I}^p(\sigma)$ such that the p-forms $w(v)$ corresponding to $v \in \hat{\mathring{S}}_k^p(\sigma)$ constitute a basis for $\mathring{I}^p(\sigma)$. In other words, we drop redundant small simplices from the set $\mathring{S}_k^p(\sigma)$ to obtain the set $\hat{\mathring{S}}_k^p(\sigma)$. There are multiple ways to select the subset $\hat{\mathring{S}}_k^p(\sigma)$, but some care is required to ensure that the corresponding forms span $\mathring{I}^p(\sigma)$; for more details, see Article PII. The same subset $\hat{\mathring{S}}_k^p(\sigma)$ can be used to define the interpolation operator as explained earlier (by requiring $\int_v \Im X = X(v)$ for all $X \in C_p^*(K_k)$ and $v \in \hat{S}_k^p(K)$).

Next, we make use of the dual decomposition. Suppose $X \in C_p^*(K_k)$ and $\sigma \in S^p(K)$. For all other cells $\tau \in S^q(K)$ of dimension $q \geq p$, the trace of all

p-forms in $\mathring{I}^p(\tau)$ vanishes on σ, and hence the coefficients of $\mathfrak{I}X$ corresponding to basis functions in $\mathring{I}^p(\sigma)$ are uniquely determined by the values of X on elements of $\hat{\mathring{S}}^p_k(\sigma)$. Let us denote these coefficients by $c[\hat{\mathring{S}}^p_k(\sigma)]$ and these values by $X[\hat{\mathring{S}}^p_k(\sigma)]$, both intended as vectors (i.e. arrays) indexed over elements of $\hat{\mathring{S}}^p_k(\sigma)$. The coefficients are solved by simple means of linear algebra. For all $p \leq q \leq n$, define a matrix $A(p,q)$, indexed over $\hat{\mathring{S}}^p_k(\tau)$ as chosen in the generic q-cell τ, such that $A(p,q)_{ij} = \int_{v_i} w(v_j)$. Then the condition $\int_v \mathfrak{I}X = X(v)$ for all $v \in \hat{\mathring{S}}^p_k(\sigma)$ reads $A(p,p)c[\hat{\mathring{S}}^p_k(\sigma)] = X[\hat{\mathring{S}}^p_k(\sigma)]$, so the coefficients $c[\hat{\mathring{S}}^p_k(\sigma)]$ are obtained by solving this linear system.

The coefficients $c[\hat{\mathring{S}}^p_k(\sigma)]$ for $\sigma \in S^q(K)$ are solved almost similarly. If $q > p$, σ contains r-faces τ (with $p \leq r < q$) such that p-forms in $\mathring{I}^p(\tau)$ have a nonvanishing trace on σ, and hence the coefficients $c[\hat{\mathring{S}}^p_k(\sigma)]$ are not determined by the values $X[\hat{\mathring{S}}^p_k(\sigma)]$ alone. However, we may assume that the coefficients $c[\hat{\mathring{S}}^p_k(\tau)]$ for these faces τ have already been solved at a previous step, and the coefficients $c[\hat{\mathring{S}}^p_k(\sigma)]$ can be obtained when this is taken into account. To this end, for each r-face τ of σ, we define a matrix $B(p,\sigma,\tau)$ by

$$B(p,\sigma,\tau)_{ij} = \int_{v_i} w(v_j), \quad v_i \in \hat{\mathring{S}}^p_k(\sigma),\ v_j \in \hat{\mathring{S}}^p_k(\tau).$$

Then the condition $\int_v \mathfrak{I}X = X(v)$ for all $v \in \hat{\mathring{S}}^p_k(\sigma)$ reads

$$A(p,q)c[\hat{\mathring{S}}^p_k(\sigma)] + \sum_{\tau \subset \sigma} B(p,\sigma,\tau)c[\hat{\mathring{S}}^p_k(\tau)] = X[\hat{\mathring{S}}^p_k(\sigma)].$$

Here the $c[\hat{\mathring{S}}^p_k(\tau)]$ are known, and the coefficients $c[\hat{\mathring{S}}^p_k(\sigma)]$ are hence obtained from this linear system.

Due to affine invariancy, the matrix $A(p,q)$ does not depend on σ and can be precomputed in a generic q-cell. The coefficients can be solved using the LU decomposition; since the matrix $A(p,q)$ stays the same, it suffices to compute this once. The matrices $B(p,\sigma,\tau)$ only depend on the order of the vertices of τ with respect to σ, and it is possible to precompute the finite number of these possibilities. The integrals involved in the matrices $A(p,q)$ and $B(p,\sigma,\tau)$ can be computed analytically as explained in Appendix B of Article PII. In Article PII we discuss also other details not covered in this summary. This includes algorithms for building the refinement K_k and evaluating the interpolant $\mathfrak{I}X$ at a given point after the coefficients in the chosen basis have been obtained with the described strategy.

Remark 6. The same strategy applies to cubical forms, but the cubical case allows of some simplifications. The selection of the sets $\hat{\mathring{S}}^p_k(\sigma)$ can be skipped altogether (one puts $\hat{\mathring{S}}^p_k(\sigma) = \mathring{S}^p_k(\sigma)$). In addition, the space $\mathring{I}^p(\sigma)$ could be further decomposed into subspaces that correspond to different coordinate planes; for more details, see Article PIII. The integrals involved in the matrices $A(p,q)$ and $B(p,\sigma,\tau)$ can be precomputed using the analytical formulas provided in Subsection 3.1 of Article PIII.

4.3 Bounds for the interpolation error

The higher order interpolation framework presented in the previous sections provides kth order approximations for p-forms in simplicial and cubical meshes in n dimensions. The following result establishes the convergence of these approximations for arbitrary k, p, and n when the mesh K is suitably refined.

Theorem 2. *Let ω be a smooth p-form in Ω. There exists a constant $C_{\omega,k}$ such that*

$$|\mathfrak{I}\mathcal{C}_k\omega(x) - \omega(x)| \leq \frac{C_{\omega,k}}{C_\Theta^p} h^k \quad \text{for all } x \text{ in all } \sigma \in S^n(K)$$

whenever $h > 0$, $C_\Theta > 0$, and K is a simplicial or cubical mesh in Ω such that all cells σ in K satisfy $\operatorname{diam}(\sigma) \leq h$ *and* $\Theta(\sigma) \geq C_\Theta$.

The proof is given in Article PI for the simplicial case and in Article PIII for the cubical case. It is based on the property (16), which implies that the approximation is exact for polynomials up to order $k-1$. (For $p = 0$, this actually holds for polynomials up to order k, and one may replace h^k in Theorem 2 with h^{k+1}.)

Theorem 2 is formulated in the spirit of Whitney's book [139], bringing the approximation property of finite elements to the framework of discrete exterior calculus. Its counterparts in finite element analysis are typically based on some version of the Bramble–Hilbert lemma, with the constant C_Θ implicitly hidden in shape regularity requirements; for more information, see [62]. To the best of the author's knowledge, Theorem 2 has not been published before in this form, and no existing result immediately implies the statement, although the techniques used in the proof are fairly standard.

The interpretation of Theorem 2 is that the constant $C_{\omega,k}$ is determined when n, p, k, Ω, and ω are fixed; one is then allowed to vary h, C_Θ, and K, and the estimate holds with the same constant $C_{\omega,k}$. Hence we can consider a sequence K^i of meshes in Ω and the convergence of the corresponding approximations when $i \to \infty$; note that K^{i+1} need not be a refinement of K^i. If C_Θ stays unaltered when $i \to \infty$, Theorem 2 immediately implies kth order convergence, but if the cells flatten limitlessly ($C_\Theta \to 0$), the order of convergence may begin to deteriorate. Theorem 2 provides a worst-case bound for this deterioration. The bound is based on Proposition 1, which limits how values of p-forms can enlarge through pullback. If $p = n$, the bound is not strict; in this case one may replace C_Θ^p in Theorem 2 with C_Θ. (If $\phi : \sigma \to \tau$ is an affine bijection between simplices or cubes, the pullback of an n-form ω obeys the rule $|\phi^*\omega(x)| \cdot |\sigma| = |\omega(\phi(x))| \cdot |\tau|$, which can be used directly in the proof to avoid any recourse to Proposition 1.) We conclude this chapter with an example illustrating that shape regularity is not a necessary condition for convergence.

Example 1. Let $\Omega = [0,1] \times [0,1]$. For integers $l, m > 1$, we define a sequence of meshes such that K^i is obtained by dividing Ω into $l^i \times m^i$ boxes and each of these boxes into two triangles. To show the idea, the meshes K^0, K^1, and K^2 for parameters $l = 3$ and $m = 2$ are displayed in Figure 5. In general, the mesh K^i consists of right triangles with legs of length l^{-i} and m^{-i}. What can be said about convergence if (a) $l = 3$ and $m = 2$, or (b) $l = 29$ and $m = 3$?

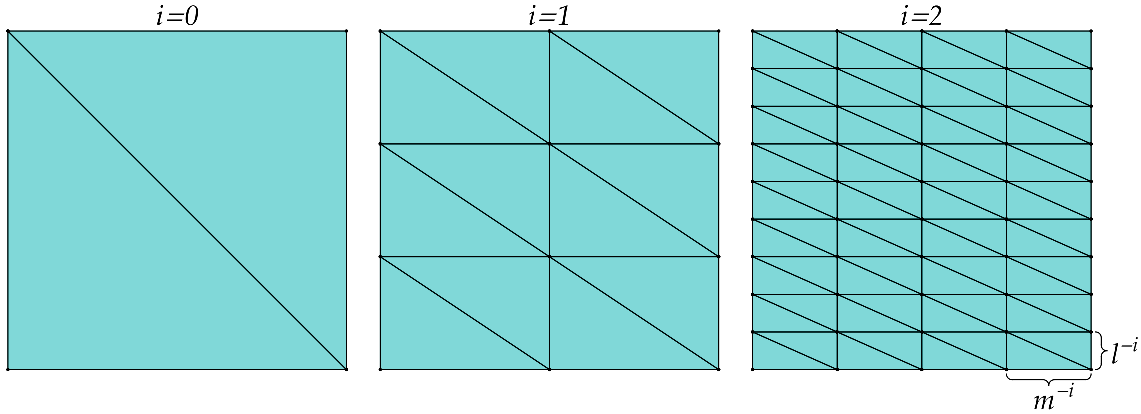

FIGURE 5 The first three meshes of the sequence K^i for parameters $l = 3$ and $m = 2$. The triangles flatten without limit when $i \to \infty$.

We work out the general case. Convergence is clear if $l = m$ or $p = 0$, so let us that assume $l > m$ and $p = 1$. (The case $p = 2$ concerns n-forms and is treated similarly.) All triangles of K^i have the same diameter h_i and fullness Θ_i:

$$h_i = \sqrt{l^{-2i} + m^{-2i}} = \sqrt{l^{2i} + m^{2i}}/(lm)^i, \quad \Theta_i = \frac{1}{2}\frac{l^{-i}m^{-i}}{h_i^2} = \frac{1}{2}\frac{(lm)^i}{l^{2i} + m^{2i}}.$$

Let us denote $B_i = h_i^k/\Theta_i^p$. We obtain the following limits:

$$\frac{h_i}{h_{i+1}} = \frac{\sqrt{l^{2i} + m^{2i}}}{(lm)^i} \cdot \frac{(lm)^{i+1}}{\sqrt{l^{2(i+1)} + m^{2(i+1)}}} = lm \cdot \sqrt{\frac{l^{2i}/l^{2(i+1)} + m^{2i}/l^{2(i+1)}}{1 + m^{2(i+1)}/l^{2(i+1)}}}$$

$$\to lm \cdot \sqrt{\frac{l^{-2} + 0}{1 + 0}} = m \text{ when } i \to \infty,$$

$$\frac{\Theta_{i+1}}{\Theta_i} = \frac{(lm)^{i+1}}{l^{2(i+1)} + m^{2(i+1)}} \cdot \frac{l^{2i} + m^{2i}}{(lm)^i} = lm \cdot \frac{l^{2i}/l^{2(i+1)} + m^{2i}/l^{2(i+1)}}{1 + m^{2(i+1)}/l^{2(i+1)}}$$

$$\to lm \cdot \frac{l^{-2} + 0}{1 + 0} = \frac{m}{l} \text{ when } i \to \infty,$$

$$\frac{B_i}{B_{i+1}} = \left(\frac{h_i}{h_{i+1}}\right)^k \cdot \left(\frac{\Theta_{i+1}}{\Theta_i}\right)^p \to m^k \cdot \left(\frac{m}{l}\right)^p = m^{k+p}/l^p \text{ when } i \to \infty.$$

Hence the bounds $C_{\omega,k}B_i$ given by Theorem 2 tend to zero as $i \to \infty$ if and only if $m^{k+p}/l^p > 1$, which amounts to $k > p(\log(l) - \log(m))/\log(m)$. Convergence is hence obtained with (a) $k \geq 1$ if $l = 3$ and $m = 2$, or (b) $k \geq 3$ if $l = 29$ and $m = 3$.

5 HIGHER ORDER DISCRETE HODGE OPERATORS

The interpolation framework presented in the previous chapter provides a natural way to define discrete Hodge operators of higher order on simplicial and cubical meshes. If one recalls from Subsection 2.2.2 interpolating approaches to the construction of the discrete Hodge operator, the following definition does not come as a surprise.

Definition 7 (Higher order discrete Hodge operators)**.** The discrete Hodge operator of order k is defined by

$$* : C_p^*(K_k) \to C^{n-p}(\tilde{K}_k), \quad * = \tilde{\mathcal{C}}_k \star \mathfrak{I},$$

where $\tilde{\mathcal{C}}_k$ denotes the de Rham map of $\tilde{K}_k$.

Definition 7 depends on the choices of $\mathfrak{I}$ and $\tilde{K}_k$, but regardless of the choices (16) implies

$$* \, \mathcal{C}_k \omega = \tilde{\mathcal{C}}_k \star \omega \quad \text{for all } \omega \in I^p(K),$$

which can be seen as a rationale for the definition. In this sense, the discrete Hodge operator of Definition 7 is exact for elements of $W_k^p(K)$ or $Q_k^p(K)$ and hence "a discrete Hodge operator of order k".

If K is simplicial and $k = 1$, the discrete Hodge operator of Definition 7 reduces to the one given in [128] using lowest order Whitney forms. Otherwise we obtain new discrete Hodge operators. We remark that in general the matrix of $*$ need not be symmetric or even invertible: when $\mathfrak{I}$ is not injective, neither is $*$, and this is the case with Whitney forms when $k > 1$, $p > 0$ and $n > 1$. The matrix is sparse to the following extent: for $\sigma_j \in S^p(K_k)$ and $\tilde{\sigma}_i \in S^{n-p}(\tilde{K}_k)$, the corresponding element $*_{ij}$ can be nonzero only if σ_j is a small cell of some cell that intersects $\tilde{\sigma}_i$.

The properties of the discrete Hodge operators of higher order are discussed in more detail in Section 4 of Article PIV. In the following we briefly state the main results; for proofs, see Article PIV. Henceforth, let us assume that K is simplicial or cubical and $*$ is defined according to Definition 7.

Theorem 3. *Let ω be a smooth p-form in Ω. There exists a constant $C_{\omega,k}$ such that*

$$\frac{|(*\,\mathcal{C}_k\omega - \tilde{\mathcal{C}}_k \star \omega)(\tilde{\sigma})|}{|\tilde{\sigma}|} \leq \frac{C_{\omega,k}}{C_\Theta^p} h^k \quad \text{for all dual } (n-p)\text{-cells } \tilde{\sigma} \in S^{n-p}(\tilde{K}_k)$$

whenever $h > 0$, $C_\Theta > 0$, and all cells σ in K satisfy $\operatorname{diam}(\sigma) \leq h$ *and* $\Theta(\sigma) \geq C_\Theta$.

Theorem 4. *Suppose $p < n$ and let ω be a smooth p-form in Ω. There exists a constant $C_{\omega,k}$ such that*

$$\frac{|(\mathrm{d}^t * \mathrm{d}\, \mathcal{C}_k\omega - \tilde{\mathcal{C}}_k\, \mathrm{d} \star \mathrm{d}\, \omega)(\tilde{\sigma}) + \int_{\partial\tilde{\sigma}\cap\partial\Omega} \star\, \mathrm{d}\, \omega|}{|\partial\tilde{\sigma}|} \leq \frac{C_{\omega,k}}{C_\Theta^{p+1}} h^k \quad \text{for all } \tilde{\sigma} \in S^{n-p}(\tilde{K}_k)$$

whenever $h > 0$, $C_\Theta > 0$, and all cells σ in K satisfy $\operatorname{diam}(\sigma) \leq h$ *and* $\Theta(\sigma) \geq C_\Theta$.

Theorem 3 has a clear interpretation: it gives a bound for the consistency error of $*$. Theorem 4 is more involved. First, note that we have included the term $\int_{\partial\tilde{\sigma}\cap\partial\Omega} \star\, \mathrm{d}\, \omega$ on the left-hand side. This can be omitted if $\tilde{\sigma}$ does not intersect $\partial\Omega$ but is otherwise required because all faces of $\tilde{\sigma}$ are not in $\tilde{K}_k$. (In DEC-based schemes, this extra term corresponds to a boundary condition; we return to this later.) Note also that the divisor on the left-hand side is $|\partial\tilde{\sigma}|$ instead of $|\tilde{\sigma}|$. Unfortunately, this means that the order of consistency (in the present sense) that is attained with the operator $\mathrm{d}^t * \mathrm{d}$ is typically one lower than that of $*$. To deduce this from Theorem 4, we assume $|\partial\tilde{\sigma}| \leq C_1 |\tilde{\sigma}| \operatorname{diam}(\tilde{\sigma})^{-1}$ for some constant C_1. If also $h \leq C_2 \operatorname{diam}(\tilde{\sigma})$, one obtains a bound of the form

$$\frac{|(\mathrm{d}^t * \mathrm{d}\, \mathcal{C}_k\omega - \tilde{\mathcal{C}}_k\, \mathrm{d} \star \mathrm{d}\, \omega)(\tilde{\sigma}) + \int_{\partial\tilde{\sigma}\cap\partial\Omega} \star\, \mathrm{d}\, \omega|}{|\tilde{\sigma}|} \leq \frac{C}{C_\Theta^{p+1}} h^{k-1}, \tag{20}$$

which is valid if the constants C_1 and C_2 can be chosen independently of K and $\tilde{\sigma}$. In other words, the bound (20) requires some conditions from the primal–dual mesh pair. We will hereafter assume that these conditions are fulfilled, excluding sequences of meshes whose cells flatten limitlessly (like the K^i in Example 1).

Remark 7 (On implementation). When the higher order interpolation framework has been implemented systematically, also discrete Hodge operators of arbitrary order can be acquired with the same code. For each small cell $v \in S_k^p(\sigma)$ in each $\sigma \in S^n(K)$, we integrate the Hodge star of the interpolant of the basis cochain $v \in C_p^*(K_k)$ over the dual $(n-p)$ cells that are in σ. The matrix of $*$ is assembled from these integrals. Although the integrals are no longer affine-invariant quantities, simplifications are possible in special cases. For example, if the Hodge star is taken with respect to the Euclidean metric, the integrals are rotationally and translationally invariant; in this case it suffices to compute them only once for cells that have the same shape. Integration can be performed numerically by dividing the dual cells into simplices and using known quadrature rules of appropriate order (see e.g. [75]).

Remark 8 (On the literature). Prior to this work, few authors have considered higher order discrete Hodge operators. The material matrices of [124], derived using local polynomial approximations, can be interpreted as discrete Hodge operators, but this formulation is limited to Cartesian grids. Chilton and Lee [44] define higher order Hodge matrices using the Lobatto cell based on Gauss–Lobatto integration points. However, these are not compatible with DEC: the authors do not introduce any dual mesh at all. In [51] second and fourth order discrete Hodge operators are obtained using overlapping grids; also these operators are of a different kind because there is no primal or dual mesh but several collocated meshes can be used simultaneously. Alotto and Freschi [4] use Kameari's elements [84] to define a second order discrete Hodge operator for 1-cochains, which fits into the framework of DEC. Unfortunately, its performance is worse than expected, and the improvements provided in [5] are no longer compatible with DEC. Finally, we mention the work [119]; there discrete Hodge operators are discussed in the context of spectral methods.

6 APPLICATION TO POISSON'S AND THE WAVE EQUATION

We have now constructed the tools required for higher order approximations in DEC, but it remains to show that these tools are actually applicable and lead to higher order methods. In this chapter we demonstrate their application to second order boundary value problems, summarising the results of Article PIV. For simplicity, we will mainly focus on Poisson's equation (representing elliptic, time-independent problems) and the wave equation (representing hyperbolic, time-dependent problems), but let us first review the unifying approach of Article PIV that covers different elliptic and hyperbolic problems with different choices of Riemannian and Lorentzian metrics.

Consider elliptic and hyperbolic partial differential equations, expressed in divergence form (see [63]) as follows:

$$\begin{aligned}
&\text{elliptic:} && \sum_{i=1}^{n}\sum_{j=1}^{n} \frac{\partial}{\partial x_i}\left(a_{ij}(x)\frac{\partial}{\partial x_j}u(x)\right) = f(x),\\
&\text{hyperbolic:} && \sum_{i=1}^{n-1}\sum_{j=1}^{n-1} \frac{\partial}{\partial x_i}\left(a_{ij}(x,t)\frac{\partial}{\partial x_j}u(x,t)\right) - \frac{\partial^2}{\partial t^2}u(x,t) = f(x,t),
\end{aligned}$$

where u is the unknown function and f is a given source term. Remarkably, any equation of this kind can be written simply as $\mathrm{d}\star\mathrm{d}\,u = f$ when the Hodge star is taken with respect to a suitable metric and the source term f is interpreted as an n-form. Defining the Hodge star using Riemannian metrics leads to elliptic problems, and hyperbolic equations result from Lorentzian metrics when the last coordinate x_n is identified as the time coordinate t. We illustrate this with the following example; for more details, see Article PIV.

Example 2. Let u be a smooth 0-form in n dimensions. Then $\mathrm{d}\,u$ is given by

$$\mathrm{d}\,u(x) = \sum_{i=1}^{n} \frac{\partial u}{\partial x_i}(x)\,\mathrm{d}\,x_i.$$

Suppose first that the Hodge star is defined using the Euclidean metric (i.e. the metric tensor satisfies $g_x(\mathrm{d}\, x_i, \mathrm{d}\, x_j) = \delta_{ij}$ at all $x \in \Omega$). Then

$$\star \mathrm{d}\, x_i = (-1)^{i-1} \mathrm{d}\, x_1 \wedge \ldots \wedge \widehat{\mathrm{d}\, x_i} \wedge \ldots \mathrm{d}\, x_n \quad \text{for all } i = 1, \ldots, n$$

and

$$\begin{aligned} \mathrm{d} \star \mathrm{d}\, u(x) &= \mathrm{d} \left(\sum_{i=1}^{n} (-1)^{i-1} \frac{\partial u}{\partial x_i}(x)\, \mathrm{d}\, x_1 \wedge \ldots \wedge \widehat{\mathrm{d}\, x_i} \wedge \ldots \mathrm{d}\, x_n \right) \\ &= \sum_{i=1}^{n} \frac{\partial^2 u}{\partial x_i^2}(x)\, \mathrm{d}\, x_1 \wedge \ldots \wedge \mathrm{d}\, x_n. \end{aligned}$$

Hence $\mathrm{d} \star \mathrm{d}\, u = 0$ amounts to Laplace's equation.

Suppose then that the Hodge star is taken with respect to the Minkowski metric. (This means that $g_x(\mathrm{d}\, x_i, \mathrm{d}\, x_j) = \delta_{ij}$ with the exception $g_x(\mathrm{d}\, t, \mathrm{d}\, t) = -1$.) Then

$$\begin{aligned} &\star \mathrm{d}\, x_i = (-1)^{i-1} \mathrm{d}\, x_1 \wedge \ldots \wedge \widehat{\mathrm{d}\, x_i} \wedge \ldots \mathrm{d}\, x_{n-1} \wedge \mathrm{d}\, t \quad \text{for all } i = 1, \ldots, n-1, \\ &\star \mathrm{d}\, t = (-1)^n \mathrm{d}\, x_1 \wedge \ldots \wedge \mathrm{d}\, x_{n-1}, \end{aligned}$$

and

$$\mathrm{d} \star \mathrm{d}\, u(x) = \mathrm{d} \left(\sum_{i=1}^{n-1} (-1)^{i-1} \frac{\partial u}{\partial x_i}(x)\, \mathrm{d}\, x_1 \wedge \ldots \wedge \widehat{\mathrm{d}\, x_i} \wedge \ldots \wedge \mathrm{d}\, x_{n-1} \wedge \mathrm{d}\, t + \right.$$
$$\left. (-1)^n \frac{\partial u}{\partial t}(x)\, \mathrm{d}\, x_1 \wedge \ldots \wedge \mathrm{d}\, x_{n-1} \right) = \left(\sum_{i=1}^{n-1} \frac{\partial^2 u}{\partial x_i^2}(x) - \frac{\partial^2 u}{\partial t^2}(x) \right) \mathrm{d}\, x_1 \wedge \ldots \wedge \mathrm{d}\, x_{n-1} \wedge \mathrm{d}\, t.$$

We see that now the operator $\mathrm{d} \star \mathrm{d}$ yields the wave equation.

Henceforth we can justifiably consider the equation $\mathrm{d} \star \mathrm{d}\, u = f$, where u is a 0-form and f is an n-form. Its discretisation based on discrete exterior calculus reads $\mathrm{d}^t * \mathrm{d}\, X = \tilde{\mathcal{C}}_k f$, where the primal 0-cochain X is an approximation of u. In other words, we attach unknowns to primal nodes and obtain one equation for each dual n-cell. For simplicity, let us assume that either the Euclidean metric or the Minkowski metric defines the Hodge star, which means that we are dealing with Poisson's or the wave equation. Of course, the discrete Hodge operator $* = \tilde{\mathcal{C}}_k \star \mathfrak{I}$ is defined accordingly.

Although the approach is unified, it is apparent that the resulting schemes cannot be identical for static and time-dependent problems. First of all, the equation $\mathrm{d} \star \mathrm{d}\, u = f$ is accompanied with boundary conditions which determine a unique solution. In the time-dependent case this includes initial conditions. Let us denote $\Omega_t = \{(x_1, \ldots, x_n) \in \Omega \mid x_n = t\}$, assuming $t \in [0, T]$. Appropriate boundary conditions can be written

$$\text{elliptic: } \begin{array}{l} u = g_D \text{ on } \partial_D \Omega, \\ \star \mathrm{d}\, u = g_N \text{ on } \partial_N \Omega, \end{array} \qquad \text{hyperbolic: } \begin{array}{l} u = g_D \text{ on } \partial_D \Omega \cup \Omega_0, \\ \star \mathrm{d}\, u = g_N \text{ on } \partial_N \Omega \cup \Omega_0, \end{array}$$

where $\partial_D\Omega$ and $\partial_N\Omega$ denote parts of the boundary where Dirichlet and Neumann boundary conditions are imposed. (In the hyperbolic case these comprise the spatial boundary $\cup_{t\in[0,T]}\partial\Omega_t$.) Note that g_D is a 0-form and g_N is an $(n-1)$-form.

These boundary conditions are incorporated in the discretisation by rewriting the equations that correspond to dual cells of boundary nodes. The nodes on which the solution is given directly by g_D are considered inactive; we denote this subset of $S^0(K_k)$ by B. All other nodes are considered active. In the elliptic case active dual cells are exactly the dual cells of active nodes. In the hyperbolic case the same holds apart from the following exceptions: $\tilde{\sigma}$ is active also if $\sigma \in \Omega_0 \setminus \partial\Omega_0$ but inactive if $\sigma \in \Omega_T \setminus \partial\Omega_T$. We denote by A_1 the set of interior dual n-cells (i.e. those not intersecting $\partial\Omega$) and by A_2 all other active dual n-cells. The discrete problem is to find $X \in C_0^*(K_k)$ such that

$$\begin{aligned}
&\mathrm{d}^t * \mathrm{d}\, X(\tilde{\sigma}) = \tilde{\mathcal{C}}_k f(\tilde{\sigma}) \text{ for all } \tilde{\sigma} \in A_1,\\
&\mathrm{d}^t * \mathrm{d}\, X(\tilde{\sigma}) = \tilde{\mathcal{C}}_k f(\tilde{\sigma}) - \int_{\partial\tilde{\sigma}\cap\partial\Omega} g_N \text{ for all } \tilde{\sigma} \in A_2,\\
&X(\sigma) = g_D(\sigma) \text{ for all } \sigma \in B.
\end{aligned} \tag{21}$$

Above we assume that the mesh pair is created such that $\partial\tilde{\sigma} \cap \partial\Omega \subset \partial_N\Omega$ if $\sigma \in A_2$ so that $\int_{\partial\tilde{\sigma}\cap\partial\Omega} g_N$ is defined. In the hyperbolic case we require also that the sets $\Omega_0 \setminus \partial\Omega_0$ and $\Omega_T \setminus \partial\Omega_T$ contain the same number of mesh nodes. This guarantees that (21) yields an equal number of equations and variables.

Besides the differences in the sets of active cells, static and time-dependent problems differ in the structure of the linear system (21). The wave equation conforms to a finite propagation speed [63], and the solution at a time t_1 is unaffected by the values of the source term at a future time $t_2 > t_1$. As a consequence, the system (21) admits a time stepping strategy that can be used to solve the values of X in chronological order. In the following we briefly explain the idea; for more details, see Article PIV.

Suppose that the mesh K (in spacetime) is structural (i.e. obtained by repeating some structure) in the time direction. Figure 6 provides an example: we can identify one time step that has been repeated three times to obtain the whole mesh. Conceptually, we can use the initial condition to solve the values of X in the first time step and then use known values to determine an initial condition for the next time step. This procedure can be repeated step by step; we can continue as long as desired by expanding the mesh forward in time.

Each time step can be regarded as a function that takes the values of the initial and boundary conditions and the source term as input and gives the values of X as output. The initial condition for the next time step is determined by values that have been solved on the two latest time steps. Since the mesh is obtained by repeating the same structure, each time step is identical. Hence the resulting scheme for the wave equation becomes much more efficient than the one for Poisson's equation. We emphasise that the time stepping strategy is not a separate scheme but merely a way to solve (21). It can also be described in terms of linear algebra by identifying certain blocks in the system matrix of (21) (see Article PIV).

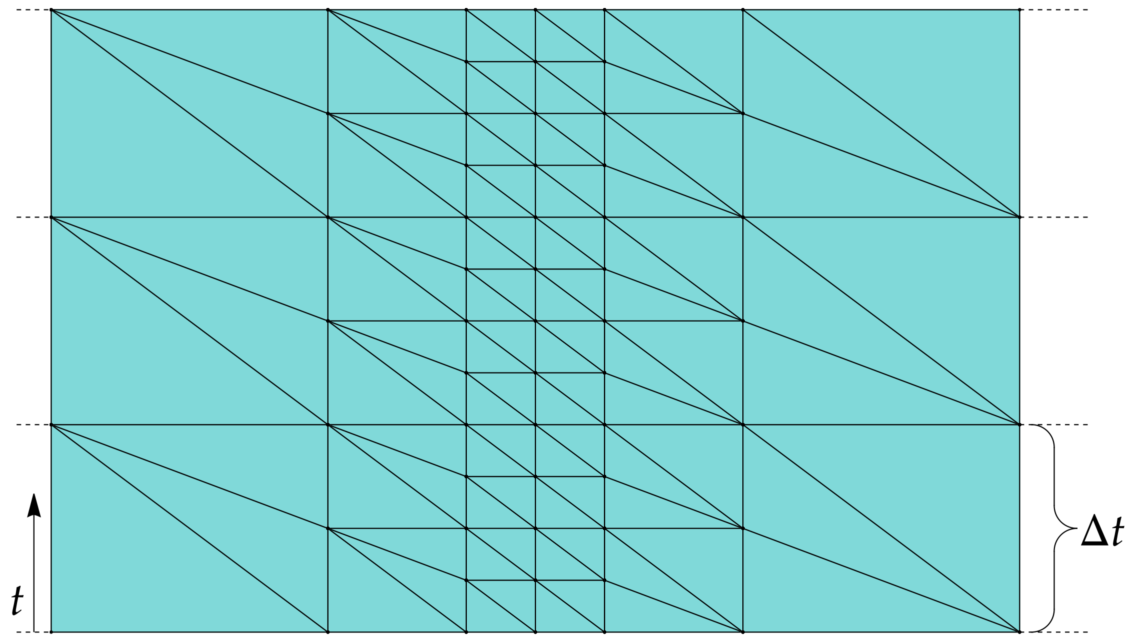

FIGURE 6 An example of a structural mesh that is obtained by repeating one time step (of length Δt) three times.

If the actual solution u is in the space $I^0(K)$, the solution of the discrete problem (21) is exact (in the sense that $X = \mathcal{C}_k u$). Otherwise it is an approximation, whose consistency follows from (20). Indeed, if we define a norm $\|\cdot\|_{\underline{\infty}}$ for dual n-cochains by

$$\|\sum_{\tilde{\sigma}_i \in S^n(\tilde{K}_k)} a_i \tilde{\sigma}_i\|_{\underline{\infty}} = \max_{\tilde{\sigma}_i \in S^n(\tilde{K}_k)} \frac{|a_i|}{|\tilde{\sigma}_i|},$$

the bound (20) implies consistency of order $k-1$. For convergence, also stability has to be ensured in a suitable norm. Let L denote the system matrix of (21) restricted to active cells. Stability is attained if the norm of L^{-1} remains bounded when the mesh is suitably refined. To bound the error in the maximum norm $\|X - \mathcal{C}_k u\|_\infty = \max_{\sigma \in S^0(K_k)} |X(\sigma) - u(\sigma)|$, an appropriate matrix norm to consider is the one induced by the norms $\|\cdot\|_{\underline{\infty}}$ and $\|\cdot\|_\infty$.

Unfortunately, a rigorous stability proof turns out to be elusive. We do not have explicit expressions for the elements of L, which rules out standard analysis based on eigenvalues or Fourier series (see e.g. [81, 8]). For this reason we have studied stability numerically by computing the norm of L^{-1}. In the following we provide two test examples that include this kind of stability analysis. Both examples illustrate the discrete scheme (21) in three dimensions. The first one deals with Poisson's equation using simplicial meshes, and in the second example we solve the wave equation using cubical meshes. More examples can be found in Article PIV.

Example 3. Let Ω be the octahedron with vertices $(\pm 1, -1, 0)$, $(\pm 1, 1, 0)$, and $(0, 0, \pm 1)$, $\partial_D \Omega = \partial \Omega$, and $\partial_N \Omega = \emptyset$. We choose the boundary condition and the source term for Poisson's equation such that the 0-form

$$u(x,y,z) = e^{x+z}\sin(x+y+2)\cos(yz)$$

is the exact solution. The objective is to assess the accuracy of the approximations obtained using the scheme (21) with Whitney forms on simplicial meshes. Let us call these "DEC solutions", and consider for comparison also "FEM solutions" that are obtained with the standard finite element method using the same basis functions (see Article PIV for details). Convergence is studied by measuring the H^1 norm of the error on four different meshes. For this we first interpolate the DEC solution and its coboundary. H^1 norms are computed numerically using a sufficiently fine mesh and 11th order quadrature rules for tetrahedra [83].

The first two of the four meshes are shown in Figure 7, and the relevant information regarding the meshes is given in Table 1. In this example, we consider orders $k \in \{1,2,4,8\}$ and build the initial mesh K such that the refined mesh K_k is always one of the meshes in Table 1. In other words, the meshes in Table 1 are not further divided into small simplices — they contain the small simplices already. (The only exception is that the first (coarsest) mesh does not contain 8th order small simplices, so the 8th order case is studied using meshes 2–4 only.) This enables a fair comparison in that the number of degrees of freedom is the same for all solutions on a given mesh.

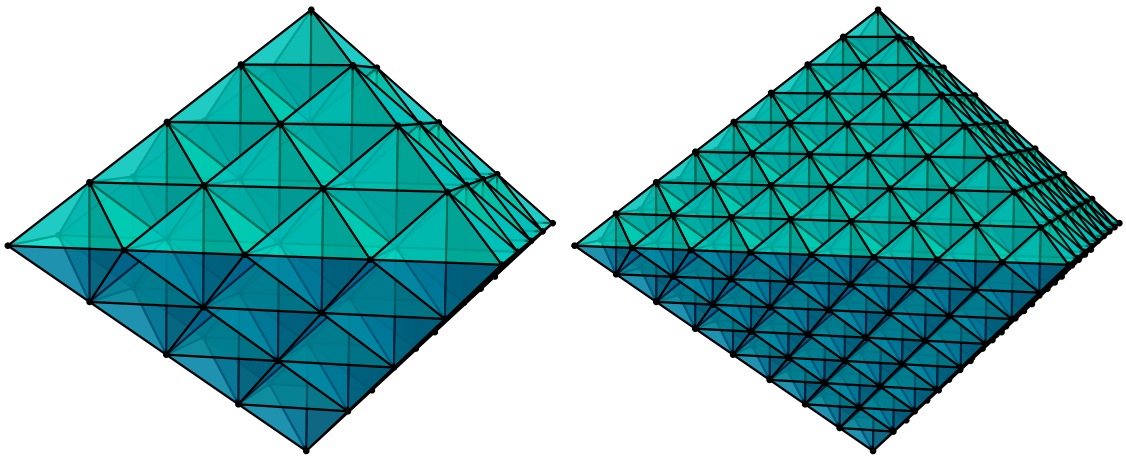

FIGURE 7 The first two of the four meshes used in Example 3.

TABLE 1 Information about the four meshes used in Example 3.

	Mesh 1	Mesh 2	Mesh 3	Mesh 4
maximum edge length	1/2	1/4	1/8	1/16
number of tetrahedra	256	2048	16384	131072
number of vertices	85	489	3281	23969

The results are displayed in Table 2 and illustrated in Figure 8. We see that higher order DEC does not outperform higher order FEM, but the results are comparable and the order of convergence seems to be the same (i.e. optimal) in H^1

norm. This is better than what was theoretically predicted. For stability analysis, we have also computed the norm of L^{-1}; the results are displayed in Table 3. Although this does not constitute a proof, it seems that $\|L^{-1}\|$ remains bounded when the mesh is suitably refined.

TABLE 2 H^1 norms of the error in Example 3.

	Mesh 1	Mesh 2	Mesh 3	Mesh 4
$k = 1$, DEC	6.73042e-01	3.38886e-01	1.69743e-01	8.49090e-02
$k = 1$, FEM	6.72936e-01	3.38870e-01	1.69741e-01	8.49087e-02
$k = 2$, DEC	2.23368e-01	5.97159e-02	1.51593e-02	3.80370e-03
$k = 2$, FEM	2.22407e-01	5.95299e-02	1.51350e-02	3.79999e-03
$k = 4$, DEC	5.02907e-02	4.63521e-03	3.15646e-04	2.01149e-05
$k = 4$, FEM	4.89353e-02	4.22144e-03	2.79932e-04	1.75908e-05
$k = 8$, DEC	-	9.60229e-05	7.77152e-07	3.70156e-09
$k = 8$, FEM	-	6.79247e-05	3.91215e-07	1.62228e-09

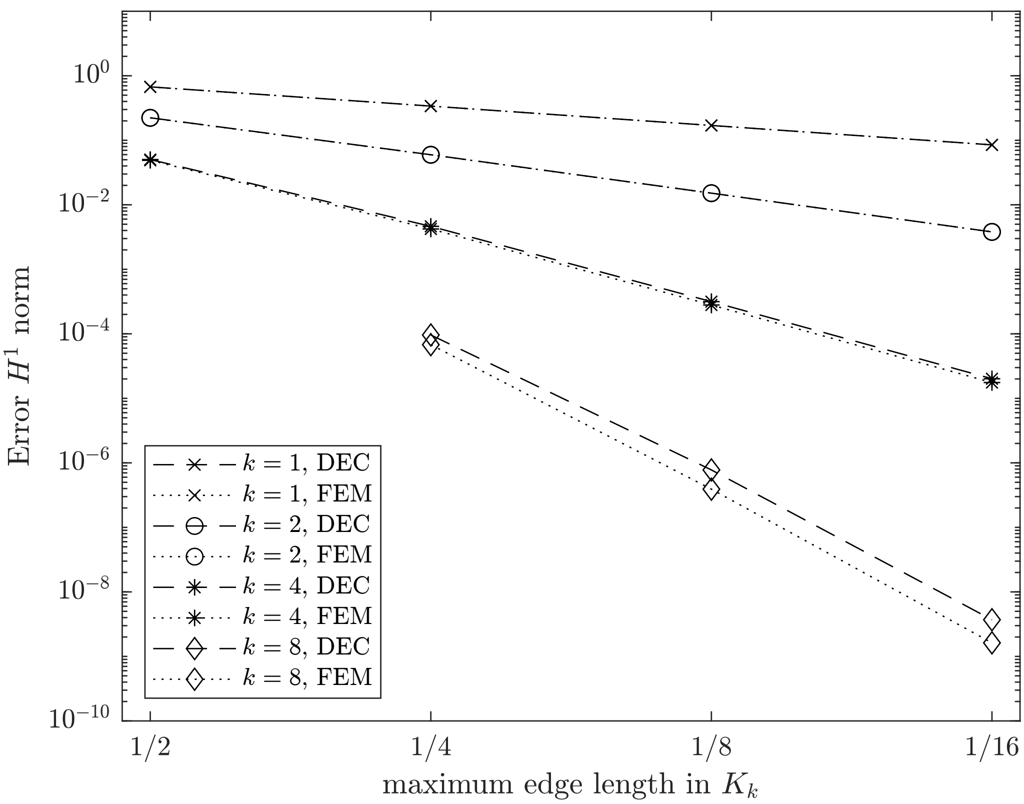

FIGURE 8 Illustration of the results displayed in Table 2.

TABLE 3 Values of $\|L^{-1}\|$ in the stability analysis of Example 3.

	Mesh 1	Mesh 2	Mesh 3	Mesh 4
$k = 1$	1.08631e-01	1.07627e-01	1.07844e-01	1.07945e-01
$k = 2$	1.06740e-01	1.08048e-01	1.08018e-01	1.07995e-01
$k = 4$	1.08094e-01	1.11758e-01	1.08055e-01	1.07993e-01
$k = 8$	-	2.63535e-01	1.70704e-01	1.22657e-01

Example 4. Let $\Omega = [0,2] \times [0,2] \times [0,T]$, $\partial_D \Omega = \cup_{t \in [0,T]} \partial \Omega_t$, and $\partial_N \Omega = \emptyset$. We choose the boundary and initial conditions and the source term for the wave equation such that the 0-form

$$u(x,y,t) = e^{x/4} \sin(x+y+t+1) \cos(y)(2 - 0.003t - 0.00002t^2)$$

is the exact solution. We use cubical meshes and forms with the scheme (21) to produce approximations for u. Convergence is studied by measuring the maximum norm of the error on different meshes. Each mesh K consists of identical cubes that are all obtained by translating the cube $[0, \Delta l] \times [0, \Delta l] \times [0, \Delta t]$. We can hence describe the meshes with the parameters Δl and Δt. In this example, we consider orders $k \in \{1,2,3,4,5\}$. For each order, the values of the parameter Δl for the meshes used are displayed in Table 4.

TABLE 4 Values of the parameter Δl for the meshes used in Example 4.

	Mesh 1	Mesh 2	Mesh 3	Mesh 4	Mesh 5
$k=1$	1/2	1/4	1/8	1/16	1/32
$k=2$	1	1/2	1/4	1/8	1/16
$k=3$	2	1	1/2	1/4	1/8
$k=4$	2	1	1/2	1/4	1/8
$k=5$	-	2	1	1/2	1/4

To ensure stability, the time step sizes Δt were selected carefully based on the following stability analysis. For each k and Δl, we computed the norm of L^{-1} for different values of Δt when the duration T is sufficiently long. This experiment suggests that the scheme (21) for the wave equation requires a typical stability criterion for the time step size Δt: it cannot be too large when compared to Δl. This is demonstrated by the values of $\|L^{-1}\|$ in Table 5. For example, in the first order case $\|L^{-1}\|$ blows up already for $T < 30$ when $\Delta t = 0.71\Delta l$, but this does not occur even after $T > 140$ when $\Delta t = 0.705\Delta l$. (The limit seems to be the usual one: $\Delta t \leq \Delta l/\sqrt{2}$.) The stability limit becomes stricter when moving to higher orders. For $k = 5$ the limit seems similar to the one for $k = 4$, but cases $k \geq 6$ are excluded because the schemes appear to be unstable regardless of Δt.

TABLE 5 Values of $\|L^{-1}\|$ in the stability analysis of Example 4.

	Mesh 1	Mesh 2	Mesh 3	Mesh 4
$k=1$, $\Delta t = 0.705\Delta l$, $T = 141$	1.44533e+02	1.95811e+02	2.28832e+02	2.47293e+02
$k=1$, $\Delta t = 0.71\Delta l$, $T = 28.4$	2.90634e+01	4.04550e+01	5.29431e+01	2.65088e+22
$k=2$, $\Delta t = 0.355\Delta l$, $T = 142$	1.35038e+02	1.66944e+02	1.86032e+02	1.99260e+02
$k=2$, $\Delta t = 0.375\Delta l$, $T = 37.5$	3.61421e+01	4.63148e+01	3.74518e+08	3.16672e+33
$k=3$, $\Delta t = 0.25\Delta l$, $T = 500$	2.33128e+02	6.36183e+02	7.11727e+02	7.66676e+02
$k=3$, $\Delta t = 0.265\Delta l$, $T = 106$	4.94310e+01	1.37435e+02	1.88688e+02	1.40144e+25
$k=4$, $\Delta t = 0.2\Delta l$, $T = 40$	2.76939e+01	6.18803e+01	6.61323e+01	7.02919e+01
$k=4$, $\Delta t = 0.21\Delta l$, $T = 42$	2.91784e+01	6.56954e+01	7.82796e+01	1.36919e+02

For convergence analysis we fix $T = 100$ and choose the time step sizes as follows: $\Delta t = \frac{50}{71}\Delta l$ for $k = 1$, $\Delta t = \frac{50}{142}\Delta l$ for $k = 2$, $\Delta t = 0.25\Delta l$ for $k = 3$, and $\Delta t = 0.2\Delta l$ for $k = 4$ and $k = 5$. The choices are below the estimated stability limits and multiply exactly to $T = 100$ after a suitable number of time steps, so we can study the error maximum norm in Ω. The results are displayed in Table 6 and illustrated in Figure 9. Note that in this example number of degrees of freedom is not exactly the same for all k. This is taken into account by considering the diameter of the cubes in the refined mesh K_k (which is $\sqrt{2(\Delta l)^2 + (\Delta t)^2/k}$) when plotting the results. The order of convergence seems to be two for $k = 1$ and $k = 2$, four for $k = 3$ and $k = 4$, and six for $k = 5$. This is again better than what was theoretically predicted.

TABLE 6 Maximum norms of the error in Example 4.

	Mesh 2	Mesh 3	Mesh 4	Mesh 5
$k = 1$	4.36612e-02	1.10626e-02	2.76855e-03	6.93555e-04
$k = 2$	2.34829e-02	6.02590e-03	1.52140e-03	3.81456e-04
$k = 3$	1.66525e-02	1.35834e-03	9.19698e-05	5.96036e-06
$k = 4$	3.46360e-03	1.93251e-04	1.12072e-05	6.83310e-07
$k = 5$	1.64667e-02	3.57679e-04	6.24342e-06	1.08734e-07

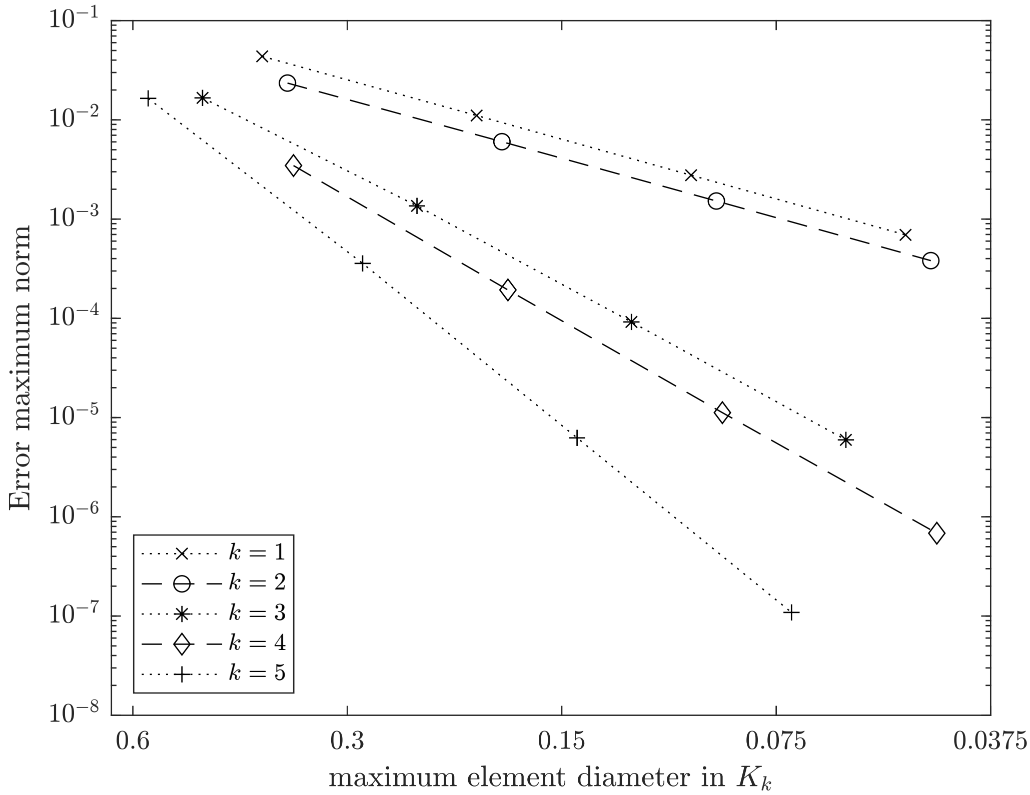

FIGURE 9 Illustration of the results displayed in Table 6.

Remark 9. We could also apply higher order Whitney forms to the wave equation by dividing each cube in Example 4 into tetrahedra. However, the resulting scheme (21) appears to be stable only in the case $k = 1$. For more information, see Example 7.10 in Article PIV.

7 CONCLUSIONS AND FUTURE WORK

We can conclude that the framework of discrete exterior calculus generalises rather naturally to higher order approximations. The role of interpolation is emphasised: the key point is to create the mesh such that cochains can be interpolated with higher order interpolants. The small cells of order k provide a systematic way of accomplishing this on simplicial and cubical meshes. Higher order interpolation reduces the interpolation error and enables one to define higher order discrete Hodge operators in a natural manner, resulting in higher order convergence. A major asset of the presented approach is that it preserves the exact nature of the discrete exterior derivative, which is fundamental to DEC. Changes are made only to the discrete Hodge operator (along with the modifications at the pre-processing and post-processing stages).

The framework enables a unified treatment of second order boundary value problems: both elliptic and hyperbolic problems are obtained from the scheme (21) with different choices of metric and active cells. Dirichlet and Neumann boundary conditions are naturally built in the scheme without producing additional error. This is a significant positive aspect in comparison with complicated special remedies (such as the introduction of ghost points) required in some other methods (see e.g. [135, 37]). From theoretical foundations, the contribution of this thesis ranges all the way to the implementation of arbitrary orders in three dimensions. We emphasise that this is quite remarkable; existing software packages that cover arbitrary orders are rather rare and typically have dozens of contributors. For example, the MFEM package [6] used to produce FEM solutions in Example 3 has about a hundred contributors.

Despite these strengths, this work has some shortcomings, and several issues are left for future research. Some assertions are based on computational evidence. We do not have a proof that the system matrix of (21) is invertible, nor a proof that (21) yields a stable scheme. Numerical experiments indicate stability in the elliptic case, but for hyperbolic problems stability seems to impose additional conditions on the spacetime mesh. The lack of proof is a serious disadvantage because the stability limit for the time step size is difficult to find numerically. If the limit is only slightly exceeded, time stepping may seem stable at first but lead to late-time instabilities. Moreover, on some occasions the resulting method seems to be unstable regardless of the time step size. Whether these stability issues can be remedied is left for future research.

Accuracy has been studied only with respect to the number of degrees of freedom. Although this kind of analysis demonstrates a great benefit from higher order methods, it does not take account of the required computation time. Low order methods could handle more degrees of freedom in a fixed amount of time, so the comparisons performed in this work do not give a complete picture of the situation. The efficiency of the approach should be studied further, preferably after the presented approach is first accompanied with a competitive implementation tailored to high performance computing.

The efficiency of the presented approach could possibly be improved also with methodological enhancements. For high orders, the cubical forms used in this work require more degrees of freedom than ideally necessary for the same order of convergence. Serendipity spaces [9, 71] require fewer degrees of freedom, but these do not seem definable using small cells. The search for new suitable interpolants, also for other cell types, is a potential source of improvements. Since the higher order framework uses a coarser mesh K and a finer mesh K_k, it is reasonable to ask whether it could be recasted as a multigrid method [134]. Although Whitney forms have been used with multigrid [77, 10], we do not know if DEC could benefit from it in some way. The form of the small cells could likely be optimised. We have only considered small cells with equal spacing, but it is known that distorting the small cells can lead to better results [39]. Also the role of the dual mesh deserves further investigation; an optimal choice is predicted to yield superconvergence [94, 95]. Our numerical examples indicate faster convergence than our theoretical estimates, but the reason for this is not fully understood yet.

Finally, we emphasise that the applicability of the tools developed in this work is not restricted to the scheme (21); they can be used whenever one applies DEC. For example, one may use the higher order discrete Hodge operators for spatial discretisation and choose some other strategy for temporal discretisation. Although Chapter 6 focused on scalar problems ($p = 0$), the tools have been developed for all p. DEC is known to befit a general class of second order boundary values problems [111], and the value of this work can be properly acknowledged only after the tools developed here have been applied with different types of problems.

YHTEENVETO (SUMMARY IN FINNISH)

Numeerisen analyysin tieteenalalle sijoittuva väitöskirja *Korkeamman asteen approksimaatiot differentiaalimuodoille* käsittelee differentiaalimuotojen approksimointia diskreettiin ulkoiseen laskentaan (engl. *discrete exterior calculus*, DEC) perustuen. Differentiaalimuotojen avulla voidaan mallintaa fysikaalisia ilmiöitä, mutta mallien ratkaiseminen eksaktisti on usein hankalaa tai mahdotonta. Numeeriset menetelmät tuottavat likimääräisiä ratkaisuja, jotka voidaan laskea tietokoneella. Mallin esittämiseksi tietokoneelle sopivassa muodossa differentiaalimuodot tulee approksimoida äärellisulotteisissa avaruuksissa. Väitöskirja tarjoaa siis työkaluja numeerisia menetelmiä varten.

Diskreetissä ulkoisessa laskennassa tarkasteltava alue jaetaan pieniin soluihin, jotka muodostavat verkon. Differentiaalimuodot approksimoidaan verkon diskreetteinä muotoina (engl. *cochain*). Väitöskirjan otsikko käsittää myös differentiaalimuotojen välisten operaattorien approksimoinnin. Kaksi tärkeintä operaattoria ovat ulkoderivaatta ja Hodge-operaattori. Ulkoderivaatan diskreetti vastine perustuu Stokesin lauseeseen eikä aiheuta lainkaan virhettä. Tämä on DEC-pohjaisten menetelmien merkittävä etu. Toinen hyvä puoli on, että metrisen tensorin vaikutus on selvästi tunnistettavissa ja rajoittuu Hodge-operaattoriin ja sen diskreettiin vastineeseen. Kuten muissakin numeerisissa menetelmissä, ideana on että likimääräinen ratkaisu lähestyy tarkkaa ratkaisua eli suppenee, kun käytettävien solujen kokoa pienennetään ja määrää kasvatetaan, mikä puolestaan vaatii enemmän laskentakapasiteettia tietokoneelta.

DEC-pohjaiset menetelmät on aiemmin mielletty alimman asteen menetelmiksi; niiden tuottamat ratkaisut suppenevat hitaammin kuin korkeamman asteen menetelmissä. Väitöskirjan pääkontribuutiona on korkeamman asteen approksimaatioiden sovittaminen teoriaan. Diskreettien muotojen interpoloinnilla on keskeinen rooli: ideana on muodostaa verkko siten, että interpolointi onnistuu korkeamman asteen funktioilla. Tätä varten kehitetään systemaattinen strategia verkoille, joiden solut ovat simpleksejä tai hyperkuutioita. Ensin valitaan haluttu aste ja jaetaan solut pienempiin soluihin, joita käytetään interpolointiin soveltuvien kyseisen asteen funktioiden määrittelemiseen. Diskreettiin ulkoiseen laskentaan käytettävä verkko muodostetaan siten, että se sisältää halutun asteiset pienemmät solut. Näin korkeamman asteen interpoloinnista tulee mahdollista.

Hodge-operaattorin diskreettiä vastinetta varten tarvitaan toinenkin verkko, jota kutsutaan duaaliverkoksi. Korkeamman asteen interpolointistrategia tarjoaa luonnollisen tavan määritellä korkeamman asteen diskreettejä Hodge-operaattoreja, joilla on ratkaiseva rooli DEC-pohjaisten menetelmien suppenemisnopeudessa. Diskreeteille Hodge-operaattoreille saadaan johdettua virhe-estimaatteja, joiden perusteella menetelmien suppeneminen on stabiilisuudesta kiinni. Hodge-operaattorin määrittävää metristä tensoria muuntelemalla saadaan katettua useita tehtäviä samalla menetelmällä. Tätä havainnollistaa toisen kertaluvun reuna-arvotehtäville esitetty DEC-pohjainen diskreetti malli, joka toimii esimerkkinä väitöskirjassa kehitettyjen työkalujen soveltamisesta.

Väitöskirja ei rajoitu pelkästään teoreettisiin tuloksiin, vaan kehitetyt työkalut on myös toteutettu tietokoneella ja testattu esimerkkitehtävien avulla. Korkeamman asteen approksimaatioille esitetään systemaattinen toteutustapa, jolla kaikenasteiset approksimaatiot saadaan samalla koodilla; haluttu aste voidaan siis antaa ohjelmalle parametrina. Testiesimerkit havainnollistavat, että menetelmät ovat toteutettavissa. Lisäksi niiden avulla tarkastellaan menetelmien stabiilisuutta ja todennetaan suppenemisnopeudessa saavutettu hyöty. Väitöskirjan teoreettinen kontribuutio ja kehitettyjen työkalujen tietokonetoteutus osoittavat, että DEC-pohjaiset menetelmät yleistyvät korkeamman asteen menetelmiksi.

REFERENCES

[1] Ralph Abraham, Jerrold E. Marsden, and Tudor Ratiu. *Manifolds, Tensor Analysis, and Applications*, volume 75 of *Applied Mathematical Sciences*. Springer, 2. edition, 1988. doi:10.1007/978-1-4612-1029-0.

[2] David H. Adams. R-torsion and linking numbers from simplicial abelian gauge theories. *arXiv preprint hep-th/9612009*, 1996. doi:10.48550/ARXIV.HEP-TH/9612009.

[3] Pierre Alliez, David Cohen-Steiner, Mariette Yvinec, and Mathieu Desbrun. Variational tetrahedral meshing. In *ACM SIGGRAPH 2005 Papers*, pages 617–625, 2005. doi:10.1145/1186822.1073238.

[4] Piergiorgio Alotto and Fabio Freschi. A second-order cell method for Poisson's equation. *IEEE Transactions on Magnetics*, 47(5):1430–1433, 2011. doi:10.1109/TMAG.2010.2092419.

[5] Piergiorgio Alotto, Fabio Freschi, and Maurizio Repetto. Algebraic second order Hodge operator for Poisson's equation. *IEEE Transactions on Magnetics*, 49(5):1761–1764, 2013. doi:10.1109/TMAG.2013.2241406.

[6] Robert Anderson, Julian Andrej, Andrew Barker, Jamie Bramwell, Jean-Sylvain Camier, Jakub Cerveny, Veselin Dobrev, Yohann Dudouit, Aaron Fisher, Tzanio Kolev, Will Pazner, Mark Stowell, Vladimir Tomov, Ido Akkerman, Johann Dahm, David Medina, and Stefano Zampini. MFEM: A modular finite element methods library. *Computers and Mathematics with Applications*, 81:42–74, 2021. doi:10.1016/j.camwa.2020.06.009.

[7] Douglas Arnold and Anders Logg. Periodic table of the finite elements. *SIAM News*, 47(9), 2014.

[8] Douglas N. Arnold. Stability, consistency, and convergence of numerical discretizations. In *Encyclopedia of Applied and Computational Mathematics*, pages 1358–1364. Springer, 2015. doi:10.1007/978-3-540-70529-1_407.

[9] Douglas N. Arnold and Gerard Awanou. Finite element differential forms on cubical meshes. *Mathematics of Computation*, 83(288):1551–1570, 2014. doi:10.1090/S0025-5718-2013-02783-4.

[10] Douglas N. Arnold, Richard S. Falk, and Ragnar Winther. Multigrid in $H(\mathrm{div})$ and $H(\mathrm{curl})$. *Numerische Mathematik*, 85(2):197–217, 2000. doi:10.1007/PL00005386.

[11] Douglas N. Arnold, Richard S. Falk, and Ragnar Winther. Finite element exterior calculus, homological techniques, and applications. *Acta Numerica*, 15:1–155, 2006. doi:10.1017/S0962492906210018.

[12] Douglas N. Arnold, Richard S. Falk, and Ragnar Winther. Geometric decompositions and local bases for spaces of finite element differential forms. *Computer Methods in Applied Mechanics and Engineering*, 198(21-26):1660–1672, 2009. doi:10.1016/j.cma.2008.12.017.

[13] Douglas N. Arnold, Richard S. Falk, and Ragnar Winther. Finite element exterior calculus: From Hodge theory to numerical stability. *Bulletin of the American Mathematical Society*, 47(2):281–354, 2010. doi:10.1090/S0273-0979-10-01278-4.

[14] Rachel F. Arnold. *The Discrete Hodge Star Operator and Poincaré Duality*. PhD thesis, Virginia Tech, 2012.

[15] Bernhard Auchmann and Stefan Kurz. A geometrically defined discrete Hodge operator on simplicial cells. *IEEE Transactions on Magnetics*, 42(4):643–646, 2006. doi:10.1109/TMAG.2006.870932.

[16] Franz Aurenhammer, Rolf Klein, and Der-Tsai Lee. *Voronoi Diagrams and Delaunay Triangulations*. World Scientific, 2013. doi:10.1142/8685.

[17] John Baez and Javier P. Muniain. *Gauge Fields, Knots and Gravity*, volume 4 of *Series on Knots and Everything*. World Scientific, 1994. doi:10.1142/2324.

[18] Nathan Bell and Anil N. Hirani. PyDEC: Software and algorithms for discretization of exterior calculus. *ACM Transactions on Mathematical Software*, 39(1):3, 2012. doi:10.1145/2382585.2382588.

[19] R. Beltman, M. J. H. Anthonissen, and B. Koren. Conservative polytopal mimetic discretization of the incompressible Navier–Stokes equations. *Journal of Computational and Applied Mathematics*, 340:443–473, 2018. doi:10.1016/j.cam.2018.02.007.

[20] Pavel B. Bochev and James M. Hyman. Principles of mimetic discretizations of differential operators. In *Compatible Spatial Discretizations*, volume 142 of *The IMA Volumes in Mathematics and its Applications*, pages 89–119. Springer, 2006. doi:10.1007/0-387-38034-5_5.

[21] Marcella Bonazzoli, Victorita Dolean, Frédéric Hecht, and Francesca Rapetti. An example of explicit implementation strategy and preconditioning for the high order edge finite elements applied to the time-harmonic Maxwell's equations. *Computers and Mathematics with Applications*, 75(5):1498–1514, 2018. doi:10.1016/j.camwa.2017.11.013.

[22] Pieter D. Boom, Odysseas Kosmas, Lee Margetts, and Andrey P. Jivkov. A geometric formulation of linear elasticity based on discrete exterior calculus. *International Journal of Solids and Structures*, 236:111345, 2022. doi:10.1016/j.ijsolstr.2021.111345.

[23] Pieter D. Boom, Ashley Seepujak, Odysseas Kosmas, Lee Margetts, and Andrey Jivkov. Parallelized discrete exterior calculus for three-dimensional elliptic problems. *Computer Physics Communications*, 279:108456, 2022. doi:10.1016/j.cpc.2022.108456.

[24] Alain Bossavit. Whitney forms: A class of finite elements for three-dimensional computations in electromagnetism. *IEE Proceedings A (Physical Science, Measurement and Instrumentation, Management and Education, Reviews)*, 135(8):493–500, 1988. doi:10.1049/ip-a-1.1988.0077.

[25] Alain Bossavit. On the geometry of electromagnetism. (1): Affine space. *Journal of the Japan Society of Applied Electromagnetics and Mechanics*, 6(1):17–28, 1998.

[26] Alain Bossavit. On the geometry of electromagnetism. (4): "Maxwell's house". *Journal of the Japan Society of Applied Electromagnetics and Mechanics*, 6(1):17–28, 1998.

[27] Alain Bossavit. Computational electromagnetism and geometry. (1): Network equations. *Journal of the Japan Society of Applied Electromagnetics and Mechanics*, 7(2):150–159, 1999.

[28] Alain Bossavit. Computational electromagnetism and geometry. (2): Network constitutive laws. *Journal of the Japan Society of Applied Electromagnetics and Mechanics*, 7(3):294–301, 1999.

[29] Alain Bossavit. Computational electromagnetism and geometry. (5): "The Galerkin hodge". *Journal of the Japan Society of Applied Electromagnetics and Mechanics*, 8(2):203–209, 2000.

[30] Alain Bossavit. 'Generalized finite differences' in computational electromagnetics. *Progress In Electromagnetics Research*, 32:45–64, 2001. doi:10.2528/PIER00080102.

[31] Alain Bossavit. Extrusion, contraction: Their discretization via Whitney forms. *COMPEL: The International Journal for Computation and Mathematics in Electrical and Electronic Engineering*, 22(3):470–480, 2003. doi:10.1108/03321640310474877.

[32] Alain Bossavit. Discretization of electromagnetic problems: The "generalized finite differences" approach. In *Numerical Methods in Electromagnetics*, volume 13 of *Handbook of Numerical Analysis*, pages 105–197. Elsevier, 2005. doi:10.1016/S1570-8659(04)13002-0.

[33] Alain Bossavit. Geometrical methods in computational electromagnetism. In *Proceedings of ICAP 2006*, pages 75–80, 2006.

[34] Alain Bossavit and Lauri Kettunen. Yee-like schemes on a tetrahedral mesh, with diagonal lumping. *International Journal of Numerical Modelling: Electronic Networks, Devices and Fields*, 12(1-2):129–142, 1999. doi:10.1002/(SICI)1099-1204(199901/04)12:1/2<129::AID-JNM327>3.0.CO;2-G.

[35] Alain Bossavit and Lauri Kettunen. Yee-like schemes on staggered cellular grids: A synthesis between FIT and FEM approaches. *IEEE Transactions on Magnetics*, 36(4):861–867, 2000. doi:10.1109/20.877580.

[36] Susanne C. Brenner and L. Ridgway Scott. *The Mathematical Theory of Finite Element Methods*, volume 15 of *Texts in Applied Mathematics*. Springer, 3. edition, 2008. doi:10.1007/978-0-387-75934-0.

[37] Steven Britt, Eli Turkel, and Semyon Tsynkov. A high order compact time/space finite difference scheme for the wave equation with variable speed of sound. *Journal of Scientific Computing*, 76(2):777–811, 2018. doi:10.1007/s10915-017-0639-9.

[38] Arne Brøndsted. *An Introduction to Convex Polytopes*, volume 90 of *Graduate Texts in Mathematics*. Springer, 1983. doi:10.1007/978-1-4612-1148-8.

[39] Ludovico Bruni Bruno. *Weights as Degrees of Freedom for High Order Whitney Finite Elements*. PhD thesis, University of Trento, 2022.

[40] Annalisa Buffa and Snorre H. Christiansen. A dual finite element complex on the barycentric refinement. *Mathematics of Computation*, 76(260):1743–1769, 2007. doi:10.1090/S0025-5718-07-01965-5.

[41] William L. Burke. *Applied Differential Geometry*. Cambridge University Press, 1985.

[42] Daniele Casati, Lorenzo Codecasa, Ralf Hiptmair, and Federico Moro. Trefftz co-chain calculus. *Zeitschrift für angewandte Mathematik und Physik*, 73(1):43, 2022. doi:10.1007/s00033-021-01671-y.

[43] Shu C. Chen and Weng Cho Chew. Numerical electromagnetic frequency domain analysis with discrete exterior calculus. *Journal of Computational Physics*, 350:668–689, 2017. doi:10.1016/j.jcp.2017.08.068.

[44] Ryan A. Chilton and Robert Lee. The Lobatto cell: Robust, explicit, higher order FDTD that handles inhomogeneous media. *IEEE Transactions on Antennas and Propagation*, 56(8):2167–2177, 2008. doi:10.1109/TAP.2008.926758.

[45] M. Cinalli, F. Edelvik, R. Schuhmann, and T. Weiland. Consistent material operators for tetrahedral grids based on geometrical principles. *International Journal of Numerical Modelling: Electronic Networks, Devices and Fields*, 17(5):487–507, 2004. doi:10.1002/jnm.553.

[46] Markus Clemens and Thomas Weiland. Discrete electromagnetism with the finite integration technique. *Progress In Electromagnetics Research*, 32:65–87, 2001. doi:10.2528/PIER00080103.

[47] Lorenzo Codecasa, Ruben Specogna, and Francesco Trevisan. Base functions and discrete constitutive relations for staggered polyhedral grids. *Computer Methods in Applied Mechanics and Engineering*, 198(9–12):1117–1123, 2009. doi:10.1016/j.cma.2008.11.021.

[48] Justin Crum, Joshua A. Levine, and Andrew Gillette. Extending discrete exterior calculus to a fractional derivative. *Computer-Aided Design*, 114:64–72, 2019. doi:10.1016/j.cad.2019.05.018.

[49] L. D. da Silva, C. A. Batista, I. R. R. González, A. M. S. Macêdo, W. R. de Oliveira, and S. B. Melo. A discrete exterior calculus approach to quantum transport and quantum chaos on surface. *Journal of Computational and Theoretical Nanoscience*, 16(9):3670–3682, 2019. doi:10.1166/jctn.2019.8364.

[50] Richard W. R. Darling. *Differential Forms and Connections*. Cambridge University Press, 1994. doi:10.1017/CBO9780511805110.

[51] C. Deimert, M. E. Potter, and M. Okoniewski. Collocated electrodynamic FDTD schemes using overlapping Yee grids and higher-order Hodge duals. *Journal of Computational Physics*, 326:629–649, 2016. doi:10.1016/j.jcp.2016.08.048.

[52] Mathieu Desbrun, Anil N. Hirani, Melvin Leok, and Jerrold E. Marsden. Discrete exterior calculus. *arXiv preprint math/0508341*, 2005. doi:10.48550/ARXIV.MATH/0508341.

[53] Mathieu Desbrun, Eva Kanso, and Yiying Tong. Discrete differential forms for computational modeling. In *Discrete Differential Geometry*, volume 38 of *Oberwolfach Seminars*, pages 287–324. Springer, 2008. doi:10.1007/978-3-7643-8621-4_16.

[54] Georges A. Deschamps. Electromagnetics and differential forms. *Proceedings of the IEEE*, 69(6):676–696, 1981. doi:10.1109/PROC.1981.12048.

[55] Daniele A. Di Pietro and Jérôme Droniou. An arbitrary-order discrete de Rham complex on polyhedral meshes: Exactness, Poincaré inequalities, and consistency. *Foundations of Computational Mathematics*, 23(1):85–164, 2023. doi:10.1007/s10208-021-09542-8.

[56] A. DiCarlo, F. Milicchio, A. Paoluzzi, and V. Shapiro. Discrete physics using metrized chains. In *2009 SIAM/ACM Joint Conference on Geometric and Physical Modeling*, pages 135–145, 2009. doi:10.1145/1629255.1629273.

[57] Tevian Dray. *Differential Forms and the Geometry of General Relativity*. CRC Press, 2014.

[58] Qiang Du and Max Gunzburger. Grid generation and optimization based on centroidal Voronoi tessellations. *Applied Mathematics and Computation*, 133(2–3):591–607, 2002. doi:10.1016/S0096-3003(01)00260-0.

[59] Qiang Du and Desheng Wang. Tetrahedral mesh generation and optimization based on centroidal Voronoi tessellations. *International Journal for Numerical Methods in Engineering*, 56(9):1355–1373, 2003. doi:10.1002/nme.616.

[60] A. F. El Ouafdi, H. El Houari, and D. Ziou. Adaptive estimation of Hodge star operator on simplicial surfaces. *The Visual Computer*, 37(6):1433–1445, 2021. doi:10.1007/s00371-020-01879-5.

[61] Bjorn Engquist and Andrew Majda. Absorbing boundary conditions. *Mathematics of Computation*, 31(139):629–651, 1977. doi:10.1090/S0025-5718-1977-0436612-4.

[62] Alexandre Ern and Jean-Luc Guermond. *Finite Elements I: Approximation and Interpolation*, volume 72 of *Texts in Applied Mathematics*. Springer, 2021. doi:10.1007/978-3-030-56341-7.

[63] Lawrence C. Evans. *Partial Differential Equations*, volume 19 of *Graduate Studies in Mathematics*. American Mathematical Society, 2. edition, 2010.

[64] Robert Eymard, Thierry Gallouët, and Raphaèle Herbin. Finite volume methods. In *Solution of Equation in $\mathbb{R}^n$ (Part 3), Techniques of Scientific Computing (Part 3)*, volume 7 of *Handbook of Numerical Analysis*, pages 713–1018. Elsevier, 2000. doi:10.1016/S1570-8659(00)07005-8.

[65] Harley Flanders. *Differential Forms with Applications to the Physical Sciences*. Courier Corporation, 1963.

[66] Theodore Frankel. *The Geometry of Physics: An Introduction*. Cambridge University Press, 3. edition, 2011. doi:10.1017/CBO9781139061377.

[67] Jörg Frauendiener. Discrete differential forms in general relativity. *Classical and Quantum Gravity*, 23(16):S369, 2006. doi:10.1088/0264-9381/23/16/S05.

[68] Sahil Garg and Mohit Pant. Meshfree methods: A comprehensive review of applications. *International Journal of Computational Methods*, 15(04):1830001, 2018. doi:10.1142/S0219876218300015.

[69] Andrew Gillette and Chandrajit Bajaj. A generalization for stable mixed finite elements. In *Proceedings of the 14th ACM Symposium on Solid and Physical Modeling*, pages 41–50, 2010. doi:10.1145/1839778.1839785.

[70] Andrew Gillette and Chandrajit Bajaj. Dual formulations of mixed finite element methods with applications. *Computer-Aided Design*, 43(10):1213–1221, 2011. doi:10.1016/j.cad.2011.06.017.

[71] Andrew Gillette and Tyler Kloefkorn. Trimmed serendipity finite element differential forms. *Mathematics of Computation*, 88(316):583–606, 2019. doi:10.1090/mcom/3354.

[72] Andrew Kruse Gillette. *Stability of Dual Discretization Methods for Partial Differential Equations*. PhD thesis, University of Texas at Austin, 2011.

[73] Gene H. Golub and Charles F. Van Loan. *Matrix Computations*. The Johns Hopkins University Press, 3. edition, 1996.

[74] Leo J. Grady and Jonathan R. Polimeni. *Discrete Calculus: Applied Analysis on Graphs for Computational Science*. Springer, 2010. doi:10.1007/978-1-84996-290-2.

[75] Axel Grundmann and H. M. Möller. Invariant integration formulas for the n-simplex by combinatorial methods. *SIAM Journal on Numerical Analysis*, 15(2):282–290, 1978. doi:10.1137/0715019.

[76] J. Harrison. Operator calculus of differential chains and differential forms. *The Journal of Geometric Analysis*, 25(1):357–420, 2015. doi:10.1007/s12220-013-9433-6.

[77] R. Hiptmair. Multigrid method for Maxwell's equations. *SIAM Journal on Numerical Analysis*, 36(1):204–225, 1998. doi:10.1137/S0036142997326203.

[78] R. Hiptmair. Discrete Hodge operators. *Numerische Mathematik*, 90(2):265–289, 2001. doi:10.1007/s002110100295.

[79] A. N. Hirani, K. B. Nakshatrala, and J. H. Chaudhry. Numerical method for Darcy flow derived using discrete exterior calculus. *International Journal for Computational Methods in Engineering Science and Mechanics*, 16(3):151–169, 2015. doi:10.1080/15502287.2014.977500.

[80] Anil N. Hirani. *Discrete Exterior Calculus*. PhD thesis, California Institute of Technology, 2003. doi:10.7907/ZHY8-V329.

[81] Eugene Isaacson and Herbert Bishop Keller. *Analysis of Numerical Methods*. Dover Publications, 2. edition, 1994.

[82] Pankaj Jagad, Abdullah Abukhwejah, Mamdouh Mohamed, and Ravi Samtaney. A primitive variable discrete exterior calculus discretization of incompressible Navier–Stokes equations over surface simplicial meshes. *Physics of Fluids*, 33(1):017114, 2021. doi:10.1063/5.0035981.

[83] Jan Jaśkowiec and N. Sukumar. High-order cubature rules for tetrahedra. *International Journal for Numerical Methods in Engineering*, 121(11):2418–2436, 2020. doi:10.1002/nme.6313.

[84] Akihisa Kameari. Symmetric second order edge elements for triangles and tetrahedra. *IEEE Transactions on Magnetics*, 35(3):1394–1397, 1999. doi:10.1109/20.767224.

[85] Bernard Kapidani and Rafael Vázquez Hernandez. High order geometric methods with splines: An analysis of discrete Hodge-star operators. *SIAM Journal on Scientific Computing*, 44(6):A3673–A3699, 2022. doi:10.1137/22M1481762.

[86] Janne Keränen. *Towards Computational Electromagnetics in Spacetime*. PhD thesis, Tampere University of Technology, 2011.

[87] Lauri Kettunen, Jonni Lohi, Jukka Räbinä, Sanna Mönkölä, and Tuomo Rossi. Generalized finite difference schemes with higher order Whitney forms. *ESAIM: Mathematical Modelling and Numerical Analysis*, 55(4):1439–1460, 2021. doi:10.1051/m2an/2021026.

[88] Markus Kivioja, Sanna Mönkölä, and Tuomo Rossi. GPU-accelerated time integration of Gross-Pitaevskii equation with discrete exterior calculus. *Computer Physics Communications*, 278:108427, 2022. doi:10.1016/j.cpc.2022.108427.

[89] P. Robert Kotiuga. Theoretical limitations of discrete exterior calculus in the context of computational electromagnetics. *IEEE Transactions on Magnetics*, 44(6):1162–1165, 2008. doi:10.1109/TMAG.2007.915998.

[90] John M. Lee. *Introduction to Smooth Manifolds*, volume 218 of *Graduate Texts in Mathematics*. Springer, 2. edition, 2013. doi:10.1007/978-1-4419-9982-5.

[91] Konstantin Lipnikov, Gianmarco Manzini, and Mikhail Shashkov. Mimetic finite difference method. *Journal of Computational Physics*, 257:1163–1227, 2014. doi:10.1016/j.jcp.2013.07.031.

[92] Jonni Lohi. Discrete exterior calculus and higher order Whitney forms. Master's thesis, University of Jyväskylä, 2019.

[93] Jonni Lohi. Source code for higher order approximations in discrete exterior calculus. GitHub repository, 2023. URL: https://github.com/higher-order-dec/code.

[94] Claudio Mattiussi. An analysis of finite volume, finite element, and finite difference methods using some concepts from algebraic topology. *Journal of Computational Physics*, 133(2):289–309, 1997. doi:10.1006/jcph.1997.5656.

[95] Claudio Mattiussi. The finite volume, finite element, and finite difference methods as numerical methods for physical field problems. In *Advances in Imaging and Electron Physics*, volume 113, pages 1–146. Elsevier, 2000. doi:10.1016/S1076-5670(00)80012-9.

[96] Mamdouh S. Mohamed, Anil N. Hirani, and Ravi Samtaney. Comparison of discrete Hodge star operators for surfaces. *Computer-Aided Design*, 78:118–125, 2016. doi:10.1016/j.cad.2016.05.002.

[97] Mamdouh S. Mohamed, Anil N. Hirani, and Ravi Samtaney. Discrete exterior calculus discretization of incompressible Navier–Stokes equations over surface simplicial meshes. *Journal of Computational Physics*, 312:175–191, 2016. doi:10.1016/j.jcp.2016.02.028.

[98] Mamdouh S. Mohamed, Anil N. Hirani, and Ravi Samtaney. Numerical convergence of discrete exterior calculus on arbitrary surface meshes. *International Journal for Computational Methods in Engineering Science and Mechanics*, 19(3):194–206, 2018. doi:10.1080/15502287.2018.1446196.

[99] Sanna Mönkölä and Joona Räty. Discrete exterior calculus for photonic crystal waveguides. *International Journal for Numerical Methods in Engineering*, 124(5):1035–1054, 2023. doi:10.1002/nme.7144.

[100] P. Mullen, A. McKenzie, D. Pavlov, L. Durant, Y. Tong, E. Kanso, J. E. Marsden, and M. Desbrun. Discrete Lie advection of differential forms. *Foundations of Computational Mathematics*, 11(2):131–149, 2011. doi:10.1007/s10208-010-9076-y.

[101] Patrick Mullen, Pooran Memari, Fernando de Goes, and Mathieu Desbrun. HOT: Hodge-optimized triangulations. In *ACM SIGGRAPH 2011 Papers*, pages 1–12, 2011. doi:10.1145/1964921.1964998.

[102] R. A. Nicolaides. Direct discretization of planar div-curl problems. *SIAM Journal on Numerical Analysis*, 29(1):32–56, 1992. doi:10.1137/0729003.

[103] R. A. Nicolaides and K. A. Trapp. Covolume discretization of differential forms. In *Compatible Spatial Discretizations*, volume 142 of *The IMA Volumes in Mathematics and its Applications*, pages 161–171. Springer, 2006. doi:10.1007/0-387-38034-5_8.

[104] R. A. Nicolaides and D.-Q. Wang. Convergence analysis of a covolume scheme for Maxwell's equations in three dimensions. *Mathematics of Computation*, 67(223):947–963, 1998. doi:10.1090/S0025-5718-98-00971-5.

[105] Roy A. Nicolaides and Xiaonan Wu. Covolume solutions of three-dimensional div-curl equations. *SIAM Journal on Numerical Analysis*, 34(6):2195–2203, 1997. doi:10.1137/S0036142994277286.

[106] Ingo Nitschke, Sebastian Reuther, and Axel Voigt. Discrete exterior calculus (DEC) for the surface Navier–Stokes equation. In *Transport Processes at Fluidic Interfaces*, pages 177–197. Springer, 2017. doi:10.1007/978-3-319-56602-3_7.

[107] Marco A. Noguez, Salvador Botello, Rafael Herrera, and Humberto Esqueda. Discretization of the 2D convection–diffusion equation using discrete exterior calculus. *Journal of Applied and Computational Mechanics*, 6(Special Issue):1348–1363, 2020. doi:10.22055/JACM.2020.34246.2370.

[108] Richard S. Palmer and Vadim Shapiro. Chain models of physical behavior for engineering analysis and design. *Research in Engineering Design*, 5(3):161–184, 1993. doi:10.1007/BF01608361.

[109] Jukka Räbinä. *On a Numerical Solution of the Maxwell Equations by Discrete Exterior Calculus*. PhD thesis, University of Jyväskylä, 2014.

[110] Jukka Räbinä. Generalized finite differences (GFD) source code for solving large scale wave equations. GitHub repository, 2019. URL: https://github.com/juolrabi/gfd.

[111] Jukka Räbinä, Lauri Kettunen, Sanna Mönkölä, and Tuomo Rossi. Generalized wave propagation problems and discrete exterior calculus. *ESAIM: Mathematical Modelling and Numerical Analysis*, 52(3):1195–1218, 2018. doi:10.1051/m2an/2018017.

[112] Jukka Räbinä, Pekko Kuopanportti, Markus I. Kivioja, Mikko Möttönen, and Tuomo Rossi. Three-dimensional splitting dynamics of giant vortices in Bose–Einstein condensates. *Physical Review A*, 98(2):023624, 2018. doi:10.1103/PhysRevA.98.023624.

[113] Jukka Räbinä, Sanna Mönkölä, and Tuomo Rossi. Efficient time integration of Maxwell's equations with generalized finite differences. *SIAM Journal on Scientific Computing*, 37(6):B834–B854, 2015. doi:10.1137/140988759.

[114] Jukka Räbinä, Sanna Mönkölä, and Tuomo Rossi. High-quality discretizations for microwave simulations. In *2016 URSI International Symposium on Electromagnetic Theory (EMTS)*, pages 129–132. IEEE, 2016. doi:10.1109/URSI-EMTS.2016.7571332.

[115] Jukka Räbinä, Sanna Mönkölä, Tuomo Rossi, Johannes Markkanen, Maria Gritsevich, and Karri Muinonen. Controlled time integration for the numerical simulation of meteor radar reflections. *Journal of Quantitative Spectroscopy and Radiative Transfer*, 178:295–305, 2016. doi:10.1016/j.jqsrt.2016.02.009.

[116] Jukka Räbinä, Sanna Mönkölä, Tuomo Rossi, Antti Penttilä, and Karri Muinonen. Comparison of discrete exterior calculus and discrete-dipole approximation for electromagnetic scattering. *Journal of Quantitative Spectroscopy and Radiative Transfer*, 146:417–423, 2014. doi:10.1016/j.jqsrt.2014.02.011.

[117] Francesca Rapetti. High order edge elements on simplicial meshes. *ESAIM: Mathematical Modelling and Numerical Analysis*, 41(6):1001–1020, 2007. doi:10.1051/m2an:2007049.

[118] Francesca Rapetti and Alain Bossavit. Whitney forms of higher degree. *SIAM Journal on Numerical Analysis*, 47(3):2369–2386, 2009. doi:10.1137/070705489.

[119] Dzhelil Rufat, Gemma Mason, Patrick Mullen, and Mathieu Desbrun. The chain collocation method: A spectrally accurate calculus of forms. *Journal of Computational Physics*, 257:1352–1372, 2014. doi:10.1016/j.jcp.2013.08.011.

[120] Mahbod Salmasi and Michael Potter. Discrete exterior calculus approach for discretizing Maxwell's equations on face-centered cubic grids for FDTD. *Journal of Computational Physics*, 364:298–313, 2018. doi:10.1016/j.jcp.2018.03.019.

[121] T. Satoh and T. Yaguchi. On the equivalence of the norms of the discrete differential forms in discrete exterior calculus. *Japan Journal of Industrial and Applied Mathematics*, 36(1):3–24, 2019. doi:10.1007/s13160-018-0334-8.

[122] Bernard Schutz. *Geometrical Methods of Mathematical Physics*. Cambridge University Press, 1980.

[123] Jie Shen, Tao Tang, and Li-Lian Wang. *Spectral Methods: Algorithms, Analysis and Applications*, volume 41 of *Springer Series in Computational Mathematics*. Springer, 2011. doi:10.1007/978-3-540-71041-7.

[124] Holger Spachmann, Rolf Schuhmann, and Thomas Weiland. Higher order spatial operators for the finite integration theory. *The Applied Computational Electromagnetics Society Journal (ACES)*, 17(1):11–22, 2002.

[125] Ari Stern, Yiying Tong, Mathieu Desbrun, and Jerrold E. Marsden. Geometric computational electrodynamics with variational integrators and discrete differential forms. In *Geometry, Mechanics, and Dynamics*, volume 73 of *Fields Institute Communications*, pages 437–475. Springer, 2015. doi:10.1007/978-1-4939-2441-7_19.

[126] John C. Strikwerda. *Finite Difference Schemes and Partial Differential Equations*. SIAM, 2. edition, 2004. doi:10.1137/1.9780898717938.

[127] Timo Tarhasaari and Lauri Kettunen. Wave propagation and cochain formulations. *IEEE Transactions on Magnetics*, 39(3):1195–1198, 2003. doi:10.1109/TMAG.2003.810220.

[128] Timo Tarhasaari, Lauri Kettunen, and Alain Bossavit. Some realizations of a discrete Hodge operator: A reinterpretation of finite element techniques.

IEEE Transactions on Magnetics, 35(3):1494–1497, 1999. doi:10.1109/20.767250.

[129] F. L. Teixeira and W. C. Chew. Lattice electromagnetic theory from a topological viewpoint. *Journal of Mathematical Physics*, 40(1):169–187, 1999. doi:10.1063/1.532767.

[130] Fernando Lisboa Teixeira. Geometric aspects of the simplicial discretization of Maxwell's equations. *Progress In Electromagnetics Research*, 32:171–188, 2001. doi:10.2528/PIER00080107.

[131] Fernando Lisboa Teixeira. Lattice Maxwell's equations. *Progress In Electromagnetics Research*, 148:113–128, 2014. doi:10.2528/PIER14062904.

[132] E. Tonti. The reason for analogies between physical theories. *Applied Mathematical Modelling*, 1(1):37–50, 1976. doi:10.1016/0307-904X(76)90023-8.

[133] F. Trevisan and L. Kettunen. Geometric interpretation of discrete approaches to solving magnetostatic problems. *IEEE Transactions on Magnetics*, 40(2):361–365, 2004. doi:10.1109/TMAG.2004.824107.

[134] Ulrich Trottenberg, Cornelis Oosterlee, and Anton Schüller. *Multigrid*. Academic Press, 2001.

[135] Eli Turkel, Dan Gordon, Rachel Gordon, and Semyon Tsynkov. Compact 2D and 3D sixth order schemes for the Helmholtz equation with variable wave number. *Journal of Computational Physics*, 232(1):272–287, 2013. doi:10.1016/j.jcp.2012.08.016.

[136] Ursula van Rienen. Finite integration technique on triangular grids revisited. *International Journal of Numerical Modelling: Electronic Networks, Devices and Fields*, 12(1-2):107–128, 1999. doi:10.1002/(SICI)1099-1204(199901/04)12:1/2<107::AID-JNM322>3.0.CO;2-2.

[137] Steven Vandekerckhove, Bart Vandewoestyne, Herbert De Gersem, Koen Van Den Abeele, and Stefan Vandewalle. Mimetic discretization and higher order time integration for acoustic, electromagnetic and elastodynamic wave propagation. *Journal of Computational and Applied Mathematics*, 259:65–76, 2014. doi:10.1016/j.cam.2013.02.027.

[138] T. Weiland. Time domain electromagnetic field computation with finite difference methods. *International Journal of Numerical Modelling: Electronic Networks, Devices and Fields*, 9(4):295–319, 1996. doi:10.1002/(SICI)1099-1204(199607)9:4<295::AID-JNM240>3.0.CO;2-8.

[139] Hassler Whitney. *Geometric Integration Theory*. Princeton University Press, 1957.

[140] Scott O. Wilson. Cochain algebra on manifolds and convergence under refinement. *Topology and its Applications*, 154(9):1898–1920, 2007. doi:10.1016/j.topol.2007.01.017.

[141] Arash Yavari. On geometric discretization of elasticity. *Journal of Mathematical Physics*, 49(2):022901, 2008. doi:10.1063/1.2830977.

[142] Kane S. Yee. Numerical solution of initial boundary value problems involving Maxwell's equations in isotropic media. *IEEE Transactions on Antennas and Propagation*, 14(3):302–307, 1966. doi:10.1109/TAP.1966.1138693.

[143] Boyuan Zhang, Dong-Yeop Na, Dan Jiao, and Weng Cho Chew. An A-Φ formulation solver in electromagnetics based on discrete exterior calculus. In *2021 Photonics & Electromagnetics Research Symposium (PIERS)*, pages 2394–2399. IEEE, 2021. doi:10.1109/PIERS53385.2021.9694901.

ORIGINAL PAPERS

PI

WHITNEY FORMS AND THEIR EXTENSIONS

by

Jonni Lohi and Lauri Kettunen

Journal of Computational and Applied Mathematics, 393:113520, 2021

Journal of Computational and Applied Mathematics 393 (2021) 113520

Contents lists available at ScienceDirect

Journal of Computational and Applied Mathematics

journal homepage: www.elsevier.com/locate/cam

Whitney forms and their extensions☆

Jonni Lohi *, Lauri Kettunen

Faculty of Information Technology, University of Jyväskylä, PO Box 35, FI 40014, Finland

ARTICLE INFO

Article history:
Received 20 August 2020
Received in revised form 15 January 2021

MSC:
primary 65N30
secondary 58A10

Keywords:
Whitney forms

ABSTRACT

Whitney forms are widely known as finite elements for differential forms. Whitney's original definition yields first order functions on simplicial complexes, and a lot of research has been devoted to extending the definition to nonsimplicial cells and higher order functions. As a result, the term Whitney forms has become somewhat ambiguous in the literature. Our aim here is to clarify the concept of Whitney forms and explicitly explain their key properties. We discuss Whitney's initial definition with more depth than usually, giving three equivalent ways to define Whitney forms. We give a comprehensive exposition of their main properties, including the proofs. Understanding of these properties is important as they can be taken as a guideline on how to extend Whitney forms to nonsimplicial cells or higher order functions. We discuss several generalisations of Whitney forms and check which of the properties can be preserved.

Contents

1. Introduction 2
2. Preliminaries and notation 2
3. Three equivalent definitions of Whitney forms 3
   3.1. Proxy fields 5
4. Properties of Whitney forms 7
5. Generalisations of Whitney forms 12
   5.1. Whitney forms on a manifold 12
   5.2. Higher order Whitney forms 13
   5.3. Whitney forms on other cells than simplices 15
      5.3.1. Construction based on generalised barycentric functions 16
      5.3.2. Construction based on conation and extrusion 17
      5.3.3. Formulas on cubes, triangular prisms, and pyramids 17
Acknowledgements 18
References 18

☆ Funding: University of Jyväskylä, Finland.
* Corresponding author.
E-mail addresses: jonni.j.lohi@student.jyu.fi (J. Lohi), lauri.y.o.kettunen@jyu.fi (L. Kettunen).

https://doi.org/10.1016/j.cam.2021.113520

1. Introduction

Whitney forms first appeared in the book of Hassler Whitney [1], which did not originally have any relation to numerical mathematics or to finite element and finite difference kind of approaches. Instead, Whitney formulated a theory of p-dimensional integration in n-dimensional affine space with chains and cochains. In a proof relating the cohomology of flat cochains to simplicial cohomology, he introduced elementary flat cochains and the corresponding differential forms [1, VII, §11]. Jozef Dodziuk used these forms (or their generalisations onto a manifold, to be precise) to approximate continuous Hodge theory with combinatorial Hodge theory and introduced the name Whitney forms in his thesis [2]. Unlike Whitney's work, Dodziuk's ideas were closely related to finite difference approaches.

Whitney forms became popular within the computational electromagnetics community in late 1980s and early 1990s after the pioneering work of Alain Bossavit [3–8]. He revealed their immediate relation to mixed finite elements [9,10] and emphasised the benefits of presenting the field equations in terms of differential forms instead of scalar and vector fields. Thereafter cochains and Whitney forms were shown to yield a natural framework to explain the finite difference method and its relation to the finite element method [11–14]. Differential forms have since been accepted as an appropriate tool to present both of these methods [15–20], and Whitney forms are widely used to build finite-dimensional subspaces of differential forms; for more examples of the use of Whitney forms (or their proxy fields) in the literature, see e.g. [21–27].

Whitney's original definition yields first order functions on simplicial complexes. In practice, the assumption of simplices behind Whitney forms is restrictive. Hence, in the literature one can find extensions to other cell types [18,28,29]. Furthermore, there have also been attempts to generalise them to higher order functions [30–32]. While the literature recognises several extensions of Whitney forms, the usage of the term "Whitney forms" is not unambiguous. The term is used for different type of objects by different authors, and the other way around, some instances of Whitney forms are sometimes called with a completely different name.

In this paper we clarify the concept of Whitney forms and create a synthesis of papers published on them. Our aim is to explain explicitly the key properties of Whitney forms and provide foundations for extending Whitney forms beyond their original assumptions. For this, in Section 3, we discuss Whitney's initial definition in more depth than usually and give three equivalent definitions, each emphasising a certain aspect of Whitney forms. In Section 4 we give a comprehensive exposition of their main properties, including the proofs. To further clarify the concept of Whitney forms, in Section 5 we consider generalisations that are called Whitney forms in the literature and check which of the properties are preserved. This reveals the trade-offs involved in extending Whitney forms to non-simplicial complexes and higher order functions. That is, to bypass assumptions involved in Whitney's initial setting, one also has to give up on some properties.

Regarding our contribution to the scientific literature, there is no prior paper which systematically lists all the key properties of Whitney forms with proofs. Although the results included in this paper can be considered as known, there are new aspects and some technical details that have not been published before. Our definitions and results are given in the spirit of Whitney's book and do not require Lebesgue theory or Sobolev spaces. This includes Theorems 4.9 and 5.1, which bring the approximation property of finite element theory into Whitney's setting. The proof of Theorem 4.3 has also not appeared elsewhere. This theorem could also be shown using Proposition 4.4 and the known fact that constants are in the span of Whitney forms, but the authors are not aware of such a proof – or even the proof of Proposition 4.4 – in the literature.

2. Preliminaries and notation

In this section some of the prerequisite concepts are briefly recalled. We expect the reader is familiar with exterior algebra and differential forms (see e.g. [1, Chapters I–III]).

Standard Whitney forms are differential forms in a simplicial complex. *Simplicial complex K* is a finite set of simplices such that

- each face of every simplex in K is also in K.
- The intersection of two simplices in K is either a common face of theirs or the empty set.

Complexes consisting of more general cells can be defined similarly. As in the initial context of Whitney forms [1], we assume that the simplices are embedded in affine space and tile a domain Ω. For simplicity, we may take $\mathbb{R}^n$ as the affine space, keeping in mind that only the affine structure of $\mathbb{R}^n$ is required, so that Ω is a polyhedron in $\mathbb{R}^n$. The general case where Ω is a manifold is covered in Section 5, which discusses generalisations of Whitney forms. We denote simplices by labels σ and τ, and $\sigma = x_0 \dots x_p$ means that σ is the oriented p-simplex whose vertices are $x_0, \dots, x_p$ and whose orientation is implied by this order of vertices. S^p denotes the set of p-simplices and $\operatorname{vect}(\sigma)$ the vectorial volume of σ (i.e. the p-vector of σ, see [1, III, §1]).

Recall that to each 0-simplex x_i of K corresponds a *barycentric function* λ_i — it is the unique function which is affine in each simplex and whose value is one at x_i and zero at other 0-simplices. Barycentric functions are the main building block for Whitney forms. We remark that they are exclusive to simplicial complexes, but we will discuss the generalisation of barycentric coordinates for other cells than simplices when considering extensions of Whitney forms.

Differential p-form in a complex K [1, p. 226] is a set of smooth p-forms ω_σ in the cells σ of K satisfying the following *patch condition*: if τ is a face of σ, then the trace $\omega_\sigma|_\tau$ of ω_σ equals ω_τ in τ. In other words, $\langle \omega_\sigma(x), \alpha \rangle = \langle \omega_\tau(x), \alpha \rangle$ for all

$x \in \tau$ and all p-vectors α in the plane of τ. (Here and throughout the paper, we denote the action of a p-covector ω on a p-vector α by $\langle \omega, \alpha \rangle$.) This means that if τ is the cell for which $x \in \tau - \partial\tau$ and α is in the plane of τ, then $\langle \omega_\sigma(x), \alpha \rangle$ is the same for all σ containing x. Hence the set of p-forms ω_σ induces a single p-form ω such that $\langle \omega(x), \alpha \rangle$ is single-valued (i.e. well-defined) for such p-vectors α.

The patch condition ensures that differential p-forms in K can be integrated over p-cells in K. Denote by $F^p(K)$ the space of differential p-forms in K. Note that since the exterior derivative d commutes with trace, we have $\mathrm{d}\,\omega \in F^{p+1}(K)$ if $\omega \in F^p(K)$, but the Hodge star $\star\omega$ is not necessarily in $F^{n-p}(K)$.

When K is a simplicial complex, formal sums $\sum_{\sigma_i \in S^p} a_i\sigma_i$ of oriented p-simplices with real coefficients are called *p-chains of K* [1, App. II, §6]. These form a vector space $C_p(K)$ for which the p-simplices σ_i constitute a natural basis (here $\sigma_i = 1\sigma_i$, the sum in which $a_j = \delta_{ij}$, the Kronecker delta). The elements of the dual space $C_p^*(K)$ are *p-cochains of K*. Following [1], we use σ_i to denote also the cochain whose value is δ_{ij} at the chain σ_j. Then the p-simplices σ_i constitute the dual basis for $C_p^*(K)$, and also cochains can be written as formal sums of simplices. Negative coefficients indicate change of orientation so that $-\sigma$ is the simplex σ with opposite orientation. Chains and cochains for more general cell complexes are defined similarly.

Since p-forms can be integrated over p-cells, each p-form ω yields a p-cochain whose values on chains are determined by integration of ω. Namely, the *de Rham map* $\mathcal{C} : F^p(K) \to C_p^*(K)$ is a linear map defined by

$$\mathcal{C}\omega(\sum_i a_i\sigma_i) = \int_{\sum_i a_i\sigma_i} \omega = \sum_i a_i \int_{\sigma_i} \omega,$$

where the second equality is the definition of integration on p-chains. *Coboundary operator* $\mathrm{d} : C_p^*(K) \to C_{p+1}^*(K)$ is a linear map defined by $\mathrm{d}\,X(c) = X(\partial c)$. We use the same notation d as for the exterior derivative of forms. Stokes' theorem then implies that $\mathcal{C}\,\mathrm{d} = \mathrm{d}\,\mathcal{C}$.

3. Three equivalent definitions of Whitney forms

Whitney p-forms are a finite-dimensional subspace of differential p-forms in a simplicial complex K. To each p-simplex σ corresponds a Whitney p-form $\mathcal{W}\sigma$. Since σ also denotes a basis cochain of $C_p^*(K)$ (and linear maps are uniquely determined by their action on basis elements), this correspondence defines a linear map $\mathcal{W} : C_p^*(K) \to F^p(K)$. $\mathcal{W}$ is known as the Whitney map, and Whitney forms are its images. This is made precise in the following definition.

Definition 3.1. The Whitney 0-form corresponding to the 0-simplex x_i is the barycentric function $\mathcal{W}x_i = \lambda_i$. For $p > 0$, the Whitney p-form corresponding to the p-simplex $x_0 \dots x_p$ is [1, VII, 11.16]

$$\mathcal{W}(x_0 \dots x_p) = p! \sum_{i=0}^{p} (-1)^i \lambda_i \,\mathrm{d}\,\lambda_0 \wedge \cdots \wedge \widehat{\mathrm{d}\,\lambda_i} \wedge \cdots \wedge \mathrm{d}\,\lambda_p, \tag{3.1}$$

where $\widehat{\ }$ indicates a term omitted from the product.

For each p, the Whitney map $\mathcal{W} : C_p^*(K) \to F^p(K)$ is defined by setting

$$\mathcal{W}(\sum_{\sigma_i \in S^p} a_i\sigma_i) = \sum_{\sigma_i \in S^p} a_i \mathcal{W}(\sigma_i).$$

The image $\mathcal{W}(C_p^*(K)) = \mathrm{span}\{\mathcal{W}\sigma \mid \sigma \in S^p\} \subset F^p(K)$ is the space of Whitney p-forms and denoted by W^p.

Note that although the λ_i are not globally smooth, they are smooth in each simplex, so (3.1) defines a p-form in each simplex of K. The patch condition holds because barycentric functions in σ restrict to barycentric functions on the faces of σ (and trace commutes with $\wedge$ and d). Hence (3.1) yields a well-defined differential form in K. Note also that the right hand side of (3.1) changes sign when the orientation changes, so $\mathcal{W}(-\sigma) = -\mathcal{W}\sigma$ and the Whitney map is well-defined.

Since the definition of Whitney forms is the main issue here, we cover it in more detail than usually and from different viewpoints. First, we give an alternative but equivalent definition. Set $\mathcal{W}\sigma = 0$ in τ if σ is not a face of τ. If it is, say $\sigma = x_0 \dots x_p$ and τ has vertices $\{x_0, \dots, x_p, x_{p+1} \dots, x_q\}$, set [1, VII, 11.12]

$$\langle \mathcal{W}\sigma(x), \alpha \rangle = p! \frac{\alpha \wedge (x_{p+1} - x) \wedge (x_{p+2} - x_{p+1}) \wedge \cdots \wedge (x_q - x_{p+1})}{(x_1 - x_0) \wedge \cdots \wedge (x_q - x_0)} \quad \text{in } \tau; \tag{3.2}$$

that is, the value of the p-form $\mathcal{W}\sigma$ at point $x \in \tau$ is the p-covector whose value on a p-vector α is defined as the ratio of the two q-vectors in the plane of τ. This can be written equivalently as

$$\langle \mathcal{W}\sigma(x), \alpha \rangle = \frac{p!(q-p)!}{q!} \frac{\alpha \wedge \mathrm{vect}(x x_{p+1} \dots x_q)}{\mathrm{vect}(x_0 \dots x_p \dots x_q)},$$

from which we see that $\mathcal{W}\sigma$ in τ does not depend on the orientation of τ but changes sign when the orientation of σ changes. For $x \in y_0 \dots y_p \subset \tau$, (3.2) becomes

$$\langle \mathcal{W}\sigma(x), \mathrm{vect}(y_0 \dots y_p) \rangle = \frac{\mathrm{vect}(y_0 \dots y_p x_{p+1} \dots x_q)}{\mathrm{vect}(x_0 \dots x_q)}. \tag{3.3}$$

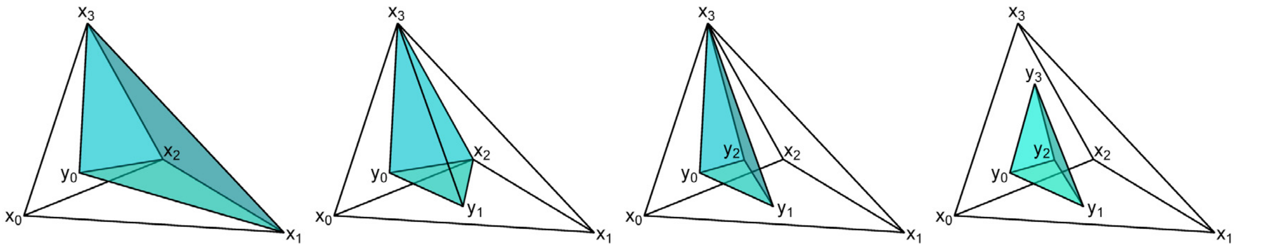

Fig. 1. Illustration of (3.3) in tetrahedron $\tau = x_0x_1x_2x_3$ for the cases $\sigma = x_0$, $\sigma = x_0x_1$, $\sigma = x_0x_1x_2$, and $\sigma = x_0x_1x_2x_3$. In each case, $\langle \mathcal{W}\sigma(x), \mathrm{vect}(y_0 \dots y_p)\rangle$ is the ratio of the highlighted volume and the volume of the whole tetrahedron. This holds for all $x \in y_0 \dots y_p$.

To see this, note that $\mathrm{vect}(y_0 \dots y_p) \wedge (x_{p+1} - x) = \mathrm{vect}(y_0 \dots y_p) \wedge (x_{p+1} - y_p - (x - y_p)) = \mathrm{vect}(y_0 \dots y_p) \wedge (x_{p+1} - y_p)$ since $x - y_p$ is in the plane of $y_0 \dots y_p$.

Although volumes depend on the metric, their ratios do not, and the above formula is meaningful in affine space. This definition beautifully illustrates the geometric character of Whitney forms (see Fig. 1), while Definition 3.1 offers an explicit formula in terms of barycentric functions. Whitney showed that these two definitions are indeed equivalent.

Proposition 3.2. *The definition with the geometric formula (3.2) is equivalent to Definition 3.1.*

Proof. Let $\sigma = x_0 \dots x_p \in S^p$ and $\tau \in S^q$, and denote by $\mathcal{W}_1\sigma$ the Whitney form of σ given by (3.1) and by $\mathcal{W}_2\sigma$ that given by (3.2). To show that $\mathcal{W}_1\sigma = \mathcal{W}_2\sigma$ in τ, we first note that both $\mathcal{W}_1\sigma$ and $\mathcal{W}_2\sigma$ zero in τ if σ is not a face of τ. Moreover, both are affine in τ, are zero at those vertices of τ that are not in σ, and change sign when the orientation of σ changes. Hence it suffices to consider the case $\tau = x_0 \dots x_p x_{p+1} \dots x_q$ and show that $\mathcal{W}_1\sigma(x_0) = \mathcal{W}_2\sigma(x_0)$.

Since the edge vectors $x_i - x_0$ span the plane of τ, all p-vectors in τ can be written as linear combinations of their wedge products. Hence it suffices to show $\langle \mathcal{W}_1\sigma(x_0), \alpha\rangle = \langle \mathcal{W}_2\sigma(x_0), \alpha\rangle$ for p-vectors α of the form $\alpha = (x_{i_1} - x_0) \wedge \dots \wedge (x_{i_p} - x_0)$ for $i_1 < \dots < i_p$. Since $\lambda_i(x_0) = 0$ and $\langle \mathrm{d}\,\lambda_i(x_0), x_j - x_0\rangle = \delta_{ij}$ if $i \neq 0$, we have

$$\langle \mathcal{W}_1\sigma(x_0), (x_{i_1} - x_0) \wedge \dots \wedge (x_{i_p} - x_0)\rangle = 0 \quad \text{if any of the indices } i_j \text{ are not in } \{1, \dots, p\}$$
$$\langle \mathcal{W}_1\sigma(x_0), (x_1 - x_0) \wedge \dots \wedge (x_p - x_0)\rangle = p!$$

By (3.2) the same is true for $\mathcal{W}_2\sigma(x_0)$; hence $\mathcal{W}_1\sigma(x_0) = \mathcal{W}_2\sigma(x_0)$. □

At this point, it is instructive to briefly discuss Whitney's book [1] and the role of Whitney forms there. The book is about p-dimensional integration in n-dimensional space. What we call chains (and cochains) of K are called algebraic chains (and cochains) in [1] where p-chains have a more general meaning as p-dimensional domains of integration. Whitney starts from polyhedral p-chains – formal sums of polyhedral p-cells with real coefficients and invariance under subdivision – which form an infinite-dimensional vector space. This space can be equipped with a norm and then completed with respect to that norm; for example, the flat norm [1, V, §3] yields the space of flat p-chains $C_p^\flat$. Its (continuous) dual space $C_p^{\flat *}$ is the space of flat p-cochains and consists of bounded linear functionals $C_p^\flat \to \mathbb{R}$. Similarly, the sharp norm [1, V, §6] yields the spaces of sharp p-chains $C_p^\sharp$ and sharp p-cochains $C_p^{\sharp *}$.

We saw that Whitney forms correspond to (algebraic) cochains of a simplicial complex K, but they also correspond to certain flat cochains in K. This explains why Whitney forms are sometimes called flat forms. A correspondence between flat forms and flat cochains is made precise in Wolfe's theorem [1, IX, Theorem 7C]. Without going into details, p-form ω and p-cochain X correspond if $\int_\sigma \omega = X(\sigma)$ for all p-cells σ. In his work [1, VII, §11], Whitney defined a linear injection ϕ from the algebraic cochains of K to flat cochains in K, which he used to prove that the cohomology ring of flat cochains is isomorphic to that of algebraic cochains. The images of ϕ he called elementary flat cochains in K, and these are in correspondence with Whitney forms.

Whitney's theory of p-chains as p-dimensional domains of integration had some shortcomings. For instance, sharp chains do not have a continuous boundary operator, while the Hodge star of a flat form is not flat. The theory has since been extended by Jenny Harrison [33]. We need not go deeper into this. However, now that we have mentioned chains, we can briefly discuss another way to look at the definition of Whitney forms, as emphasised by Alain Bossavit [14,29,34]: approximating p-chains with algebraic p-chains.

To explain this, we extend the notation $\langle \omega, c\rangle := \int_c \omega$ for differential forms ω and chains c. This expression is bilinear and can be interpreted either as the evaluation of ω on c or (by duality) as the evaluation of c on ω. Similarly, denote $\langle X, c\rangle = X(c)$ for cochains X and chains c. Whitney forms have the property $\langle \mathcal{W}\sigma_j, \sigma_i\rangle = \delta_{ij}$ and hence enable one to approximate a p-form ω in W^p with $\tilde{\omega} = \sum_{\sigma_i \in S^p} \langle \omega, \sigma_i\rangle \mathcal{W}\sigma_i$. The approximation $\tilde{\omega}$ has the property that $\langle \tilde{\omega}, c\rangle = \langle \omega, c\rangle$ — not for all p-chains c, but for algebraic chains, namely those in $C_p(K)$. This has a dual viewpoint: one can approximate a p-chain c in $C_p(K)$ with $\tilde{c} = \sum_{\sigma_i \in S^p} \langle \mathcal{W}\sigma_i, c\rangle \sigma_i$, and the approximation $\tilde{c}$ has the property that $\langle \omega, c\rangle = \langle \omega, \tilde{c}\rangle$ — not for all p-forms ω, but for those in W^p. Letting $\mathcal{W}^t$ denote the map $c \mapsto \tilde{c}$, we have $\langle \mathcal{W}X, c\rangle = \langle X, \mathcal{W}^t c\rangle$ for all p-chains c and all $X \in C_p^*(K)$.

On the other hand, if we have such a map $\mathcal{W}^t$ to approximate p-chains in $C_p(K)$, this defines a map $\mathcal{W}$ from $C^*_p(K)$ to $F^p(K)$ by requiring that $\langle \mathcal{W}X, c\rangle = \langle X, \mathcal{W}^t c\rangle$ hold for all p-chains c and all $X \in C^*_p(K)$. This approach to the definition of Whitney forms is used e.g. in [14,29,31,34,35]. When suitable conditions are imposed for the map $\mathcal{W}^t$, this approach leads to the following, yet another equivalent definition of Whitney forms, which first appeared in [34]. Setting $\mathcal{W}x_i = \lambda_i$ for $p = 0$, the Whitney form corresponding to p-simplex σ for $p > 0$ is obtained recursively by

$$\mathcal{W}\sigma = \sum_{\tau \in S^{p-1}} \mathbf{d}^\sigma_\tau \lambda_{\sigma-\tau}\, \mathrm{d}\,\mathcal{W}\tau, \tag{3.4}$$

where $\mathbf{d}^\sigma_\tau$ is the incidence number relating τ and σ (which is 0 if τ is not a face of σ and ± 1 if it is, the sign depending on whether the orientations agree or not) and $\sigma - \tau$ denotes the vertex opposite to the $(p-1)$-face τ of σ.

It is easy to show that this definition is equivalent to Definition 3.1, after we first note that the exterior derivative of the Whitney p-form $\mathcal{W}(x_0 \dots x_p)$ for any p-simplex $x_0 \dots x_p \in S^p$ is

$$\mathrm{d}\,\mathcal{W}(x_0 \dots x_p) = p! \sum_{i=0}^{p} (-1)^i\, \mathrm{d}\,\lambda_i \wedge \mathrm{d}\,\lambda_0 \wedge \dots \wedge \widehat{\mathrm{d}\,\lambda_i} \wedge \dots \wedge \mathrm{d}\,\lambda_p = (p+1)!\, \mathrm{d}\,\lambda_0 \wedge \dots \wedge \mathrm{d}\,\lambda_p. \tag{3.5}$$

Proposition 3.3. *The definition with the recursive formula (3.4) is equivalent to Definition 3.1.*

Proof. First note that writing $\sigma = x_0 \dots x_p$ we get

$$\sum_{\tau \in S^{p-1}} \mathbf{d}^\sigma_\tau \lambda_{\sigma-\tau}\, \mathrm{d}\,\mathcal{W}\tau = \sum_{i=0}^{p} (-1)^i \lambda_i\, \mathrm{d}\,\mathcal{W}(x_0 \dots \widehat{x_i} \dots x_p).$$

For $\sigma = x_0x_1$ this becomes $\lambda_0\, \mathrm{d}\,\mathcal{W}x_1 - \lambda_1\, \mathrm{d}\,\mathcal{W}x_0 = \lambda_0\, \mathrm{d}\,\lambda_1 - \lambda_1\, \mathrm{d}\,\lambda_0$, which is the same as $\mathcal{W}x_0x_1$ of Definition 3.1, proving the claim for 1-simplices. Suppose as induction hypothesis that it holds for $(p-1)$-simplices, and let $\sigma = x_0 \dots x_p$ be a p-simplex. By (3.5) we get

$$\begin{aligned}\sum_{\tau \in S^{p-1}} \mathbf{d}^\sigma_\tau \lambda_{\sigma-\tau}\, \mathrm{d}\,\mathcal{W}\tau &= \sum_{i=0}^{p} (-1)^i \lambda_i\, \mathrm{d}\,\mathcal{W}(x_0 \dots \widehat{x_i} \dots x_p) \\ &= \sum_{i=0}^{p} (-1)^i \lambda_i p!\, \mathrm{d}\,\lambda_0 \wedge \dots \wedge \widehat{\mathrm{d}\,\lambda_i} \wedge \dots \mathrm{d}\,\lambda_p = \mathcal{W}(x_0 \dots x_p). \quad \square\end{aligned}$$

3.1. Proxy fields

The definition of Whitney forms does not require the notion of metric; only the affine structure of the ambient space is invoked. However, metric structure allows one to identify certain differential forms with scalar or vector fields, so-called proxy fields. Indeed, Whitney forms are often presented in terms of these proxy fields. To clarify such seemingly different definitions, let us look at the 3-dimensional case with Euclidean metric and standard orientation (so that right-hand rule is used for cross product).

0-forms are scalar functions, so there is no distinction between a 0-form and its proxy field. In each simplex of K, flat map $\flat$ from vector fields to 1-forms is defined by $\langle \flat u(x), v\rangle = u(x) \cdot v$; that is, the value of $\flat u$ at point x is the covector whose value on vector v is the dot product $u(x) \cdot v$. This is an isomorphism with inverse $\sharp$, and the proxy field of a 1-form ω is the vector field $\sharp\omega$. Similarly, if u is a vector field, the rule $v_1 \wedge v_2 \mapsto u(x) \cdot v_1 \times v_2$ defines a 2-form, and this yields a correspondence between vector fields and 2-forms. The proxy field of a 2-form ω can be written as $\sharp \star \omega$, where $\star$ is the Hodge star. Finally, a scalar field f defines a 3-form by the rule $v_1 \wedge v_2 \wedge v_3 \mapsto f(x)\det(v_1, v_2, v_3)$, and any 3-form is obtained this way from a scalar field f, its proxy field. When considered globally in K, the proxy fields of 1- and 2-forms in K have a well-defined tangential and normal component on inter-element boundaries (respectively).

In this case the proxy fields are perhaps more easily explained in terms of standard coordinates. The proxy field of the 1-form $\omega_1\, \mathrm{d}\,x^1 + \omega_2\, \mathrm{d}\,x^2 + \omega_3\, \mathrm{d}\,x^3$ is the vector field $(\omega_1, \omega_2, \omega_3)$, the proxy field of the 2-form $\omega_{12}\, \mathrm{d}\,x^1 \wedge \mathrm{d}\,x^2 + \omega_{13}\, \mathrm{d}\,x^1 \wedge \mathrm{d}\,x^2 + \omega_{23}\, \mathrm{d}\,x^2 \wedge \mathrm{d}\,x^3$ is the vector field $(\omega_{23}, -\omega_{13}, \omega_{12})$, and the proxy field of the 3-form $\omega_{123}\, \mathrm{d}\,x^1 \wedge \mathrm{d}\,x^2 \wedge \mathrm{d}\,x^3$ is the scalar field ω_{123}. (This holds more generally when Ω is an oriented Riemannian manifold and $\{x^1, x^2, x^3\}$ is any positively oriented orthonormal frame.) When ω is a differential form, denote by $\omega^\sharp$ its proxy field.

Theorem 3.4. *In a tetrahedron $x_0x_1x_2x_3$, the proxy fields of Whitney forms are*

$$\begin{aligned}(\mathcal{W}x_0x_1)^\sharp &= \lambda_0 \nabla\lambda_1 - \lambda_1 \nabla\lambda_0 \\ (\mathcal{W}x_0x_1x_2)^\sharp &= 2(\lambda_0 \nabla\lambda_1 \times \nabla\lambda_2 - \lambda_1 \nabla\lambda_0 \times \nabla\lambda_2 + \lambda_2 \nabla\lambda_0 \times \nabla\lambda_1)\end{aligned}$$

$$(\mathcal{W}x_0x_1x_2x_3)^\sharp = 6\Big(\lambda_0(\nabla\lambda_1 \times \nabla\lambda_2)\cdot\nabla\lambda_3 - \lambda_1(\nabla\lambda_0 \times \nabla\lambda_2)\cdot\nabla\lambda_3$$
$$+ \lambda_2(\nabla\lambda_0 \times \nabla\lambda_1)\cdot\nabla\lambda_3 - \lambda_3(\nabla\lambda_0 \times \nabla\lambda_1)\cdot\nabla\lambda_2\Big)$$

and their values at $x \in x_0x_1x_2x_3$ can be written as

$$(\mathcal{W}x_0x_1)^\sharp(x) = a \times x + b$$
$$(\mathcal{W}x_0x_1x_2)^\sharp(x) = cx + d$$
$$(\mathcal{W}x_0x_1x_2x_3)^\sharp(x) = \pm\frac{1}{|x_0x_1x_2x_3|},$$

where the vectors $a = \pm\frac{x_3-x_2}{6|x_0x_1x_2x_3|}$, $b = \mp\frac{x_3-x_2}{6|x_0x_1x_2x_3|} \times x_2$, and $d = \pm\frac{1}{3|x_0x_1x_2x_3|}x_3$ and the scalar $c = \mp\frac{1}{3|x_0x_1x_2x_3|}$ are constants and the signs depend on whether $\{x_1 - x_0, x_2 - x_0, x_3 - x_0\}$ is a right-handed frame or not.

Proof. Since the gradient ∇f of a function f is $(\mathrm{d}f)^\sharp$ and for 1-forms ω, η, and ξ we have

$$(\omega \wedge \eta)^\sharp = \omega^\sharp \times \eta^\sharp, \quad (\omega \wedge \eta \wedge \xi)^\sharp = (\omega^\sharp \times \eta^\sharp)\cdot\xi^\sharp,$$

the first part follows from Definition 3.1. Since the gradients of barycentric functions are constants, we omit the variable x from them and write

$$\begin{aligned}
(\mathcal{W}x_0x_1)^\sharp(x) &= \lambda_0(x)\nabla\lambda_1 - \lambda_1(x)\nabla\lambda_0 = \nabla\lambda_0\cdot(x-x_2)\nabla\lambda_1 - \nabla\lambda_1\cdot(x-x_2)\nabla\lambda_0 \\
&= (\nabla\lambda_0\cdot x)\nabla\lambda_1 - (\nabla\lambda_1\cdot x)\nabla\lambda_0 - (\nabla\lambda_0\cdot x_2)\nabla\lambda_1 + (\nabla\lambda_1\cdot x_2)\nabla\lambda_0 \\
&= (\nabla\lambda_0 \times \nabla\lambda_1)\times x - (\nabla\lambda_0 \times \nabla\lambda_1)\times x_2.
\end{aligned}$$

Here we used the identity

$$(a \times b)\times c = (a\cdot c)b - (b\cdot c)a. \tag{3.6}$$

Note that in place of x_2 in the vector b we could use any point of x_2x_3.

For any permutation $i_1i_2i_3i_4$ of 1234, the vector $(x_{i_2} - x_{i_3}) \times (x_{i_4} - x_{i_3})$ is orthogonal to $x_{i_2}x_{i_3}x_{i_4}$ and has length equal to $2|x_{i_2}x_{i_3}x_{i_4}|$. On the other hand, $\nabla\lambda_{i_1}$ is orthogonal to $x_{i_2}x_{i_3}x_{i_4}$ and has length equal to the reciprocal of the height of the tetrahedron with respect to the face $x_{i_2}x_{i_3}x_{i_4}$. Hence we have

$$\nabla\lambda_{i_1} = \pm\frac{(x_{i_2} - x_{i_3}) \times (x_{i_4} - x_{i_3})}{6|x_0x_1x_2x_3|}.$$

The sign is $+$ if $\{x_{i_2} - x_{i_3}, x_{i_4} - x_{i_3}, x_{i_1} - x_{i_3}\}$ is a right-handed frame and $-$ otherwise. Using (3.6) again we get

$$\begin{aligned}
\nabla\lambda_{i_1} \times \nabla\lambda_{i_2} &= \pm\frac{(x_{i_2} - x_{i_3}) \times (x_{i_4} - x_{i_3})}{6|x_0x_1x_2x_3|} \times \nabla\lambda_{i_2} = \pm\frac{x_{i_4} - x_{i_3}}{6|x_0x_1x_2x_3|}, \\
(\nabla\lambda_{i_1} \times \nabla\lambda_{i_2})\cdot\nabla\lambda_{i_3} &= \pm\frac{x_{i_4} - x_{i_3}}{6|x_0x_1x_2x_3|}\cdot\nabla\lambda_{i_3} = \frac{\mp 1}{6|x_0x_1x_2x_3|},
\end{aligned}$$

the signs depending as above. Using the handedness of $\{x_1-x_0, x_2-x_0, x_3-x_0\}$ to determine the signs for each permutation, these formulas yield

$$\begin{aligned}
&(\mathcal{W}x_0x_1)^\sharp(x) = (\nabla\lambda_0 \times \nabla\lambda_1)\times x - (\nabla\lambda_0 \times \nabla\lambda_1)\times x_2 = a \times x + b, \\
&(\mathcal{W}x_0x_1x_2)^\sharp(x) = 2(\lambda_0(x)\nabla\lambda_1 \times \nabla\lambda_2 - \lambda_1(x)\nabla\lambda_0 \times \nabla\lambda_2 + \lambda_2(x)\nabla\lambda_0 \times \nabla\lambda_1) \\
&= 2\left(\lambda_0(x)\left(\pm\frac{x_3 - x_0}{6|x_0x_1x_2x_3|}\right) - \lambda_1(x)\left(\pm\frac{x_1 - x_3}{6|x_0x_1x_2x_3|}\right) + \lambda_2(x)\left(\pm\frac{x_3 - x_2}{6|x_0x_1x_2x_3|}\right)\right) \\
&= \pm\frac{1}{3|x_0x_1x_2x_3|}\Big(\big(\lambda_0(x) + \lambda_1(x) + \lambda_2(x)\big)x_3 - \lambda_0(x)x_0 - \lambda_1(x)x_1 - \lambda_2(x)x_2\Big) \\
&= \pm\frac{1}{3|x_0x_1x_2x_3|}\Big(\big(1 - \lambda_3(x)\big)x_3 - \lambda_0(x)x_0 - \lambda_1(x)x_1 - \lambda_2(x)x_2\Big) = \pm\frac{x_3 - x}{3|x_0x_1x_2x_3|} = cx + d, \\
&(\mathcal{W}x_0x_1x_2x_3)^\sharp(x) = 6\Big(\lambda_0(x)(\nabla\lambda_1 \times \nabla\lambda_2)\cdot\nabla\lambda_3 - \lambda_1(x)(\nabla\lambda_0 \times \nabla\lambda_2)\cdot\nabla\lambda_3 \\
&+ \lambda_2(x)(\nabla\lambda_0 \times \nabla\lambda_1)\cdot\nabla\lambda_3 - \lambda_3(x)(\nabla\lambda_0 \times \nabla\lambda_1)\cdot\nabla\lambda_2\Big) = 6\Big(\lambda_0(x)\frac{\pm 1}{6|x_0x_1x_2x_3|} \\
&- \lambda_1(x)\frac{\mp 1}{6|x_0x_1x_2x_3|} + \lambda_2(x)\frac{\pm 1}{6|x_0x_1x_2x_3|} - \lambda_3(x)\frac{\mp 1}{6|x_0x_1x_2x_3|}\Big) = \pm\frac{1}{|x_0x_1x_2x_3|}. \quad \square
\end{aligned}$$

The proxy fields of Whitney forms first appeared in [10] and are sometimes called Whitney elements or Nedelec elements; 1-forms correspond to "edge elements". Be aware that in some places the proxy fields are called just Whitney forms and are given as the definition of Whitney forms. We make the distinction that Whitney forms are always differential forms and Whitney elements mean their proxy fields.

4. Properties of Whitney forms

In this section we discuss the main properties of Whitney forms. Although these are mostly well-known, the kind of list that we have compiled is not easily found in the literature. In particular, we include proofs for all properties that are not evident from the discussion of Section 3. We also try to put emphasis on why these properties are relevant, to explain why one would like to preserve them for generalisations of Whitney forms.

Property 1: Whitney forms are differential forms in a complex

"Whitney forms are differential forms in a complex" concisely summarises their conformity properties on inter-element boundaries. Whitney p-form is an element of the space $F^p(K)$, so it is a set of p-forms ω_σ in the cells σ of K. Thanks to the patch condition in the definition of $F^p(K)$, we can consider this set of p-forms as a single p-form ω such that $\langle \omega(x), \alpha \rangle$ is well-defined for p-vectors α in the plane of the cell τ for which $x \in \tau - \partial\tau$. This reflects how finite element spaces for differential forms are built in FEEC theory [19,36] by first constructing them in each cell and then assembling the local constructions together.

This property ensures that Whitney forms can be used as conforming finite elements and p-forms can be integrated over p-cells in K. Perhaps most importantly, it prescribes what type of objects Whitney forms are in the first place. Hence we propose that all generalisations of Whitney forms should at the very least be differential forms in a complex to be called Whitney forms.

Property 2: W^p is isomorphic to $C_p^*(K)$

That Whitney forms correspond to the cells of K can already be seen from Definition 3.1: to the cochain σ corresponds the Whitney form $\mathcal{W}\sigma$, and Whitney p-forms are the images of the map $\mathcal{W} : C_p^*(K) \to F^p(K)$. The following proposition makes the correspondence more precise.

Proposition 4.1. *The map $\mathcal{W} : C_p^*(K) \to F^p(K)$ is an isomorphism onto its image W^p. Moreover, $\mathcal{C}\mathcal{W}X = X$ for all $X \in C_p^*(K)$.*

Proof. For the first claim it suffices to show that $\mathcal{W}$ is injective, which follows from the second claim. To prove $\mathcal{C}\mathcal{W}X = X$ for all $X \in C_p^*(K)$ it suffices to show that $\int_{\sigma_i} \mathcal{W}\sigma_j = \delta_{ij}$, whence the claim follows by linearity.

That $\int_{\sigma_i} \mathcal{W}\sigma_j = \delta_{ij}$ is perhaps most easily seen using (3.2) or (3.3) and Proposition 3.2. □

Because of this property, integrals on p-cells of K serve as unisolvent degrees of freedom for Whitney p-forms. This means that values of the integrals are in one-to-one correspondence with elements of W^p. Moreover, this correspondence is the simplest possible since $\int_{\sigma_i} \mathcal{W}\sigma_j = \delta_{ij}$. Note that $\sum_{\sigma_i \in S^p} a_i \mathcal{W}\sigma_i = 0$ implies $a_j = \int_{\sigma_j} \sum_{\sigma_i \in S^p} a_i \mathcal{W}\sigma_i = 0\ \forall j$, so the set $\{\mathcal{W}\sigma_i \mid \sigma_i \in S^p\}$ is linearly independent. Since it also spans W^p, it constitutes a basis for W^p.

There are two consequences. Firstly, we can interpolate the cochain $X \in C_p^*(K)$ with the p-form $\mathcal{W}X$, and the integrals of this interpolant match with the values of the cochain on p-simplices: $\mathcal{C}\mathcal{W}X = X$. Secondly, we can approximate the p-form $\omega \in F^p(K)$ with the Whitney form $\mathcal{W}\mathcal{C}\omega$, and the integrals of this approximation match with those of ω on p-simplices: $\mathcal{C}\mathcal{W}\mathcal{C}\omega = \mathcal{C}\omega$. Indeed, Whitney p-forms are commonly considered as a tool for either interpolating p-cochains or approximating differential p-forms.

Property 3: Whitney forms are first order polynomials in each cell

In each cell, barycentric functions are affine and hence their exterior derivatives are constant, so we see from Definition 3.1 that Whitney forms are affine. Hence they are at most first order polynomials in each cell. (That is, if $\omega \in W^p$, the function $x \mapsto \langle \omega(x), \alpha \rangle$ is a first order polynomial for each p-vector α.) This of course implies that they are also smooth in each cell.

Property 4: Whitney forms are affine invariant

In addition to being affine in each cell, Whitney forms are affine objects in the following two senses. First, their definition is meaningful in affine space without any choice of metric. Furthermore, they are invariant under affine transformations.

Proposition 4.2. *Let $\sigma = x_0 \dots x_n$ and $\tau = y_0 \dots y_n$ be two n-simplices and $\varphi : \sigma \to \tau$ affine map such that $\varphi(x_i) = y_i$. Then*

$$\mathcal{W}(x_0 \dots x_p) = \varphi^*(\mathcal{W}(y_0 \dots y_p)) \quad \text{in } \sigma.$$

Proof. Let λ_i denote the barycentric coordinates in σ and μ_i those in τ. Since $\mu_i \circ \varphi$ is affine in σ and $(\mu_i \circ \varphi)(x_j) = \delta_{ij}$, it follows that $\varphi^*(\mu_i) = \mu_i \circ \varphi = \lambda_i$. Hence by the naturality of pullback with respect to wedge product and exterior derivative we have

$$\varphi^*(\mathcal{W}(y_0 \dots y_p)) = \varphi^*(p! \sum_{i=0}^{p} (-1)^i \mu_i \, \mathrm{d}\,\mu_0 \wedge \cdots \wedge \widehat{\mathrm{d}\,\mu_i} \wedge \cdots \wedge \mathrm{d}\,\mu_p)$$

$$= p! \sum_{i=0}^{p} (-1)^i \mu_i \, \mathrm{d}\,\varphi^*(\mu_0) \wedge \cdots \wedge \mathrm{d}\,\widehat{\varphi^*(\mu_i)} \wedge \cdots \wedge \mathrm{d}\,\varphi^*(\mu_p) = \mathcal{W}(x_0 \dots x_p). \quad \square$$

This property is useful because computations done in a reference simplex transfer to all simplices by affine transformations and hence need be done only once. For example, using (3.3),

$$\int_{\varphi(z_0 z_1)} \mathcal{W} y_0 y_1 = \int_{z_0 z_1} \varphi^*(\mathcal{W} y_0 y_1) = \int_{z_0 z_1} \mathcal{W} x_0 x_1 = \frac{\mathrm{vect}(z_0 z_1 x_2 \dots x_n)}{\mathrm{vect}(x_0 \dots x_n)} \quad \text{for } z_0 z_1 \subset \sigma.$$

This equality is also seen from (3.3), since volume ratios are preserved by affine transformations.

Property 5: locality

Whitney form $\mathcal{W}\sigma$ is nonzero only on those simplices that include σ as a face. Locality is needed to make system matrices sparse in numerical methods that utilise Whitney forms.

Property 6: Whitney forms constitute a partition of unity

Barycentric functions sum up to one, forming a partition of unity. The following theorem generalises this property for other Whitney forms.

Theorem 4.3. *In any q-simplex $\tau \in S^q$, for all points x and all p-vectors α in τ,*

$$\sum_{\sigma_i \in S^p} \langle \mathcal{W}\sigma_i(x), \alpha \rangle \, \mathrm{vect}(\sigma_i) = \alpha.$$

Proof. Suppose $\tau = x_0 \dots x_q \in S^q$ and $x \in \tau$. Since the edge vectors $x_i - x_0$ span the plane of τ, all p-vectors in τ can be written as linear combinations of their wedge products. Hence it suffices to consider the case $\alpha = (x_1 - x_0) \wedge \cdots \wedge (x_p - x_0)$, whereafter the claim follows by linearity.

At all points of τ

$$\langle \mathrm{d}\,\lambda_i, x_k - x_j \rangle = \begin{cases} 0 & \text{if } i \notin \{j, k\} \\ 1 & \text{if } i = k \\ -1 & \text{if } i = j \end{cases}$$

and hence for $i_1 < \cdots < i_p$ we have

$$\langle \mathrm{d}\,\lambda_{i_1} \wedge \cdots \wedge \mathrm{d}\,\lambda_{i_p}, (x_1 - x_0) \wedge \cdots \wedge (x_p - x_0) \rangle = \begin{cases} 0 & \text{if } \{i_1, \dots, i_p\} \not\subset \{0, \dots, p\} \\ (-1)^k & \text{if } \{i_1, \dots, i_p\} \subset \{0, \dots, \widehat{k}, \dots, p\} \end{cases}$$

Using this we see that

$$\langle \mathcal{W}(x_{i_0} \dots x_{i_p})(x), \alpha \rangle = 0 \quad \text{if at least two of the indices } i_j \text{ are not in } \{0, \dots, p\}$$

$$\langle \mathcal{W}(x_0 \dots x_{k-1} x_{i_k} x_{k+1} \dots x_p)(x), \alpha \rangle = p!(-1)^k \lambda_{i_k}(x)(-1)^k = p! \lambda_{i_k}(x) \quad \text{for } i_k \notin \{0, \dots, p\}$$

$$\langle \mathcal{W}(x_0 \dots x_p)(x), \alpha \rangle = p! \sum_{j=0}^{p} (-1)^j \lambda_j(x)(-1)^j = p! \sum_{j=0}^{p} \lambda_j(x)$$

Recalling that $\mathcal{W}\sigma_i = 0$ in τ if σ_i is not a face of τ, we can therefore write

$$\sum_{\sigma_i \in S^p} \langle \mathcal{W}\sigma_i(x), \alpha \rangle \operatorname{vect}(\sigma_i)$$
$$= p! \sum_{j=0}^{p} \lambda_j(x) \operatorname{vect}(x_0 \dots x_p) + \sum_{j=p+1}^{q} p! \lambda_j(x) \Big(\sum_{k=0}^{p} \operatorname{vect}(x_0 \dots x_{k-1} x_j x_{k+1} \dots x_p) \Big)$$

After rewriting the first term of the inner sum as

$$\operatorname{vect}(x_j x_1 \dots x_p) = \frac{1}{p!}(x_1 - x_j) \wedge \dots \wedge (x_p - x_j)$$
$$= \frac{1}{p!}\Big(x_1 - x_0 - (x_j - x_0)\Big) \wedge \dots \wedge \Big(x_p - x_0 - (x_j - x_0)\Big) = \frac{1}{p!}(x_1 - x_0) \wedge \dots \wedge (x_p - x_0)$$
$$- \frac{1}{p!} \sum_{l=1}^{p} (x_1 - x_0) \wedge \dots \wedge (x_{l-1} - x_0) \wedge (x_j - x_0) \wedge (x_{l+1} - x_0) \wedge \dots \wedge (x_p - x_0)$$
$$= \operatorname{vect}(x_0 \dots x_p) - \sum_{l=1}^{p} \operatorname{vect}(x_0 \dots x_{l-1} x_j x_{l+1} \dots x_p)$$

the other terms cancel, and we find out that

$$\sum_{\sigma_i \in S^p} \langle \mathcal{W}\sigma_i(x), \alpha \rangle \operatorname{vect}(\sigma_i) = p! \sum_{j=0}^{p} \lambda_j(x) \operatorname{vect}(x_0 \dots x_p) + \sum_{j=p+1}^{q} p! \lambda_j(x) \operatorname{vect}(x_0 \dots x_p)$$
$$= p! \operatorname{vect}(x_0 \dots x_p) = (x_1 - x_0) \wedge \dots \wedge (x_p - x_0) = \alpha. \quad \square$$

As we show next, this partition of unity property actually amounts to saying that W^p contains all constant forms.

Proposition 4.4. *Let $\widetilde{\mathcal{W}} : C_p^*(K) \to F^p(K)$ be any linear map such that $\mathcal{C}\widetilde{\mathcal{W}}X = X$ for all $X \in C_p^*(K)$, and denote by $\widetilde{W}^p$ its image in $F^p(K)$. Then*

i. *a p-form $\omega \in F^p(K)$ is in $\widetilde{W}^p$ if and only if $\widetilde{\mathcal{W}}\mathcal{C}\omega = \omega$.*
ii. *The partition of unity property of Theorem 4.3 holds for $\widetilde{\mathcal{W}}$ if and only if $\widetilde{W}^p$ contains all constant p-forms.*

Proof. i: If $\widetilde{\mathcal{W}}\mathcal{C}\omega = \omega$, then ω is in the image of $\widetilde{\mathcal{W}}$, while if $\omega \in \widetilde{W}^p$, then $\omega = \widetilde{W}X$ for some $X \in C_p^*(K)$, so $\widetilde{\mathcal{W}}\mathcal{C}\omega = \widetilde{\mathcal{W}}\mathcal{C}\widetilde{W}X = \widetilde{\mathcal{W}}X = \omega$.

ii: Suppose first that the partition of unity property holds, and let ω be a constant p-covector. For all points x and all p-vectors α

$$\langle \widetilde{\mathcal{W}}\mathcal{C}\omega(x), \alpha \rangle = \Big\langle \sum_{\sigma_i \in S^p} \Big(\int_{\sigma_i} \omega \Big) \widetilde{\mathcal{W}}\sigma_i(x), \alpha \Big\rangle = \sum_{\sigma_i \in S^p} \Big(\int_{\sigma_i} \omega \Big) \langle \widetilde{\mathcal{W}}\sigma_i(x), \alpha \rangle$$
$$= \sum_{\sigma_i \in S^p} \langle \omega, \operatorname{vect}(\sigma_i) \rangle \langle \widetilde{\mathcal{W}}\sigma_i(x), \alpha \rangle = \Big\langle \omega, \sum_{\sigma_i \in S^p} \langle \widetilde{\mathcal{W}}\sigma_i(x), \alpha \rangle \operatorname{vect}(\sigma_i) \Big\rangle = \langle \omega, \alpha \rangle.$$

Since this holds for all p-vectors α, the p-covectors $\widetilde{\mathcal{W}}\mathcal{C}\omega(x)$ and ω are the same, and since this holds for all x, we have $\widetilde{\mathcal{W}}\mathcal{C}\omega = \omega$. Hence $\omega \in \widetilde{\mathcal{W}}$.

Suppose then that $\widetilde{W}^p$ contains all constant p-forms, and take any point x and any p-vector α. Since constants are in $\widetilde{W}^p$, we have $\widetilde{\mathcal{W}}\mathcal{C}\omega = \omega$ for all p-covectors ω, and hence

$$\langle \omega, \alpha \rangle = \langle \widetilde{\mathcal{W}}\mathcal{C}\omega(x), \alpha \rangle = \Big\langle \sum_{\sigma_i \in S^p} \Big(\int_{\sigma_i} \omega \Big) \widetilde{\mathcal{W}}\sigma_i(x), \alpha \Big\rangle = \sum_{\sigma_i \in S^p} \Big(\int_{\sigma_i} \omega \Big) \langle \widetilde{\mathcal{W}}\sigma_i(x), \alpha \rangle$$
$$= \sum_{\sigma_i \in S^p} \langle \omega, \operatorname{vect}(\sigma_i) \rangle \langle \widetilde{\mathcal{W}}\sigma_i(x), \alpha \rangle = \Big\langle \omega, \sum_{\sigma_i \in S^p} \langle \widetilde{\mathcal{W}}\sigma_i(x), \alpha \rangle \operatorname{vect}(\sigma_i) \Big\rangle.$$

Since this holds for all p-covectors ω, we have $\alpha = \sum_{\sigma_i \in S^p} \langle \widetilde{\mathcal{W}}\sigma_i(x), \alpha \rangle \operatorname{vect}(\sigma_i)$, so the partition of unity property holds. $\square$

Corollary 4.5. *W^p contains all constant p-forms.*

This property ensures that approximating constants with Whitney forms yields exact approximations. It is useful in error analysis [29] and may be needed in convergence proofs [34].

Property 7: exactness

The exactness property or exact sequence property makes precise the good behaviour of Whitney forms with respect to the exterior derivative. We first state a closely related result. Recall that Stokes' theorem implies $\mathcal{C}\,\mathrm{d}\,\omega = \mathrm{d}\,\mathcal{C}\omega$ for all $\omega \in F^p(K)$. Similar property holds for the map $\mathcal{W}$.

Proposition 4.6. *$\mathcal{W}\,\mathrm{d}\,X = \mathrm{d}\,\mathcal{W}X$ for all p-cochains $X \in C_p^*(K)$.*

Proof. By linearity it is sufficient to consider the case $X = \sigma = x_0 \dots x_p$. Let $x_{i_1}, \dots, x_{i_m}$ be the vertices opposite to σ in those $(p+1)$-simplices that have σ as a face. Then the coboundary $\mathrm{d}\,\sigma$ can be written as $\mathrm{d}\,\sigma = \sum_{j=1}^m x_{i_j} x_0 \dots x_p$. By locality property $\mathcal{W}\,\mathrm{d}\,\sigma = 0 = \mathrm{d}\,\mathcal{W}\sigma$ in those simplices that do not have σ as a face, and in σ itself all $(p+1)$-forms are zero. Hence it suffices to show $\mathcal{W}\,\mathrm{d}\,\sigma = \mathrm{d}\,\mathcal{W}\sigma$ in any q-simplex $\tau \in S^q$ of the form $\tau = x_0 \dots x_p x_{p+1} \dots x_q$ for $q > p$.

In τ we have

$$
\begin{aligned}
\mathcal{W}\,\mathrm{d}\,\sigma &= \mathcal{W}\Bigg(\sum_{i=p+1}^{q} x_i x_0 \dots x_p\Bigg) \\
&= \sum_{i=p+1}^{q} (p+1)!\Bigg(\lambda_i\,\mathrm{d}\,\lambda_0 \wedge \dots \wedge \mathrm{d}\,\lambda_p - \sum_{j=0}^{p} (-1)^j \lambda_j\,\mathrm{d}\,\lambda_i \wedge \mathrm{d}\,\lambda_0 \wedge \dots \wedge \widehat{\mathrm{d}\,\lambda_j} \wedge \dots \wedge \mathrm{d}\,\lambda_p\Bigg) \\
&= (p+1)!\Bigg(\sum_{i=p+1}^{q} \lambda_i\,\mathrm{d}\,\lambda_0 \wedge \dots \wedge \mathrm{d}\,\lambda_p - \sum_{j=0}^{p} (-1)^j \lambda_j\,\mathrm{d}\Bigg(\sum_{i=p+1}^{q} \lambda_i\Bigg) \wedge \mathrm{d}\,\lambda_0 \wedge \dots \wedge \widehat{\mathrm{d}\,\lambda_j} \wedge \dots \wedge \mathrm{d}\,\lambda_p\Bigg) \\
&= (p+1)!\Bigg(\sum_{i=p+1}^{q} \lambda_i\,\mathrm{d}\,\lambda_0 \wedge \dots \wedge \mathrm{d}\,\lambda_p + \sum_{j=0}^{p} (-1)^j \lambda_j\,\mathrm{d}\Bigg(\sum_{i=0}^{p} \lambda_i\Bigg) \wedge \mathrm{d}\,\lambda_0 \wedge \dots \wedge \widehat{\mathrm{d}\,\lambda_j} \wedge \dots \wedge \mathrm{d}\,\lambda_p\Bigg) \\
&= (p+1)!\Bigg(\sum_{i=p+1}^{q} \lambda_i\,\mathrm{d}\,\lambda_0 \wedge \dots \wedge \mathrm{d}\,\lambda_p + \sum_{j=0}^{p} \lambda_j\,\mathrm{d}\,\lambda_0 \wedge \dots \wedge \mathrm{d}\,\lambda_p\Bigg) = (p+1)!\,\mathrm{d}\,\lambda_0 \wedge \dots \wedge \mathrm{d}\,\lambda_p
\end{aligned}
$$

By (3.5), this is the same as $\mathrm{d}\,\mathcal{W}\sigma$. □

The exactness property follows from Proposition 4.6. The statement can be formulated as follows.

Proposition 4.7. $\mathrm{d}\,W^p \subset W^{p+1}$*, so we may consider the sequence*

$$
0 \to \mathbb{R} \xrightarrow{\subset} W^0 \xrightarrow{\mathrm{d}} W^1 \xrightarrow{\mathrm{d}} \dots \xrightarrow{\mathrm{d}} W^n \xrightarrow{\mathrm{d}} 0.
$$

In addition, if Ω has trivial homology, then this sequence is exact, so $\ker \mathrm{d}_p = \operatorname{im} \mathrm{d}_{p-1}$ *for $p > 1$.*

Proof. Any Whitney p-form is the image $\mathcal{W}X$ of some $X \in C_p^*(K)$, and $\mathrm{d}\,\mathcal{W}X = \mathcal{W}\,\mathrm{d}\,X$ then says that $\mathrm{d}\,\mathcal{W}X$ is the image of $\mathrm{d}\,X$ and hence a Whitney $(p+1)$-form. Thus $\mathrm{d}\,W^p \subset W^{p+1}$.

Trivial homology implies that also the cohomology groups are trivial, so every p-cochain $X \in C_p^*(K)$ for $p > 0$ such that $\mathrm{d}\,X = 0$ is a coboundary of some $(p-1)$-cochain Y. Suppose $\mathcal{W}X$ is a Whitney p-form such that $\mathrm{d}\,\mathcal{W}X = 0$. Then $\mathcal{W}\,\mathrm{d}\,X = \mathrm{d}\,\mathcal{W}X = 0$, and $\mathrm{d}\,X = 0$ by injectivity of $\mathcal{W}$. Hence $X = \mathrm{d}\,Y$ for some $Y \in C_{p-1}^*(K)$, and $\mathcal{W}X \in \operatorname{im} \mathrm{d}_{p-1}$ since $\mathrm{d}\,\mathcal{W}Y = \mathcal{W}\,\mathrm{d}\,Y = \mathcal{W}X$. Thus $\ker \mathrm{d}_p \subset \operatorname{im} \mathrm{d}_{p-1}$, and by $\mathrm{d}^2 = 0$ we get $\ker \mathrm{d}_p = \operatorname{im} \mathrm{d}_{p-1}$. □

This property is a standard requirement for finite element spaces in FEEC theory [19,36], and it may be decisive for the convergence of numerical methods. For example, in the case of computational electromagnetism it is useful in eliminating finite-dimensional solutions that do not correspond with solutions of Maxwell's equations in cavity resonators, as emphasised by Alain Bossavit [7,29,34].

Property 8: convergence

As discussed before, we can approximate a p-form ω with $\mathcal{W}\mathcal{C}\omega$, and the integrals of this approximation match with those of ω on all p-simplices of K. We also saw by Proposition 4.4 that this approximation is exact if and only if ω is in W^p. We have yet to show the desired property that $\mathcal{W}\mathcal{C}\omega$ converges to ω when the mesh is refined.

This is indeed true, as long as the simplices are not allowed to flatten limitlessly during the refinement process. To make this precise, we employ the metric of $\mathbb{R}^n$ to define the fullness $\Theta(\sigma)$ of the p-simplex σ as the ratio

$$
\Theta(\sigma) = \frac{|\sigma|}{\operatorname{diam}(\sigma)^p}.
$$

The simplices do not flatten limitlessly if there is a uniform lower bound for their fullness. Properties of fullness are discussed in [1]. We need only the following lemma.

Lemma 4.8. *Let $\sigma = x_0 \dots x_p$ be a p-simplex, and denote by h_i the distance from vertex x_i to the plane of the opposite $(p-1)$-face of σ. Let $x = \sum_{i=0}^n \lambda_i x_i$ be any point in σ. Then*

$$h_i \geq p!\Theta(\sigma)\operatorname{diam}(\sigma), \quad \operatorname{dist}(x, \partial\sigma) \geq p!\Theta(\sigma)\operatorname{diam}(\sigma) \min_{i\in\{0,\dots,p\}} \lambda_i.$$

Proof. Let τ_i be the $(p-1)$-face opposite to vertex x_i. Since $|\tau_i| \leq \frac{1}{(p-1)!}\operatorname{diam}(\tau_i)^{p-1}$ and $|\sigma| = \frac{1}{p}|\tau_i|h_i$,

$$h_i = \frac{p|\sigma|}{|\tau_i|} \geq \frac{p|\sigma|}{\frac{1}{(p-1)!}\operatorname{diam}(\tau_i)^{p-1}} \geq p!\Theta(\sigma)\operatorname{diam}(\sigma).$$

The distance from x to the plane of τ_i is $\lambda_i h_i$, so also the second claim follows. □

Now we are ready to prove the convergence property. A similar result has been proved by Jozef Dodziuk [2, Theorem 3.7], but our statement is slightly different and does not restrict to standard subdivisions. We are also in a position to give a much simpler proof using previous results. Below we use the Euclidean metric, as in the definition of fullness, but the choice of metric will only affect the result by up to a constant.

Theorem 4.9. *Let ω be a smooth p-form in Ω. There exists a constant C_ω such that*

$$|\mathcal{WC}\omega(x) - \omega(x)| \leq \frac{C_\omega}{C_\Theta^p} h \quad \text{for all } x \in \tau \text{ in all } \tau \in S^n$$

whenever $h > 0$, $C_\Theta > 0$, and K is a simplicial complex in Ω such that $\operatorname{diam}(\sigma) \leq h$ and $\Theta(\sigma) \geq C_\Theta$ for all simplices σ of K.

Proof. It suffices to prove this for $\omega = \omega_I \,\mathrm{d}x^{i_1} \wedge \dots \wedge \mathrm{d}x^{i_p}$ where $1 \leq i_1 < \dots < i_p \leq n$. Since ω is smooth in the polyhedron Ω, ω_I admits a smooth extension to a neighbourhood of Ω. The partial derivatives of ω_I are hence bounded in Ω, and we can find a constant C_I such that $|\omega_I(x) - \omega_I(y)| \leq C_I|x-y|$ whenever $yx \subset \Omega$.

Fix $\tau \in S^n$ and $y \in \tau$. We can write

$$\begin{aligned} &\omega(x) = \omega_I(x)\,\mathrm{d}x^{i_1} \wedge \dots \wedge \mathrm{d}x^{i_p} = (\omega_I(y) + g(x))\,\mathrm{d}x^{i_1} \wedge \dots \wedge \mathrm{d}x^{i_p}, \quad \text{where} \\ &g(x) = \omega_I(x) - \omega_I(y), \quad |g(x)| \leq C_I|x-y| \leq C_I h \quad \text{if } x \in \tau. \end{aligned}$$

Using Proposition 4.4 and Corollary 4.5,

$$\begin{aligned} &\mathcal{WC}\omega(x) = \omega_I(y)\,\mathrm{d}x^{i_1} \wedge \dots \wedge \mathrm{d}x^{i_p} + \mathcal{WC}(g\,\mathrm{d}x^{i_1} \wedge \dots \wedge \mathrm{d}x^{i_p})(x), \\ &\mathcal{WC}\omega(x) - \omega(x) = \mathcal{WC}(g\,\mathrm{d}x^{i_1} \wedge \dots \wedge \mathrm{d}x^{i_p})(x) - g(x)\,\mathrm{d}x^{i_1} \wedge \dots \wedge \mathrm{d}x^{i_p}. \end{aligned}$$

When σ is a p-face of τ, we have $|\int_\sigma g\,\mathrm{d}x^{i_1} \wedge \dots \wedge \mathrm{d}x^{i_p}| \leq |\sigma|C_I h$, and hence in τ

$$|\mathcal{WC}(g\,\mathrm{d}x^{i_1} \wedge \dots \wedge \mathrm{d}x^{i_p})(x)| = \left| \sum_{\sigma\subset\tau} \left(\int_\sigma g\,\mathrm{d}x^{i_1} \wedge \dots \wedge \mathrm{d}x^{i_p} \right) \mathcal{W}\sigma(x) \right| \leq \sum_{\sigma\subset\tau} |\sigma|C_I h|\mathcal{W}\sigma(x)|,$$

where the sum is over the p-faces σ of τ.

Now the affine invariance property proves useful since we can work in the standard n-simplex $\Delta^n = y_0 y_1 \dots y_n$, where $y_0 = (0,\dots,0)$ and $y_i = (0,\dots,0,1,0,\dots,0)$ has 1 in the ith slot for $1 \leq i \leq n$. Consider one of the p-faces σ and label the vertices of $\tau = x_0 x_1 \dots x_n$ such that $\sigma = x_0 \dots x_p$. Let φ be the affine map from τ to Δ^n such that $\varphi(x_i) = y_i$. Proposition 4.2 and the pullback inequality $|f^*\omega(x)| \leq |Df(x)|^p \cdot |\omega(f(x))|$ of p-forms [1, II, 4.12] give

$$|\mathcal{W}\sigma(x)| = |\mathcal{W}(x_0 \dots x_p)(x)| = |\varphi^*(\mathcal{W}(y_0 \dots y_p))(x)| \leq |D\varphi(x)|^p |\mathcal{W}(y_0 \dots y_p)(\varphi(x))|.$$

Next we find a bound for $|D\varphi(x)|$. Denote by $z = \sum_{i=0}^n \frac{1}{n+1} x_i$ the barycentre of τ, and take v such that $|v| = 1$ and $|D\varphi(z)v| = \max_{|w|=1} |D\varphi(z)w|$. Let $t = \operatorname{dist}(z, \partial\tau)$; by Lemma 4.8 we have $t \geq \frac{n!}{n+1}\Theta(\tau)\operatorname{diam}(\tau)$. Now z and $z + tv$ are both in τ, so $\varphi(z)$ and $\varphi(z+tv)$ are in Δ^n, which has diameter $\sqrt{2}$. Since φ is affine,

$$|D\varphi(x)| = |D\varphi(z)| = |D\varphi(z)v| = \frac{|\varphi(z+tv) - \varphi(z)|}{t} \leq \frac{\sqrt{2}}{\frac{n!}{n+1}\Theta(\tau)\operatorname{diam}(\tau)}.$$

To compute $\mathcal{W}(y_0 \dots y_p)$ we note that the barycentric coordinates in Δ^n are $\lambda_i = x^i$ for $1 \le i \le n$ and $\lambda_0 = 1 - \sum_{i=1}^n x^i$. Hence

$$\begin{aligned}
&\mathcal{W}(y_0 \dots y_p) \\
&= p!\Big((1 - \sum_{i=1}^n x^i)\,\mathrm{d}x^1 \wedge \cdots \wedge \mathrm{d}x^p + \sum_{j=1}^p (-1)^j x^j\,\mathrm{d}(1 - \sum_{i=1}^n x^i) \wedge \mathrm{d}x^1 \wedge \cdots \wedge \widehat{\mathrm{d}x^j} \wedge \cdots \wedge \mathrm{d}x^p\Big) \\
&= p!\Big((1 - \sum_{i=p+1}^n x^i)\,\mathrm{d}x^1 \wedge \cdots \wedge \mathrm{d}x^p + \sum_{j=1}^p \sum_{i=p+1}^n (-1)^{p+j} x^j\,\mathrm{d}x^1 \wedge \cdots \wedge \widehat{\mathrm{d}x^j} \wedge \cdots \wedge \mathrm{d}x^p \wedge \mathrm{d}x^i\Big)
\end{aligned}$$

and

$$|\mathcal{W}(y_0 \dots y_p)| = p! \sqrt{\Big(1 - \sum_{i=p+1}^n x^i\Big)^2 + (n-p)\sum_{i=1}^p (x^i)^2} \le p!\sqrt{1+n-p} \quad \text{in } \Delta^n.$$

Using these estimates and the facts that $\operatorname{diam}(\tau) \ge \operatorname{diam}(\sigma)$ and $|\sigma| \le \frac{1}{p!}\operatorname{diam}(\sigma)^p$, we get

$$\begin{aligned}
&\sum_{\sigma \subset \tau} |\sigma| C_I h |\mathcal{W}\sigma(x)| \le \sum_{\sigma \subset \tau} |\sigma| C_I h \Big(\frac{\sqrt{2}}{\frac{n!}{n+1}\Theta(\tau)\operatorname{diam}(\tau)}\Big)^p p!\sqrt{1+n-p} \\
&\le \sum_{\sigma \subset \tau} C_I h \Big(\frac{\sqrt{2}}{\frac{n!}{n+1}\Theta(\tau)}\Big)^p \sqrt{1+n-p} = \frac{C_I \binom{n+1}{p+1}\big(\frac{\sqrt{2}(n+1)}{n!}\big)^p \sqrt{1+n-p}}{\Theta(\tau)^p} h.
\end{aligned}$$

This holds for all $\tau \in S^n$, so we may choose $C_\omega = C_I\binom{n+1}{p+1}\big(\frac{\sqrt{2}(n+1)}{n!}\big)^p\sqrt{1+n-p} + C_I$, and then

$$\begin{aligned}
&|\mathcal{W}\mathcal{C}\omega(x) - \omega(x)| \le |\mathcal{W}\mathcal{C}(g\,\mathrm{d}x^{i_1} \wedge \cdots \wedge \mathrm{d}x^{i_p})(x)| + |g(x)\,\mathrm{d}x^{i_1} \wedge \cdots \wedge \mathrm{d}x^{i_p}| \\
&\le \sum_{\sigma \subset \tau} |\sigma| C_I h |\mathcal{W}\sigma(x)| + C_I h \le \frac{C_\omega}{C_\Theta^p} h \quad \text{for all } x \in \tau \text{ in all } \tau \in S^n,
\end{aligned}$$

which concludes the proof of the theorem. □

5. Generalisations of Whitney forms

To further clarify the concept of Whitney forms, we consider what other possibilities go by this name in the literature. In contrast to the three equivalent definitions given in Section 3, the Whitney forms considered in this section are generalisations of Whitney forms. By this we mean that they are not equivalent to the standard Whitney forms but are sufficiently related so that calling them by the same name is justified. As we shall see, they also preserve certain properties of standard Whitney forms.

5.1. Whitney forms on a manifold

In the initial context of Whitney forms, the simplicial complex K is embedded in affine space. In this subsection we consider the generalisation to the case where K is a smooth simplicial complex on a compact smooth manifold Ω. Now p-simplices are maps $\sigma : \Delta^p \to \Omega$ from the standard p-simplex Δ^p to Ω. The faces of σ are its restrictions $\sigma|_\tau$ to the faces τ of Δ^p. Since the q-faces of Δ^p can be identified with Δ^q, each q-face of σ yields a map from Δ^q to Ω. Hence the q-faces of σ are q-simplices.

In this subsection we assume K is a finite set of simplices σ such that

- The restriction of each $\sigma : \Delta^p \to \Omega$ to $\Delta^p - \partial\Delta^p$ is a diffeomorphism onto its image, and each point $x \in \Omega$ is contained in the image of exactly one such restriction
- Each face of every simplex in K is also in K
- The intersection of the images of two simplices in K is either the image of a common face of theirs or the empty set
- Each p-simplex has $p+1$ distinct vertices (0-faces), and no other p-simplex has this same set of vertices

Chains and cochains of K can be defined similarly as before. Now $\sigma = x_0 \dots x_p$ means that the p-simplex σ maps the vertices of Δ^p to $x_0, \dots, x_p$. Differential p-form in K is a set of smooth p-forms ω_σ in the images of the simplices σ of K satisfying the following patch condition: if τ is a q-face of σ, then the trace $\omega_\sigma|_{\tau(\Delta^q)}$ equals ω_τ in $\tau(\Delta^q)$. The exterior derivative and the de Rham map are well-defined.

Barycentric functions in Ω can be defined as follows. Let $x \in \Omega$ and let $\sigma = x_0 \dots x_p$ be the p-simplex (p depending on x) such that x is in the image of the restriction of σ to $\Delta^p - \partial\Delta^p$. Then the $\lambda_i(x)$ for $0 \le i \le p$ are the barycentric coordinates of $\sigma^{-1}(x)$ with respect to the corresponding vertices of Δ^p. For other vertices $\lambda_i(x) = 0$. The Whitney

p-form $\mathcal{W}\sigma$ corresponding to a p-simplex σ of K can now be defined with the same formula (3.1). Define the map $\mathcal{W} : C_p^*(K) \to F^p(K)$ by extending linearly and the space of Whitney p-forms W^p as its image. By the same arguments as before, $\mathcal{W}\sigma$ is in $F^p(K)$, so property 1 is fulfilled.

The definition given above amounts to taking pullback as follows. If $\sigma \in S^p$ is a face of $\tau \in S^q$ and σ' is the p-face of Δ^q such that $\sigma = \tau|_{\sigma'}$, then $\mathcal{W}\sigma$ is the pullback $\tau^{-1*}(\mathcal{W}\sigma')$ in $\tau(\Delta^q)$, where $\mathcal{W}\sigma'$ is the Whitney p-form corresponding to σ' in Δ^q. Hence

$$\int_{\sigma_i(\Delta^p)} \mathcal{W}\sigma_j = \int_{\tau(\sigma_i')} \tau^{-1*}(\mathcal{W}\sigma_j') = \int_{\sigma_i'} \mathcal{W}\sigma_j' = \delta_{ij}$$

if σ_i and σ_j are p-faces of τ, so our earlier discussion about property 2 applies here as well. If σ is not a face of τ, then $\mathcal{W}\sigma = 0$ in $\tau(\Delta^q)$, so property 5 holds too.

The same proof as before shows that property 7 holds. A convergence property similar to property 8 has been proved in [2] using standard subdivisions. For this Ω is assumed to be a Riemannian manifold so that the Riemannian metric induces a norm for p-covectors at each point of Ω.

However, not all of the properties are preserved. On a manifold we do not have the affine structure of affine space. We can no longer identify the tangent spaces of different points, so there are no such things as p-vector of σ or constant p-forms (for $p > 0$). Thus properties 3 and 6 do not make sense as such, and the partition of unity property only holds for 0-forms. Property 4 is also lost, although Proposition 4.2 works if σ is a diffeomorphism that preserves barycentric functions.

Although most of the properties of Whitney forms hold also when the complex K is on a manifold Ω, the affine character of Whitney forms – a central property in their initial context – is not visible on a manifold since there is no affine structure. This is the reason why we consider Whitney forms on a manifold to be generalisations of Whitney forms.

5.2. Higher order Whitney forms

Higher order finite elements are appreciated for better accuracy and convergence properties. There are also higher order Whitney forms, or at least this term has appeared in the literature several times [30–32,34,36,37]. In this subsection, we explain what these are and which properties of Whitney forms are preserved by their higher order generalisations. The discussion is limited to higher order differential forms on simplices. In the literature one can find higher order finite elements also on other cell types (see e.g. [38–43]). However, these are typically not called Whitney forms in the literature, and one would have to give up on even more of the properties, so we leave this kind of extensions out of scope of this paper.

Higher order Whitney forms are differential forms in a simplicial complex K. (Here the complex K is again embedded in affine space, and we assume Ω is a polyhedron in $\mathbb{R}^n$.) Property 1 is hence to be fulfilled by construction. We denote by W_k^p the space of Whitney p-forms of order k. We will next define W_k^p by giving a set of elements of $F^p(K)$ that span W_k^p.

Let $\mathcal{I}(n+1,k)$ denote the set of multi-indices with $n+1$ components that sum to k; that is, $\mathcal{I}(n+1,k)$ consists of arrays $\mathbf{k} = (k_0, k_1, \dots, k_n)$ where the k_i are nonnegative integers such that $\sum_{i=0}^n k_i = k$. For a fixed n-simplex $\sigma = x_0 \dots x_n$, denote by $\lambda_\sigma^{\mathbf{k}}$ the function $\prod_{i=0}^n (\lambda_i)^{k_i}$. This is a continuous function in Ω, and hence its product with any Whitney p-form is in $F^p(K)$. We may therefore define for $k \geq 1$

$$W_k^p = \operatorname{span}\{\lambda_\sigma^{\mathbf{k}} \mathcal{W}\tau \mid \sigma = x_0 \dots x_n \in S^n,\ \mathbf{k} \in \mathcal{I}(n+1, k-1),\ \text{and } \tau \text{ is a } p\text{-face of } \sigma\}. \tag{5.1}$$

Note that $W_1^p = W^p$.

The spaces of higher order Whitney forms could also be defined using the Koszul operator [19,36]. In terms of their proxy fields, the 1-forms in 2D were first given in [9] and the 1- and 2-forms in 3D in [10]. They have subsequently been studied e.g. in [44–51]. It is shown in [52] that W_k^p by our definition is the same as the space $\mathcal{P}_k^- \Lambda^p$ in FEEC theory [19,36]. This space is constructed such that it includes all polynomials of order $\leq k-1$ and its elements are at most kth order polynomials in each simplex. Property 3 hence takes the obvious form for kth order Whitney forms.

Since W^p is already isomorphic to $C_p^*(K)$ and increasing the order increases the dimension of the space, one immediately sees that property 2 cannot hold. The de Rham map $\mathcal{C}$ from W_k^p to $C_p^*(K)$ is not injective, and we do not even have the map $\mathcal{W}$ from $C_p^*(K)$ to W_k^p. To approximate elements of $F^p(K)$ in W_k^p, one must first determine suitable degrees of freedom, as the integrals over p-cells no longer define a unique element of W_k^p. There are at least three ways to do this [37]. We consider the so-called small simplices of [32], for this yields us at least some kind of map from cochains to W_k^p and enables us to interpret generalisations of properties that involved the map $\mathcal{W}$.

Small simplices are homothetic images of the simplices of K. For a fixed n-simplex $\sigma = x_0 \dots x_n$, each multi-index $\mathbf{k} \in \mathcal{I}(n+1, k-1)$ defines a map, which we denote by $\mathbf{k}_\sigma$, from σ to itself such that the point x whose barycentric coordinates are λ_i maps to the point whose barycentric coordinates are $\frac{\lambda_i + k_i}{k}$. In other words, $\mathbf{k}_\sigma$ is defined by

$$\mathbf{k}_\sigma : \sigma \to \sigma, \quad \lambda_0 x_0 + \dots + \lambda_n x_n \mapsto \frac{\lambda_0 + k_0}{k} x_0 + \dots + \frac{\lambda_n + k_n}{k} x_n.$$

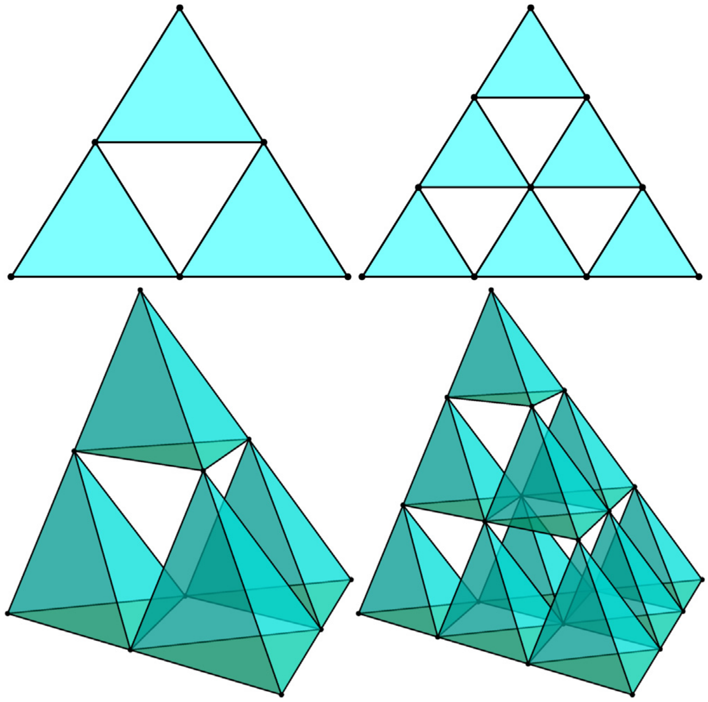

Fig. 2. Second and third order small simplices $\mathbf{k}_\sigma(\sigma)$ in the cases when σ is a triangle in two dimensions and a tetrahedron in three dimensions.

The set of kth order small p-simplices of K is

$$S_k^p = \{\mathbf{k}_\sigma(\tau) \mid \sigma = x_0 \dots x_n \in S^n,\ \mathbf{k} \in \mathcal{I}(n+1, k-1), \text{ and } \tau \text{ is a } p\text{-face of } \sigma\}. \tag{5.2}$$

Note from (5.1) and (5.2) that the small p-simplices of order k correspond exactly to the spanning p-forms of W_k^p. When required, we use label υ for elements of S_k^p and denote by $w(\upsilon)$ the corresponding p-form. See Fig. 2 for examples of small simplices.

Although the small n-simplices do not pave Ω, we can form a subdivision of K that contains the kth order small simplices of K as cells; denote this subdivision by K_k. Not all the cells of K_k are necessarily simplices, but it is a cell complex nevertheless, and we may hence consider p-chains $C_p(K_k)$, p-cochains $C_p^*(K_k)$, and the de Rham map of K_k.

Integrals over the small simplices S_k^p serve as degrees of freedom for W_k^p, but these are overdetermining, as the spanning p-forms in (5.1) are not linearly independent. To obtain unisolvent degrees of freedom, one can choose a subset of S_k^p such that the integrals over this subset uniquely determine an element of W_k^p by omitting redundant small simplices. This yields a linear map $\mathcal{V} : C_p^*(K_k) \to W_k^p$ such that the values of all cochains $X \in C_p^*(K_k)$ match with the integrals of $\mathcal{V}X$ on the chosen subset of S_k^p. Then we have $\mathcal{C}\mathcal{V}X = X$ for all $X \in \mathcal{C}(W_k^p)$ and $\mathcal{V}\mathcal{C}\omega = \omega$ for all $\omega \in W_k^p$ — this is closest to property 2 that one can get.

We immediately see that $w(\upsilon)$ is nonzero in n-simplex $\sigma \in S^n$ only if $\upsilon \subset \sigma$, so the spanning p-forms in (5.1) are local; this is the counterpart of property 5. Likewise, the affine invariance property continues to hold, and Proposition 4.2 now says $w(\mathbf{k}_\sigma(x_0 \dots x_p)) = \varphi^*(w(\mathbf{k}_\tau(y_0 \dots y_p)))$. It has been proved e.g. in [19] that also the exact sequence property holds.

As for the partition of unity property, there are two interpretations. On one hand, Theorem 4.3 implies that in any n-simplex $\tau \in S^n$, for all p-vectors α and all points x in τ

$$\sum_{\substack{\tau \supset \sigma_i \in S^p \\ \mathbf{k} \in \mathcal{I}(n+1,k-1)}} \frac{(k-1)!}{k_0! k_1! \dots k_n!} \langle w(\mathbf{k}_\tau(\sigma_i))(x), \alpha \rangle \operatorname{vect}(\sigma_i) = \alpha;$$

this follows from the multinomial theorem. On the other hand, we have

$$\sum_{\upsilon_i \in S_k^p} \langle \mathcal{V}\upsilon_i(x), \alpha \rangle \operatorname{vect}(\upsilon_i) = \alpha. \tag{5.3}$$

To show (5.3), note that the requirement $\mathcal{C}\widetilde{\mathcal{W}}X = X$ for all $X \in C_p^*(K)$ in Proposition 4.4 can be replaced with $\mathcal{C}\widetilde{\mathcal{W}}X = X$ for all $X \in \mathcal{C}(\widetilde{W}^p)$ by requiring in addition that $\mathcal{C}$ be injective in $\widetilde{W}^p$. Using this for the map $\mathcal{V}$ yields (5.3), since W_k^p contains all constant p-forms.

Finally, for the convergence property one expects an improvement: higher order Whitney forms should enable higher order convergence. This is indeed true. The proof is similar as in the lowest order case, but we have included it below to bring also the higher order approximation property into Whitney's setting.

Theorem 5.1. *Let $\mathcal{V} : C_p^*(K_k) \to W_k^p$ be the linear map obtained with a choice of kth order small simplices as explained above, and let ω be a smooth p-form in Ω. There exists a constant $C_{\omega,k}$ such that*

$$|\mathcal{V}\mathcal{C}\omega(x) - \omega(x)| \le \frac{C_{\omega,k}}{C_\Theta^p} h^k \quad \text{for all } x \in \tau \text{ in all } \tau \in S^n$$

whenever $h > 0$, $C_\Theta > 0$, and K is a simplicial complex in Ω such that $\operatorname{diam}(\sigma) \le h$ and $\Theta(\sigma) \ge C_\Theta$ for all simplices σ of K.

Proof. It suffices to prove this for $\omega = \omega_I \,\mathrm{d}x^{i_1} \wedge \cdots \wedge \mathrm{d}x^{i_p}$ where $1 \le i_1 < \cdots < i_p \le n$. Denote by T_y the $(k-1)$th order Taylor polynomial of ω_I at y. Since ω is smooth in the polyhedron Ω, we can find a constant C_I such that $|\omega_I(x) - T_y(x)| \le C_I |x-y|^k$ whenever $yx \subset \Omega$.

Fix $\tau \in S^n$ and $y \in \tau$. We can write

$$\omega(x) = \omega_I(x)\,\mathrm{d}x^{i_1} \wedge \cdots \wedge \mathrm{d}x^{i_p} = (T_y(x) + g(x))\,\mathrm{d}x^{i_1} \wedge \cdots \wedge \mathrm{d}x^{i_p}, \quad \text{where}$$
$$g(x) = \omega_I(x) - T_y(x), \quad |g(x)| \le C_I|x-y|^k \le C_I h^k \quad \text{if } x \in \tau.$$

Since the constant $\mathrm{d}x^{i_1} \wedge \cdots \wedge \mathrm{d}x^{i_p}$ is in W^p (by Corollary 4.5) and T_y is in the span of the products $\lambda^{\mathbf{k}}$ with $\mathbf{k} \in \mathcal{I}(n+1, k-1)$ (it is a polynomial of order $k-1$), we see from (5.1) that $T_y\,\mathrm{d}x^{i_1} \wedge \cdots \wedge \mathrm{d}x^{i_p}$ is in W_k^p. Hence $\mathcal{V}\mathcal{C}(T_y\,\mathrm{d}x^{i_1} \wedge \cdots \wedge \mathrm{d}x^{i_p}) = T_y\,\mathrm{d}x^{i_1} \wedge \cdots \wedge \mathrm{d}x^{i_p}$ and

$$\mathcal{V}\mathcal{C}\omega(x) = T_y(x)\,\mathrm{d}x^{i_1} \wedge \cdots \wedge \mathrm{d}x^{i_p} + \mathcal{V}\mathcal{C}(g\,\mathrm{d}x^{i_1} \wedge \cdots \wedge \mathrm{d}x^{i_p})(x),$$
$$\mathcal{V}\mathcal{C}\omega(x) - \omega(x) = \mathcal{V}\mathcal{C}(g\,\mathrm{d}x^{i_1} \wedge \cdots \wedge \mathrm{d}x^{i_p})(x) - g(x)\,\mathrm{d}x^{i_1} \wedge \cdots \wedge \mathrm{d}x^{i_p}.$$

Denote by $\hat{S}_k^p$ the chosen subset of S_k^p and by $\hat{S}_k^p(\tau)$ its restriction to those small simplices that are in τ. The interpolant $\mathcal{V}\mathcal{C}(g\,\mathrm{d}x^{i_1} \wedge \cdots \wedge \mathrm{d}x^{i_p})$ is a linear combination $\sum_{\upsilon_i \in \hat{S}_k^p} \alpha_i w(\upsilon_i)$ of the spanning forms $w(\upsilon_i)$. Since $w(\upsilon) = 0$ in τ if $\upsilon \not\subset \tau$, it suffices to consider $\sum_{\upsilon_i \in \hat{S}_k^p(\tau)} \alpha_i w(\upsilon_i)$. Each coefficient α_i is a linear combination of the integrals $\int_{\upsilon_j} g\,\mathrm{d}x^{i_1} \wedge \cdots \wedge \mathrm{d}x^{i_p}$, $\upsilon_j \in \hat{S}_k^p(\tau)$. The coefficients of this latter linear combination are constant and affine-invariant quantities (determined by the inverse of the matrix A with components $A_{ij} = \int_{\upsilon_i} w(\upsilon_j)$). Hence there exists a constant C_α such that

$$|\alpha_i| \le C_\alpha \sum_{\upsilon_j \in \hat{S}_k^p(\tau)} \left|\int_{\upsilon_j} g\,\mathrm{d}x^{i_1} \wedge \cdots \wedge \mathrm{d}x^{i_p}\right| \le C_\alpha \sum_{\upsilon_j \in \hat{S}_k^p(\tau)} C_I h^k |\upsilon_j|$$

holds for all of the coefficients α_i. Using the facts that $\operatorname{diam}(\tau) \ge \operatorname{diam}(\upsilon_j)$ and $|\upsilon_j| \le \frac{1}{p!}\operatorname{diam}(\upsilon_j)^p$ and denoting by C_k the cardinality of $\hat{S}_k^p(\tau)$, we get

$$|\alpha_i| \le C_\alpha C_k C_I h^k \frac{1}{p!} \operatorname{diam}(\tau)^p.$$

To find a bound for the $|w(\upsilon_i)|$, suppose that υ_i is the image of the p-face $\sigma \subset \tau$. Then clearly $|w(\upsilon_i)(x)| \le |\mathcal{W}\sigma(x)|\ \forall x \in \tau$, and hence using the affine map to the standard n-simplex exactly in the same way as in the proof of Theorem 4.9 we find

$$|w(\upsilon_i)(x)| \le \left(\frac{\sqrt{2}}{\frac{n!}{n+1}\Theta(\tau)\operatorname{diam}(\tau)}\right)^p p!\sqrt{1+n-p} \quad \text{for all } x \in \tau.$$

Combining these estimates yields

$$|\mathcal{V}\mathcal{C}(g\,\mathrm{d}x^{i_1} \wedge \cdots \wedge \mathrm{d}x^{i_p})(x)| = \Big|\sum_{\upsilon_i \in \hat{S}_k^p(\tau)} \alpha_i w(\upsilon_i)(x)\Big| \le \sum_{\upsilon_i \in \hat{S}_k^p(\tau)} |\alpha_i||w(\upsilon_i)(x)|$$
$$\le C_k^2 C_\alpha C_I \left(\frac{\sqrt{2}}{\frac{n!}{n+1}\Theta(\tau)}\right)^p \sqrt{1+n-p} \cdot h^k \quad \text{for all } x \in \tau.$$

This holds for all $\tau \in S^n$, so we may choose $C_{\omega,k} = C_k^2 C_\alpha C_I \left(\frac{\sqrt{2}}{\frac{n!}{n+1}}\right)^p \sqrt{1+n-p} + C_I$, and then

$$|\mathcal{V}\mathcal{C}\omega(x) - \omega(x)| \le |\mathcal{V}\mathcal{C}(g\,\mathrm{d}x^{i_1} \wedge \cdots \wedge \mathrm{d}x^{i_p})(x)| + |g(x)\,\mathrm{d}x^{i_1} \wedge \cdots \wedge \mathrm{d}x^{i_p}|$$
$$\le C_k^2 C_\alpha C_I \left(\frac{\sqrt{2}}{\frac{n!}{n+1}\Theta(\tau)}\right)^p \sqrt{1+n-p} \cdot h^k + C_I h^k \le \frac{C_{\omega,k}}{C_\Theta^p} h^k \quad \text{for all } x \in \tau \text{ in all } \tau \in S^n. \quad \square$$

5.3. Whitney forms on other cells than simplices

Standard Whitney forms are differential forms in a simplicial complex. For flexibility in modelling and mesh generation, also other kind of cells should be allowed, and there have been several approaches to generalising Whitney forms for nonsimplicial cells. In this subsection, we consider the case where K is a cell complex of convex polyhedral cells.

When moving to nonsimplicial cells, we would like to preserve at least properties 1 and 2 of Whitney forms, so we take these as a guideline. Firstly, as stated earlier, all Whitney forms should be differential forms in the complex K — elements of $F^p(K)$. Secondly, there should be a Whitney p-form $\mathcal{W}\sigma$ corresponding to each p-cell σ of K, so that we get a linear map $\mathcal{W} : C^*_p(K) \to F^p(K)$ whose image is the space of Whitney p-forms W^p. In addition, $\mathcal{W}$ should be an isomorphism onto its image, so that integrals over p-cells uniquely determine an element of W^p and serve as degrees of freedom. Without loss of generality, we may then also require that $\int_{\sigma_i} \mathcal{W}\sigma_j = \delta_{ij}$, which is probably the best-known property of Whitney forms. Property 5, locality, will be fulfilled by all constructions without further mention.

In general, properties 3 and 4 as such will be lost. This is inevitable: a first order polynomial would already be fixed by its values on $n+1$ vertices, and there is no affine map like in Proposition 4.2 between more general cells. However, for some cell types there is a same kind of canonical map (maybe not affine) and Whitney forms on one cell move onto another through taking pullback. For example, any cube is obtained from the reference cube $[0, 1]^3$ with the obvious map after the image of one vertex is fixed, and to define Whitney forms on cubes it suffices to consider the reference cube. The same applies to for example triangular prisms and pyramids.

To define Whitney forms for a convex polyhedral cell, we may consider the cell and its faces as the cell complex K so that there is only one n-cell. In doing so, we must ensure that traces on faces depend only on the face itself, so that the same Whitney forms belong to $F^p(K)$ also in the case when K has many n-cells. The complex K may even contain different kind of cells, as long as traces on faces shared by two such cells are the same according to both constructions.

From the literature, we have chosen two constructions that we believe best preserve the properties of Whitney forms. These will be discussed below. More options can be found in the literature if one is willing to give up on more of the properties (see e.g. [53–56]). In particular we would like to mention [54], where the author shows a way to construct finite-dimensional spaces of differential forms on arbitrary polytopes in any dimension such that the basis p-forms correspond to the p-cells and the spaces fulfil the exact sequence property. It requires auxiliary spaces on a simplicial refinement of the complex, and as these one can use Whitney forms. However, the resulting forms are in $F^p(K')$ with respect to the refinement K' and not necessarily in $F^p(K)$ with respect to the initial complex K (discontinuities are allowed in the cells of K). Another downside is that explicit expressions for the basis forms are not given on general polytopes, so they might not be easily computable.

The rest of this subsection is divided into parts as follows. First we briefly discuss two relevant approaches to generalising Whitney forms. The first approach is based on the construction of [57] and generalised barycentric coordinates. The second approach [29] is based on geometric conation and extrusion operations and constructs Whitney forms for cells obtained with these operations recursively. Finally, we summarise the Whitney forms resulting from these approaches on cubes, triangular prisms, and pyramids in 3D.

5.3.1. Construction based on generalised barycentric functions

Whitney forms in a simplicial complex were built using barycentric functions. These are exclusive to simplicial complexes, but for nonsimplicial cells there are generalised barycentric coordinates, which are no longer unique. Suppose σ is a convex polyhedral p-cell in $\mathbb{R}^n$ with m vertices $x_1, \ldots, x_m$. Any set of m nonnegative functions $\lambda_i : \sigma \to \mathbb{R}$ are called generalised barycentric coordinates in σ if for all $x \in \sigma$

$$\sum_{i=1}^{m} \lambda_i(x) = 1, \quad \sum_{i=1}^{m} \lambda_i(x) x_i = x. \tag{5.4}$$

Note that generalised barycentric coordinates in σ restrict to generalised barycentric coordinates on its faces.

The functions λ_i are not uniquely determined by (5.4) for general cells, and there are different kind of generalised barycentric coordinates (see the references in [56] and [57]). On simplices, these all reduce to the standard barycentric coordinates. Generalised barycentric functions in K are defined after we choose barycentric coordinates in each cell such that their restrictions agree on inter-element faces. This is typically ensured by using the same kind of coordinates on incident cells [56].

In [56] and [57], Whitney forms are generalised for nonsimplicial cells by taking generalised barycentric functions as Whitney 0-forms and using the same formula (3.1) (without the multiplier $p!$) for 1- and 2-forms. This gives the 1-form $\lambda_i \, \mathrm{d}\lambda_j - \lambda_j \, \mathrm{d}\lambda_i$ for any two vertices x_i and x_j and the 2-form $\lambda_i \, \mathrm{d}\lambda_j \wedge \mathrm{d}\lambda_k - \lambda_j \, \mathrm{d}\lambda_i \wedge \mathrm{d}\lambda_k + \lambda_k \, \mathrm{d}\lambda_i \wedge \mathrm{d}\lambda_j$ for any three vertices x_i, x_j, and x_k. (In [56] and [57], the forms are given in terms of their proxy fields.) These do not correspond to the cells of K, but they are used in [57] to construct finite elements in 2D and 3D that (although not called Whitney forms in [57]) actually better fulfil the properties of Whitney forms.

The construction of [57] uses Wachspress coordinates [58]. In both two and three dimensions, we get linear maps $\mathcal{W} : C^*_p(K) \to F^p(K)$ such that the spaces of Whitney p-forms $W^p = \mathcal{W}(C^*_p(K))$ constitute an exact sequence. Moreover, we have $\int_{\sigma_i} \mathcal{W}\sigma_j = \delta_{ij}$, and integrals over p-cells serve as degrees of freedom. In 2D any convex nondegenerate polygons are allowed, but in 3D the complex K is restricted by the additional requirement that the faces of the polyhedral cells be triangles or parallelograms.

As Whitney 0-forms we take the generalised barycentric functions resulting from Wachspress coordinates. In 2D, define the Whitney 1-forms corresponding to the edges of K such that their proxy fields are the $\mathbf{q}_i$ in Lemma 3.1 of [57] rotated 90 degrees counterclockwise and divided by the edge length. In 3D, define the Whitney 1- and 2-forms corresponding to the edges and the faces of K such that their proxy fields are the $\mathbf{p}_e$ and the $\mathbf{q}_f$ in Lemmas 4.7 and 4.6 of [57] divided by the edge length and the face area, respectively. Define the n-forms corresponding to the polygons/polyhedra of K such that their proxy fields equal the reciprocal of the area/volume in the corresponding polygon/polyhedron and zero elsewhere.

Then $\int_{\sigma_i} \mathcal{W}\sigma_j = \delta_{ij}$ by Lemmas 3.1, 4.7, and 4.6 of [57]. In 2D, it follows from Lemma 3.4 of [57] that constants are in W^p, and hence the partition of unity property holds by Proposition 4.4. In 3D this holds for certain types of cells by Lemma 4.14 of [57]. The counterpart to property 8 in 2D is Lemma 3.10 of [57], but we do not know if this has been proved in 3D yet. As discussed, properties 3 and 4 are lost. In general, Wachspress coordinates are rational functions. However, we remark that in the case of simplices everything reduces to normal Whitney forms. Thus, the construction of [57] truly generalises Whitney forms while preserving many of their properties.

5.3.2. Construction based on conation and extrusion

To present how Whitney forms for polytopal cells are obtained systematically, one approach is to first consider a systematic construction of the cells themselves. In [29] Whitney forms are defined recursively for cells that are obtained through conation and extrusion operations. Consider an n-dimensional cell σ with plane P in $\mathbb{R}^{n+1}$, a point $a \in \mathbb{R}^{n+1}$ outside P, and a vector v not parallel to P. Conation yields the $(n+1)$-dimensional cell

$$\mathrm{cone}(\sigma) = \{\lambda a + (1-\lambda)x \mid x \in \sigma,\ 0 \le \lambda \le 1\},$$

and extrusion yields the $(n+1)$-dimensional cell

$$\mathrm{extr}(\sigma) = \{x + \lambda v \mid x \in \sigma,\ 0 \le \lambda \le 1\}.$$

In [29], it is shown how Whitney forms lift up onto either of these $(n+1)$-dimensional cells, supposing we know them on σ.

The requirements (1)–(3) on page 1570 of [29] ensure $\int_{\sigma_i} \mathcal{W}\sigma_j = \delta_{ij}$, the exact sequence property, and the inclusion of constant p-forms in W^p (which by Proposition 4.4 implies the partition of unity property). Properties 3 and 4 are again understandably lost. In the case of simplices, this construction yields the usual Whitney forms (with repeated conation starting from a 0-cell). In 3D, other cell types that fit this approach are parallelepipeds (conation, extrusion, extrusion), pyramids (conation, extrusion, conation), and triangular prisms (conation, conation, extrusion).

Recently in [59], the authors combined these conation and extrusion techniques with their earlier construction [57] to define Whitney forms on polygon-based prisms and cones. The work [59] covers both theoretical analysis and implementation instructions. As mentioned in [59], any convex polyhedral cell can be divided into polygon-based cones by connecting the vertices with a chosen interior point. Hence one could define Whitney forms for cell complexes of arbitrary convex polyhedra by refining the complex this way — if one does not mind that the resulting forms are in $F^p(K')$ only with respect to the refined complex K'.

5.3.3. Formulas on cubes, triangular prisms, and pyramids

Finally, to show examples of Whitney forms on other cells than simplices, we give formulas of Whitney forms on cubes, triangular prisms, and pyramids. These three cell types are suitable for examples since the Whitney forms on them have sufficiently simple explicit formulas. In addition, both of the approaches we considered in this subsection yield these Whitney forms.

In all of the examples, we use Cartesian xyz-coordinates. The cell σ is defined by giving its vertices x_i in $\mathbb{R}^3$. Its edges are oriented so that $i < j$ for any edge x_ix_j, and its facets are oriented such that the normal vector (prescribed by the right hand rule) points outward.

Example 5.2 (*Cubes*)**.** Consider the cube σ with vertices

$$\begin{array}{llll} x_1 = (0,0,0) & x_2 = (1,0,0) & x_3 = (0,1,0) & x_4 = (1,1,0) \\ x_5 = (0,0,1) & x_6 = (1,0,1) & x_7 = (0,1,1) & x_8 = (1,1,1) \end{array}$$

The Whitney forms on σ are

$$\begin{array}{lll} \mathcal{W}x_1 = (1-x)(1-y)(1-z) & \mathcal{W}x_2 = x(1-y)(1-z) & \mathcal{W}x_3 = (1-x)y(1-z) \\ \mathcal{W}x_4 = xy(1-z) & \mathcal{W}x_5 = (1-x)(1-y)z & \mathcal{W}x_6 = x(1-y)z \\ \mathcal{W}x_7 = (1-x)yz & \mathcal{W}x_8 = xyz & \end{array}$$

$$\begin{array}{lll} \mathcal{W}x_1x_2 = (1-y)(1-z)\,\mathrm{d}x & \mathcal{W}x_3x_4 = y(1-z)\,\mathrm{d}x & \mathcal{W}x_5x_6 = (1-y)z\,\mathrm{d}x \\ \mathcal{W}x_7x_8 = yz\,\mathrm{d}x & \mathcal{W}x_1x_3 = (1-x)(1-z)\,\mathrm{d}y & \mathcal{W}x_2x_4 = x(1-z)\,\mathrm{d}y \\ \mathcal{W}x_5x_7 = (1-x)z\,\mathrm{d}y & \mathcal{W}x_6x_8 = xz\,\mathrm{d}y & \mathcal{W}x_1x_5 = (1-x)(1-y)\,\mathrm{d}z \\ \mathcal{W}x_2x_6 = x(1-y)\,\mathrm{d}z & \mathcal{W}x_3x_7 = (1-x)y\,\mathrm{d}z & \mathcal{W}x_4x_8 = xy\,\mathrm{d}z \end{array}$$

$$\begin{array}{lll} \mathcal{W}x_5x_6x_8x_7 = z\,\mathrm{d}x \wedge \mathrm{d}y & \mathcal{W}x_1x_3x_4x_2 = -(1-z)\,\mathrm{d}x \wedge \mathrm{d}y & \mathcal{W}x_1x_2x_6x_5 = (1-y)\,\mathrm{d}x \wedge \mathrm{d}z \\ \mathcal{W}x_3x_7x_8x_4 = -y\,\mathrm{d}x \wedge \mathrm{d}z & \mathcal{W}x_1x_5x_7x_3 = -(1-x)\,\mathrm{d}y \wedge \mathrm{d}z & \mathcal{W}x_2x_4x_8x_6 = x\,\mathrm{d}y \wedge \mathrm{d}z \\ \mathcal{W}\sigma = \mathrm{d}x \wedge \mathrm{d}y \wedge \mathrm{d}z & & \end{array}$$

The proxy fields of the 1- and 2-forms above first appeared in [10].

Example 5.3 (*Triangular Prisms*)**.** Consider the triangular prism σ with vertices

$$\begin{array}{lll} x_1 = (0,0,0) & x_2 = (1,0,0) & x_3 = (0,1,0) \\ x_4 = (0,0,1) & x_5 = (1,0,1) & x_6 = (0,1,1) \end{array}$$

The Whitney forms on σ are

$$\begin{array}{lll} \mathcal{W}x_1 = (1-y-x)(1-z) & \mathcal{W}x_2 = x(1-z) & \mathcal{W}x_3 = y(1-z) \\ \mathcal{W}x_4 = (1-y-x)z, & \mathcal{W}x_5 = xz, & \mathcal{W}x_6 = yz \\ \mathcal{W}x_1x_4 = (1-y-x)\,\mathrm{d}z & \mathcal{W}x_2x_5 = x\,\mathrm{d}z & \mathcal{W}x_3x_6 = y\,\mathrm{d}z \end{array}$$

$$\begin{array}{ll} \mathcal{W}x_1x_2 = (1-y)(1-z)\,\mathrm{d}x + x(1-z)\,\mathrm{d}y & \mathcal{W}x_2x_3 = -y(1-z)\,\mathrm{d}x + x(1-z)\,\mathrm{d}y \\ \mathcal{W}x_1x_3 = y(1-z)\,\mathrm{d}x + (1-x)(1-z)\,\mathrm{d}y & \mathcal{W}x_4x_5 = (1-y)z\,\mathrm{d}x + xz\,\mathrm{d}y \\ \mathcal{W}x_5x_6 = -yz\,\mathrm{d}x + xz\,\mathrm{d}y & \mathcal{W}x_4x_6 = yz\,\mathrm{d}x + (1-x)z\,\mathrm{d}y \\ \mathcal{W}x_1x_2x_5x_4 = (1-y)\,\mathrm{d}x\wedge\mathrm{d}z + x\,\mathrm{d}y\wedge\mathrm{d}z & \mathcal{W}x_2x_3x_6x_5 = -y\,\mathrm{d}x\wedge\mathrm{d}z + x\,\mathrm{d}y\wedge\mathrm{d}z \\ \mathcal{W}x_1x_4x_6x_3 = -y\,\mathrm{d}x\wedge\mathrm{d}z - (1-x)\,\mathrm{d}y\wedge\mathrm{d}z & \mathcal{W}x_1x_3x_2 = -2(1-z)\,\mathrm{d}x\wedge\mathrm{d}y \\ \mathcal{W}x_4x_5x_6 = 2z\,\mathrm{d}x\wedge\mathrm{d}y & \mathcal{W}\sigma = 2\,\mathrm{d}x\wedge\mathrm{d}y\wedge\mathrm{d}z \end{array}$$

The proxy fields of the 1- and 2-forms above first appeared in [60].

Example 5.4 (*Pyramids*)**.** Consider the pyramid σ with vertices

$$x_1 = (0,0,0) \quad x_2 = (1,0,0) \quad x_3 = (0,1,0) \quad x_4 = (1,1,0) \quad x_5 = (0,0,1)$$

The Whitney forms on σ are

$$\mathcal{W}x_1 = \tfrac{(1-z-x)(1-z-y)}{1-z} \quad \mathcal{W}x_2 = \tfrac{x(1-z-y)}{1-z} \quad \mathcal{W}x_3 = \tfrac{(1-z-x)y}{1-z} \quad \mathcal{W}x_4 = \tfrac{xy}{1-z} \quad \mathcal{W}x_5 = z$$

$$\begin{array}{l} \mathcal{W}x_1x_2 = (1-z-y)\,\mathrm{d}x + \tfrac{x(1-z-y)}{1-z}\,\mathrm{d}z \quad \mathcal{W}x_2x_4 = x\,\mathrm{d}y + \tfrac{xy}{1-z}\,\mathrm{d}z \\ \mathcal{W}x_3x_4 = y\,\mathrm{d}x + \tfrac{xy}{1-z}\,\mathrm{d}z \quad \mathcal{W}x_1x_3 = (1-z-x)\,\mathrm{d}y + \tfrac{(1-z-x)y}{1-z}\,\mathrm{d}z \\ \mathcal{W}x_1x_5 = (z - \tfrac{yz}{1-z})\,\mathrm{d}x + (z - \tfrac{xz}{1-z})\,\mathrm{d}y + (1-x-y+\tfrac{xy}{1-z} - \tfrac{xyz}{(1-z)^2})\,\mathrm{d}z \\ \mathcal{W}x_2x_5 = (-z + \tfrac{yz}{1-z})\,\mathrm{d}x + \tfrac{xz}{1-z}\,\mathrm{d}y + (x - \tfrac{xy}{1-z} + \tfrac{xyz}{(1-z)^2})\,\mathrm{d}z \\ \mathcal{W}x_3x_5 = \tfrac{yz}{1-z}\,\mathrm{d}x + (-z + \tfrac{xz}{1-z})\,\mathrm{d}y + (y - \tfrac{xy}{1-z} + \tfrac{xyz}{(1-z)^2})\,\mathrm{d}z \\ \mathcal{W}x_4x_5 = -\tfrac{yz}{1-z}\,\mathrm{d}x - \tfrac{xz}{1-z}\,\mathrm{d}y + (\tfrac{xy}{1-z} - \tfrac{xyz}{(1-z)^2})\,\mathrm{d}z \\ \mathcal{W}x_1x_2x_5 = z\,\mathrm{d}x\wedge\mathrm{d}y + (2-y-\tfrac{y}{1-z})\,\mathrm{d}x\wedge\mathrm{d}z - \tfrac{xz}{1-z}\,\mathrm{d}y\wedge\mathrm{d}z \\ \mathcal{W}x_1x_5x_3 = z\,\mathrm{d}x\wedge\mathrm{d}y + \tfrac{yz}{1-z}\,\mathrm{d}x\wedge\mathrm{d}z + (-2+x+\tfrac{x}{1-z})\,\mathrm{d}y\wedge\mathrm{d}z \\ \mathcal{W}x_2x_4x_5 = z\,\mathrm{d}x\wedge\mathrm{d}y + \tfrac{yz}{1-z}\,\mathrm{d}x\wedge\mathrm{d}z + (x + \tfrac{x}{1-z})\,\mathrm{d}y\wedge\mathrm{d}z \\ \mathcal{W}x_4x_3x_5 = z\,\mathrm{d}x\wedge\mathrm{d}y + (-y - \tfrac{y}{1-z})\,\mathrm{d}x\wedge\mathrm{d}z - \tfrac{xz}{1-z}\,\mathrm{d}y\wedge\mathrm{d}z \\ \mathcal{W}x_1x_3x_4x_2 = -(1-z)\,\mathrm{d}x\wedge\mathrm{d}y - y\,\mathrm{d}x\wedge\mathrm{d}z + x\,\mathrm{d}y\wedge\mathrm{d}z \\ \mathcal{W}\sigma = 3\,\mathrm{d}x\wedge\mathrm{d}y\wedge\mathrm{d}z \end{array}$$

Whitney forms on pyramids first appeared in [28].

Acknowledgements

The authors thank Sanna Mönkölä, Tuomo Rossi, and two anonymous reviewers for their helpful comments on the manuscript.

References

[1] H. Whitney, Geometric Integration Theory, Princeton University Press, 1957.
[2] J. Dodziuk, Finite-difference approach to the Hodge theory of harmonic forms, Amer. J. Math. 98 (1) (1976) 79–104.
[3] A. Bossavit, Whitney forms: A class of finite elements for three-dimensional computations in electromagnetism, IEE Proc. A 135 (8) (1988) 493–500.
[4] A. Bossavit, A rationale for 'edge-elements' in 3-D fields computations, IEEE Trans. Magn. 24 (1) (1988) 74–79.
[5] A. Bossavit, Mixed finite elements and the complex of Whitney forms, Math. Finite Elem. Appl. VI (1988) 137–144.
[6] A. Bossavit, I. Mayergoyz, Edge-elements for scattering problems, IEEE Trans. Magn. 25 (4) (1989) 2816–2821.
[7] A. Bossavit, Solving Maxwell equations in a closed cavity, and the question of 'spurious modes', IEEE Trans. Magn. 26 (2) (1990) 702–705.
[8] A. Bossavit, A new viewpoint on mixed elements, Meccanica 27 (1) (1992) 3–11.
[9] P.-A. Raviart, J.-M. Thomas, A mixed finite element method for 2-nd order elliptic problems, in: Mathematical Aspects of Finite Element Methods, Springer, 1977, pp. 292–315.
[10] J.-C. Nédélec, Mixed finite elements in $\mathbb{R}^3$, Numer. Math. 35 (3) (1980) 315–341.
[11] A. Bossavit, Computational Electromagnetism: Variational Formulations, Complementarity, Edge Elements, Academic Press, 1998.
[12] A. Bossavit, L. Kettunen, Yee-like schemes on a tetrahedral mesh, with diagonal lumping, Int. J. Numer. Modelling, Electron. Netw. Devices Fields 12 (1–2) (1999) 129–142.
[13] A. Bossavit, L. Kettunen, Yee-like schemes on staggered cellular grids: A synthesis between FIT and FEM approaches, IEEE Trans. Magn. 36 (4) (2000) 861–867.
[14] A. Bossavit, 'Generalized finite differences' in computational electromagnetics, Prog. Electromagn. Res. 32 (2001) 45–64.

[15] R. Hiptmair, Canonical construction of finite elements, Math. Comp. 68 (228) (1999) 1325–1346.
[16] R. Hiptmair, Finite elements in computational electromagnetism, Acta Numer. 11 (2002) 237–339.
[17] P. Castillo, J. Koning, R. Rieben, D. White, A discrete differential forms framework for computational electromagnetism, Comput. Model. Eng. Sci. 5 (4) (2004) 331–345.
[18] A. Bossavit, Discretization of electromagnetic problems: The ''generalized finite differences'' approach, Handb. Numer. Anal. 13 (2005) 105–197.
[19] D. Arnold, R. Falk, R. Winther, Finite element exterior calculus, homological techniques, and applications, Acta Numer. 15 (2006) 1–155.
[20] S. Christiansen, H. Munthe-Kaas, B. Owren, Topics in structure-preserving discretization, Acta Numer. 20 (2011) 1–119.
[21] M.-F. Wong, O. Picon, V. Fouad-Hanna, A finite element method based on Whitney forms to solve Maxwell equations in the time domain, IEEE Trans. Magn. 31 (3) (1995) 1618–1621.
[22] R. Hiptmair, Multigrid method for Maxwell's equations, SIAM J. Numer. Anal. 36 (1) (1998) 204–225.
[23] T. Tarhasaari, L. Kettunen, A. Bossavit, Some realizations of a discrete Hodge operator: A reinterpretation of finite element techniques, IEEE Trans. Magn. 35 (3) (1999) 1494–1497.
[24] D. Arnold, R. Falk, R. Winther, Multigrid in $H(\mathrm{div})$ and $H(\mathrm{curl})$, Numer. Math. 85 (2) (2000) 197–217.
[25] A. Bossavit, Computational electromagnetism and geometry: (4): From degrees of freedom to fields, J. Japan Soc. Appl. Electromagn. Mech. 8 (1) (2000) 102–109.
[26] S. Wilson, Cochain algebra on manifolds and convergence under refinement, Topology Appl. 154 (9) (2007) 1898–1920.
[27] C. Nore, H. Zaidi, F. Bouillault, A. Bossavit, J.-L. Guermond, Approximation of the time-dependent induction equation with advection using Whitney elements, COMPEL (2016).
[28] V. Gradinaru, R. Hiptmair, Whitney elements on pyramids, Electron. Trans. Numer. Anal. 8 (1999) 154–168.
[29] A. Bossavit, A uniform rationale for Whitney forms on various supporting shapes, Math. Comput. Simulation 80 (8) (2010) 1567–1577.
[30] R. Hiptmair, Higher order Whitney forms, Prog. Electromagn. Res. 32 (2001) 271–299.
[31] F. Rapetti, High order edge elements on simplicial meshes, ESAIM Math. Model. Numer. Anal. 41 (6) (2007) 1001–1020.
[32] F. Rapetti, A. Bossavit, Whitney forms of higher degree, SIAM J. Numer. Anal. 47 (3) (2009) 2369–2386.
[33] J. Harrison, Operator calculus of differential chains and differential forms, J. Geom. Anal. 25 (1) (2015) 357–420.
[34] A. Bossavit, Generating Whitney forms of polynomial degree one and higher, IEEE Trans. Magn. 38 (2) (2002) 341–344.
[35] F. Rapetti, Weights computation for simplicial Whitney forms of degree one, C. R. Math. 341 (8) (2005) 519–523.
[36] D. Arnold, R. Falk, R. Winther, Finite element exterior calculus: From Hodge theory to numerical stability, Bull. Amer. Math. Soc. 47 (2) (2010) 281–354.
[37] S. Christiansen, F. Rapetti, On high order finite element spaces of differential forms, Math. Comp. 85 (298) (2016) 517–548.
[38] N. Nigam, J. Phillips, High-order conforming finite elements on pyramids, IMA J. Numer. Anal. 32 (2) (2012) 448–483.
[39] M. Bergot, M. Duruflé, High-order optimal edge elements for pyramids, prisms and hexahedra, J. Comput. Phys. 232 (1) (2013) 189–213.
[40] F. Fuentes, B. Keith, L. Demkowicz, S. Nagaraj, Orientation embedded high order shape functions for the exact sequence elements of all shapes, Comput. Math. Appl. 70 (4) (2015) 353–458.
[41] D. Arnold, G. Awanou, Finite element differential forms on cubical meshes, Math. Comp. 83 (288) (2014) 1551–1570.
[42] S. Christiansen, A. Gillette, Constructions of some minimal finite element systems, ESAIM Math. Model. Numer. Anal. 50 (3) (2016) 833–850.
[43] A. Gillette, T. Kloefkorn, Trimmed serendipity finite element differential forms, Math. Comp. 88 (316) (2019) 583–606.
[44] P. Monk, On the p- and hp-extension of Nédélec's curl-conforming elements, J. Comput. Appl. Math. 53 (1) (1994) 117–137.
[45] J.S. Savage, A.F. Peterson, Higher-order vector finite elements for tetrahedral cells, IEEE Trans. Microw. Theory Tech. 44 (6) (1996) 874–879.
[46] J. Webb, Hierarchal vector basis functions of arbitrary order for triangular and tetrahedral finite elements, IEEE Trans. Antennas and Propagation 47 (8) (1999) 1244–1253.
[47] D.-K. Sun, J.-F. Lee, Z. Cendes, Construction of nearly orthogonal Nedelec bases for rapid convergence with multilevel preconditioned solvers, SIAM J. Sci. Comput. 23 (4) (2001) 1053–1076.
[48] M. Ainsworth, J. Coyle, Hierarchic finite element bases on unstructured tetrahedral meshes, Internat. J. Numer. Methods Engrg. 58 (14) (2003) 2103–2130.
[49] L. Demkowicz, I. Babuska, p Interpolation error estimates for edge finite elements of variable order in two dimensions, SIAM J. Numer. Anal. 41 (4) (2003) 1195–1208.
[50] J. Schöberl, S. Zaglmayr, High order Nédélec elements with local complete sequence properties, COMPEL (2005).
[51] M. Bonazzoli, F. Rapetti, High-order finite elements in numerical electromagnetism: Degrees of freedom and generators in duality, Numer. Algorithms 74 (1) (2017) 111–136.
[52] D. Arnold, R. Falk, R. Winther, Geometric decompositions and local bases for spaces of finite element differential forms, Comput. Methods Appl. Mech. Engrg. 198 (21–26) (2009) 1660–1672.
[53] A. Buffa, S. Christiansen, A dual finite element complex on the barycentric refinement, Math. Comp. 76 (260) (2007) 1743–1769.
[54] S. Christiansen, A construction of spaces of compatible differential forms on cellular complexes, Math. Models Methods Appl. Sci. 18 (5) (2008) 739–757.
[55] A. Gillette, C. Bajaj, Dual formulations of mixed finite element methods with applications, Comput. Aided Des. 43 (10) (2011) 1213–1221.
[56] A. Gillette, A. Rand, C. Bajaj, Construction of scalar and vector finite element families on polygonal and polyhedral meshes, Comput. Methods Appl. Math. 16 (4) (2016) 667–683.
[57] W. Chen, Y. Wang, Minimal degree $H(\mathrm{curl})$ and $H(\mathrm{div})$ conforming finite elements on polytopal meshes, Math. Comp. 86 (307) (2017) 2053–2087.
[58] M. Floater, A. Gillette, N. Sukumar, Gradient bounds for Wachspress coordinates on polytopes, SIAM J. Numer. Anal. 52 (1) (2014) 515–532.
[59] W. Chen, Y. Wang, H^1, $H(\mathrm{curl})$ and $H(\mathrm{div})$ conforming elements on polygon-based prisms and cones, Numer. Math. 145 (4) (2020) 973–1004.
[60] J.-C. Nédélec, A new family of mixed finite elements in $\mathbb{R}^3$, Numer. Math. 50 (1) (1986) 57–81.

PII

SYSTEMATIC IMPLEMENTATION OF HIGHER ORDER WHITNEY FORMS IN METHODS BASED ON DISCRETE EXTERIOR CALCULUS

by

Jonni Lohi

Numerical Algorithms, 91(3):1261–1285, 2022

Numerical Algorithms
https://doi.org/10.1007/s11075-022-01301-2

ORIGINAL PAPER

Systematic implementation of higher order Whitney forms in methods based on discrete exterior calculus

Jonni Lohi[1]

Received: 16 September 2021 / Accepted: 12 March 2022

Abstract

We present a systematic way to implement higher order Whitney forms in numerical methods based on discrete exterior calculus. Given a simplicial mesh, we first refine the mesh into smaller simplices which can be used to define higher order Whitney forms. Cochains on this refined mesh can then be interpolated using higher order Whitney forms. Hence, when the refined mesh is used with methods based on discrete exterior calculus, the solution can be expressed as a higher order Whitney form. We present algorithms for the three required steps: refining the mesh, solving the coefficients of the interpolant, and evaluating the interpolant at a given point. With our algorithms, the order of the Whitney forms one wishes to use can be given as a parameter so that the same code covers all orders, which is a significant improvement on previous implementations. Our algorithms are applicable with all methods in which the degrees of freedom are integrals over mesh simplices — that is, when the solution is a cochain on a simplicial mesh. They can also be used when one simply wishes to approximate differential forms in finite-dimensional spaces. Numerical examples validate the generality of our algorithms.

Keywords Higher order Whitney forms · Cochains · Differential forms · Interpolation · Discrete exterior calculus · Simplicial mesh

Mathematics Subject Classification (2010) Primary 65D05 · Secondary 58A10 · 65D15 · 65N50

1 Introduction

Partial differential equations describing field theories such as electromagnetism and elasticity often admit a natural expression in terms of differential forms. In the past

✉ Jonni Lohi
jonni.j.lohi@student.jyu.fi

[1] Faculty of Information Technology, University of Jyväskylä, PO Box 35, FI-40014, Jyväskylä, Finland

Published online: 18 April 2022

decades, the role of differential forms has increased also in numerical methods and their practical implementations. The growth of their popularity has been accelerated by finite element exterior calculus [1, 3] for the finite element method and by discrete exterior calculus [13, 16] for finite difference kind of methods. For computations, differential forms are approximated in finite-dimensional spaces using a mesh consisting of a finite number of cells. In finite element exterior calculus these finite-dimensional spaces are spanned by suitable finite elements, while discrete exterior calculus is based on cochains (also known as discrete forms) as approximations for differential forms.

Methods based on discrete exterior calculus (DEC) may go by different names, e.g. Yee-like schemes [9, 10], finite integration technique [12], or generalised finite differences [6, 8]. These methods enable one to distinguish the features that depend on metric from those that do not, and in a way they preserve the geometric structure of the continuous model at the discrete level. The methods can typically be made explicit, which enables a very large number of degrees of freedom. In the literature there are many examples where discrete exterior calculus has been successfully applied (see e.g. [17, 22–26, 29]).

Although methods based on cochains have their benefits, there are also some drawbacks. When the solution is given as a cochain, it cannot be evaluated at a given point. In some situations evaluating the solution at a given point is preferable, and then one has to interpolate the cochain somehow. This raises the question: in which space does the interpolant lie? In the case of simplicial meshes, it is well known that Whitney forms [31] can be used to approximate differential forms and interpolate cochains in methods based on discrete exterior calculus. However, this only applies to lowest order Whitney forms. Although higher order Whitney forms have been defined and used elsewhere [4, 5, 7, 11, 15, 21, 27, 28], they have not been used with cochain-based methods. Indeed, these are often considered low-order methods in that they seem to lack natural higher order generalisations.

In this paper, we provide an alternative viewpoint and show how higher order Whitney forms can be used to interpolate cochains in methods based on discrete exterior calculus. As with lowest order Whitney forms, we require a simplicial mesh to begin with. This mesh is refined into smaller simplices which have been used to define higher order Whitney forms in [28]. Cochains on this refined mesh can then be interpolated using higher order Whitney forms, so when we apply methods based on discrete exterior calculus with the refined mesh, the solution can be expressed as a higher order Whitney form.

With this approach, we can reduce the interpolation error without any modifications in the methods themselves; the only changes are in preprocessing (preparing the mesh) and postprocessing (interpolating the cochain) stages. For this reason, we do not focus on any specific method here, but instead provide a framework for interpolating cochains with higher order Whitney forms. This framework can then be applied with any method — our algorithms are applicable whenever the solution is a cochain on a simplicial mesh. They can also be used if one simply wishes to approximate differential forms in finite-dimensional spaces and might be relevant for the finite element method as well, if integrals over small simplices are chosen as degrees of freedom.

Although reducing the interpolation error alone does not lead to higher order DEC methods, it is a necessary step toward them. To obtain higher order convergence, one would also have to improve the accuracy of discrete Hodge operators. This is possible using higher order Whitney forms and the interpolation framework presented here. It would of course require changes in specific methods, and hence, we will study higher order discrete Hodge operators in a future article.

The main novelty of this paper is the systematic implementation strategy that is usable with DEC and yields Whitney forms of all orders with the same code. The idea of using small simplices to construct bases and degrees of freedom for higher order Whitney forms is not new [11, 28]; however, although systematic implementations for more traditional bases and dofs exist, the approach with small simplices still lacks a systematic implementation strategy. The implementation in 3D is a delicate issue. For FEM, it has been studied in [4], but only second- and third-order 1-forms were implemented. Similarly, only second-order forms were implemented in our previous studies for DEC [18, 19]. Without general algorithms, the implementation process has to be repeated separately for each order, while the workload becomes unreasonably laborious very quickly. The systematic implementation strategy of this paper and in particular Algorithms 1–3 are a significant novelty, yielding all orders with the same code. Without such algorithms, the implementation of, for example, 8th-order 1-forms in 3D would be practically impossible using small simplices (to define both basis functions and dofs).

The outline of this paper is as follows. We start with some preliminaries in Section 2. Section 3 covers lowest order Whitney forms, and in Section 4 we recall the small simplices of [28] and use them to define higher order Whitney forms. In Section 5 we give the general idea for interpolating cochains with higher order Whitney forms. The implementation of this idea is discussed in Section 6. This section contains three subsections where we present algorithms for the three required steps: refining the mesh, solving the coefficients of the interpolant, and evaluating the interpolant at a given point. Numerical examples of Section 7 validate the generality of our algorithms — the order of Whitney forms can be given as a parameter, and hence, all cases are covered by the same code.

2 Some preliminary concepts

In this section we recall some prerequisite concepts that are used in this paper. The discussion is brief, but readers unfamiliar with these concepts can consult the given references for more information.

We start by defining a mesh in a domain $\Omega \subset \mathbb{R}^n$. Bounded and convex p-dimensional polytopes in $\mathbb{R}^n$ are called p-cells for short. Cell complex K is a finite set of cells such that

- each face of every cell in K is also in K.

- The intersection of two cells in K is either a common face of theirs or the empty set.

The set of p-cells in K is denoted by $S^p(K)$. A cell complex K is a mesh in Ω if the union of the cells of K is Ω. To enable this we assume that our domain Ω is a bounded polytope in $\mathbb{R}^n$. A cell complex (or mesh) is simplicial if its cells are all simplices. In this case there is a unique barycentric function [31, App. II, §2] corresponding to each 0-simplex x_i — this is denoted by λ_i.

We will also need the concept of orientation [31, App. II, §5]. Recall that p-cell σ is oriented by orienting its plane. If $\tau \in S^{p+1}(K)$ is oriented and $\sigma \in S^p(K)$ is a face of τ, the orientation of τ induces an orientation on σ; we say that the orientation of σ agrees with that of τ if σ is equipped with the induced orientation. For $\tau \in S^{p+1}(K)$ and $\sigma \in S^p(K)$, the incidence number d_σ^τ is defined as

$$\mathrm{d}_\sigma^\tau = \begin{cases} 1 & \text{if } \sigma \text{ is a } p\text{-face of } \tau \text{ and their orientations agree,} \\ -1 & \text{if } \sigma \text{ is a } p\text{-face of } \tau \text{ and their orientations do not agree,} \\ 0 & \text{otherwise.} \end{cases}$$

In the case of simplices, we denote by $x_0 \dots x_p$ the oriented p-simplex whose vertices are $x_0, \dots, x_p$ and whose orientation is implied by this order of vertices.

We assume the reader is familiar with exterior algebra and differential forms (see e.g. [31, I–III] and [1]). Let $\langle \omega, \alpha \rangle$ denote the action of p-covector ω on p-vector α. Differential p-form in a complex K [31, p. 226] is a set of smooth p-forms ω_σ in the cells σ of K satisfying the following patch condition: if τ is a face of σ, then the trace $\omega_\sigma|_\tau$ of ω_σ equals ω_τ in τ. In other words, $\langle \omega_\sigma(x), \alpha \rangle = \langle \omega_\tau(x), \alpha \rangle$ for all $x \in \tau$ and all p-vectors α in the plane of τ. This enables us to consider the set of p-forms ω_σ as single p-form ω such that $\langle \omega(x), \alpha \rangle$ is well-defined for those p-vectors α that are in the plane of the cell σ for which $x \in \sigma - \partial\sigma$. Hence, differential p-forms in K can be integrated over p-cells. Denote by $F^p(K)$ the space of differential p-forms in K. Note that since the exterior derivative d commutes with trace, we have $\mathrm{d}\omega \in F^{p+1}(K)$ if $\omega \in F^p(K)$, but the Hodge star $\star\omega$ is not necessarily in $F^{n-p}(K)$.

Formal sums $\sum_{\sigma_i \in S^p(K)} a_i \sigma_i$ of oriented p-cells with real coefficients are called p-chains of K [31, App. II, §6]. These form a vector space $C_p(K)$ for which the p-cells σ_i constitute a natural basis (here $\sigma_i = 1\sigma_i$, the sum in which $a_j = \delta_{ij}$, the Kronecker delta). The elements of the dual space $C_p^*(K)$ are p-cochains of K. Following [31], we use σ_i to denote also the cochain whose value is δ_{ij} at the chain σ_j. Then the p-cells σ_i constitute the dual basis for $C_p^*(K)$, and also cochains can be written as formal sums of cells. Negative coefficients indicate change of orientation so that $-\sigma$ is the cell σ with opposite orientation. For computer implementations, chains and cochains can be considered as vectors consisting of the coefficients a_i after a numbering has been chosen for the cells of K.

The boundary $\partial\tau$ of a $(p+1)$-cell $\tau \in S^{p+1}(K)$ is the p-chain $\sum_{\sigma \in S^p(K)} \mathrm{d}_\sigma^\tau \sigma$. This defines the boundary map $\partial : C_{p+1}(K) \to C_p(K)$ for all chains by requiring it be linear. The coboundary map $\mathrm{d} : C_p^*(K) \to C_{p+1}^*(K)$ for cochains is defined by $\mathrm{d}X(c) = X(\partial c)$. We use the same notation d as for the exterior derivative of forms. When cochains are considered as vectors, we can denote by d also the matrix with components $\mathrm{d}_{ij} = \mathrm{d}_{\sigma_j}^{\tau_i}$ for $\tau_i \in S^{p+1}(K)$ and $\sigma_j \in S^p(K)$, since this is the matrix of the coboundary map. This notation is not explicitly needed in this paper, but we mention it so that $\mathrm{d}X$ makes sense also when cochain X is considered as a vector.

Since p-forms can be integrated over p-cells, each p-form ω yields a p-cochain whose values on chains are determined by integration of ω. Namely, the de Rham map $\mathcal{C} : F^p(K) \to C_p^*(K)$ is the linear map defined by

$$\mathcal{C}\omega\Big(\sum_{\sigma_i \in S^p(K)} a_i \sigma_i \Big) = \int_{\sum_{\sigma_i \in S^p(K)} a_i \sigma_i} \omega = \sum_{\sigma_i \in S^p(K)} a_i \int_{\sigma_i} \omega,$$

where the second equality is the definition of integration on p-chains. The cochain $\mathcal{C}\omega$ can be considered as an approximation of ω. In vector presentation, its components are the integrals of ω over the p-cells of K. We remark that Stokes' theorem implies $\mathcal{C}\mathrm{d}\omega = \mathrm{d}\mathcal{C}\omega$ for p-forms ω.

We invoke the inner product of $\mathbb{R}^n$ to define norms as follows. If ω is a p-covector, denote by $|\omega|$ the norm induced by the inner product of $\mathbb{R}^n$ [31, I, §12]. If ω is a p-form, then $|\omega|$ denotes the function whose value at x is $|\omega(x)|$. Hence, we may define the L^2 norm of the p-form ω as the L^2 norm of the function $|\omega|$. This is denoted by $\||\omega|\|_{L^2(\Omega)}$. In other words, $\||\omega|\|_{L^2(\Omega)} = (\int_\Omega |\omega(x)|^2 dx)^{1/2}$. For p-simplex σ, denote by $|\sigma|$ its p-dimensional volume and define its fullness $\Theta(\sigma)$ by $\Theta(\sigma) = |\sigma|/\mathrm{diam}(\sigma)^p$.

Discrete exterior calculus [13, 14, 16] enables a discrete presentation of boundary value problems expressed in terms of differential forms. When differential forms are approximated with cochains, the coboundary operator naturally replaces the exterior derivative. Indeed, if $\mathcal{C}\omega$ approximates ω, then $\mathcal{C}\mathrm{d}\omega = \mathrm{d}\mathcal{C}\omega$ suggests that $\mathrm{d}\mathcal{C}\omega$ is the right approximation for $\mathrm{d}\omega$. One also has to express the Hodge star operator for cochains. There are several ways to do this, and one typically employs a dual complex so that p-cochains of K are mapped to $(n-p)$-cochains of the dual complex. We need not consider any specific approach to deal with the Hodge operator or any specific boundary value problem. The framework we present in this paper can be applied as long as the solution is a cochain on a simplicial mesh which is meant to approximate a differential form — that is, its coefficients correspond to the integrals of the form.

3 Lowest order Whitney forms

In this section, we briefly recall Whitney forms as a tool for interpolating cochains. More information can be found in [20]. Let us henceforth assume that the mesh K is simplicial.

Definition 3.1 The Whitney 0-form corresponding to the 0-simplex x_i is the barycentric function $\mathcal{W}x_i = \lambda_i$. For $p > 0$, the Whitney p-form corresponding to the p-simplex $x_0 \ldots x_p$ is [31, VII, 11.16]

$$\mathcal{W}(x_0 \ldots x_p) = p! \sum_{i=0}^{p} (-1)^i \lambda_i \mathrm{d}\lambda_0 \wedge \ldots \wedge \widehat{\mathrm{d}\lambda_i} \wedge \ldots \wedge \mathrm{d}\lambda_p, \tag{3.1}$$

where $\widehat{\mathrm{d}\lambda_i}$ indicates a term omitted from the product.

For each p, the Whitney map $\mathcal{W} : C_p^*(K) \to F^p(K)$ is defined by setting

$$\mathcal{W}\Bigg(\sum_{\sigma_i \in S^p(K)} a_i \sigma_i \Bigg) = \sum_{\sigma_i \in S^p(K)} a_i \mathcal{W}\sigma_i .$$

The image $\mathcal{W}(C_p^*(K)) = \mathrm{span}\{\mathcal{W}\sigma \mid \sigma \in S^p(K)\} \subset F^p(K)$ is the space of Whitney p-forms and denoted by $W^p(K)$.

First, recall that $\mathcal{CW}X = X$ for all $X \in C_p^*(K)$. Cochains and Whitney forms are in one-to-one correspondence in the simplest possible way, the cochain $X = \sum_{\sigma_i \in S^p(K)} a_i \sigma_i \in C_p^*(K)$ corresponding to the p-form $\mathcal{W}X = \sum_{\sigma_i \in S^p(K)} a_i \mathcal{W}\sigma_i$; we can interpolate X with $\mathcal{W}X$, and the integrals of this interpolant match with the values of X on p-simplices of K. Further, we can approximate p-form $\omega \in F^p(K)$ with the Whitney form $\mathcal{WC}\omega$, and the integrals of this approximation match with those of ω on p-simplices of K: $\mathcal{CWC}\omega = \mathcal{C}\omega$. This approximation is exact for elements of $W^p(K)$, including constant p-forms.

For computing derivatives, a useful fact is that d and $\mathcal{W}$ commute: for $X \in C_p^*(K)$, we have $\mathrm{d}\mathcal{W}X = \mathcal{W}\mathrm{d}X$. Finally, we mention the affine invariance property of Whitney forms. Let $\sigma = x_0 \ldots x_n$ and $\tau = y_0 \ldots y_n$ be two n-simplices and $\varphi : \sigma \to \tau$ the affine map such that $\varphi(x_i) = y_i$. Then $\mathcal{W}(x_0 \ldots x_p)$ in σ is the pullback $\varphi^*(\mathcal{W}(y_0 \ldots y_p))$. Because of this property, computations done in a reference simplex transfer to all simplices by affine transformations and hence need be done only once. This will be useful when we consider interpolation with higher order Whitney forms.

4 Small simplices and higher order Whitney forms

Lowest order Whitney forms defined in the previous section include constants and are at most first-order polynomials in each simplex. There are also higher order Whitney forms, or Whitney forms of order k, which include $(k-1)$th-order polynomials and are at most kth-order polynomials in each simplex. Higher order Whitney forms can be defined in different ways. We use the so-called small simplices of [28], since this approach enables us to interpolate cochains with higher order Whitney forms.

To define the small simplices, let $\mathcal{I}(n+1, k)$ denote the set of multi-indices with $n+1$ components that sum to k; that is, $\mathcal{I}(n+1, k)$ consists of arrays $\mathbf{k} = (k_0, k_1, \ldots, k_n)$ where the k_i are nonnegative integers such that $\sum_{i=0}^{n} k_i = k$. The cardinality $\#\mathcal{I}(n+1, k)$ of $\mathcal{I}(n+1, k)$ is $\binom{n+k}{k}$ (see Lemma A.1 in Appendix A). For a fixed n-simplex $\sigma = x_0 \ldots x_n$, each multi-index $\mathbf{k} \in \mathcal{I}(n+1, k-1)$ defines a map, which we denote by $\mathbf{k}_\sigma$, from σ to itself such that the point x whose barycentric coordinates are λ_i maps to the point whose barycentric coordinates are $\frac{\lambda_i + k_i}{k}$. In other words, $\mathbf{k}_\sigma$ is defined by

$$\mathbf{k}_\sigma : \sigma \to \sigma, \quad \lambda_0 x_0 + \ldots + \lambda_n x_n \mapsto \tfrac{\lambda_0 + k_0}{k} x_0 + \ldots + \tfrac{\lambda_n + k_n}{k} x_n .$$

For $k \geq 1$, the set of kth-order small p-simplices of K is

$$\begin{aligned} S_k^p(K) = \{\ &\mathbf{k}_\sigma(\tau) \mid \sigma = x_0 \dots x_n \in S^n(K), \\ &\mathbf{k} \in \mathcal{I}(n+1, k-1),\ \text{and } \tau \text{ is a } p\text{-face of } \sigma\}. \end{aligned} \tag{4.1}$$

Small simplices are homothetic images of the simplices of K. See Fig. 1 for examples of small simplices.

To each kth-order small p-simplex υ corresponds a kth-order Whitney p-form $w(\upsilon) \in F^p(K)$, as given in the following definition. Henceforth, when $\sigma = x_0 \dots x_n$ is a fixed n-simplex, we denote by $\lambda_\sigma^{\mathbf{k}}$ the function $\prod_{i=0}^n (\lambda_i)^{k_i}$.

Definition 4.1 Let $\sigma = x_0 \dots x_n \in S^n(K)$, $\mathbf{k} \in \mathcal{I}(n+1, k-1)$, and τ be a p-face of σ. The kth-order Whitney p-form corresponding to the small simplex $\mathbf{k}_\sigma(\tau)$ is

$$w(\mathbf{k}_\sigma(\tau)) = \lambda_\sigma^{\mathbf{k}} \mathcal{W}\tau.$$

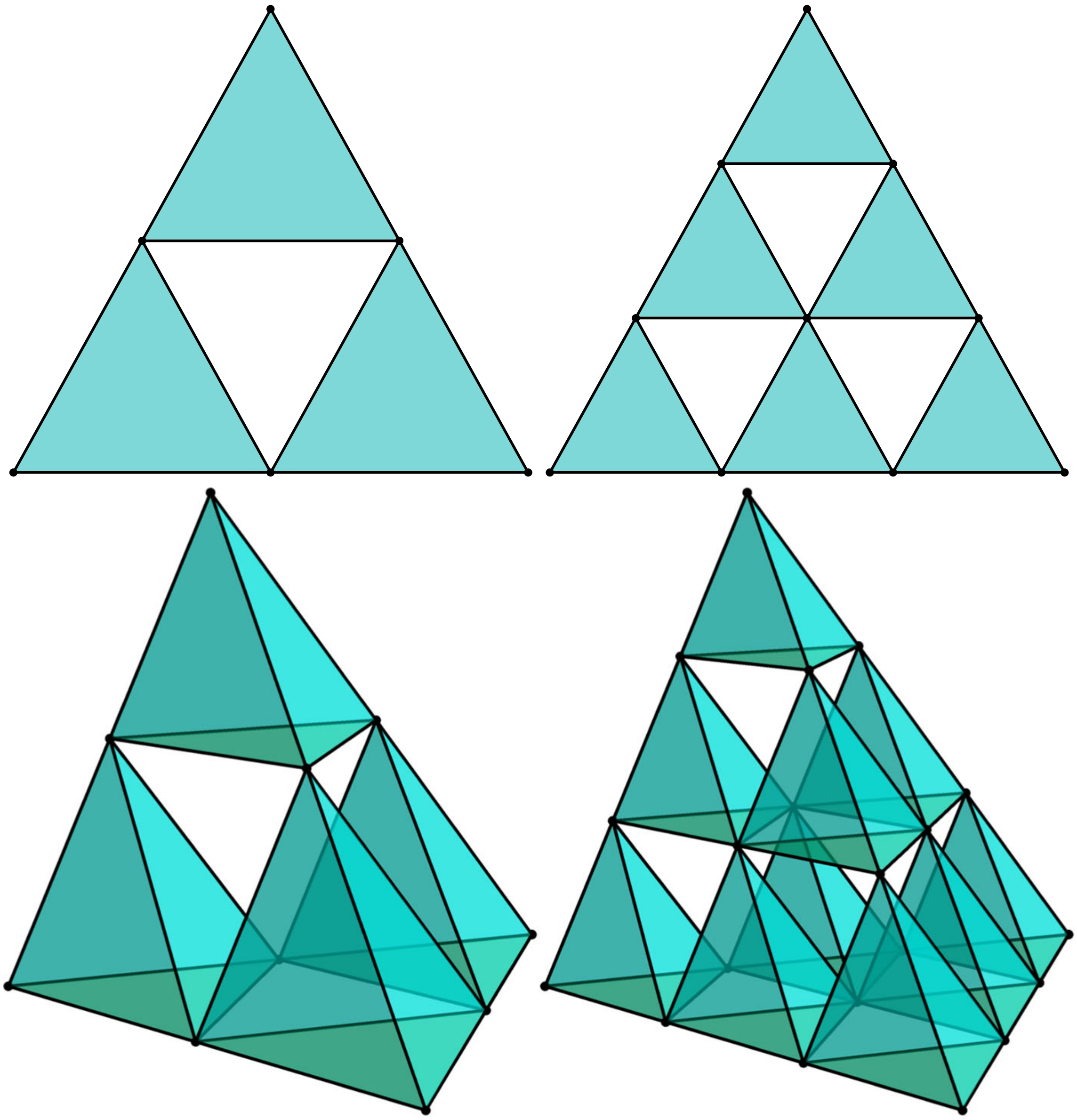

Fig. 1 Second- and third-order small simplices $\mathbf{k}_\sigma(\sigma)$ in the cases when σ is a triangle in two dimensions and a tetrahedron in three dimensions

The space of kth-order Whitney p-forms is the span of all such forms:

$$W_k^p(K) = \text{span}\{w(\upsilon) \mid \upsilon \in S_k^p(K)\}.$$

Since the higher order Whitney forms in the definition above are products of barycentric functions and lowest order Whitney forms, it is immediate that they too are affine invariant and elements of $F^p(K)$. However, it is equally evident that there is no similar correspondence between Whitney forms and cochains of $C_p^*(K)$ in the higher order case. Namely, $W^p(K)$ is already isomorphic to $C_p^*(K)$, and increasing the order increases the dimension of the space, so there is no way for $W_k^p(K)$ to be isomorphic to $C_p^*(K)$. However, it is only natural that higher order approximations require more degrees of freedom, and the spanning higher order forms in Definition 4.1 were given corresponding to small simplices of K. This suggests that instead of $C_p^*(K)$ we should concentrate on cochains over the small simplices of K — the next section makes this idea precise.

5 Interpolating with higher order Whitney forms

As can be seen from Fig. 1, the small simplices do not pave Ω, and hence, they do not form a subdivision of K. However, we can always refine the mesh K such that the refinement contains the small simplices as cells. In this section, we consider how to interpolate cochains of this refined mesh with higher order Whitney forms.

Choose k and let K_k denote a refinement of K into kth-order small simplices; more precisely, K_k can be any mesh in Ω that contains the small simplices of order k as cells. K_k is allowed to have also other cells. For instance, between the small simplices of a tetrahedron in three dimensions, there are holes that are either octahedra or inverted tetrahedra (see Fig. 1). The refinement K_k is not unique; the holes can be accepted as cells as such, or one may further divide them into simplices. The only requirements are that K_k is a mesh in Ω (i.e. satisfies the definition of mesh given in Section 2) and contains the small simplices of order k as cells. We can then consider chains $C_p(K_k)$ and cochains $C_p^*(K_k)$ of K_k and the de Rham map $\mathcal{C}_k : F^p(K) \to C_p^*(K_k)$ (which is well-defined in $F^p(K_k)$, but we restrict the domain to the subset $F^p(K)$).

To interpolate with higher order Whitney forms, we are looking for some kind of interpolating map $\mathcal{V} : C_p^*(K_k) \to F^p(K)$ akin to the Whitney map $\mathcal{W}$. Since the coefficients a_i of the cochain $X = \sum_{\sigma_i \in S^p(K_k)} a_i \sigma_i$ can be considered as integrals of some differential form that X is meant to approximate, we would like to find $\mathcal{V}X \in W_k^p(K)$ such that $\int_{\sigma_i} \mathcal{V}X = a_i \ \forall \sigma_i \in S^p(K_k)$. In other words, we would like to have $\mathcal{C}_k \mathcal{V} X = X$ for all $X \in C_p^*(K_k)$, preserving the property of $\mathcal{W}$. However, it is evident that this is generally not possible, since the number of cells in K_k is greater than the dimension of $W_k^p(K)$. We will therefore have to relax the condition $\int_{\sigma_i} \mathcal{V}X = a_i \ \forall \sigma_i \in S^p(K_k)$ somehow.

Since the spanning higher order forms in Definition 4.1 were given corresponding to small simplices of K, the first relaxation that comes to mind is to require $\int_{\sigma_i} \mathcal{V}X = a_i$ not for all $\sigma_i \in S^p(K_k)$ but for all $\sigma_i \in S_k^p(K)$ — that is, for those cells that are small simplices. However, the spanning forms in Definition 4.1 are not linearly independent, so the dimension of $W_k^p(K)$ is lower than the number of small simplices in $S^p(K_k)$. Hence, we must relax the condition even further.

A simple and feasible way to deal with this linear dependency is to choose a subset $\hat{S}_k^p(K)$ of $S_k^p(K)$ such the forms corresponding to small simplices in $\hat{S}_k^p(K)$ form a basis for $W_k^p(K)$. The subset $\hat{S}_k^p(K)$ of $S_k^p(K)$ is chosen by omitting redundant small simplices. Then those coefficients a_i of the cochain $X = \sum_{\sigma_i \in S^p(K_k)} a_i \sigma_i$ that correspond to $\sigma_i \in \hat{S}_k^p(K)$ determine a unique element $\mathcal{V}X \in W_k^p(K)$ such that $\int_{\sigma_i} \mathcal{V}X = a_i \ \forall \sigma_i \in \hat{S}_k^p(K)$, defining a linear map $\mathcal{V} : C_p^*(K_k) \to F^p(K)$. The map $\mathcal{V}$ does not satisfy $\mathcal{C}_k \mathcal{V}X = X$ for all $X \in C_p^*(K_k)$ since we do not necessarily have $\int_{\sigma_i} \mathcal{V}X = a_i$ if $\sigma_i \notin \hat{S}_k^p(K)$. Now we only have $\mathcal{C}_k \mathcal{V}X = X$ for $X \in \mathcal{C}_k(W_k^p(K))$. This is how our earlier requirement has been relaxed. To summarise, $\mathcal{V}X$ has the correct integrals on the chosen subset of small simplices.

To make the above precise, we have to specify some details — namely, how to choose the subset $\hat{S}_k^p(K)$ such that the corresponding Whitney forms constitute a basis for $W_k^p(K)$. In the following we give the general idea in n-dimensions; details specific to three dimensions are considered in the next section.

Let σ^n denote a generic n-simplex considered as a cell complex, and let $\mathring{W}_k^p(\sigma^n)$ denote the subspace of p-forms in $W_k^p(\sigma^n)$ with zero trace on the boundary of σ^n. We rely on the decomposition [2, Theorem 7.3]

$$W_k^p(\sigma^n) = \bigoplus_{\substack{\sigma^q \in S^q(\sigma^n) \\ p \le q \le n}} \mathring{W}_k^p(\sigma^q), \tag{5.1}$$

where we have extended elements in $W_k^p(\sigma^q)$ to elements of $W_k^p(\sigma^n)$ using the barycentric extension (see [2, (7.1)]; simply consider all barycentric functions in σ^n instead of σ^q), which will henceforth be applied implicitly when appropriate. This implies the global decomposition

$$W_k^p(K) = \bigoplus_{\substack{\sigma^q \in S^q(K) \\ p \le q \le n}} \mathring{W}_k^p(\sigma^q). \tag{5.2}$$

Hence, it suffices to choose the subset $\hat{S}_k^p(\sigma^q)$ in a generic q-simplex σ^q, considering only those small simplices that are not contained in the boundary of σ^q. The same choice can then be applied throughout the mesh, yielding the required map $\mathcal{V} : C_p^*(K_k) \to F^p(K)$.

Let us therefore consider q-simplex σ^q and let $\mathring{S}_k^p(\sigma^q)$ denote the set of those small simplices in $S_k^p(\sigma^q)$ that are not contained in the boundary of σ^q. The dimension of $\mathring{W}_k^p(\sigma^q)$ compares with the cardinality of $\mathring{S}_k^p(\sigma^q)$ as follows:

$$\dim(\mathring{W}_k^p(\sigma^q)) = \binom{q}{p} \binom{p+k-1}{q},$$

$$\#\mathring{S}_k^p(\sigma^q) = \begin{cases} \begin{pmatrix} k-1 \\ q \end{pmatrix}, & p = 0, \\ \begin{pmatrix} q+1 \\ p+1 \end{pmatrix} \begin{pmatrix} p+k-1 \\ q \end{pmatrix}, & p > 0. \end{cases} \tag{5.3}$$

The first line has been proved in [1], and the second line is proved as Lemma A.3 in Appendix A.

These counts determine how many small simplices one must omit before their cardinality matches the dimension of the Whitney forms in each simplex. The omitted simplices can be chosen in many ways, as long as the remaining forms span the same space. For this, let us recall the linear relations between higher order Whitney forms. When σ is a p-face of a $(p+1)$-simplex τ, let $\tau - \sigma$ denote the node of τ that is opposite to σ. Then, for each $\tau \in S^{p+1}(\sigma^q)$ we have (see e.g. [19] for a proof)

$$\sum_{\sigma \in S^p(\sigma^q)} \mathrm{d}_\sigma^\tau \lambda_{\tau-\sigma} \mathcal{W}\sigma = 0. \tag{5.4}$$

This shows that second-order p-forms are linearly dependent, and multiplying both sides by $\lambda_{\sigma^q}^{\mathbf{k}}$ with $\mathbf{k} \in \mathcal{I}(q+1, k-2)$ gives relations for kth-order p-forms. These relations can be used to ensure that we only omit redundant small simplices and the remaining p-forms still span the same space.

When $p = 0$ or $p = q$, (5.3) says $\dim(\mathring{W}_k^p(\sigma^q)) = \#\mathring{S}_k^p(\sigma^q)$. Thus none of the small simplices will be omitted in that case. When $0 < p < q$, we multiply (5.4) applied to each $(p+1)$-face τ of $\sigma^q = x_0 \ldots x_q$ by $\lambda_{\sigma^q}^{\mathbf{k}}$ with $\mathbf{k} \in \mathcal{I}(q+1, k-2)$ such that $k_i \neq 0$ if $x_i \notin \tau$. (This requirement on $\mathbf{k}$ is set to obtain relations specifically for $\mathring{W}_k^p(\sigma^q)$ instead of $W_k^p(\sigma^q)$.) By Lemma A.2 in Appendix A, the number of such $\mathbf{k}$ is $\begin{pmatrix} p+k-1 \\ q \end{pmatrix}$, and hence, we get $\begin{pmatrix} q+1 \\ p+2 \end{pmatrix} \begin{pmatrix} p+k-1 \\ q \end{pmatrix}$ relations for $\mathring{W}_k^p(\sigma^q)$. Notice that the binomial coefficient $\begin{pmatrix} p+k-1 \\ q \end{pmatrix}$ involved in (5.3) appears here too; these formulas have a nice geometric interpretation which will be helpful in implementations. All of this will be clarified in practice in the next section.

We conclude this section with the approximation property of higher order Whitney forms [20] and some remarks.

Theorem 5.1 *Let $\mathcal{V} : C_p^*(K_k) \to F^p(K)$ be the linear map obtained with a choice of kth-order small simplices as explained above, and let ω be a smooth p-form in Ω. There exists a constant $C_{\omega,k}$ such that*

$$|\mathcal{V}\mathcal{C}_k\omega(x) - \omega(x)| \leq \frac{C_{\omega,k}}{C_\Theta^p} h^k \quad \text{for all } x \in \tau \text{ in all } \tau \in S^n(K)$$

whenever $h > 0$, $C_\Theta > 0$, and K is a simplicial mesh in Ω such that $\mathrm{diam}(\sigma) \leq h$ *and $\Theta(\sigma) \geq C_\Theta$ for all simplices σ of K.*

Remark 5.2 To vary the order of Whitney forms in different subdomains of Ω, one has to divide adjacent elements into small simplices of different orders. This results in a division that is not a mesh in the sense of discrete exterior calculus. The interfaces of such subdomains require special treatment and changes in specific methods.

Remark 5.3 d and $\mathcal{V}$ commute for 0-cochains, i.e. $\mathrm{d}\mathcal{V}X = \mathcal{V}\mathrm{d}X$ for $X \in C_0^*(K_k)$. For $p > 0$, this property cannot be achieved without giving up on other properties. In general $\mathrm{d}\mathcal{V}X$ is given by $\mathcal{V}\mathrm{d}\mathcal{C}_k\mathcal{V}X$, so the derivative can still be computed after one first corrects the values of X on omitted small simplices.

6 Systematic implementation strategy

Let us next turn our attention to the implementation of the ideas presented in the previous section. For simplicity and due to practical interests, we will henceforth restrict to the three-dimensional case $n = 3$. Although more work would be required in the case $n > 3$, it should be visible how the same algorithms generalise to any dimension. In contrast, we will not restrict to any specific order k. Our algorithms enable the implementation of kth-order 0-, 1-, 2-, and 3-forms in $\mathbb{R}^3$ such that the order k can be given as a parameter and the same code covers all orders.

Let us first consider kth-order small simplices and the choice of the subsets $\hat{S}_k^p(\sigma^q)$ in three dimensions. As explained, we will work in a generic q-simplex σ^q and consider only those small simplices that are not contained in the boundary of σ^q. Using (5.3) with $0 \leq p \leq q \leq 3$, we find that there are three types of small simplices that require attention:

- $\mathring{W}_k^1(\sigma^2)$ has dimension $2\binom{k}{2}$, while $\#\mathring{S}_k^1(\sigma^2) = 3\binom{k}{2}$. This means we have to omit $\binom{k}{2}$ small 1-simplices in σ^2.
- $\mathring{W}_k^1(\sigma^3)$ has dimension $3\binom{k}{3}$, while $\#\mathring{S}_k^1(\sigma^3) = 6\binom{k}{3}$. This means we have to omit $3\binom{k}{3}$ small 1-simplices in σ^3.
- $\mathring{W}_k^2(\sigma^3)$ has dimension $3\binom{k+1}{3}$, while $\#\mathring{S}_k^2(\sigma^3) = 4\binom{k+1}{3}$. This means we have to omit $\binom{k+1}{3}$ small 2-simplices in σ^3.

Our strategy to omit redundant small simplices was inspired by the example with $k = 3$ given in [11, p. 31]. We make use of the following geometrical observation, illustrated in Fig. 2 (recall also Fig. 1). In σ^2, the holes that are not small simplices are inverted triangles and in correspondence to elements of $\mathcal{I}(3, k-2)$. Their cardinality is $\binom{k}{2}$, which is also the number of relations we get for $\mathring{W}_k^1(\sigma^2)$. These relations correspond to the inverted triangles, and we omit one small 1-simplex for each. In σ^3, there are two kind of holes: $\binom{k}{3}$ inverted tetrahedra corresponding to elements of $\mathcal{I}(4, k-3)$ and $\binom{k+1}{3}$ octahedra corresponding to elements of $\mathcal{I}(4, k-2)$. We have $4\binom{k}{3}$ relations for $\mathring{W}_k^1(\sigma^3)$; 4 per inverted tetrahedron (one for each of its 2-faces). These relations allow us to omit any 3 of the edges of each inverted tetrahedron to obtain a basis for $\mathring{W}_k^1(\sigma^3)$. For $\mathring{W}_k^2(\sigma^3)$, we have one relation per octahedron, and omitting one 2-face for each octahedron yields a basis for $\mathring{W}_k^2(\sigma^3)$.

As stated, it suffices to make these choices only once in a generic q-simplex, and the same choice can then be applied throughout the mesh. For other small simplices

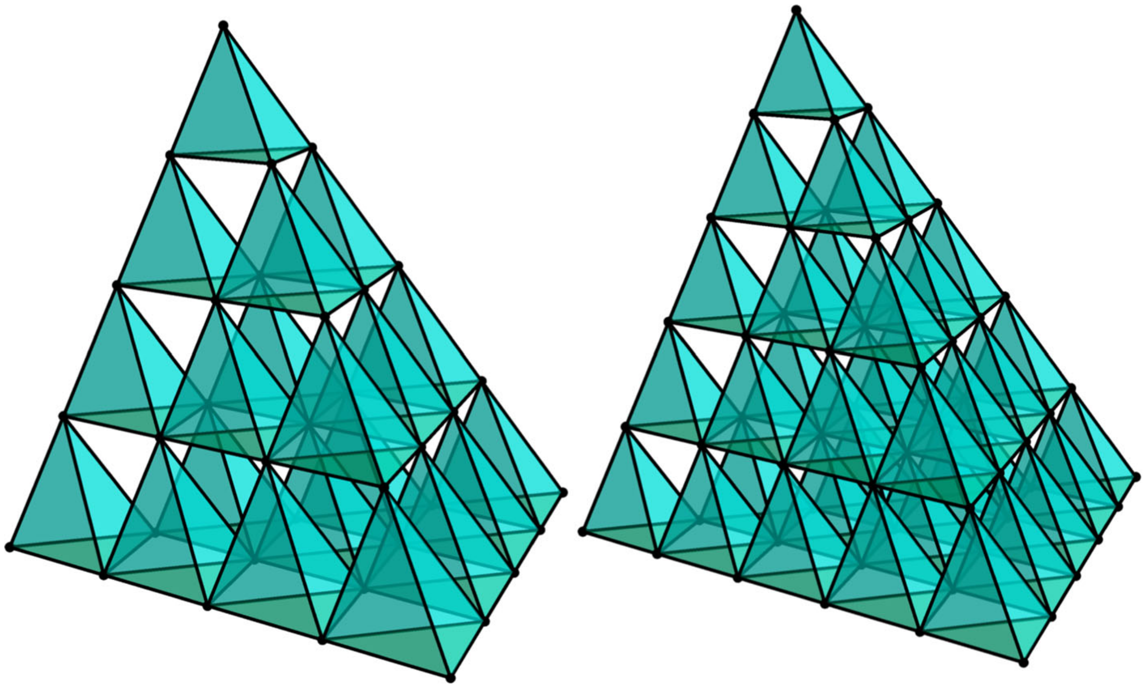

Fig. 2 Illustration of the holes between kth-order small simplices for $k = 4$ and $k = 5$. In σ^2, there are $\binom{k}{2}$ inverted triangles. In σ^3, there are $\binom{k}{3}$ inverted tetrahedra and $\binom{k+1}{3}$ octahedra

than the three types covered above, none of the small simplices are omitted. However, we remark that in practice one should exclude duplicate entries from the sets $\mathring{S}^0_k(\sigma^q)$. Namely, the same small 0-simplex may appear multiple times in (4.1). To handle this, we can choose to always label the small 0-simplices as the images of the first vertex of σ^q.

Let us denote the chosen subsets of $\mathring{S}^p_k(\sigma^q)$ by $\hat{\mathring{S}}^p_k(\sigma^q)$ and choose a numbering for their elements. As explained in the previous section, these subsets determine a map $\mathcal{V} : C^*_p(K_k) \to F^p(K)$ which enables us to interpolate cochains of K_k with kth-order Whitney forms. The implementation process can be divided into three steps:

1. Given a simplicial mesh K in Ω, we form a refinement K_k containing the kth-order small simplices as cells.
2. Given a cochain $X \in C^*_p(K_k)$, we solve the coefficients of the interpolant $\mathcal{V}X$ in the chosen basis.
3. Given the coefficients of the interpolant $\mathcal{V}X$, we show how to evaluate it at a given point $x \in \Omega$.

These steps are discussed in detail in the following three subsections.

6.1 Refining the mesh

Suppose we have a three-dimensional simplicial mesh K in Ω. In this subsection, we discuss how the mesh can be refined systematically to obtain a refinement K_k that contains the kth-order small simplices as cells. We make the following assumptions for the mesh as data structure:

- The p-simplices of K have been indexed, and the positions of the 0-simplices (which are points in Ω) are contained in a list.
- The vertices of each p-simplex $\sigma \in S^p(K)$ can be accessed in a definite order, and this order determines the orientation of σ.
- Given a list of vertices $x_0, \ldots, x_p$, we have means of finding the p-simplex with these vertices (if one exists).

These can be achieved when, in addition to the position list, we store the indices of the $(p-1)$-faces and the parent $(p+1)$-simplices of each p-simplex σ.

When refining the mesh, one might wish to store the indices of the small simplices that correspond to the elements of the sets $\hat{\mathring{S}}^p_k(\sigma^q)$ in each q-simplex $\sigma^q \in S^q(K)$. They will be needed when interpolating cochains, and having saved the indices in memory, one need not repeatedly find them for each interpolation. While possible, this is not necessary if new indices are allocated in increasing order, as the indices of the small simplices will then be implied from those of the big simplices. In this case finding them is a very small task, while storing the indices can use a lot of memory. Nevertheless, if desired, the index of each small simplex can be stored right after it is added to K_k, and hence, we need not make this explicit in the rest of this subsection.

The strategy for refining the mesh is as follows. We start with an empty mesh K_k and make it the desired refinement of K by going through the simplices of K in the order of increasing dimension and adding the corresponding small simplices into K_k. With this order, we only have to consider the small simplices that are not in the boundary of the simplices, since those in the boundary have already been covered along with some lower-dimensional simplex. For 2- and 3-simplices, we will also fill the holes that would otherwise be left between the small simplices. Multi-indices are needed to label both small simplices and the holes, and hence, we assume access to the sets $\mathcal{I}(l, m)$ stored in some data structure.

The first step is straightforward: we copy the 0-simplices of K into K_k. Second, the small 0- and 1-simplices of each 1-simplex of K are added into K_k. Third, we go through the 2-simplices of K and add the corresponding small 0-, 1-, and 2-simplices into K, also filling the inverted triangles in between. Fourth, we add the small 0-, 1-, 2-, and 3-simplices and the holes of each 3-simplex of K into K_k. The holes that are octahedra are the only cells in K_k that are not simplices; however, it is possible to divide them into four tetrahedra. In discrete exterior calculus, it is sometimes desirable that cells are well-centered. In this case one might wish to divide each octahedron into four tetrahedra by adding a 1-simplex of smallest possible length. If this is not uniquely determined, the octahedron can accordingly be divided into two pyramids or kept as it is. The potential division has no effect on the algorithms of this paper.

When adding the small simplices of $\sigma^q = x_0 \ldots x_q \in S^q(K)$ into K_k, we first add the small 0-simplices that are in the interior of σ^q. These are obtained as images of x_0 through $\mathbf{k}_\sigma$ with $\mathbf{k} \in \mathcal{I}(q, k-1)$ such that $k_i \neq 0$ for $i > 0$. Each small 0-simplex is covered exactly once, so we do not have to check if another 0-simplex has already been added in the same position. For adding other small simplices (and the holes), we need means of finding the indices of the small 0-simplices corresponding to their vertices (which have already been added into K_k). It is useful to have a function that returns the index of the small 0-simplex $\mathbf{k}_\sigma(x_i)$ for any $\mathbf{k}$, $\sigma = x_0 \dots x_q$, and $i \in \{0, \dots, q\}$. The indices of the 0-simplices can then be used to add higher-dimensional cells (or find if they exist); these are added in the order of increasing dimension.

The approach is simple on paper and also relatively easy to implement. Algorithm 1 summarises our strategy for refining the mesh.

Algorithm 1 Refining the mesh.

Data: Simplicial mesh K.
Result: Refinement K_k containing the kth-order small simplices as cells.

```
initialise empty mesh K_k
foreach σ ∈ S^0(K) do
    add a 0-simplex into K_k at the location of σ
foreach σ = x_0x_1 ∈ S^1(K) do
    foreach k ∈ I(2, k − 1) such that k_1 ≠ 0 do
        add the small 0-simplex k_σ(x_0) into K_k
    foreach k ∈ I(2, k − 1) do
        add the small 1-simplex k_σ(x_0x_1) into K_k
foreach σ = x_0x_1x_2 ∈ S^2(K) do
    foreach k ∈ I(3, k − 1) such that k_1, k_2 ≠ 0 do
        add the small 0-simplex k_σ(x_0) into K_k
    foreach k ∈ I(3, k − 1) do
        add the small 1-simplices k_σ(x_0x_1), k_σ(x_0x_2), and k_σ(x_1x_2) into K_k (if
        not in K_k already)
        add the small 2-simplex k_σ(x_0x_1x_2) into K_k
    foreach k ∈ I(3, k − 2) do
        add the inverted triangle corresponding to k into K_k
foreach σ = x_0x_1x_2x_3 ∈ S^3(K) do
    foreach k ∈ I(4, k − 1) such that k_1, k_2, k_3 ≠ 0 do
        add the small 0-simplex k_σ(x_0) into K_k
    foreach k ∈ I(4, k − 1) do
        add the small 1-simplices k_σ(x_0x_1), k_σ(x_0x_2), k_σ(x_0x_3), k_σ(x_1x_2),
        k_σ(x_1x_3), and k_σ(x_2x_3) into K_k (if not in K_k already)
        add the small 2-simplices k_σ(x_0x_1x_2), k_σ(x_0x_1x_3), k_σ(x_0x_2x_3), and
        k_σ(x_1x_2x_3) into K_k (if not in K_k already)
        add the small 3-simplex k_σ(x_0x_1x_2x_3) into K_k
    foreach k ∈ I(4, k − 2) do
        add the octahedron corresponding to k into K_k
    foreach k ∈ I(4, k − 3) do
        add the inverted tetrahedron corresponding to k into K_k
```

6.2 Solving the coefficients of the interpolant

Suppose we have a cochain $X \in C^*_p(K_k)$ on the refined mesh K_k. In this subsection, we discuss how to determine the coefficients of the interpolant $\mathcal{V}X$ in the chosen basis.

The idea is to first solve the coefficients corresponding to small p-simplices that are in $\hat{\mathring{S}}^p_k(\sigma^p)$ for some $\sigma^p \in S^p(K)$. These can then be used to solve the coefficients corresponding to small p-simplices that are in $\hat{\mathring{S}}^p_k(\sigma^{p+1})$ for some $\sigma^{p+1} \in S^{p+1}(K)$. Continuing in this order, we can solve the coefficients of the interpolant in all simplices.

When $\sigma^p \in S^p(K)$, the coefficients corresponding to small p-simplices that are in $\hat{\mathring{S}}^p_k(\sigma^p)$ are uniquely determined by the values of X on the elements of $\hat{\mathring{S}}^p_k(\sigma^p)$; let $X[\hat{\mathring{S}}^p_k(\sigma^p)]$ denote these components of X when it is considered as a vector. To solve the coefficients, observe that if for each p and q we define matrix $A(p, q)$, indexed over $\upsilon \in \hat{\mathring{S}}^p_k(\sigma^q)$, by

$$A(p, q)_{ij} = \int_{\upsilon_i} w(\upsilon_j),$$

and define c_i as ith component of the vector $A(p, p)^{-1}X[\hat{\mathring{S}}^p_k(\sigma^p)]$, then the Whitney form $\sum_{\upsilon_i \in \hat{\mathring{S}}^p_k(\sigma^p)} c_i w(\upsilon_i)$ has the correct integrals on elements of $\hat{\mathring{S}}^p_k(\sigma^p)$. Hence, the coefficients can be solved using the inverse of the matrix $A(p, p)$.

The same idea works when $q > p$ and $\sigma^q \in S^q(K)$, but now we first have to take into account the Whitney forms corresponding to small simplices of the faces of σ^q whose coefficients have been solved earlier. Therefore we first subtract their integrals over elements of $\hat{\mathring{S}}^p_k(\sigma^q)$ from the vector $X[\hat{\mathring{S}}^p_k(\sigma^q)]$. Then multiplying by $A(p, q)^{-1}$ yields the correct coefficients corresponding to small p-simplices in $\hat{\mathring{S}}^p_k(\sigma^q)$.

At first glance, this approach might seem inefficient because we have to integrate functions and invert matrices to even solve the coefficients of the interpolant. However, we stress that the integrals of higher order Whitney forms over small simplices are affine invariant quantities, and hence, it suffices to build the matrices $A(p, q)$ only once! Of course, in practice we can use the LU decomposition of $A(p, q)$ to solve the coefficients instead of explicitly computing the inverse; this yields better numerical accuracy. We write $A(p, q)^{-1}$ only for notational simplicity.

The integrals of the basis functions corresponding to small simplices of faces of σ^q over elements of $\hat{\mathring{S}}^p_k(\sigma^q)$ can also be precomputed. We only have to remember that the vertices of the faces may be in different possible orders, and these yield different integrals. For this, let us define matrices $B(p, \sigma^q, \sigma^r)$, where σ^r is an r-face of σ^q, such that

$$B(p, \sigma^q, \sigma^r)_{ij} = \int_{\upsilon_i} w(\upsilon_j), \quad \upsilon_i \in \hat{\mathring{S}}^p_k(\sigma^q),\ \upsilon_j \in \hat{\mathring{S}}^p_k(\sigma^r).$$

This time the matrix $B(p, \sigma^q, \sigma^r)$ is not the same for all σ^q and σ^r since it depends on which face σ^r is and on the order of its vertices. However, there is only a finite number of possibilities we have to precompute, and then the matrix $B(p, \sigma^q, \sigma^r)$ will always be one of these. For example, consider $B(1, \sigma^3, \sigma^2)$. There are four 2-faces of σ^3, and there are six permutations for the vertices for σ^2. Hence, there are 24 possibilities for the matrix $B(p, \sigma^q, \sigma^r)$. In 3D, the number of possibilities never exceeds 24 (see Table 1).

Having precomputed these matrices $B(p, \sigma^q, \sigma^r)$, we do not have to integrate anything when solving the coefficients. When σ^r is a face of σ^q and we wish to take the Whitney forms corresponding to small simplices of σ^r into account, we use the matrix $B(p, \sigma^q, \sigma^r)$ (the one appropriate for σ^q and σ^r) and the coefficients we have solved in σ^r earlier. Matrix-vector multiplication yields the integrals over elements of $\hat{\mathring{S}}_k^p(\sigma^q)$.

The integrals of higher order Whitney forms over small simplices that are needed for the matrices $A(p, q)$ and $B(p, \sigma^q, \sigma^r)$ can be computed analytically; we elaborate on this in Appendix B. Another option is to use at least kth-order quadrature formulas for numerical integration. The matrices are formed only once, and hence, we can precompute them in as high numerical precision as desired.

Algorithm 2 summarises our strategy for solving the coefficients of the interpolant.

Algorithm 2 Solving the coefficients of the interpolant.

Data: Cochain $X \in C_p^*(K_k)$ on the refined mesh K_k.

Result: Coefficients $c[\hat{\mathring{S}}_k^p(\sigma^q)]$ of the interpolant $\mathcal{V}X$ in the chosen basis of $\mathring{W}_k^p(\sigma^q)$, for all $\sigma^q \in S^q(K)$, $p \leq q \leq 3$.

```
foreach σ^p ∈ S^p(K) do
    set c[Ŝ_k^p(σ^p)] = A(p, p)^{-1} X[Ŝ_k^p(σ^p)]
for q = p + 1 to 3 do
    foreach σ^q ∈ S^q(K) do
        for r = p to q − 1 do
            foreach r-face σ^r of σ^q do
                subtract B(p, σ^q, σ^r) c[Ŝ_k^p(σ^r)] from X[Ŝ_k^p(σ^q)]
        set c[Ŝ_k^p(σ^q)] = A(p, q)^{-1} X[Ŝ_k^p(σ^q)]
```

Table 1 The number of different possibilities for the matrix $B(p, \sigma^q, \sigma^r)$

	$\#B(p, \sigma^q, \sigma^r)$
$p = 0, q = 1, r = 0$	2
$p = 0, q = 2, r = 0$	3
$p = 0, q = 3, r = 0$	4
$p \in \{0, 1\}, q = 2, r = 1$	6
$p \in \{0, 1\}, q = 3, r = 1$	12
$p \in \{0, 1, 2\}, q = 3, r = 2$	24

6.3 Evaluating the interpolant at a given point

Suppose we have solved the coefficients $c[\upsilon_i]$ of the interpolant in the chosen basis for $W_k^p(K)$ and we wish to evaluate the interpolant at a given point $x \in \Omega$. In this subsection, we discuss how to compute the value of $\sum_{\upsilon_i \in \hat{S}_k^p(K)} c[\upsilon_i]w(\upsilon_i)$ at x. Note that this is not an entirely trivial task, for we have used the decomposition (5.2) when forming a basis and hence have to accumulate contributions of $\mathring{W}_k^p(\sigma^q)$ for different $\sigma^q \in S^q(K)$, $p \le q \le 3$.

We assume it is possible to search for a 3-simplex $\sigma^3 \in S^3(K)$ that contains x (or one is known in advance). Notice that $w(\upsilon)$ is zero in σ^3 if υ is not contained in σ^3, and hence, it suffices to consider the basis forms corresponding to small simplices of σ^3. If x happens to be in multiple 3-simplices, their intersection is some q-simplex $\sigma^q \in S^q(K)$ for $q < 3$. In this case we may either compute the value in σ^q (considering only the small simplices of σ^q) or choose one of them and compute the value there; the trace on σ^q agrees with the value computed in σ^q.

Supposing we have found a 3-simplex σ^3 containing x, the next step is to compute the barycentric coordinates of x and the values of the lowest order Whitney forms corresponding to p-faces of σ^3. These can then be used with the coefficients $c[\upsilon_i]$ to compute the value of the interpolant. Indeed, since the basis forms are products of barycentric functions and lowest order Whitney forms, we can write the interpolant as

$$\sum_{\upsilon_i \in \hat{S}_k^p(\sigma^3)} c[\upsilon_i]w(\upsilon_i) = \sum_{\sigma_i^p \subset \sigma^3} d_i \mathcal{W}\sigma_i^p,$$

where the second sum is over p-faces σ_i^p of σ^3 and d_i is a linear combination of products of barycentric functions. To compute d_i, recall the decomposition (5.1) and accumulate the contributions from all faces of σ^3 using the coefficients $c[\upsilon_i]$. Taking orientations into account, our strategy for evaluating the interpolant at a given point is formulated in Algorithm 3.

Algorithm 3 Evaluating the interpolant at a given point.

Data: Point $x \in \Omega$ and the coefficients $c[\upsilon_i]$ of the interpolant.
Result: Value of the interpolant $\sum_{\upsilon_i \in \hat{S}_k^p(K)} c[\upsilon_i]w(\upsilon_i)$ at x.

find a 3-simplex $\sigma^3 = x_0x_1x_2x_3 \in S^3(K)$ containing x
compute the barycentric functions λ_0, λ_1, λ_2, and λ_3 at x
foreach *p-face σ_i^p of σ^3* **do**
    compute $\mathcal{W}\sigma_i^p(x)$
    initialise d_i as zero
for $q = p$ **to** *3* **do**
    foreach *q-face σ^q of σ^3* **do**
        foreach *small p-simplex $\upsilon = \mathbf{k}_{\sigma^q}(\tau) \in \mathring{\hat{S}}_k^p(\sigma^q)$* **do**
            set $d_i = d_i \pm c[\upsilon]\lambda_{\sigma^q}^{\mathbf{k}}$ if $\tau = \pm\sigma_i^p$
the result is $\sum d_i \mathcal{W}\sigma_i^p(x)$, where the sum is over the p-faces σ_i^p of σ^3

7 Numerical examples

To show that our algorithms can be implemented in practice, we provide numerical examples with higher order Whitney forms. In all of the test cases, our domain Ω is the rhombic dodecahedron with vertices $(\pm 1, \pm 1, \pm 1)$, $(\pm 2, 0, 0)$, $(0, \pm 2, 0)$, and $(0, 0, \pm 2)$. We build a simplicial mesh K in Ω and its refinement K_k. For a p-form ω, the cochain $\mathcal{C}_k\omega$ is obtained by integrating ω using high-order quadrature formulas for p-simplices. Then we can approximate ω with the kth-order Whitney form $\mathcal{VC}_k\omega$. We compute the L^2 norm (again using quadrature formulas) of the error $|\mathcal{VC}_k\omega - \omega|$. The experiments are performed for $k \in \{1, \ldots, 12\}$ using several test functions ω. All test functions have L^2 norm close to one so that the use of absolute error is appropriate. To study convergence properly before running out of machine accuracy, computations are done in quadruple precision.

First, we confirm that our algorithms work as expected using polynomial test functions on a coarse mesh. The mesh has 24 tetrahedra and the maximum edge length is 2.0. Our test functions $\omega_{p,j}$ are (where the label $j \in \{1, 2, 3\}$)

$$
\begin{aligned}
&\omega_{0,1}(x, y, z) = 0.25,\ \ \omega_{0,2}(x, y, z) = \frac{64}{75}x^2y^2z - \frac{8}{75}z^5,\\
&\omega_{0,3}(x, y, z) = \frac{32}{11}x^4y^4z^2 - \frac{1}{176}z^{10},\ \ \omega_{1,1}(x, y, z) = \frac{30}{128}\mathrm{d}x - \frac{10}{128}\mathrm{d}y + \frac{10}{252}\mathrm{d}z,\\
&\omega_{1,2}(x, y, z) = x^2y^2z\mathrm{d}x + x^2yz^2\mathrm{d}y + xy^2z^2\mathrm{d}z,\\
&\omega_{1,3}(x, y, z) = \frac{20}{9}(x^2y^4z^4\mathrm{d}x + x^4y^2z^4\mathrm{d}y + x^4y^4z^2\mathrm{d}z),\\
&\omega_{2,1}(x, y, z) = \frac{30}{128}\mathrm{d}y \wedge \mathrm{d}z - \frac{10}{128}\mathrm{d}z \wedge \mathrm{d}x + \frac{10}{252}\mathrm{d}x \wedge \mathrm{d}y,\\
&\omega_{2,2}(x, y, z) = x^2y^2z\mathrm{d}y \wedge \mathrm{d}z + x^2yz^2\mathrm{d}z \wedge \mathrm{d}x + xy^2z^2\mathrm{d}x \wedge \mathrm{d}y,\\
&\omega_{2,3}(x, y, z) = \frac{20}{9}(x^2y^4z^4\mathrm{d}y \wedge \mathrm{d}z + x^4y^2z^4\mathrm{d}z \wedge \mathrm{d}x + x^4y^4z^2\mathrm{d}x \wedge \mathrm{d}y),\\
&\omega_{3,1}(x, y, z) = 0.25\mathrm{d}x \wedge \mathrm{d}y \wedge \mathrm{d}z,\\
&\omega_{3,2}(x, y, z) = \left(\frac{64}{75}x^2y^2z - \frac{8}{75}z^5\right)\mathrm{d}x \wedge \mathrm{d}y \wedge \mathrm{d}z,\\
&\omega_{3,3}(x, y, z) = \left(\frac{32}{11}x^4y^4z^2 - \frac{1}{176}z^{10}\right)\mathrm{d}x \wedge \mathrm{d}y \wedge \mathrm{d}z.
\end{aligned}
$$

The results are displayed in Table 2. As expected, the approximation becomes exact as soon as the test function is in the space of kth-order Whitney forms.

We also study the convergence of the approximations with respect to the maximum edge length h of the initial mesh K. Our test function is the 1-form

$$
\begin{aligned}
\omega(x, y, z) = \frac{1}{4}\Big(&\sin(2y)\cos(2z)e^{x^2/4}\mathrm{d}x + \sin(2z)\cos(2x)e^{y^2/4}\mathrm{d}y\\
&+ \sin(2x)\cos(2y)e^{z^2/4}\mathrm{d}z\Big).
\end{aligned}
$$

Table 2 Values of $\||\mathcal{V}\mathcal{C}_k\omega_{p,j} - \omega_{p,j}|\|_{L^2(\Omega)}$ for polynomial test functions $\omega_{p,j}$

	$k=1$	$k=2$	$k=3$	$k=4$	$k=5$	$k=6$	$k=7$	$k=8$	$k=9$	$k=10$	$k=11$	$k=12$
$\omega_{0,1}$	9.2e-35	1.9e-34	2.6e-34	3.8e-34	6.5e-34	6.7e-34	7.8e-34	7.4e-34	1.5e-33	1.6e-33	1.8e-33	5.3e-33
$\omega_{0,2}$	1.6	3.4e-01	5.7e-02	5.1e-03	5.4e-34	7.4e-34	9.1e-34	8.2e-34	1.8e-33	2.0e-33	2.4e-33	5.1e-33
$\omega_{0,3}$	5.9	1.8	5.8e-01	2.0e-01	5.4e-02	1.1e-02	2.2e-03	2.7e-04	1.9e-05	1.8e-33	2.6e-33	4.7e-33
$\omega_{1,1}$	1.6e-34	3.1e-34	4.9e-34	3.8e-34	9.5e-34	9.9e-34	1.2e-33	1.0e-33	2.7e-33	4.0e-33	6.7e-33	1.5e-32
$\omega_{1,2}$	1.5	8.1e-01	2.4e-01	4.7e-02	5.1e-03	1.1e-33	1.3e-33	9.7e-34	2.5e-33	4.0e-33	5.7e-33	1.0e-32
$\omega_{1,3}$	2.7	1.6	9.8e-01	3.3e-01	1.2e-01	3.4e-02	7.4e-03	1.2e-03	1.4e-04	9.0e-06	4.6e-33	7.7e-33
$\omega_{2,1}$	1.9e-34	2.9e-34	4.5e-34	4.2e-34	8.7e-34	1.1e-33	1.4e-33	1.3e-33	2.8e-33	4.8e-33	6.8e-33	1.7e-32
$\omega_{2,2}$	9.8e-01	6.7e-01	2.2e-01	4.1e-02	4.3e-03	1.1e-33	1.2e-33	1.0e-33	1.9e-33	2.9e-33	4.8e-33	1.0e-32
$\omega_{2,3}$	1.0	9.7e-01	6.0e-01	3.3e-01	1.4e-01	4.1e-02	8.5e-03	1.4e-03	1.6e-04	1.2e-05	3.6e-33	8.6e-33
$\omega_{3,1}$	0	1.3e-34	2.5e-34	2.6e-34	7.4e-34	7.0e-34	7.8e-34	6.9e-34	1.4e-33	2.2e-33	3.9e-33	6.7e-33
$\omega_{3,2}$	9.0e-01	5.2e-01	1.6e-01	3.2e-02	3.8e-03	8.0e-34	7.8e-34	6.3e-34	1.2e-33	2.6e-33	4.1e-33	7.8e-33
$\omega_{3,3}$	9.6e-01	8.3e-01	5.0e-01	2.5e-01	9.7e-02	2.8e-02	6.0e-03	1.0e-03	1.4e-04	1.2e-05	2.5e-33	5.2e-33

Table 3 Values of $\||\mathcal{V}\mathcal{C}_k\omega - \omega|\|_{L^2(\Omega)}$ using four meshes with maximum edge length h

	$h = 2.0$	$h = 1.0$	$h = 0.5$	$h = 0.25$
$k = 1$	9.0649e-01	4.4526e-01	2.2121e-01	1.1029e-01
$k = 2$	3.3087e-01	8.0654e-02	1.9448e-02	4.8134e-03
$k = 3$	9.8547e-02	1.2599e-02	1.5579e-03	1.9377e-04
$k = 4$	2.6463e-02	1.4660e-03	8.9684e-05	5.5870e-06
$k = 5$	4.5029e-03	1.5825e-04	4.9643e-06	1.5484e-07
$k = 6$	9.9236e-04	1.3688e-05	2.1085e-07	3.2889e-09
$k = 7$	1.2736e-04	1.0950e-06	8.5536e-09	6.6710e-11
$k = 8$	2.0474e-05	7.2193e-08	2.8066e-10	1.0957e-12
$k = 9$	2.2874e-06	4.7448e-09	9.2150e-12	1.7954e-14
$k = 10$	2.9958e-07	2.6627e-10	2.5915e-13	2.5269e-16
$k = 11$	2.9673e-08	1.5551e-11	7.5258e-15	3.6695e-18
$k = 12$	3.4667e-09	7.9114e-13	1.9458e-16	4.7636e-20

We approximate ω using four meshes that have 24, 192, 1536, and 12288 tetrahedra with maximum edge lengths 2.0, 1.0, 0.5, and 0.25 respectively. The results are displayed in Table 3 and illustrated in Fig. 3 (in log–log scale). We conclude that higher

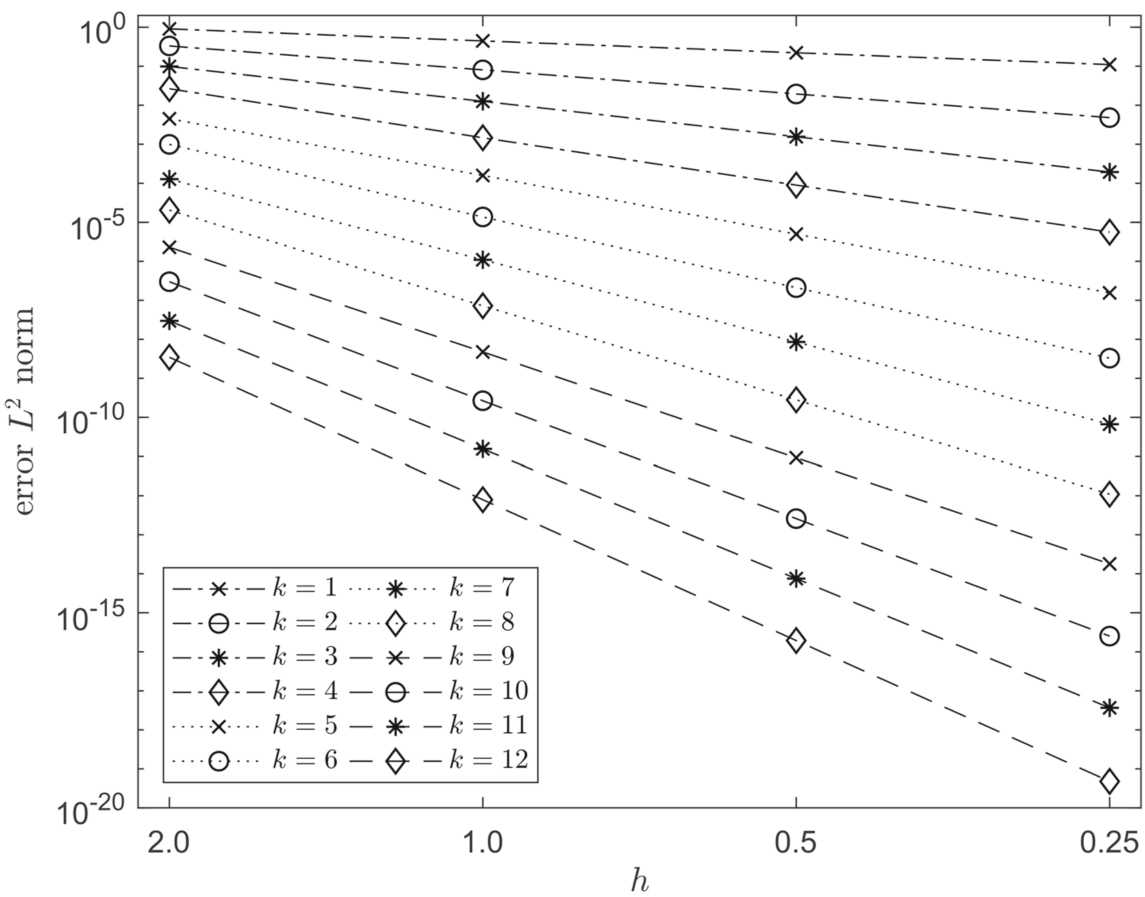

Fig. 3 Illustration of the results displayed in Table 3

order convergence as predicted theoretically by Theorem 5.1 can also be attained in practice with the help of our algorithms.

Appendix A. Some combinatorial results

This Appendix contains some combinatorial results that are used in this paper.

Lemma A.1 *For integers $l > 0$ and $m \geq 0$, we have*

$$\#\mathcal{I}(l, m) = \binom{l+m-1}{m}.$$

Proof This is seen using the well-known stars and bars technique from combinatorics. □

Lemma A.2 *Let τ be a p-face of $\sigma^q = x_0 \dots x_q$. We have*

$$\#\{\mathbf{k} \in \mathcal{I}(q+1, k) \mid k_i \neq 0 \text{ if } x_i \notin \tau\} = \binom{p+k}{q}.$$

Proof

$$\begin{aligned}&\#\{\mathbf{k} \in \mathcal{I}(q+1, k) \mid k_i \neq 0 \text{ if } x_i \notin \tau\} = \#\mathcal{I}(q+1, k-(q+1-(p+1)))\\&= \#\mathcal{I}(q+1, p+k-q) = \binom{p+k}{p+k-q} = \binom{p+k}{q},\end{aligned}$$

where Lemma A.1 was applied in the second to last step. □

Lemma A.3 *Let $\mathring{S}_k^p(\sigma^q)$ denote the set of those small simplices in $S_k^p(\sigma^q)$ that are not contained in the boundary of σ^q. The cardinality of $\mathring{S}_k^p(\sigma^q)$ is*

$$\#\mathring{S}_k^p(\sigma^q) = \begin{cases} \binom{k-1}{q}, & p = 0, \\ \binom{q+1}{p+1}\binom{p+k-1}{q}, & p > 0. \end{cases}$$

Proof When a p-face σ^p of σ^q is mapped through $\mathbf{k}_{\sigma^q}$ with $\mathbf{k} \in \mathcal{I}(q+1, k-1)$, the image $\mathbf{k}_{\sigma^q}(\sigma^p)$ is not contained in the boundary of σ^q precisely when $k_i \neq 0$ if $x_i \notin \sigma^p$. By Lemma A.2, the number of such $\mathbf{k}$ is $\binom{p+k-1}{q}$. When $p = 0$, the small simplices not in the boundary are all obtained as image of one vertex; when $p > 0$, the images of the $\binom{q+1}{p+1}$ p-faces are distinct. □

Appendix B. Integrating higher order Whitney forms over small simplices

This Appendix discusses how the integrals of higher order Whitney forms over small simplices can be computed analytically. We start with a well-known integration rule for products of barycentric functions [30].

Lemma B.1 *Let $\sigma = x_0 \dots x_q$ be a q-simplex and $\mathbf{k} \in \mathcal{I}(q+1, k)$. The average of $\lambda_\sigma^{\mathbf{k}}$ over σ is*

$$\frac{1}{|\sigma|}\int_\sigma \lambda_\sigma^{\mathbf{k}} = \frac{\prod_{i=0}^q k_i!}{(q+k)!}.$$

This result is extended for small q-simplices in [27, Proposition 3.6]. We extend the result further for small p-simplices, $p \le q$. For $\mathbf{k} \in \mathcal{I}(q+1, k)$, we say $\mathbf{r} \le \mathbf{k}$ if $\mathbf{r} = (r_0, \dots, r_q)$ is a multi-index such that $r_i \le k_i$ for all i. In this case we can define $\binom{\mathbf{k}}{\mathbf{r}} = \prod_{i=0}^q \binom{k_i}{r_i}$. With these notations, Lemma B.1 generalises for small p-simplices as follows.

Lemma B.2 *Let $\sigma = x_0 \dots x_q$ be a q-simplex, and suppose $\tau = x_{i_0} \dots x_{i_p}$ is a p-face of σ and $x_{i_{p+1}}, \dots, x_{i_q}$ are the vertices of σ that are not in τ. Let $\mathbf{k} \in \mathcal{I}(q+1, k)$, $\mathbf{k}' \in \mathcal{I}(q+1, k')$, $\tilde{\mathbf{k}} = (k_{i_0}, \dots, k_{i_p})$, and $\upsilon = \mathbf{k}'_\sigma(\tau)$. The average of $\lambda_\sigma^{\mathbf{k}}$ over the small p-simplex υ is*

$$\frac{1}{|\upsilon|}\int_\upsilon \lambda_\sigma^{\mathbf{k}} = \frac{1}{(k'+1)^k}\left(\prod_{j=p+1}^{q} (k'_{i_j})^{k_{i_j}}\right)\sum_{\mathbf{r}\le\tilde{\mathbf{k}}}\binom{\tilde{\mathbf{k}}}{\mathbf{r}}\left(\prod_{j=0}^{p}(k'_{i_j})^{k_{i_j}-r_j}\right)\frac{1}{|\tau|}\int_\tau \lambda_\tau^{\mathbf{r}}.$$

Proof Recall that $\mathbf{k}'_\sigma$ maps the point x with barycentric coordinates λ_i to the point whose barycentric coordinates are $\frac{\lambda_i + k'_i}{k'+1}$. Hence, the λ_{i_j} with $j > p$ are constant on υ and we can write

$$\int_\upsilon \lambda_\sigma^{\mathbf{k}} = \left(\frac{k'_{i_{p+1}}}{k'+1}\right)^{k_{i_{p+1}}} \cdot \dots \cdot \left(\frac{k'_{i_q}}{k'+1}\right)^{k_{i_q}} \int_\upsilon \lambda_{i_0}^{k_{i_0}} \cdot \dots \cdot \lambda_{i_p}^{k_{i_p}},$$

$$\int_\upsilon \lambda_{i_0}^{k_{i_0}} \cdot \dots \cdot \lambda_{i_p}^{k_{i_p}} = \int_\tau \left(\frac{\lambda_{i_0}+k'_{i_0}}{k'+1}\right)^{k_{i_0}} \cdot \dots \cdot \left(\frac{\lambda_{i_p}+k'_{i_p}}{k'+1}\right)^{k_{i_p}} \cdot \frac{1}{(k'+1)^p},$$

where $\frac{1}{(k'+1)^p}$ is the Jacobian determinant of $\mathbf{k}'_\sigma$ considered as a map from τ onto υ.

Since $|\upsilon| = \frac{|\tau|}{(k'+1)^p}$, we get

$$\frac{1}{|\upsilon|}\int_\upsilon \lambda_\sigma^{\mathbf{k}} = \left(\frac{k'_{i_{p+1}}}{k'+1}\right)^{k_{i_{p+1}}} \cdot \dots \cdot \left(\frac{k'_{i_q}}{k'+1}\right)^{k_{i_q}} \frac{1}{|\tau|}\int_\tau$$
$$\left(\frac{\lambda_{i_0}+k'_{i_0}}{k'+1}\right)^{k_{i_0}} \cdot \dots \cdot \left(\frac{\lambda_{i_p}+k'_{i_p}}{k'+1}\right)^{k_{i_p}}$$

$$= \frac{1}{(k'+1)^k}\left(\prod_{j=p+1}^{q}(k'_{i_j})^{k_{i_j}}\right)\frac{1}{|\tau|}\int_\tau \underbrace{(\lambda_{i_0}+k'_{i_0})^{k_{i_0}}}_{\sum_{r_0=0}^{k_{i_0}}\binom{k_{i_0}}{r_0}\lambda_{i_0}^{r_0}(k'_{i_0})^{k_{i_0}-r_0}} \cdot\dots\cdot \underbrace{(\lambda_{i_p}+k'_{i_p})^{k_{i_p}}}_{\sum_{r_p=0}^{k_{i_p}}\binom{k_{i_p}}{r_p}\lambda_{i_p}^{r_p}(k'_{i_p})^{k_{i_p}-r_p}}$$

$$= \frac{1}{(k'+1)^k}\left(\prod_{j=p+1}^{q}(k'_{i_j})^{k_{i_j}}\right)\sum_{\mathbf{r}\le\tilde{\mathbf{k}}}\binom{\tilde{\mathbf{k}}}{\mathbf{r}}\left(\prod_{j=0}^{p}(k'_{i_j})^{k_{i_j}-r_j}\right)\frac{1}{|\tau|}\int_\tau \lambda_\tau^{\mathbf{r}}. \qquad \square$$

With Lemmas B.1 and B.2 we can compute averages of barycentric products over small simplices. The integrals of higher order Whitney forms over small simplices are then easily obtained using the following result.

Proposition B.3 *Let σ^q be a q-simplex, $\tau \in S^p(\sigma^q)$ a p-face of σ^q, and ω a smooth 0-form. For any p-simplex $\upsilon \subset \sigma^q$, we have*

$$\int_\upsilon \omega \mathcal{W}\tau = \left(\frac{1}{|\upsilon|}\int_\upsilon \omega\right)\langle \mathcal{W}\tau(x), \mathrm{vect}(\upsilon)\rangle,$$

where $\frac{1}{|\upsilon|}\int_\upsilon \omega$ is the average of ω over υ, x is any point in υ, and $\mathrm{vect}(\upsilon)$ *is the p-vector of υ.*

Proof The quantity $\langle \mathcal{W}\tau(x), \mathrm{vect}(\upsilon)\rangle$ is constant in υ (see [20]), and hence,

$$\int_\upsilon \omega \mathcal{W}\tau = \int_\upsilon \left\langle \omega(x)\mathcal{W}\tau(x), \frac{\mathrm{vect}(\upsilon)}{|\upsilon|}\right\rangle dx = \left(\frac{1}{|\upsilon|}\int_\upsilon \omega\right)\langle \mathcal{W}\tau(x), \mathrm{vect}(\upsilon)\rangle. \qquad \square$$

Acknowledgements The author thanks Lauri Kettunen and two anonymous reviewers for their helpful comments on the manuscript.

Funding Open Access funding provided by University of Jyväskylä (JYU). University of Jyväskylä.

Declarations

Conflict of interest The author declares no competing interests.

References

1. Arnold, D., Falk, R., Winther, R.: Finite element exterior calculus, homological techniques, and applications. Acta Numerica **15**, 1–155 (2006)

2. Arnold, D., Falk, R., Winther, R.: Geometric decompositions and local bases for spaces of finite element differential forms. Comput. Methods Appl. Mech. Eng. **198**(21–26), 1660–1672 (2009)
3. Arnold, D., Falk, R., Winther, R.: Finite element exterior calculus: From Hodge theory to numerical stability. Bull. Am. Math. Soc. **47**(2), 281–354 (2010)
4. Bonazzoli, M., Dolean, V., Hecht, F., Rapetti, F.: An example of explicit implementation strategy and preconditioning for the high order edge finite elements applied to the time-harmonic Maxwell's equations. Comput. and Math. Appl. **75**(5), 1498–1514 (2018)
5. Bonazzoli, M., Rapetti, F.: High-order finite elements in numerical electromagnetism: Degrees of freedom and generators in duality. Numer. Algo. **74**(1), 111–136 (2017)
6. Bossavit, A.: 'Generalized finite differences' in computational electromagnetics. Prog. Electromagn. Res. **32**, 45–64 (2001)
7. Bossavit, A.: Generating Whitney forms of polynomial degree one and higher. IEEE Trans. Magn. **38**(2), 341–344 (2002)
8. Bossavit, A.: Discretization of electromagnetic problems: The "generalized finite differences" approach. Handbook of Numerical Analysis **13**, 105–197 (2005)
9. Bossavit, A., Kettunen, L.: Yee-like schemes on a tetrahedral mesh, with diagonal lumping. International Journal of Numerical Modelling: Electronic networks, Devices and Fields **12**(1-2), 129–142 (1999)
10. Bossavit, A., Kettunen, L.: Yee-like schemes on staggered cellular grids: A synthesis between FIT and FEM approaches. IEEE Trans. Magn. **36**(4), 861–867 (2000)
11. Christiansen, S., Rapetti, F.: On high order finite element spaces of differential forms. Math. Comput. **85**(298), 517–548 (2016)
12. Clemens, M., Weiland, T.: Discrete electromagnetism with the finite integration technique. Prog. Electromagn. Res. **32**, 65–87 (2001)
13. Desbrun, M., Hirani, A., Leok, M., Marsden, J.: Discrete exterior calculus. arXiv:math/0508341 (2005)
14. Desbrun, M., Kanso, E., Tong, Y.: Discrete Differential Forms for Computational Modeling. In: Discrete Differential Geometry. Springer, pp 287–324 (2008)
15. Hiptmair, R.: Higher order Whitney forms. Prog. Electromagn. Res. **32**, 271–299 (2001)
16. Hirani, A.: Discrete Exterior Calculus. PhD thesis, California Institute of Technology (2003)
17. Hirani, A., Nakshatrala, K., Chaudhry, J.: Numerical method for Darcy flow derived using discrete exterior calculus. International Journal for Computational Methods in Engineering Science and Mechanics **16**(3), 151–169 (2015)
18. Kettunen, L., Lohi, J., Räbinä, J., Mönkölä, S., Rossi, T.: Generalized finite difference schemes with higher order Whitney forms. ESAIM: Mathematical Modelling and Numerical Analysis **55**(4), 1439–1460 (2021)
19. Lohi, J.: Discrete Exterior Calculus and Higher Order Whitney Forms. Master's thesis, University of Jyväskylä (2019)
20. Lohi, J., Kettunen, L.: Whitney forms and their extensions. J. Comput. Appl. Math. **393**, 113520 (2021)
21. Marsic, N., Geuzaine, C.: Efficient finite element assembly of high order Whitney forms. IET Conference Proceedings (2014)
22. Mohamed, M., Hirani, A., Samtaney, R.: Discrete exterior calculus discretization of incompressible Navier–Stokes equations over surface simplicial meshes. J. Comput. Phys. **312**, 175–191 (2016)
23. Räbinä, J., Kettunen, L., Mönkölä, S., Rossi, T.: Generalized wave propagation problems and discrete exterior calculus. ESAIM: Mathematical Modelling and Numerical Analysis **52**(3), 1195–1218 (2018)
24. Räbinä, J., Kuopanportti, P., Kivioja, M., Möttönen, M., Rossi, T.: Three-dimensional splitting dynamics of giant vortices in Bose–Einstein condensates. Phys, Rev. A 98(2) (2018)
25. Räbinä, J., Mönkölä, S., Rossi, T.: Efficient time integration of Maxwell's equations with generalized finite differences. SIAM J. Sci. Comput. **37**(6), B834–B854 (2015)
26. Räbinä, J., Mönkölä, S., Rossi, T., Markkanen, J., Gritsevich, M., Muinonen, K.: Controlled time integration for the numerical simulation of meteor radar reflections. J. Quant. Spectros. Radiat. Transfer **178**, 295–305 (2016)
27. Rapetti, F.: High order edge elements on simplicial meshes. ESAIM: Mathematical Modelling and Numerical Analysis **41**(6), 1001–1020 (2007)
28. Rapetti, F., Bossavit, A.: Whitney forms of higher degree. SIAM J. Numer. Anal. **47**(3), 2369–2386 (2009)

29. Stern, A., Tong, Y., Desbrun, M., Marsden, J.: Geometric computational electrodynamics with variational integrators and discrete differential forms. In: Geometry, Mechanics, and Dynamics. Springer, pp 437–475 (2015)
30. Vermolen, F., Segal, A.: On an integration rule for products of barycentric coordinates over simplexes in $\mathbb{R}^n$. J. Comput. Appl. Math. **330**, 289–294 (2018)
31. Whitney, H.: Geometric integration theory. Princeton University Press, Princeton (1957)

PIII

NEW DEGREES OF FREEDOM FOR DIFFERENTIAL FORMS ON CUBICAL MESHES

by

Jonni Lohi

Advances in Computational Mathematics, Accepted for publication, 2022

New degrees of freedom for differential forms on cubical meshes

Jonni Lohi
Faculty of Information Technology
University of Jyväskylä

Abstract

We consider new degrees of freedom for higher order differential forms on cubical meshes. The approach is inspired by the idea of Rapetti and Bossavit to define higher order Whitney forms and their degrees of freedom using small simplices. We show that higher order differential forms on cubical meshes can be defined analogously using small cubes and prove that these small cubes yield unisolvent degrees of freedom. Significantly, this approach is compatible with discrete exterior calculus and expands the framework to cover higher order methods on cubical meshes, complementing the earlier strategy based on simplices.

1 Introduction

Finite element exterior calculus [4] highlights the importance of suitable finite element spaces in discretisations of partial differential equations. The principal finite elements for differential forms are presented in the periodic table of finite elements [1]. Along with the shape functions, the table provides degrees of freedom, defined as weighted moments, and together they specify the finite element space on a given mesh. Although these traditional dofs suit the finite element method excellently, for cochain-based methods it is desirable to obtain dofs for p-forms through integration on p-chains of the mesh. For example, in the case of (lowest order) Whitney forms (i.e. the space $\mathcal{P}_1^-\Lambda^p$), the basis p-forms are in correspondence with p-cochains of the mesh, and hence they can be used as a tool in methods that are based on discrete exterior calculus. With higher order Whitney forms ($\mathcal{P}_k^-\Lambda^p$ for $k > 1$) this is no longer the case, and the traditional dofs lack physical interpretation.

Rapetti and Bossavit [10] addressed this issue by introducing an approach based on small simplices, which are images of the mesh simplices through homothetic transformations. The idea is to define the shape functions and their dofs using these: to each small p-simplex of order k corresponds a Whitney p-form of order k, and the dofs are obtained through integration over kth order small p-simplices. Although the approach generalises the lowest order case (in that $k = 1$ yields the standard Whitney forms on the initial simplices), the higher order case is not equally simple. In particular, the small simplices do not pave the initial mesh, and the spanning forms corresponding to small simplices are not linearly independent. Despite these downsides, the approach can be reconciled with discrete exterior calculus and has been adopted for use [7, 6, 8].

In this work, we provide an analogous approach for the space $\mathcal{Q}_k^-\Lambda^p$, the (tensor product) finite element space of differential forms on cubical meshes, to which we hereafter refer as "cubical forms" for short. The approach uses small cubes, which are similar to small simplices but defined on cubical meshes. We first give a definition of the small cubes and use them to define cubical forms similarly as higher order Whitney forms are defined using small simplices. The new degrees of freedom resulting from integration over small cubes are considered next: we provide an explicit formula for integrating basis functions and prove that the dofs are unisolvent. Finally, we conclude with the properties of the resulting interpolation operator. Two improvements to the analogous strategy based on small simplices are that the small cubes completely pave the initial mesh and the spanning cubical forms are linearly independent. The approach is hence readily compatible with discrete exterior calculus and enables higher order methods on cubical meshes.

2 Small cubes and cubical forms

We first define the small cubes and the cubical forms in the unit n-cube $\square^n = [0,1]^n$. Cubical meshes are considered in Section 4.

Definition 2.1 (Small cubes)**.** Let $\mathcal{J}(n, k-1)$ denote the set of multi-indices $\mathbf{k} = (k_1, \ldots, k_n)$ with n components $k_i \le k-1$. For the unit n-cube $\square^n = [0,1]^n$, each multi-index $\mathbf{k} \in \mathcal{J}(n, k-1)$ defines a map $\mathbf{k}_{k-1} : \square^n \to \square^n$ by

$$\mathbf{k}_{k-1}(x_1, \ldots, x_n) = \frac{(k_1 + x_1, \ldots, k_n + x_n)}{k}.$$

For $k \ge 1$, the set of kth order small p-cubes of $\square^n$ is

$$S_k^p(\square^n) = \{\mathbf{k}_{k-1}(\tau) \mid \mathbf{k} \in \mathcal{J}(n, k-1) \text{ and } \tau \text{ is a } p\text{-face of } \square^n\}.$$

Remark 2.2. Since $\mathcal{J}(n, k-1) \subset \mathcal{J}(n, k)$, the map $\mathbf{k}_{k-1}$ is not defined by the components of $\mathbf{k}$ alone. The subscript specifies the set of multi-indices whose element $\mathbf{k}$ is considered.

Examples of small cubes are shown in Figure 1.

Cubical forms can be seen as counterparts of Whitney forms for cubes. These are the shape functions of the $\mathcal{Q}_k^-\Lambda^p$ family in finite element exterior calculus, and they can be obtained using a tensor product construction [3]. We define cubical forms using small cubes similarly as higher order Whitney forms are defined using small simplices. Henceforth, we say that two p-cells (or hyperplanes) are parallel if one of them can be moved to the hyperplane of the other by translation.

Definition 2.3 (Lowest order cubical forms)**.** Let σ be a p-face of $\square^n$. Let $x_{i_1}, \ldots, x_{i_p}$ be the coordinates whose plane is parallel to σ and $x_{i_{p+1}}, \ldots, x_{i_n}$ the other coodinates, whose values $y_{i_{p+1}}, \ldots, y_{i_n}$ are either 0 or 1 on σ. The lowest order cubical form $\mathcal{W}\sigma$ corresponding to σ is

$$\mathcal{W}\sigma = \left(\prod_{j=p+1}^{n} x_{i_j}^{y_{i_j}} (1 - x_{i_j})^{1-y_{i_j}} \right) \mathrm{d}\, x_{i_1} \wedge \ldots \wedge \mathrm{d}\, x_{i_p}.$$

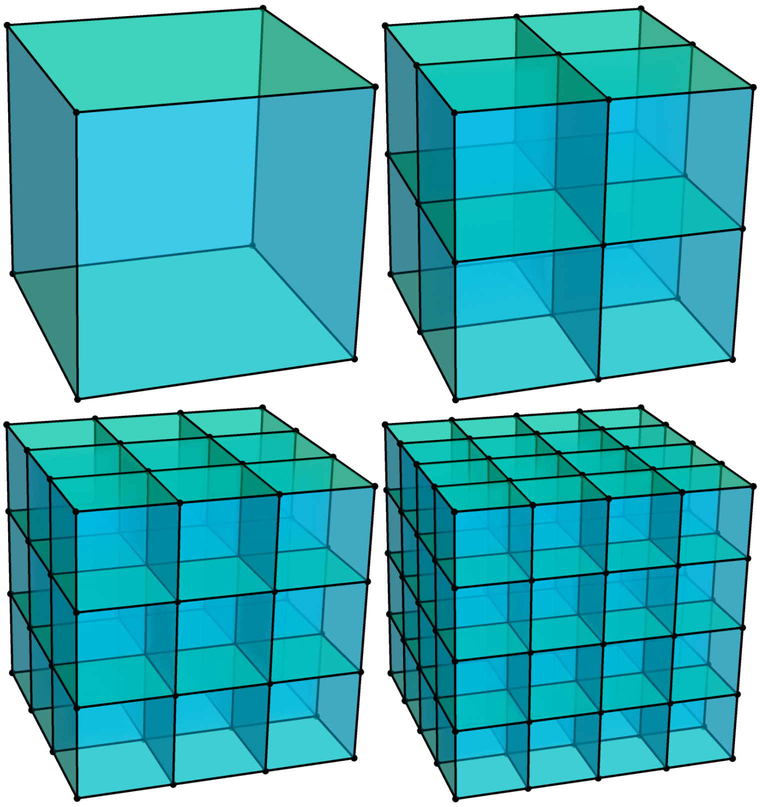

Figure 1: Small cubes of orders 1–4 in three dimensions.

Definition 2.4 (Higher order cubical forms)**.** Let $\mathbf{k} \in \mathcal{J}(n, k-1)$ and τ be a p-face of $\square^n$. The kth order cubical p-form corresponding to the small cube $\mathbf{k}_{k-1}(\tau)$ is

$$w(\mathbf{k}_{k-1}(\tau)) = \left(\prod_{i=1}^{n} x_i^{k_i}(1-x_i)^{k-1-k_i}\right)\mathcal{W}\tau.$$

The space of kth order cubical p-forms is

$$Q_k^p(\square^n) = \operatorname{span}\{w(\mathbf{k}_{k-1}(\tau)) \mid \mathbf{k} \in \mathcal{J}(n, k-1) \text{ and } \tau \text{ is a } p\text{-face of } \square^n\}.$$

Let us first verify that the forms given in Definition 2.4 indeed yield the space $\mathcal{Q}_k^- \Lambda^p$.

Proposition 2.5. *In the unit n-cube $\square^n$, we have $Q_k^p(\square^n) = \mathcal{Q}_k^- \Lambda^p(\square^n)$.*

Proof. Recall that $\mathcal{Q}_k^- \Lambda^p(\square^n)$ is spanned by p-forms of the form $f \,\mathrm{d}\, x_{i_1} \wedge \ldots \wedge \mathrm{d}\, x_{i_p}$, where f is at most kth order polynomial in all variables and at most $(k-1)$th order polynomial in the variables $x_{i_1}, \ldots, x_{i_p}$. Hence $Q_k^p(\square^n) \subset \mathcal{Q}_k^- \Lambda^p(\square^n)$ follows directly from Definitions 2.3 and 2.4. It remains to prove $\mathcal{Q}_k^- \Lambda^p(\square^n) \subset Q_k^p(\square^n)$, and for this it is sufficent to show that $Q_k^p(\square^n)$ contains all p-forms of the form $x_1^{y_1} \cdot \ldots \cdot x_n^{y_n} \,\mathrm{d}\, x_{i_1} \wedge \ldots \wedge \mathrm{d}\, x_{i_p}$, where the y_i are integers such that $0 \le y_i \le k$ for all i and $y_i \le k-1$ if $i \in \{i_1, \ldots, i_p\}$.

Let $\omega = x_1^{y_1} \cdot \ldots \cdot x_n^{y_n} \,\mathrm{d}\, x_{i_1} \wedge \ldots \wedge \mathrm{d}\, x_{i_p}$ for such integers y_i. We choose $z_i = y_i + 1$ if $i \in \{i_1, \ldots, i_p\}$, $z_i = y_i$ if $i \notin \{i_1, \ldots, i_p\}$, and write

$$x_i^{y_i} = x_i^{y_i}(x_i + (1-x_i))^{k-z_i} = x_i^{y_i} \sum_{j=0}^{k-z_i} \binom{k-z_i}{j} x_i^j (1-x_i)^{k-z_i-j}.$$

Expanding ω in this way, we get a linear combination of terms of the form

$$\left(\prod_{i=1}^{n} x_i^{a_i}(1-x_i)^{b_i}\right) \mathrm{d}\, x_{i_1} \wedge \ldots \wedge \mathrm{d}\, x_{i_p},$$

where $a_i + b_i = k-1$ if $i \in \{i_1, \ldots, i_p\}$ and $a_i + b_i = k$ otherwise. From Definitions 2.3 and 2.4, we see that such terms are in $Q_k^p(\square^n)$. $\square$

From existing results for $\mathcal{Q}_k^- \Lambda^p$ (see [3]), we know that the exterior derivative d satisfies $\mathrm{d}(Q_k^p(\square^n)) \subset Q_k^{p+1}(\square^n)$ and the dimension of the space $Q_k^p(\square^n)$ is $\binom{n}{p} k^p (k+1)^{n-p}$. It is easy to see that this is also the number of distinct kth order small p-cubes of $\square^n$. The spanning forms given in Definition 2.4 are hence linearly independent, which is an improvement to the analogous approach based on small simplices and higher order Whitney forms.

3 New degrees of freedom

Since p-forms can be integrated over small p-cubes, we can take the integrals over kth order small p-cubes as degrees of freedom for kth order cubical p-forms. Note that each dof can be associated with a specific face of $\square^n$ — the one that contains the small simplex but has no faces of lower dimension that also contain it. Hence the basic requirement for degrees of freedom is fulfilled: the values of dofs associated with a face only depend on the trace of the differential form on that face.

3.1 Integrating basis functions over small simplices

In this subsection we provide a formula for computing the values of the new dofs for basis functions. The following lemmas play a key role.

Lemma 3.1. *For integers $m, n \geq 0$ and for $y, z \in \mathbb{R}$,*

$$\int_0^1 (z+x)^n (y+1-x)^m dx = \sum_{i=0}^{m} \sum_{j=0}^{n} \binom{m}{i} \binom{n}{j} y^{m-i} z^{n-j} \frac{i!j!}{(i+j+1)!}.$$

Proof.

$$\int_0^1 (z+x)^n (y+1-x)^m dx = \int_0^1 \left(\sum_{j=0}^{n} \binom{n}{j} z^{n-j} \cdot x^j\right) \left(\sum_{i=0}^{m} \binom{m}{i} y^{m-i} \cdot (1-x)^i\right) dx$$

$$= \sum_{i=0}^{m} \sum_{j=0}^{n} \binom{m}{i} \binom{n}{j} y^{m-i} z^{n-j} \int_0^1 (1-x)^i x^j dx = \sum_{i=0}^{m} \sum_{j=0}^{n} \binom{m}{i} \binom{n}{j} y^{m-i} z^{n-j} \frac{i!j!}{(i+j+1)!},$$

where we used a well-known integration rule for products of barycentric functions [11] in the last step. $\square$

Lemma 3.2. *Let τ be a p-face of $\square^n$. Let $x_{i_1}, \ldots, x_{i_p}$ be the coordinates whose plane is parallel to τ and $x_{i_{p+1}}, \ldots, x_{i_n}$ the other coodinates, whose values $y_{i_{p+1}}, \ldots, y_{i_n}$ are* *either 0 or 1 on τ. Let $\mathbf{k} \in \mathcal{J}(n,k)$, $\mathbf{k}' \in \mathcal{J}(n,k')$, and $\upsilon = \mathbf{k}'_{k'}(\tau)$. The average of $\prod_{i=1}^n x_i^{k_i}(1-x_i)^{k-k_i}$ over the small p-cube υ is*

$$\frac{1}{|\upsilon|}\int_\upsilon \prod_{i=1}^n x_i^{k_i}(1-x_i)^{k-k_i} = \frac{1}{(k'+1)^{nk}}\left(\prod_{j=p+1}^n (k'_{i_j}+y_{i_j})^{k_{i_j}}(k'-k'_{i_j}+1-y_{i_j})^{k-k_{i_j}}\right)$$
$$\cdot\left(\prod_{j=1}^p\int_0^1 (k'_{i_j}+x)^{k_{i_j}}(k'-k'_{i_j}+1-x)^{k-k_{i_j}}\,dx\right).$$

Proof. Recall that $\mathbf{k}'_{k'}$ maps $(x_1,\ldots,x_n)$ to $(k'_1+x_1,\ldots,k'_n+x_n)/(k'+1)$. For $j>p$, $x_{i_j}^{k_{i_j}}(1-x_{i_j})^{k-k_{i_j}}$ has the constant value

$$\left(\frac{k'_{i_j}+y_{i_j}}{k'+1}\right)^{k_{i_j}}\left(1-\frac{k'_{i_j}+y_{i_j}}{k'+1}\right)^{k-k_{i_j}} = \frac{1}{(k'+1)^k}(k'_{i_j}+y_{i_j})^{k_{i_j}}(k'-k'_{i_j}+1-y_{i_j})^{k-k_{i_j}}$$

on υ and hence

$$\frac{1}{|\upsilon|}\int_\upsilon \prod_{i=1}^n x_i^{k_i}(1-x_i)^{k-k_i} = \frac{1}{(k'+1)^{(n-p)k}}\cdot\left(\prod_{j=p+1}^n (k'_{i_j}+y_{i_j})^{k_{i_j}}(k'-k'_{i_j}+1-y_{i_j})^{k-k_{i_j}}\right)$$
$$\cdot\frac{1}{|\upsilon|}\int_\upsilon\prod_{j=1}^p x_{i_j}^{k_{i_j}}(1-x_{i_j})^{k-k_{i_j}}.$$

Since $1/(k'+1)^p$ is the Jacobian determinant of $\mathbf{k}'_{k'}$ regarded as a map from τ onto υ and $\frac{1}{|\upsilon|}=(k'+1)^p$, we can write

$$\frac{1}{|\upsilon|}\int_\upsilon\prod_{j=1}^p x_{i_j}^{k_{i_j}}(1-x_{i_j})^{k-k_{i_j}} = \int_\tau\prod_{j=1}^p\left(\frac{k'_{i_j}+x_{i_j}}{k'+1}\right)^{k_{i_j}}\left(1-\frac{k'_{i_j}+x_{i_j}}{k'+1}\right)^{k-k_{i_j}}$$
$$=\frac{1}{(k'+1)^{pk}}\int_\tau\prod_{j=1}^p(k'_{i_j}+x_{i_j})^{k_{i_j}}(k'-k'_{i_j}+1-x_{i_j})^{k-k_{i_j}}.$$

The result follows, since the integral above is

$$\int_\tau\prod_{j=1}^p(k'_{i_j}+x_{i_j})^{k_{i_j}}(k'-k'_{i_j}+1-x_{i_j})^{k-k_{i_j}}$$
$$=\int_{[0,1]^p}\left(\prod_{j=1}^p(k'_{i_j}+x_{i_j})^{k_{i_j}}(k'-k'_{i_j}+1-x_{i_j})^{k-k_{i_j}}\right)dx_{i_1}\ldots dx_{i_p}$$
$$=\prod_{j=1}^p\int_0^1(k'_{i_j}+x)^{k_{i_j}}(k'-k'_{i_j}+1-x)^{k-k_{i_j}}\,dx.$$

$\square$

The integral of any kth order spanning p-form given in Definition 2.4 over any kth order small p-cube can now be computed by combining Lemmas 3.1 and 3.2 with the following proposition.

Proposition 3.3. *Let σ be a p-face of the unit n-cube $\square^n$, and let ω be a smooth 0-form. For any small p-cube υ, we have*

$$\int_\upsilon \omega \mathcal{W}\sigma = \left(\frac{1}{|\upsilon|}\int_\upsilon \omega\right)\langle \mathcal{W}\sigma(x), \mathrm{vect}(\upsilon)\rangle,$$

where $\frac{1}{|\upsilon|}\int_\upsilon \omega$ is the average of ω over υ, x is any point in υ, and $\mathrm{vect}(\upsilon)$ *is the p-vector of υ.*

Proof. Let $x_{i_1}, \ldots, x_{i_p}$ be the coordinates whose plane is parallel to σ. If υ is not parallel to σ, then both sides become zero because some of the coordinates is constant and hence $\mathrm{d}\, x_{i_1} \wedge \ldots \wedge \mathrm{d}\, x_{i_p}$ vanishes on υ. But if υ is parallel to σ, $\mathcal{W}\sigma$ is constant in υ and hence

$$\int_\upsilon \omega \mathcal{W}\sigma = \int_\upsilon \left\langle \omega(x)\mathcal{W}\sigma(x), \frac{\mathrm{vect}(\upsilon)}{|\upsilon|}\right\rangle dx = \left(\frac{1}{|\upsilon|}\int_\upsilon \omega\right)\langle \mathcal{W}\sigma(x), \mathrm{vect}(\upsilon)\rangle.$$

$\square$

3.2 Proof of unisolvence

Let us next show that these new degrees of freedom are unisolvent. Note that since the number of small p-cubes is equal to the number of (linearly independent) spanning p-forms, it is sufficient to prove that $\omega \in Q_k^p(\square^n)$ has zero integral over all kth order small p-cubes only if $\omega = 0$. This is shown in Theorem 3.6, whose proof uses the following two lemmas.

Lemma 3.4. *For each $i \in \{1, \ldots, n\}$, let $k_i \geq 0$ be an integer and K_i a set of $k_i + 1$ distinct real numbers. Suppose that $f : \mathbb{R}^n \to \mathbb{R}$ is a polynomial of order k_i at most in the variable x_i, for all $i = 1, \ldots, n$. If $f(x) = 0$ for all $x \in K_1 \times \ldots \times K_n$, then $f = 0$.*

Proof. A well-known result for univariate polynomials states that a polynomial of order $k \geq 1$ can have at most k roots. Hence the case $n = 1$ is clear. Suppose as an induction hypothesis that the statement holds for $n = m - 1$, with $m \geq 2$, and consider the case $n = m$. If $f(x) = 0$ for all $x \in K_1 \times \ldots \times K_m$, then for each $y_j \in K_m$ the function $g_j : \mathbb{R}^{m-1} \to \mathbb{R}$ defined by $g_j(x) = f(x, y_j)$ is zero by the induction hypothesis. Hence for any $(x_1, \ldots, x_{m-1})$, the function $y \mapsto f(x_1, \ldots, x_{m-1}, y)$ vanishes in K_m and hence has $k_m + 1$ roots. Since it is an univariate polynomial of order k_m at most, it must be zero. Hence the statement holds for $n = m$. $\square$

Lemma 3.5. *Suppose that $f : \mathbb{R}^n \to \mathbb{R}$ is a nonzero polynomial. For any $h_1, \ldots, h_n > 0$, there exist $\epsilon, M_1, \ldots, M_n > 0$ such that $|f| \geq \epsilon$ in $[M_1, M_1 + h_1] \times \ldots \times [M_n, M_n + h_n]$.*

Proof. We can write

$$f = \sum_{i_1=0}^{k_1}\sum_{i_2=0}^{k_2}\cdots\sum_{i_n=0}^{k_n} a(i_1, i_2, \ldots, i_n) x_1^{i_1} x_2^{i_2} \cdot \ldots \cdot x_n^{i_n} = \sum_{i_1=0}^{k_1} x_1^{i_1} \sum_{i_2=0}^{k_2} x_2^{i_2} \cdots \sum_{i_n=0}^{k_n} a(i_1, i_2, \ldots, i_n) x_n^{i_n},$$

where k_i is the order of f in the variable x_i and each coefficient $a(i_1, i_2, \dots, i_n)$ is constant. For each $j \in \{1, \dots, n\}$ and $i_1, \dots, i_{n-j}$ such that $0 \le i_l \le k_l$ for all $l \in \{1, \dots, n-j\}$, let us define a function $g_j[i_1, \dots, i_{n-j}] : \mathbb{R}^j \to \mathbb{R}$ by

$$g_j[i_1, \dots, i_{n-j}](x_{n-j+1}, \dots, x_n) = \sum_{i_{n-j+1}=0}^{k_{n-j+1}} x_{n-j+1}^{i_{n-j+1}} \sum_{i_{n-j+2}=0}^{k_{n-j+2}} x_{n-j+2}^{i_{n-j+2}} \dots \sum_{i_n=0}^{k_n} a(i_1, i_2, \dots, i_n) x_n^{i_n}.$$

In other words, we have

$$g_1[i_1, \dots, i_{n-1}](x_n) = \sum_{i_n=0}^{k_n} a(i_1, i_2, \dots, i_n) x_n^{i_n},$$

$$g_j[i_1, \dots, i_{n-j}](x_{n-j+1}, \dots, x_n) = \sum_{i_{n-j+1}=0}^{k_{n-j+1}} g_{j-1}[i_1, \dots, i_{n-j+1}](x_{n-j+2}, \dots, x_n) x_{n-j+1}^{i_{n-j+1}},$$

and $g_n(x) = f(x)$.

We proceed as follows. At step 1, we can find $\epsilon_n, M_n > 0$ such that each $g_1[i_1, \dots, i_{n-1}]$ is either identically zero or satisfies $|g_1[i_1, \dots, i_{n-1}](x_n)| \ge \epsilon_n$ for all $x_n \in [M_n, M_n + h_n]$. At step j (for $2 \le j \le n$), suppose we have found $\epsilon_{n-j+2}, M_{n-j+2}, \dots, M_n > 0$ such that each $g_{j-1}[i_1, \dots, i_{n-j+1}]$ is either identically zero or satisfies

$$|g_{j-1}[i_1, \dots, i_{n-j+1}](x_{n-j+2}, \dots, x_n)| \ge \epsilon_{n-j+2}$$

for all $(x_{n-j+2}, \dots, x_n) \in [M_{n-j+2}, M_{n-j+2} + h_{n-j+2}] \times \dots \times [M_n, M_n + h_n]$. Then we can find $\epsilon_{n-j+1}, M_{n-j+1} > 0$ such that each $g_j[i_1, \dots, i_{n-j}]$ is either identically zero or satisfies

$$|g_j[i_1, \dots, i_{n-j}](x_{n-j+1}, \dots, x_n)| \ge \epsilon_{n-j+1}$$

for all $(x_{n-j+1}, \dots, x_n) \in [M_{n-j+1}, M_{n-j+1} + h_{n-j+1}] \times \dots \times [M_n, M_n + h_n]$. The proof is completed at step n, since $g_n = f$, which is nonzero by assumption. $\square$

Theorem 3.6. *Let $\omega \in Q_k^p(\square^n)$. If $\int_\upsilon \omega = 0$ for all small p-cubes $\upsilon \in S_k^p(\square^n)$, then $\omega = 0$.*

Proof. Assume $\int_\upsilon \omega = 0$ for all $\upsilon \in S_k^p(\square^n)$ and write

$$\omega = \sum_{1 \le i_1 < \dots < i_p \le n} \omega_{i_1 \dots i_p} \, \mathrm{d}\, x_{i_1} \wedge \dots \wedge \mathrm{d}\, x_{i_p}.$$

Note that $\mathrm{d}\, x_{i_1} \wedge \dots \wedge \mathrm{d}\, x_{i_p}$ is zero on υ unless υ is parallel to the corresponding coordinate plane. Hence $\int_\upsilon \omega = 0$ implies $\int_\upsilon \omega_{i_1 \dots i_p} \, \mathrm{d}\, x_{i_1} \wedge \dots \wedge \mathrm{d}\, x_{i_p} = 0$ for all $1 \le i_1 < \dots < i_p \le n$. We show that each coefficient function $\omega_{i_1 \dots i_p}$ is zero.

Let τ be the p-face of $\square^n$ which is parallel to the coordinate plane of $x_{i_1}, \dots, x_{i_p}$ and on which the other coordinates are zero, and let $\mathbf{k} = (0, \dots, 0) \in \mathcal{J}(n, k-1)$. Denote $\upsilon_0 = \mathbf{k}_{k-1}(\tau)$ and define a function $f : \mathbb{R}^n \to \mathbb{R}$ by

$$f(u) = \int_{\upsilon_0} \omega_{i_1 \dots i_p}(x + u) \, \mathrm{d}\, x_{i_1} \wedge \dots \wedge \mathrm{d}\, x_{i_p}.$$

Observe that since $\omega_{i_1\dots i_p}$ is at most kth order polynomial in all variables and at most $(k-1)$th order polynomial in the variables $x_{i_1}, \dots, x_{i_p}$, the same holds for f.

In the small p-cube υ_0, the coordinates $x_{i_1}, \dots, x_{i_p}$ vary from 0 to $1/k$ and the other coordinates are zero. The other small p-cubes of order k that are parallel to υ_0 are obtained from υ_0 through translation as follows. Let

$$K_i = \begin{cases} \{0, \frac{1}{k}, \frac{2}{k}, \dots, \frac{k-1}{k}\} & \text{if } i \in \{i_1, \dots, i_p\}, \\ \{0, \frac{1}{k}, \frac{2}{k}, \dots, \frac{k-1}{k}, 1\} & \text{if } i \notin \{i_1, \dots, i_p\}. \end{cases}$$

Then the small p-cubes of order k that are parallel to the coordinate plane of $x_{i_1}, \dots, x_{i_p}$ are precisely the translations of υ_0 by vectors $u \in K_1 \times \dots \times K_n$. In particular, we have $f(u) = 0$ for all $u \in K_1 \times \dots \times K_n$, and hence $f = 0$ by Lemma 3.4.

It remains to show how $f = 0$ implies $\omega_{i_1\dots i_p} = 0$. If $\omega_{i_1\dots i_p} \neq 0$, applying Lemma 3.5 with $h_1 = h_2 = \dots = h_n = 1$ yields $\epsilon > 0$ and $M_1, \dots, M_n > 0$ such that $|\omega_{i_1\dots i_p}| \geq \epsilon$ in $[M_1, M_1+1] \times \dots \times [M_n, M_n+1]$. But $\omega_{i_1\dots i_p}$ must attain the value 0 somewhere in this set because $f(M_1 \dots, M_n) = 0$. This is a contradiction. Hence $\omega_{i_1\dots i_p}$ must vanish identically, which concludes the proof. □

4 Interpolating with cubical forms

Similarly as Whitney forms are used to interpolate cochains on simplicial meshes, cubical forms can be used for interpolating on cubical meshes. We say that a mesh K in $\Omega \subset \mathbb{R}^n$ is cubical if for each n-cell σ in K there exists an affine bijection $\phi : \square^n \to \sigma$. In other words, we require that σ be a parallelotope. (The requirement could be relaxed to accommodate curvilinear meshes, but this would have a negative effect on the approximation properties [3]). We denote by $S^p(K)$ the set of p-cells and by $C_p^*(K)$ the space of p-cochains.

The small cubes of $\sigma \in S^n(K)$ are obtained as the images of the small cubes of $\square^n$ through the map ϕ, and the corresponding cubical forms in σ are defined as the pullbacks through ϕ^{-1}:

$$w(\phi(\mathbf{k}_{k-1}(\tau))) = (\phi^{-1})^*(w(\mathbf{k}_{k-1}(\tau))).$$

When K is a cubical mesh, we define the space of kth order cubical p-forms as the span of all kth order cubical p-forms in the cells of K. Denote this space by $Q_k^p(K)$. We remark that the space admits a geometric decomposition, in the sense of [5], as follows. Let $\mathring{S}_k^p(\sigma^q)$ denote those small p-cubes of $\sigma^q \in S^q(K)$ that are not contained in the boundary of σ^q and $\mathring{Q}_k^p(\sigma^q)$ those p-forms in $Q_k^p(\sigma^q)$ that have zero trace on the boundary of σ^q. Then $\mathring{Q}_k^p(\sigma^q) = \operatorname{span}\{w(\upsilon) \mid \upsilon \in \mathring{S}_k^p(\sigma^q)\}$ and we have the geometric decomposition

$$Q_k^p(\sigma^n) = \bigoplus_{\substack{\sigma^q \in S^q(\sigma^n), \\ p \leq q \leq n}} \mathring{Q}_k^p(\sigma^q), \quad Q_k^p(K) = \bigoplus_{\substack{\sigma^q \in S^q(K), \\ p \leq q \leq n}} \mathring{Q}_k^p(\sigma^q), \tag{4.1}$$

where we have extended elements in $Q_k^p(\sigma^q)$ to elements of $Q_k^p(\sigma^n)$ using a suitable extension operator. (If σ^q is a q-face of σ^n, then any small p-cube υ of σ^q is also a small p-cube of σ^n, so $w(\upsilon)$ extends to σ^n by regarding υ as a small p-cube of σ^n.) A dual decomposition can also be obtained by replacing Q and $\mathring{Q}$ in (4.1) with S and $\mathring{S}$.

To apply cubical forms with discrete exterior calculus, we refine the cubical mesh K into a finer mesh K_k whose cells are the kth order small cubes. Notice that the small cubes pave the initial cubes completely, so there are no holes between them and the refinement K_k is unique (unlike with small simplices). We define the interpolation operator $\mathfrak{I} : C_p^*(K_k) \to Q_k^p(K)$ by requiring that

$$\int_v \mathfrak{I}X = X(v) \tag{4.2}$$

for all $v \in S^p(K_k)$. The interpolation operator satisfies all expected properties:

$$\mathcal{C}_k \mathfrak{I} X = X \quad \forall X \in C_p^*(K_k), \tag{4.3}$$

$$\mathfrak{I}\mathcal{C}_k \omega = \omega \quad \forall \omega \in Q_k^p(K), \tag{4.4}$$

$$\mathfrak{I}\,\mathrm{d}\,X = \mathrm{d}\,\mathfrak{I}X \quad \forall X \in C_p^*(K_k), \tag{4.5}$$

where $\mathcal{C}_k$ denotes the de Rham map of K_k and d denotes both the coboundary operator and the exterior derivative.

Proposition 4.1. *The interpolation operator* $\mathfrak{I}$ *is well defined by* (4.2) *and satisfies the properties* (4.3)–(4.5).

Proof. Theorem 3.6 implies that the restriction of $\mathcal{C}_k$ to $Q_k^p(K)$ is injective; since the dimensions of $C_p^*(K_k)$ and $Q_k^p(K)$ match, it is bijective, and (4.2) defines $\mathfrak{I}$ as its inverse. Hence the properties (4.3)–(4.4) hold. For (4.5) we invoke also $\mathrm{d}(Q_k^p(K)) \subset Q_k^{p+1}(K)$: $\mathfrak{I}\,\mathrm{d}\,X = \mathfrak{I}\,\mathrm{d}\,\mathcal{C}_k\mathfrak{I}X = \mathfrak{I}\mathcal{C}_k\,\mathrm{d}\,\mathfrak{I}X = \mathrm{d}\,\mathfrak{I}X$, where we used (4.3), Stokes' theorem, and the fact that $\mathrm{d}\,\mathfrak{I}X$ is in $Q_k^{p+1}(K)$. □

Remark 4.2. At this point, we obtain an easy proof for the exact sequence property of cubical forms: if Ω has trivial homology groups, the spaces $Q_k^p(K)$ constitute an exact sequence with d. To see this, suppose $\omega \in Q_k^{p+1}(K)$ such that $\mathrm{d}\,\omega = 0$. Then $\mathrm{d}\,\mathcal{C}_k\omega = \mathcal{C}_k\,\mathrm{d}\,\omega = 0$, and it is a standard result in algebraic topology [12] that $\mathcal{C}_k\omega = \mathrm{d}\,X$ for some $X \in C_p^*(K_k)$. Hence $\omega = \mathfrak{I}\mathcal{C}_k\omega = \mathfrak{I}\,\mathrm{d}\,X = \mathrm{d}\,\mathfrak{I}X$. It seems that this exact sequence property of cubical forms has not been proven (or even stated) previously in the literature [2, 3].

The interpolation operator is implemented efficiently using the decomposition (4.1). To compute the value of $\mathfrak{I}X$ in $\sigma^n \in S^n(K)$, we consider basis functions in $\mathring{Q}_k^p(\sigma^q)$ for q-faces σ^q of σ^n, with $p \le q \le n$. The coefficients of basis functions in $\mathring{Q}_k^p(\sigma^q)$ only depend on the values of X on those small p-cubes that are in σ^q. Systematic implementation is possible by copying the approach provided in [8] for higher order Whitney forms and small simplices. With cubical forms the process is only much simpler, since the spanning forms given in Definition 2.4 are linearly independent and the refinement K_k has no other cells than small cubes. In addition, now the coefficients of basis functions with $\mathrm{d}\,x_{i_1} \wedge \ldots \wedge \mathrm{d}\,x_{i_p}$ in them only depend on the values on small cubes that are parallel to the corresponding coordinate plane, which further simplifies the computations.

Besides interpolating cochains, the operator $\mathfrak{I}$ can be used to approximate differential forms; the approximation of ω obtained with cubical forms is $\mathfrak{I}\mathcal{C}_k\omega$. We conclude the paper with a convergence proof for this approximation.

Theorem 4.3. *Let ω be a smooth p-form in Ω. There exists a constant $C_{\omega,k}$ such that*

$$|\mathfrak{I}\mathcal{C}_k\omega(x) - \omega(x)| \leq \frac{C_{\omega,k}}{C_\Theta^p} h^k \quad \text{for all } x \in \sigma \text{ in all } \sigma \in S^n(K)$$

whenever $h > 0$, $C_\Theta > 0$, and K is a cubical mesh in Ω such that $\operatorname{diam}(\sigma) \leq h$ *and* $\Theta(\sigma) \geq C_\Theta$ *for all cells σ of K.*

Here $\Theta(\sigma)$ denotes the fullness, which is defined for a p-cell σ as $\Theta(\sigma) = |\sigma|/\operatorname{diam}(\sigma)^p$. The proof of Theorem 4.3 is similar to that of Theorem 5.1 in [9] after some preparations.

Lemma 4.4. *Let σ be an n-parallelotope. There exists an n-ball $B \subset \sigma$ with diameter* $\operatorname{diam}(B) = \Theta(\sigma)\operatorname{diam}(\sigma)$*.*

Proof. We may assume that $\sigma = \{\sum_{i=1}^n \mu_i v_i \mid 0 \leq \mu_i \leq 1\ \forall i\}$, where $v_1, \ldots, v_n$ are the edge vectors of σ. Let τ be any $(n-1)$-face of σ and let h denote the distance from the plane of this face to the point $z = \frac{1}{2}(v_1 + \ldots + v_n)$. Since $|\sigma| = 2h|\tau|$ and $|\tau| \leq \operatorname{diam}(\sigma)^{n-1}$,

$$h = \frac{|\sigma|}{2|\tau|} \geq \frac{|\sigma|}{2\operatorname{diam}(\sigma)^{n-1}} = \frac{1}{2}\Theta(\sigma)\operatorname{diam}(\sigma).$$

This holds for all $(n-1)$-faces of σ, and hence the n-ball with radius $\frac{1}{2}\Theta(\sigma)\operatorname{diam}(\sigma)$ centred at z fits in σ. $\square$

Suppose $\sigma \in S^n(K)$ and consider the affine bijection $\phi : \square^n \to \sigma$ from the unit n-cube onto σ. As a consequence of Lemma 4.4, we obtain a bound for the norm of $D\phi^{-1}$ as follows. Let $B \subset \sigma$ be an n-ball with centre z such that $\operatorname{diam}(B) = \Theta(\sigma)\operatorname{diam}(\sigma)$, and pick v such that $|v| = 1$ and $|D\phi^{-1}(z)v| = \max_{|w|=1}|D\phi^{-1}(z)w|$. Since ϕ^{-1} is affine, for all $x \in \sigma$

$$\begin{aligned} |D\phi^{-1}(x)| = |D\phi^{-1}(z)v| &= \frac{|\phi^{-1}(z + \frac{1}{2}\Theta(\sigma)\operatorname{diam}(\sigma)v) - \phi^{-1}(z - \frac{1}{2}\Theta(\sigma)\operatorname{diam}(\sigma)v)|}{\Theta(\sigma)\operatorname{diam}(\sigma)} \\ &\leq \frac{\sqrt{n}}{\Theta(\sigma)\operatorname{diam}(\sigma)}, \end{aligned} \tag{4.6}$$

where we used the fact that ϕ^{-1} maps σ onto the unit cube, which has diameter $\sqrt{n}$.

Proof of Theorem 4.3. We write

$$\omega = \sum_{1 \leq i_1 < \ldots < i_p \leq n} \omega_{i_1 \ldots i_p} \,\mathrm{d}\,x_{i_1} \wedge \ldots \wedge \mathrm{d}\,x_{i_p}$$

and, for $y \in \Omega$, denote by $T_{y,i_1\ldots i_p}$ the $(k-1)$th order Taylor polynomial of $\omega_{i_1\ldots i_p}$ at y. Since ω is smooth in Ω, we may find a constant C_ω such that $|\omega_{i_1\ldots i_p}(x) - T_{y,i_1\ldots i_p}(x)| \leq C_\omega|x-y|^k$ for all $i_1 \ldots i_p$ whenever the line segment from y to x is in Ω.

Let $h > 0$ and $C_\Theta > 0$, and suppose K satisfies the assumptions. Fix $\sigma \in K$ and $y \in \sigma$, and denote $g_{i_1\ldots i_p} = \omega_{i_1\ldots i_p} - T_{y,i_1\ldots i_p}$ so that

$$\omega = \sum_{1 \leq i_1 < \ldots < i_p \leq n} (T_{y,i_1\ldots i_p} + g_{i_1\ldots i_p}) \,\mathrm{d}\,x_{i_1} \wedge \ldots \wedge \mathrm{d}\,x_{i_p}, \quad |g_{i_1\ldots i_p}(x)| \leq C_\omega h^k \text{ in } \sigma.$$

Since $\mathfrak{IC}_k T_{y,i_1\dots i_p}\,\mathrm{d}\,x_{i_1}\wedge\ldots\wedge\mathrm{d}\,x_{i_p} = T_{y,i_1\dots i_p}\,\mathrm{d}\,x_{i_1}\wedge\ldots\wedge\mathrm{d}\,x_{i_p}$ for all $i_1\dots i_p$, we have

$$\mathfrak{IC}_k\omega-\omega=\sum_{1\le i_1<\ldots<i_p\le n}\Big(\mathfrak{IC}_k(g_{i_1\dots i_p}\,\mathrm{d}\,x_{i_1}\wedge\ldots\wedge\mathrm{d}\,x_{i_p})-g_{i_1\dots i_p}\,\mathrm{d}\,x_{i_1}\wedge\ldots\wedge\mathrm{d}\,x_{i_p}\Big).$$

In σ the interpolant $\mathfrak{IC}_k(g_{i_1\dots i_p}\,\mathrm{d}\,x_{i_1}\wedge\ldots\wedge\mathrm{d}\,x_{i_p})=\sum_{\upsilon_i\in S_k^p(\sigma)}\alpha_i w(\upsilon_i)$, where each α_i is a linear combination of the integrals of $g_{i_1\dots i_p}\,\mathrm{d}\,x_{i_1}\wedge\ldots\wedge\mathrm{d}\,x_{i_p}$ over small p-cubes in σ. The coefficients in this linear combination are constant and independent of σ, so we may find a constant C_α, depending only on n, p, and k, such that for all the coefficients

$$|\alpha_i|\le C_\alpha\max_{\upsilon_j\in S_k^p(\sigma)}\Big|\int_{\upsilon_j}g_{i_1\dots i_p}\,\mathrm{d}\,x_{i_1}\wedge\ldots\wedge\mathrm{d}\,x_{i_p}\Big|\le C_\alpha C_\omega h^k\cdot\max_{\upsilon_j\in S_k^p(\sigma)}|\upsilon_j|\le C_\alpha C_\omega h^k\operatorname{diam}(\sigma)^p.$$

In the unit cube, we clearly have $|w(\upsilon)(x)|\le 1$ for all $\upsilon\in S_k^p(\square^n)$ and $x\in\square^n$. Applying the pullback inequality $|f^*\omega(x)|\le|Df(x)|^p\cdot|\omega(f(x))|$ [12, II, 4.12] to the inverse of the affine bijection $\phi:\square^n\to\sigma$ and using (4.6), we get

$$|w(\upsilon_i)(x)|\le|D\phi^{-1}(x)|^p\le\frac{\sqrt{n}^p}{\Theta(\sigma)^p\operatorname{diam}(\sigma)^p},\quad|\alpha_i w(\upsilon_i)(x)|\le\frac{C_\alpha C_\omega\sqrt{n}^p h^k}{\Theta(\sigma)^p}$$

for all $\upsilon_i\in S_k^p(\sigma)$ and $x\in\sigma$. Hence

$$|\mathfrak{IC}_k(g_{i_1\dots i_p}\,\mathrm{d}\,x_{i_1}\wedge\ldots\wedge\mathrm{d}\,x_{i_p})(x)|\le\binom{n}{p}k^p(k+1)^{n-p}\frac{C_\alpha C_\omega\sqrt{n}^p h^k}{\Theta(\sigma)^p}$$

and we may choose

$$C_{\omega,k}=\binom{n}{p}\left(\binom{n}{p}k^p(k+1)^{n-p}C_\alpha C_\omega\sqrt{n}^p+C_\omega\right)$$

to obtain

$$|\mathfrak{IC}_k\omega(x)-\omega(x)|\le\sum_{1\le i_1<\ldots<i_p\le n}|\mathfrak{IC}_k g_{i_1\dots i_p}\,\mathrm{d}\,x_{i_1}\wedge\ldots\wedge\mathrm{d}\,x_{i_p}(x)|+|g_{i_1\dots i_p}\,\mathrm{d}\,x_{i_1}\wedge\ldots\wedge\mathrm{d}\,x_{i_p}(x)|$$
$$\le\binom{n}{p}\left(\binom{n}{p}k^p(k+1)^{n-p}\frac{C_\alpha C_\omega\sqrt{n}^p h^k}{\Theta(\sigma)^p}+C_\omega h^k\right)\le\frac{C_{\omega,k}}{\Theta(\sigma)^p}h^k$$

for all $x\in\sigma$ in all $\sigma\in S^n(K)$ whenever K satisfies the assumptions. □

References

[1] Douglas Arnold and Anders Logg. Periodic table of the finite elements. *SIAM News*, 47(9), 2014.

[2] Douglas N. Arnold. Spaces of finite element differential forms. In *Analysis and Numerics of Partial Differential Equations*, volume 4 of *Springer INdAM Series*, pages 117–140. Springer, 2013.

[3] Douglas N. Arnold, Daniele Boffi, and Francesca Bonizzoni. Finite element differential forms on curvilinear cubic meshes and their approximation properties. *Numerische Mathematik*, 129(1):1–20, 2015.

[4] Douglas N. Arnold, Richard S. Falk, and Ragnar Winther. Finite element exterior calculus, homological techniques, and applications. *Acta Numerica*, 15:1–155, 2006.

[5] Douglas N. Arnold, Richard S. Falk, and Ragnar Winther. Geometric decompositions and local bases for spaces of finite element differential forms. *Computer Methods in Applied Mechanics and Engineering*, 198(21-26):1660–1672, 2009.

[6] Lauri Kettunen, Jonni Lohi, Jukka Räbinä, Sanna Mönkölä, and Tuomo Rossi. Generalized finite difference schemes with higher order Whitney forms. *ESAIM: Mathematical Modelling and Numerical Analysis*, 55(4):1439–1460, 2021.

[7] Jonni Lohi. Discrete exterior calculus and higher order Whitney forms. Master's thesis, University of Jyväskylä, 2019.

[8] Jonni Lohi. Systematic implementation of higher order Whitney forms in methods based on discrete exterior calculus. *Numerical Algorithms*, 91(3):1261–1285, 2022.

[9] Jonni Lohi and Lauri Kettunen. Whitney forms and their extensions. *Journal of Computational and Applied Mathematics*, 393:113520, 2021.

[10] Francesca Rapetti and Alain Bossavit. Whitney forms of higher degree. *SIAM Journal on Numerical Analysis*, 47(3):2369–2386, 2009.

[11] F. J. Vermolen and A. Segal. On an integration rule for products of barycentric coordinates over simplexes in $\mathbb{R}^n$. *Journal of Computational and Applied Mathematics*, 330:289–294, 2018.

[12] Hassler Whitney. *Geometric Integration Theory*. Princeton University Press, 1957.

PIV

HIGHER ORDER METHODS BASED ON DISCRETE EXTERIOR CALCULUS

by

Jonni Lohi, Lauri Kettunen, and Tuomo Rossi

Submitted, 2022

Higher order methods based on discrete exterior calculus

Jonni Lohi, Lauri Kettunen, and Tuomo Rossi
Faculty of Information Technology
University of Jyväskylä

Abstract

We propose a unifying approach to derive higher order methods for elliptic and hyperbolic boundary value problems. The approach is based on discrete exterior calculus. The problems are expressed in terms of differential forms, which are approximated using cochains. It then remains to handle the exterior derivative and the Hodge star operator, whose discrete counterparts are the coboundary and the discrete Hodge operator. Although the importance of the discrete Hodge operator has been acknowledged, methods based on discrete exterior calculus have previously been limited to lowest order. We show that higher order methods can be discovered when using discrete Hodge operators of higher approximation order. These are obtained by interpolating cochains with suitable finite element differential forms and then integrating the Hodge stars of the interpolants over dual cells. By construction, the discrete Hodge operator is, in a sense, exact for all differential forms in the chosen finite element space. We consider two possibilities, Whitney forms on simplicial meshes and cubical forms on cubical meshes, and study the properties of the resulting higher order discrete Hodge operators. Our approach enables a unified treatment of elliptic and hyperbolic problems. Defining the Hodge star operator with respect to Riemannian metrics results in elliptic problems, and the hyperbolic case is obtained when we switch to Lorentzian metrics and consider the cochains in spacetime. Although the same formulation covers both cases, the stability of the methods requires more careful consideration for hyperbolic problems. Time-dependent problems also admit time stepping schemes that can be used to efficiently solve the resulting large linear system step by step. Convergence properties are studied both theoretically and through numerical examples for Poisson's equation and the wave equation.

1 Introduction

Numerical schemes designed to solve second order boundary value problems realise the operators of the continuous level problems in finite-dimensional spaces. Of particular importance are the finite-dimensional counterparts of the differential operator and the Hodge star operator. All their properties cannot be preserved at the discrete level, and some compromise is always involved in the choice of their finite-dimensional proxies.

Explicit recognition of these proxies is highly important because they determine the properties of the finite-dimensional schemes.

This paper concerns schemes based on discrete exterior calculus. These schemes choose to realise the differential operator exactly in terms of a cochain complex. As a compromise, the Hodge star operator is handled approximatively with a discrete Hodge operator. Methods based on discrete exterior calculus may go by different names, e.g. Yee-like schemes [13, 14], finite integration technique [15], or generalised finite differences [11, 12]. Here exterior calculus refers to the calculus of differential forms; the methods are often presented without any reference to differential geometry, but a reinterpretation in terms of differential forms enables one to distinguish their metric-dependent features and hence provides deeper insight into them. The structural analysis approach based on differential geometry has been presented by Alain Bossavit and others in the computational electromagnetics community [3, 4, 5, 6, 24, 7, 8, 9, 10, 17].

Although methods based on discrete exterior calculus have gained popularity, they have previously been limited to lowest order, and extending the framework for higher order methods still remains an open issue. Steps in this direction have been taken in [19, 18], where the authors have demonstrated how higher order Whitney forms can be used with discrete exterior calculus. However, so far they have only been used in interpolating. While this reduces the interpolation error, it has not yet been examined if the error resulting from the discrete Hodge operator can also be reduced using higher order Whitney forms.

To answer this question affirmatively, the present paper proposes a systematic way to define higher order discrete Hodge operators on simplicial and cubical meshes. Given a mesh, we refine it into either the small simplices of [23] or the small cubes of [20], which enables us to interpolate cochains on the refined mesh using either Whitney or cubical forms. To map a primal p-cochain to a dual $(n-p)$-cochain, we first interpolate the cochain, next apply the actual Hodge star operator to the interpolant, and finally integrate the resulting $(n-p)$-form over dual $(n-p)$-cells to obtain a dual $(n-p)$-cochain. This prescribes our higher order discrete Hodge operator. By linearity, it clearly suffices to do the computations for basis cochains; moreover, under certain conditions it is sufficient to compute the required integrals only once in a single element.

After we have defined the discrete Hodge operators and studied their properties, we show how they provide higher order cochain-based methods. The approach we propose enables a unified treatment of elliptic and hyperbolic problems, which follow when we define the Hodge star using Riemannian or Lorentzian metrics, respectively. Although the same idea covers both classes of problems, there are certain aspects in which the hyperbolic case requires more careful consideration. Firstly, there is a difference in boundary conditions, and we show how these are dealt with. Hyperbolic problems also admit time stepping schemes that can be used to efficiently solve the resulting large linear system step by step. In addition, the stability criterion seems to be stricter in the hyperbolic case; the methods can be proven to be consistent, so convergence boils down to the stability of the schemes. Questions of convergence are considered for Poisson's equation and the wave equation.

The outline of this paper is as follows. We start with some preliminaries and explain our notation in Section 2. Section 3 summarises previous work on higher order interpolation of cochains, recalling the small simplices of [23] and the small cubes of [20]. Then we are ready to define higher order discrete Hodge operators in Section 4, where we also consider their theoretical properties. In Section 5 we present the aforementioned discretisation approach, and in Section 6 we consider its convergence for Poisson's equation and the wave equation. Section 7 provides several illustrative numerical examples, and in Section 8 we conclude the paper by summarising our findings.

2 Preliminaries

We first recall some prerequisite concepts and explain our notation. For simplicity, we assume that our domain of interest Ω is a bounded polytope in $\mathbb{R}^n$. Points $x = (x_1, \dots, x_n)$ in Ω have coordinates $x_1, \dots, x_n$. In time-dependent problems we identify x_n as the time coordinate $t \in [0, T]$ and denote $\Omega_t = \{(x_1, \dots, x_n) \in \Omega \mid x_n = t\}$.

A mesh in Ω is a finite set of cells [25, App. II, §1], denoted by K, such that

- each face of every cell in K is also in K.
- The intersection of two cells in K is either a common face of theirs or the empty set.
- The union of the cells in K is Ω.

The set of p-cells in K is denoted by $S^p(K)$. If the cells are all simplices, we say that the mesh is simplicial. Similarly, we say that the mesh is cubical if the cells are all parallelotopes. For a p-cell σ, let $|\sigma|$ denote its p-dimensional volume, and define its fullness $\Theta(\sigma)$ by $\Theta(\sigma) = |\sigma| / \operatorname{diam}(\sigma)^p$.

We assume that the cells are oriented [25, App. II, §5]. Recall that if $\sigma \in S^p(K)$ is a face of $\tau \in S^{p+1}(K)$, the orientation of τ induces an orientation on σ. The incidence number d_σ^τ is defined as

$$\mathrm{d}_\sigma^\tau = \begin{cases} 1 & \text{if } \sigma \text{ is a } p\text{-face of } \tau \text{ and } \sigma \text{ has the induced orientation,} \\ -1 & \text{if } \sigma \text{ is a } p\text{-face of } \tau \text{ but } \sigma \text{ has the opposite orientation,} \\ 0 & \text{otherwise.} \end{cases}$$

The incidence matrix d is the matrix with elements $\mathrm{d}_{ij} = \mathrm{d}_{\sigma_j}^{\tau_i}$ for $\tau_i \in S^{p+1}(K)$ and $\sigma_j \in S^p(K)$.

We denote by $C_p(K)$ the space of p-chains of K (that is, formal sums of oriented p-cells) and the dual space of p-cochains by $C_p^*(K)$ [25, App. II, §6]. Any p-chain of K can be uniquely expressed as a sum $\sum_{\sigma_i \in S^p(K)} a_i \sigma_i$, and p-chains can be considered as vectors whose components are the a_i. The same holds for p-cochains, after we adopt the standard notation that σ_i can also denote the cochain whose value is δ_{ij} at the chain σ_j. Negative coefficients correspond to a change of orientation. The boundary $\partial\tau$ of $\tau \in S^{p+1}(K)$ is the p-chain $\sum_{\sigma \in S^p(K)} \mathrm{d}_\sigma^\tau \, \sigma$, and the boundary map $\partial : C_{p+1}(K) \to C_p(K)$ follows by extending linearly. For cochains, the coboundary map $\mathrm{d} : C_p^*(K) \to C_{p+1}^*(K)$ is defined by $\mathrm{d}\, X(c) = X(\partial c)$. The incidence matrix is the matrix of the coboundary operator, hence the same notation.

We assume the reader is familiar with exterior algebra and differential forms (see e.g. [25, I–III] and [2]). We denote by $F^p(K)$ the space of differential p-forms in K [25, p. 226].

These are cellwise smooth and have a well-defined trace in all cells of K, which ensures that they can be integrated over p-cells. Integration over p-chains follows by extending linearly. The de Rham map $\mathcal{C} : F^p(K) \to C_p^*(K)$ is the linear map defined by

$$\mathcal{C}\omega\Bigg(\sum_{\sigma_i \in S^p(K)} a_i \sigma_i\Bigg) = \int_{\sum_{\sigma_i \in S^p(K)} a_i \sigma_i} \omega = \sum_{\sigma_i \in S^p(K)} a_i \int_{\sigma_i} \omega.$$

We overload the symbol d also for the exterior derivative of p-forms. Then $\mathcal{C}$ and d commute: by Stokes' theorem, we have $\mathcal{C}\,\mathrm{d}\,\omega = \mathrm{d}\,\mathcal{C}\omega$ for p-forms ω.

The definition of the Hodge star operator depends on the choice of metric. To appreciate how different problems follow from the same unifying approach, let us make the definition explicit. By metric we refer to a metric tensor g, which by definition is a symmetric and smooth 2-tensor field whose value g_x is nondegenerate at each point $x \in \Omega$. For the moment, we can assume that g_x is a bilinear map $V \times V \to \mathbb{R}$, where V is an n-dimensional vector space (that will be specified later). Then g_x is nondegenerate if $g_x(v, w) = 0$ for all $w \in V$ implies $v = 0$. If g_x is also positive definite (i.e. $g_x(v, v) > 0$ if $v \neq 0$) at each point $x \in \Omega$, the metric is Riemannian. Otherwise $g_x(v, v) < 0$ for some $v \neq 0$, and the corresponding matrix has negative eigenvalues. The metric is Lorentzian when exactly one eigenvalue is negative.

To define the Hodge star, choose as V the space of covectors, with oriented basis $\{\mathrm{d}\,x_1, \dots, \mathrm{d}\,x_n\}$. We extend the notion of metric for p-covectors as follows. First, for simple p-covectors $\omega_1 \wedge \ldots \wedge \omega_p$ and $\eta_1 \wedge \ldots \wedge \eta_p$, define $g_x(\omega_1 \wedge \ldots \wedge \omega_p, \eta_1 \wedge \ldots \wedge \eta_p)$ as the determinant of the matrix with entries $(i, j) = g_x(\omega_i, \eta_j)$. Then $g_x(\omega, \eta)$ for any p-covectors ω and η is obtained by bilinearity. Using the given metric, we define the Hodge star operator as the unique linear operator from p-covectors to $(n-p)$-covectors satisfying

$$\omega \wedge (\star\eta) = g_x(\omega, \eta)\,\mathrm{d}\,x_1 \wedge \ldots \wedge \mathrm{d}\,x_n$$

for all p-covectors ω and η. The Hodge star for differential forms is defined pointwise, and it maps p-forms to $(n-p)$-forms.

Remark 2.1. From the definition it follows that

$$\star\,\mathrm{d}\,x_j = \sum_{i=1}^{n} (-1)^{i-1} g_x(\mathrm{d}\,x_i, \mathrm{d}\,x_j)\,\mathrm{d}\,x_1 \wedge \ldots \wedge \widehat{\mathrm{d}\,x_i} \wedge \ldots \wedge \mathrm{d}\,x_n.$$

Boundary value problems related to field theories in physics can often be presented in a natural way with differential forms, the exterior derivative, and the Hodge star operator. Discrete exterior calculus provides a framework for approximating such problems in finite-dimensional spaces. Given a mesh K, differential p-forms can be approximated with p-cochains. A key point in discrete exterior calculus is that the exterior derivative can be discretised without additional error using the coboundary operator; as stated, we have $\mathcal{C}\,\mathrm{d}\,\omega = \mathrm{d}\,\mathcal{C}\omega$ for p-forms ω. This is not the case with the Hodge star operator, whose approximation is another key point. Note that if $\omega \in F^p(K)$, the Hodge star $\star\omega$ is not necessarily in $F^{n-p}(K)$. For this reason, it is not sensible to approximate the Hodge star operator using the same mesh K — instead, we use another mesh called a dual mesh [12].

The dual mesh $\tilde{K}$ is created such that for each p-cell $\sigma \in S^p(K)$, there exists a unique dual $(n-p)$-cell $\tilde{\sigma} \in S^{n-p}(\tilde{K})$, and if σ is a face of τ, then $\tilde{\tau}$ is a face of $\tilde{\sigma}$. Two examples are the barycentric dual mesh, which exists for every simplicial mesh, and the circumcentric dual mesh, which requires that all the primal cells have circumcentres inside them. Strictly speaking, the dual mesh is not a valid mesh by our definition, as dual cells of boundary cells have incomplete boundary (all their faces are not in $\tilde{K}$), but these are typically handled using boundary conditions anyway. We can consider dual p-chains $C_p(\tilde{K})$, dual p-cochains $C_p^*(\tilde{K})$, and the de Rham map $\tilde{\mathcal{C}} : F^p(\tilde{K}) \to C_p^*(\tilde{K})$. We use d^t as the incidence matrix for the dual mesh and let this imply the orientations. The coboundary of $X \in C_p^*(\tilde{K})$ is then given as $\mathrm{d}^t X$.

The discrete Hodge operator $* : C_p^*(K) \to C_{n-p}^*(\tilde{K})$ is a linear map taking p-cochains of the primal mesh to $(n-p)$-cochains of the dual mesh. It can be used to approximate the actual Hodge star operator when differential forms are approximated suitably on the two meshes; for example, if we approximate f with $\mathcal{C}f$ on the primal mesh and wish to approximate $g = \star f$ as well, this should be done with $\tilde{\mathcal{C}}g$ on the dual mesh. The map $*$ should be chosen such that $*\mathcal{C}f$ is a sensible approximation for $\tilde{\mathcal{C}}g$. To achieve this, the definition of the discrete Hodge operator should be tied to the choice of the mesh pair. Two main approaches for the definition are the diagonal Hodge (see e.g. [16]) and the Galerkin Hodge (see [11, Section 8]). We will define $*$ later in Section 4 using interpolation with suitable finite element differential forms.

3 Refined mesh and interpolation of cochains

In cochain-based discretisations, the solution cannot be directly evaluated at a given point; it must first be interpolated somehow. As a necessary step towards higher order methods based on discrete exterior calculus, some theory of interpolating cochains with higher order elements is hence required. In the case of simplicial meshes, a systematic way of doing this has been thoroughly explained in [21], and [20] complements the approach to cover cubical meshes. In this section, we summarise the main idea.

As a first step, the mesh K is suitably refined into smaller cells. For this we recall the small simplices from [23] and the small cubes from [20].

Definition 3.1 (Small simplices of [23]). Let $\mathcal{I}(n+1, k-1)$ denote the set of multi-indices $\mathbf{k} = (k_0, k_1, \ldots, k_n)$ with $n+1$ components that sum to $k-1$. For a fixed n-simplex σ with vertices $x_0, \ldots, x_n$, each multi-index $\mathbf{k} \in \mathcal{I}(n+1, k-1)$ defines a map $\mathbf{k}_\sigma : \sigma \to \sigma$ in terms of the barycentric coordinates $\lambda_1, \ldots, \lambda_n$ by

$$\mathbf{k}_\sigma : \sigma \to \sigma, \quad \lambda_0 x_0 + \ldots + \lambda_n x_n \mapsto \frac{\lambda_0 + k_0}{k} x_0 + \ldots + \frac{\lambda_n + k_n}{k} x_n.$$

For $k \geq 1$, the set of kth order small p-simplices of σ is

$$S_k^p(\sigma) = \{\mathbf{k}_\sigma(\tau) \mid \mathbf{k} \in \mathcal{I}(n+1, k-1), \text{ and } \tau \text{ is a } p\text{-face of } \sigma\}.$$

Definition 3.2 (Small cubes of [20]). Let $\mathcal{J}(n, k-1)$ denote the set of multi-indices $\mathbf{k} = (k_1, \ldots, k_n)$ with n components $k_i \leq k-1$. For the unit n-cube $\square^n = [0,1]^n$, each multi-index $\mathbf{k} \in \mathcal{J}(n, k-1)$ defines a map $\mathbf{k}_{k-1} : \Box^n \to \Box^n$ by

$$\mathbf{k}_{k-1}(x_1, \dots, x_n) = \frac{(k_1 + x_1, \dots, k_n + x_n)}{k}.$$

For $k \geq 1$, the set of kth order small p-cubes of $\Box^n$ is

$$S_k^p(\Box^n) = \{\mathbf{k}_{k-1}(\tau) \mid \mathbf{k} \in \mathcal{J}(n, k-1) \text{ and } \tau \text{ is a } p\text{-face of } \Box^n\}.$$

It is instructive to see Figure 1 for examples of small simplices and small cubes.

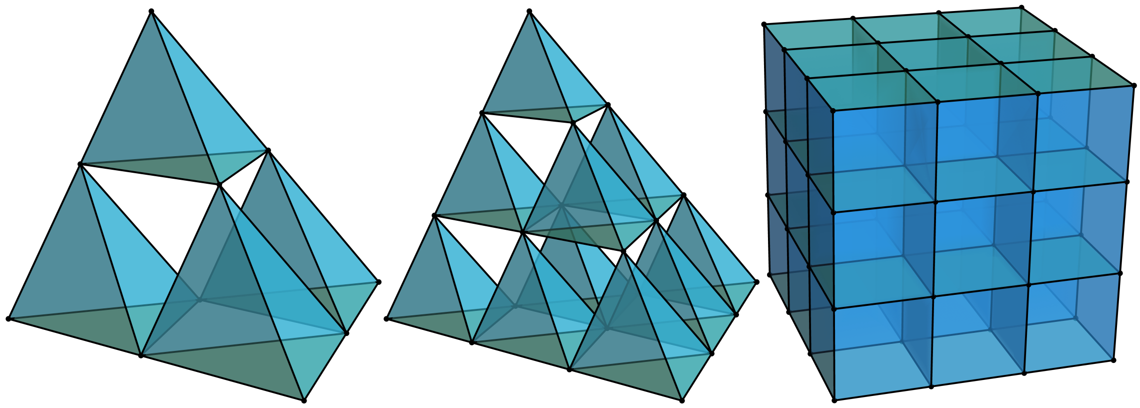

Figure 1: From left to right: second order small simplices, third order small simplices, and third order small cubes in three dimensions.

Above the small cubes were defined in the unit n-cube $\Box^n$. If σ is a parallelotope, there exists an affine bijection $\phi : \Box^n \to \sigma$, and we define the small cubes of σ as the images of the small cubes of $\Box^n$ through ϕ. Let us denote by $S_k^p(K)$ the set of all kth order small simplices (if K is simplicial) or cubes (if K is cubical) in the cells of K.

We choose k and refine the mesh K into a finer mesh K_k that contains the small cells $S_k^p(K)$ as cells. Note that the small simplices do not pave the initial simplices (see Figure 1), so if K is simplicial, the refinement K_k is not unique and it is allowed to contain also other cells. If K is cubical, K_k consists of the small cubes precisely. We denote by $C_p^*(K_k)$ the cochains of the refined mesh K_k and by $\mathcal{C}_k$ the de Rham map of K_k.

The reasoning for this refinement K_k is that we can interpolate cochains in $C_p^*(K_k)$ with suitable finite element differential forms. If K is simplicial, the suitable finite element space is the space of kth order Whitney p-forms (denoted W_k^p in [23, 22, 21] or $\mathcal{P}_k^-\Lambda^p$ in finite element exterior calculus notation). If K is cubical, a viable choice is the space of kth order cubical p-forms (denoted Q_k^p in [20] or $\mathcal{Q}_k^-\Lambda^p$ in FEEC notation). How cochains in $C_p^*(K_k)$ are interpolated is explained in the papers [21] and [20]. When $\mathfrak{I} : C_p^*(K_k) \to F^p(K)$ denotes the resulting interpolation operator, the main idea is that $\mathfrak{I}\mathcal{C}_k\omega = \omega$ holds for all ω in the used finite element space. We do not go into details here but instead summarise the properties of the resulting interpolation operator $\mathfrak{I}$.

We will use the notation $\mathfrak{I}(C_p^*(K_k))$ to denote the finite element space used in interpolating (which is also the image of $C_p^*(K_k)$ through $\mathfrak{I}$) and express our results in a way that covers both simplicial and cubical meshes. Firstly, the map $\mathfrak{I}$ is linear and satisfies $\mathfrak{I}\mathcal{C}_k\omega = \omega$ for all $\omega \in \mathfrak{I}(C_p^*(K_k))$. From the exact sequence property of the finite element spaces we obtain $\mathrm{d}\,\omega \in \mathfrak{I}(C_{p+1}^*(K_k))$ if $\omega \in \mathfrak{I}(C_p^*(K_k))$, which (together with $\mathfrak{I}\mathcal{C}_k\omega = \omega$

and Stokes' theorem) implies $\mathrm{d}\,\mathfrak{I}X = \mathfrak{I}\,\mathrm{d}\,X$ if $X = \mathcal{C}_k\omega$ for $\omega \in \mathfrak{I}(C_p^*(K_k))$. Finally, for a general $\omega \in F^p(K)$, $\mathfrak{I}\mathcal{C}\omega$ is an approximation of ω that converges as follows when the mesh is refined.

Theorem 3.3. *Let ω be a smooth p-form in Ω. There exists a constant $C_{\omega,k}$ such that*

$$|\mathfrak{I}\mathcal{C}_k\omega(x) - \omega(x)| \leq \frac{C_{\omega,k}}{C_\Theta^p} h^k \quad \text{for all } x \in \tau \text{ in all } \tau \in S^n(K)$$

whenever $h > 0$, $C_\Theta > 0$, and K is a mesh in Ω such that $\operatorname{diam}(\sigma) \leq h$ and $\Theta(\sigma) \geq C_\Theta$ for all cells σ of K.

The proof is given in [22] for simplices and Whitney forms and in [20] for cubes and cubical forms.

4 Higher order discrete Hodge operators

In a nutshell, our strategy for obtaining a discrete Hodge operator of order k can be explained as follows.

1. Given a mesh K, we form a refined mesh K_k that contains the small simplices (if K is simplicial) or the small cubes (if K is cubical) of order k as cells. We can consider p-chains $C_p(K_k)$, p-cochains $C_p^*(K_k)$, and the de Rham map $\mathcal{C}_k : F^p(K_k) \to C_p^*(K_k)$ of the refined mesh K_k.

2. We form a dual mesh $\tilde{K}_k$ for the refined mesh K_k and consider also p-chains $C_p(\tilde{K}_k)$, p-cochains $C_p^*(\tilde{K}_k)$, and the de Rham map $\tilde{\mathcal{C}}_k : F^p(\tilde{K}_k) \to C_p^*(\tilde{K}_k)$ of this dual mesh.

3. We choose an interpolating map $\mathfrak{I} : C_p^*(K_k) \to F^p(K)$ that enables us to interpolate cochains of the refined mesh K_k with higher order finite element differential forms (either Whitney forms or cubical forms).

4. Our discrete Hodge operator of order k is the composite map $\tilde{\mathcal{C}}_k \star \mathfrak{I} : C_p^*(K_k) \to C_{n-p}^*(\tilde{K}_k)$, where $\star$ is the actual Hodge star operator for p-forms.

The refinement K_k and interpolation of cochains have been explained in the previous section, and below we will only use the aforementioned properties of the interpolation operator $\mathfrak{I}$. Regarding the dual mesh $\tilde{K}_k$, there are no limitations besides the basic requirements. Although different dual meshes yield different discrete Hodge operators, the same convergence results hold for all sensible dual meshes (see Corollary 4.10). We summarise the definition as follows.

Definition 4.1 (Higher order discrete Hodge operator)**.** kth order discrete Hodge operator $*$ is defined by

$$* : C_p^*(K_k) \to C_{n-p}^*(\tilde{K}_k), \quad * = \tilde{\mathcal{C}}_k \star \mathfrak{I}.$$

To build the matrix of $*$, we take the Hodge star of the basis functions and integrate over dual $(n-p)$-cells. Note that these integrals are not affine-invariant quantities, but depending on the continuous Hodge star, they may be rotationally or translationally invariant. For example, when the Hodge star is taken with respect to the Euclidean metric and all cells have the same shape, it is sufficient to compute the integrals only once in a single element. The same integrals can then be used in all cells (when scaled suitably to take sizes into account).

Remark 4.2. Definition 4.1 can be seen as an extension of the definition given in [24] using lowest order Whitney forms, which is recovered when K is simplicial and $k = 1$.

Remark 4.3. The discrete Hodge operator $* : C_p^*(K_k) \to C_{n-p}^*(\tilde{K}_k)$ is not invertible when K is simplicial, $k > 1$, $p > 0$, and $n > 1$ because then the interpolation operator is not injective.

4.1 Properties of discrete Hodge operators

To gain insight into our higher order discrete Hodge operators, let us consider their theoretical properties. The main goal of this section is to bound the consistency error of the operator $\mathrm{d}^t * \mathrm{d}$. In the following, we assume that the discrete Hodge operator $*$ is defined according to Definition 4.1.

In discrete exterior calculus, the coboundary operator discretises the exterior derivative exactly in the sense that $\mathrm{d}\,\mathcal{C}\omega = \mathcal{C}\,\mathrm{d}\,\omega$ for all $\omega \in F^p(K)$. While such approximation is not possible for the Hodge star, our discrete Hodge operator is designed to be exact for Whitney forms (if K is simplicial) or cubical forms (if K is cubical) up to order k, in the following sense.

Corollary 4.4. *Let $\omega \in \mathfrak{I}(C_p^*(K_k))$. Then $*\,\mathcal{C}_k\omega = \tilde{\mathcal{C}}_k \star \omega$.*

Proof. Since $\mathfrak{I}\mathcal{C}_k\omega = \omega$ for $\omega \in \mathfrak{I}(C_p^*(K_k))$, we have

$$* \,\mathcal{C}_k\omega = \tilde{\mathcal{C}}_k \star \mathfrak{I}\mathcal{C}_k\omega = \tilde{\mathcal{C}}_k \star \omega.$$

□

Corollary 4.4 can be considered as a rationale for Definition 4.1. As an immediate consequence, we get the following result.

Corollary 4.5. *Let $\omega \in \mathfrak{I}(C_p^*(K_k))$. Then $\mathrm{d}^t * \mathrm{d}\,\mathcal{C}_k\omega(\tilde{\sigma}) = \tilde{\mathcal{C}}_k\,\mathrm{d} \star \mathrm{d}\,\omega(\tilde{\sigma})$ for all dual $(n-p)$-cells $\tilde{\sigma} \in S^{n-p}(\tilde{K}_k)$ that have complete boundary.*

Proof. Since $\mathrm{d}\,\omega \in \mathfrak{I}(C_{p+1}^*(K_k))$, Corollary 4.4 gives us

$$\mathrm{d}^t * \mathrm{d}\,\mathcal{C}_k\omega = \mathrm{d}^t * \mathcal{C}_k\,\mathrm{d}\,\omega = \mathrm{d}^t\,\tilde{\mathcal{C}}_k \star \mathrm{d}\,\omega.$$

Recalling that d^t gives the coboundary on the dual mesh, $\mathrm{d}^t\,\tilde{\mathcal{C}}_k \star \mathrm{d}\,\omega(\tilde{\sigma}) = \tilde{\mathcal{C}}_k\,\mathrm{d} \star \mathrm{d}\,\omega(\tilde{\sigma})$ when $\tilde{\sigma} \in S^{n-p}(\tilde{K}_k)$ has complete boundary. □

Remark 4.6. Note that $\tilde{\sigma}$ has incomplete boundary only if $\sigma \subset \partial\Omega$. In this case Corollary 4.5 is corrected by including $\int_{\partial\tilde{\sigma}\cap\partial\Omega} \star\,\mathrm{d}\,\omega$ on the left-hand side.

The consistency error of $*$ can be bound using Theorem 3.3.

Theorem 4.7. *Let ω be a smooth p-form in Ω. There exists a constant $C_{\omega,k}$ such that*

$$\frac{|(*\,\mathcal{C}_k\omega - \tilde{\mathcal{C}}_k \star \omega)(\tilde{\sigma})|}{|\tilde{\sigma}|} \leq \frac{C_{\omega,k}}{C_\Theta^p} h^k \quad \textit{for all dual } (n-p)\textit{-cells } \tilde{\sigma} \in S^{n-p}(\tilde{K}_k)$$

whenever $h > 0$, $C_\Theta > 0$, and all cells σ of K fulfill $\operatorname{diam}(\sigma) \leq h$ *and* $\Theta(\sigma) \geq C_\Theta$.

Proof. We write

$$\omega = \mathfrak{I}\mathcal{C}_k\omega + \eta,$$

where $\eta = \omega - \mathfrak{I}\mathcal{C}_k\omega$ is the residual when approximating ω with $\mathfrak{I}\mathcal{C}_k\omega$. By Theorem 3.3, there exists a constant $C_{\omega,k}$ such that

$$|\eta(x)| \leq \frac{C_{\omega,k}}{C_\Theta^p} h^k \quad \text{for all } x \in \tau \text{ in all } \tau \in S^n(K) \tag{4.1}$$

whenever $h > 0$, $C_\Theta > 0$, and all cells σ of K fulfill $\operatorname{diam}(\sigma) \leq h$ and $\Theta(\sigma) \geq C_\Theta$. Note that

$$\mathfrak{I}\mathcal{C}_k\eta = \mathfrak{I}\mathcal{C}_k(\omega - \mathfrak{I}\mathcal{C}_k\omega) = \mathfrak{I}\mathcal{C}_k\omega - \mathfrak{I}\mathcal{C}_k\mathfrak{I}\mathcal{C}_k\omega = \mathfrak{I}\mathcal{C}_k\omega - \mathfrak{I}\mathcal{C}_k\omega = 0,$$

and hence $*\,\mathcal{C}_k\eta = 0$. Using Corollary 4.4 for $\mathfrak{I}\mathcal{C}_k\omega \in \mathfrak{I}(C_p^*(K_k))$, we find

$$*\,\mathcal{C}_k\omega - \tilde{\mathcal{C}}_k \star \omega = *\,\mathcal{C}_k(\mathfrak{I}\mathcal{C}_k\omega + \eta) - \tilde{\mathcal{C}}_k \star (\mathfrak{I}\mathcal{C}_k\omega + \eta) = *\,\mathcal{C}_k\eta - \tilde{\mathcal{C}}_k \star \eta = -\tilde{\mathcal{C}}_k \star \eta.$$

Finally, let $h > 0$ and $C_\Theta > 0$, and suppose all cells σ of K fulfill $\operatorname{diam}(\sigma) \leq h$ and $\Theta(\sigma) \geq C_\Theta$. Then (4.1) implies $|\int_{\tilde{\sigma}} \star\eta| \leq |\tilde{\sigma}| \cdot \frac{C_{\omega,k}}{C_\Theta^p} h^k$ and hence

$$\frac{|(*\,\mathcal{C}_k\omega - \tilde{\mathcal{C}}_k \star \omega)(\tilde{\sigma})|}{|\tilde{\sigma}|} = \frac{|-\tilde{\mathcal{C}}_k \star \eta(\tilde{\sigma})|}{|\tilde{\sigma}|} = \frac{|-\int_{\tilde{\sigma}} \star\eta|}{|\tilde{\sigma}|} \leq \frac{C_{\omega,k}}{C_\Theta^p} h^k$$

for all dual $(n-p)$-cells $\tilde{\sigma} \in S^{n-p}(\tilde{K}_k)$. ☐

Theorem 4.8. *Let $p < n$ and suppose ω is a smooth p-form in Ω. There exists a constant $C_{\omega,k}$ such that*

$$\frac{|(\mathrm{d}^t * \mathrm{d}\,\mathcal{C}_k\omega - \tilde{\mathcal{C}}_k\,\mathrm{d} \star \mathrm{d}\,\omega)(\tilde{\sigma})|}{|\partial\tilde{\sigma}|} \leq \frac{C_{\omega,k}}{C_\Theta^{p+1}} h^k \quad \textit{for all } \tilde{\sigma} \in S^{n-p}(\tilde{K}_k) \textit{ with complete boundary}$$

whenever $h > 0$, $C_\Theta > 0$, and all cells σ of K fulfill $\operatorname{diam}(\sigma) \leq h$ *and* $\Theta(\sigma) \geq C_\Theta$.

Proof. We write

$$\mathrm{d}\,\omega = \mathfrak{I}\mathcal{C}_k\,\mathrm{d}\,\omega + \eta,$$

where $\eta = \mathrm{d}\,\omega - \mathfrak{I}\mathcal{C}_k\,\mathrm{d}\,\omega$ is the residual when approximating $\mathrm{d}\,\omega$ with $\mathfrak{I}\mathcal{C}_k\,\mathrm{d}\,\omega$. By Theorem 3.3, there exists a constant $C_{\omega,k}$ such that

$$|\eta(x)| \leq \frac{C_{\omega,k}}{C_\Theta^{p+1}} h^k \quad \text{for all } x \in \tau \text{ in all } \tau \in S^n(K) \tag{4.2}$$

whenever $h > 0$, $C_\Theta > 0$, and all cells σ of K fulfill $\operatorname{diam}(\sigma) \leq h$ and $\Theta(\sigma) \geq C_\Theta$. Note that $\mathfrak{I}\mathcal{C}_k\eta = 0$ and hence $*\,\mathcal{C}_k\eta = 0$. When restricting to dual cells with complete boundary (so that $\mathrm{d}^t\,\tilde{\mathcal{C}}_k = \tilde{\mathcal{C}}_k\,\mathrm{d}$), Corollary 4.4 applied to $\mathfrak{I}\mathcal{C}_k\,\mathrm{d}\,\omega \in \mathfrak{I}(C^*_{p+1}(K_k))$ implies

$$\mathrm{d}^t * \mathrm{d}\,\mathcal{C}_k\omega - \tilde{\mathcal{C}}_k\,\mathrm{d} \star \mathrm{d}\,\omega = \mathrm{d}^t * \mathcal{C}_k(\mathfrak{I}\mathcal{C}_k\,\mathrm{d}\,\omega + \eta) - \mathrm{d}^t\,\tilde{\mathcal{C}}_k \star (\mathfrak{I}\mathcal{C}_k\,\mathrm{d}\,\omega + \eta) = -\,\mathrm{d}^t\,\tilde{\mathcal{C}}_k \star \eta. \quad (4.3)$$

Finally, let $h > 0$ and $C_\Theta > 0$, and suppose all cells σ of K fulfill $\operatorname{diam}(\sigma) \leq h$ and $\Theta(\sigma) \geq C_\Theta$. Then (4.2) implies $|\int_{\partial\tilde{\sigma}} \star\eta| \leq |\partial\tilde{\sigma}| \cdot \frac{C_{\omega,k}}{C_\Theta^{p+1}} h^k$ and hence

$$\frac{|(\mathrm{d}^t * \mathrm{d}\,\mathcal{C}_k\omega - \tilde{\mathcal{C}}_k\,\mathrm{d} \star \mathrm{d}\,\omega)(\tilde{\sigma})|}{|\partial\tilde{\sigma}|} = \frac{|-\,\mathrm{d}^t\,\tilde{\mathcal{C}}_k \star \eta(\tilde{\sigma})|}{|\partial\tilde{\sigma}|} = \frac{|-\int_{\partial\tilde{\sigma}} \star\eta|}{|\partial\tilde{\sigma}|} \leq \frac{C_{\omega,k}}{C_\Theta^{p+1}} h^k$$

for all dual $(n-p)$-cells $\tilde{\sigma} \in S^{n-p}(\tilde{K}_k)$ with complete boundary. □

Remark 4.9. If $\tilde{\sigma}$ has incomplete boundary, (4.3) is corrected by including $\int_{\partial\tilde{\sigma}\cap\partial\Omega} \star\,\mathrm{d}\,\omega$ on the left-hand side, and the same proof yields

$$\frac{|\mathrm{d}^t * \mathrm{d}\,\mathcal{C}_k\omega(\tilde{\sigma}) + \int_{\partial\tilde{\sigma}\cap\partial\Omega} \star\,\mathrm{d}\,\omega - \tilde{\mathcal{C}}_k\,\mathrm{d} \star \mathrm{d}\,\omega(\tilde{\sigma})|}{|\partial\tilde{\sigma}|} \leq \frac{C_{\omega,k}}{C_\Theta^{p+1}} h^k.$$

Notice that in Theorem 4.8, instead of $|\tilde{\sigma}|$, we have $|\partial\tilde{\sigma}|$ as the divisor on the left-hand side. To remedy this, let us assume that the dual mesh we use is sensible in the following sense: there exists a constant C (independent of K) such that

$$|\partial\tilde{\sigma}| \leq C|\tilde{\sigma}|\operatorname{diam}(\tilde{\sigma})^{-1} \quad (4.4)$$

for all dual cells $\tilde{\sigma}$. Theorem 4.8 can then be reformulated as follows.

Corollary 4.10. *Let $p < n$ and suppose ω is a smooth p-form in Ω. Assuming a sensible dual mesh in the sense of (4.4), there exists a constant $C_{\omega,k}$ such that*

$$\frac{|(\mathrm{d}^t * \mathrm{d}\,\mathcal{C}_k\omega - \tilde{\mathcal{C}}_k\,\mathrm{d} \star \mathrm{d}\,\omega)(\tilde{\sigma})|}{|\tilde{\sigma}|} \leq \frac{C_{\omega,k}}{C_\Theta^{p+1}} \frac{h^k}{\operatorname{diam}(\tilde{\sigma})}$$

for all $\tilde{\sigma} \in S^{n-p}(\tilde{K}_k)$ with complete boundary whenever $h > 0$, $C_\Theta > 0$, and all cells σ of K fulfill $\operatorname{diam}(\sigma) \leq h$ *and* $\Theta(\sigma) \geq C_\Theta$. *If in addition $h \leq \tilde{C}\operatorname{diam}(\tilde{\sigma})$ for some $\tilde{C}$, we get the bound*

$$\frac{|(\mathrm{d}^t * \mathrm{d}\,\mathcal{C}_k\omega - \tilde{\mathcal{C}}_k\,\mathrm{d} \star \mathrm{d}\,\omega)(\tilde{\sigma})|}{|\tilde{\sigma}|} \leq \frac{C_{\omega,k}\tilde{C}}{C_\Theta^{p+1}} h^{k-1}.$$

As $\operatorname{diam}(\tilde{\sigma})$ is typically proportional to h, Corollary 4.10 reveals that in general the order of consistency attained with $\mathrm{d}^t * \mathrm{d}$ is only $k-1$. However, it is worth pointing out that above we have considered the averaged consistency error. The divisor $|\tilde{\sigma}|$ tends to zero when the mesh is refined, and hence the quantity $|(\mathrm{d}^t * \mathrm{d}\,\mathcal{C}_k\omega - \tilde{\mathcal{C}}_k\,\mathrm{d} \star \mathrm{d}\,\omega)(\tilde{\sigma})|$ alone vanishes faster.

5 Unifying approach for second order boundary value problems

Let u be a 0-form. We consider boundary value problems with the differential operator $\mathrm{d}\star\mathrm{d}$. In Euclidean space this corresponds to the Laplacian. When the Hodge star is taken with respect to the Minkowski metric, $\mathrm{d}\star\mathrm{d}$ corresponds to the d'Alembertian. More general elliptic and hyperbolic problems are obtained by considering more general Riemannian and Lorentzian metrics (see Remark 5.1 below). The application of $\mathrm{d}\star\mathrm{d}$ to a 0-form is exemplified in Table 1.

1D Euclidean space $\star\mathrm{d}\,x = 1$ $\mathrm{d}\star\mathrm{d}\,u = \frac{\partial^2 u}{\partial x^2}\,\mathrm{d}\,x$	(1+1)D Minkowski space $\star\mathrm{d}\,x = \mathrm{d}\,t,\ \star\mathrm{d}\,t = \mathrm{d}\,x$ $\mathrm{d}\star\mathrm{d}\,u = (\frac{\partial^2 u}{\partial x^2} - \frac{\partial^2 u}{\partial t^2})\,\mathrm{d}\,x\wedge\mathrm{d}\,t$
2D Euclidean space $\star\mathrm{d}\,x = \mathrm{d}\,y$ $\star\mathrm{d}\,y = -\,\mathrm{d}\,x$ $\mathrm{d}\star\mathrm{d}\,u = (\frac{\partial^2 u}{\partial x^2} + \frac{\partial^2 u}{\partial y^2})\,\mathrm{d}\,x\wedge\mathrm{d}\,y$	(2+1)D Minkowski space $\star\mathrm{d}\,x = \mathrm{d}\,y\wedge\mathrm{d}\,t,\ \star\mathrm{d}\,y = -\,\mathrm{d}\,x\wedge\mathrm{d}\,t$ $\star\mathrm{d}\,t = -\,\mathrm{d}\,x\wedge\mathrm{d}\,y$ $\mathrm{d}\star\mathrm{d}\,u = (\frac{\partial^2 u}{\partial x^2} + \frac{\partial^2 u}{\partial y^2} - \frac{\partial^2 u}{\partial t^2})\,\mathrm{d}\,x\wedge\mathrm{d}\,y\wedge\mathrm{d}\,t$
3D Euclidean space $\star\mathrm{d}\,x = \mathrm{d}\,y\wedge\mathrm{d}\,z,\ \star\mathrm{d}\,y = -\,\mathrm{d}\,x\wedge\mathrm{d}\,z$ $\star\mathrm{d}\,z = \mathrm{d}\,x\wedge\mathrm{d}\,y$ $\mathrm{d}\star\mathrm{d}\,u = (\frac{\partial^2 u}{\partial x^2} + \frac{\partial^2 u}{\partial y^2} + \frac{\partial^2 u}{\partial z^2})\,\mathrm{d}\,x\wedge\mathrm{d}\,y\wedge\mathrm{d}\,z$	(3+1)D Minkowski space $\star\mathrm{d}\,x = \mathrm{d}\,y\wedge\mathrm{d}\,z\wedge\mathrm{d}\,t,\ \star\mathrm{d}\,y = -\,\mathrm{d}\,x\wedge\mathrm{d}\,z\wedge\mathrm{d}\,t$ $\star\mathrm{d}\,z = \mathrm{d}\,x\wedge\mathrm{d}\,y\wedge\mathrm{d}\,t,\ \star\mathrm{d}\,t = \mathrm{d}\,x\wedge\mathrm{d}\,y\wedge\mathrm{d}\,z$ $\mathrm{d}\star\mathrm{d}\,u = (\frac{\partial^2 u}{\partial x^2} + \frac{\partial^2 u}{\partial y^2} + \frac{\partial^2 u}{\partial z^2} - \frac{\partial^2 u}{\partial t^2})\,\mathrm{d}\,x\wedge\mathrm{d}\,y\wedge\mathrm{d}\,z\wedge\mathrm{d}\,t$

Table 1: Applying the operator $\mathrm{d}\star\mathrm{d}$ to a 0-form u gives the Laplacian in Euclidean space and the d'Alembertian in Minkowski space.

The basic idea of the approach is the same for every problem: we attach unknowns to primal 0-cells and obtain one equation for each dual n-cell. Let us start with the equation $\mathrm{d}\star\mathrm{d}\,u = f$. We approximate 0-forms (such as u) with primal 0-cochains and n-forms (such as f) with dual n-cochains. The differential operator $\mathrm{d}\star\mathrm{d}$ is discretised as $\mathrm{d}^t * \mathrm{d}$, which maps primal 0-cochains to dual n-cochains. The discrete equation is hence $\mathrm{d}^t * \mathrm{d}\,X = \tilde{\mathcal{C}} f$, where the cochain X is an approximation of u. When cochains are considered as vectors, this reduces to a linear system with one equation for each dual n-cell.

It is also possible to add certain lower order terms by interpolating and integrating over dual n-cells. For example, consider the Helmholtz equation, $\Delta u + k^2 u = 0$. This can be discretised as $\mathrm{d}^t * \mathrm{d}\,X + \tilde{\mathcal{C}}(k^2 \star \mathfrak{I} X) = 0$, using the Euclidean metric. (The Minkowski metric yields the Klein–Gordon equation.) Again we have one equation for each dual n-cell, but now we also include the contribution of the interpolant $\mathfrak{I}X$ (which is the approximate solution), taking the term $k^2 u$ into account. Most generally, we can accept equations that can be put in the form

$$\mathrm{d}\star\mathrm{d}\,u + F(\mathrm{d}\,u, u, x, t) = 0, \tag{5.1}$$

where F is an n-covector-valued function whose value at each point can be computed from the values of $\mathrm{d}\,u$ and u. The corresponding discrete equation is

$$\mathrm{d}^t * \mathrm{d}\,X + \tilde{\mathcal{C}}(F(\mathfrak{I}\,\mathrm{d}\,X, \mathfrak{I}X,\ \cdot\ ,\ \cdot\ )) = 0,$$

and this translates into a linear system when F is integrated numerically over dual n-cells (for each basis 0-cochain in place of X).

Remark 5.1. Hyperbolic equations of the following divergence form

$$\sum_{i=1}^{n-1}\sum_{j=1}^{n-1}\frac{\partial}{\partial x_i}\left(a_{ij}(x,t)\frac{\partial}{\partial x_j}u(x,t)\right)-\frac{\partial^2}{\partial t^2}u(x,t)=0$$

can be expressed in the form $\mathrm{d}\star\mathrm{d}\,u=0$ by tweaking the metric (see Remark 2.1) such that

$$\star\,\mathrm{d}\,x_j=\sum_{i=1}^{n-1}(-1)^{i-1}a_{ij}\,\mathrm{d}\,x_1\wedge\ldots\wedge\widehat{\mathrm{d}\,x_i}\wedge\ldots\wedge\mathrm{d}\,x_{n-1}\wedge\mathrm{d}\,t,\ \star\,\mathrm{d}\,t=(-1)^n\,\mathrm{d}\,x_1\wedge\ldots\wedge\mathrm{d}\,x_{n-1}.$$

Elliptic equations can be expressed similarly (simply exclude the t-coordinate). This means that the model covers heterogenous and anisotropic media.

5.1 Handling boundary conditions

Although the basic idea of the approach is the same for both elliptic and hyperbolic problems, the obvious difference is in boundary conditions. Time-independent problems do not require initial conditions, so in this sense the boundary points are all of the same kind. In time-dependent problems also initial conditions are present and we have to make a distinction between three different types of boundary points: $\partial\Omega_t$ for all $t\in[0,T]$, Ω_0, and Ω_T. Hence boundary conditions are more involved in the hyperbolic case.

In the elliptic case, the equation (5.1) with a combination of Dirichlet and Neumann boundary conditions in parts $\partial_D\Omega$ and $\partial_N\Omega$ of the boundary becomes

$$\begin{aligned}&\mathrm{d}\star\mathrm{d}\,u+F(\mathrm{d}\,u,u,x)=0\quad\text{in }\Omega,\\&\omega=g_D\quad\text{on }\partial_D\Omega,\\&\star\,\mathrm{d}\,\omega=g_N\quad\text{on }\partial_N\Omega,\end{aligned}\tag{5.2}$$

where $\partial_D\Omega\cup\partial_N\Omega=\partial\Omega$ and $\partial_D\Omega$ should be nonempty to enforce a unique solution. For the hyperbolic case, we also need initial conditions:

$$\begin{aligned}&\mathrm{d}\star\mathrm{d}\,u+F(\mathrm{d}\,u,u,x,t)=0\quad\text{in }\Omega,\\&\omega=g_D\quad\text{on }\partial_D\Omega\cup\Omega_0,\\&\star\,\mathrm{d}\,\omega=g_N\quad\text{on }\partial_N\Omega\cup\Omega_0,\end{aligned}\tag{5.3}$$

where $\partial_D\Omega\cup\partial_N\Omega=\cup_{t\in[0,T]}\partial\Omega_t$ and $\partial_D\Omega\cap\partial\Omega_t$ should be nonempty for each t. Note that there is no boundary condition on Ω_T. In both cases g_D is a 0-form and g_N is an $(n-1)$-form.

The discrete versions of (5.2) and (5.3) should be expressed as linear systems. Consider first the elliptic case. We require that the primal–dual mesh pair is formed such that $\partial\tilde\sigma\cap\partial\Omega\subset\partial_N\Omega$ for dual n-cells $\tilde\sigma$ of nodes $\sigma\in S^0(K_k)$ that are on $\partial_N\Omega$. Then the integral $\int_{\partial\tilde\sigma\cap\partial\Omega}g_N$ is defined and we can use it to correct the value $\mathrm{d}^t*\mathrm{d}$ yields for $\tilde\sigma$. The discrete version of the problem (5.2) is to find $X\in C_0^*(K_k)$ such that

$$\begin{aligned}&\mathrm{d}^t*\mathrm{d}\,X(\tilde\sigma)=-\int_{\tilde\sigma}F(\mathfrak{I}\,\mathrm{d}\,X,\mathfrak{I}X,\ \cdot\ )\quad\forall\tilde\sigma\in S^n(\tilde K_k)\text{ dual of }\sigma\notin\partial\Omega,\\&X(\sigma)=g_D(\sigma)\quad\text{for all }\sigma\in S^0(K_k)\text{ that are on }\partial_D\Omega,\\&\mathrm{d}^t*\mathrm{d}\,X(\tilde\sigma)=-\int_{\partial\tilde\sigma\cap\partial\Omega}g_N-\int_{\tilde\sigma}F(\mathfrak{I}\,\mathrm{d}\,X,\mathfrak{I}X,\ \cdot\ )\quad\forall\tilde\sigma\in S^n(\tilde K_k)\text{ dual of }\sigma\in\partial_N\Omega.\end{aligned}\tag{5.4}$$

Note that here the number of equations is automatically equal to the number of variables. Of course, the variables whose values are immediately seen from $X(\sigma) = g_D(\sigma)$ (and the corresponding equations) can be eliminated from the system; in the rest of this section we assume that Dirichlet boundary conditions have been eliminated by modifying the right-hand side accordingly.

Similarly for (5.3), the discrete version is to find $X \in C_0^*(K_k)$ such that

$$\begin{aligned}
\mathrm{d}^t * \mathrm{d}\, X(\tilde{\sigma}) &= -\int_{\tilde{\sigma}} F(\mathfrak{I}\,\mathrm{d}\, X, \mathfrak{I}X, \,\cdot\,, \,\cdot\,) \quad \forall \tilde{\sigma} \in S^n(\tilde{K}_k) \text{ dual of } \sigma \notin \partial\Omega, \\
X(\sigma) &= g_D(\sigma) \quad \text{for all } \sigma \in S^0(K_k) \text{ that are in } \partial_D\Omega \cup \Omega_0, \\
\mathrm{d}^t * \mathrm{d}\, X(\tilde{\sigma}) &= -\int_{\tilde{\sigma}} F(\mathfrak{I}\,\mathrm{d}\, X, \mathfrak{I}X, \,\cdot\,, \,\cdot\,) \\
&\qquad - \int_{\partial\tilde{\sigma}\cap\partial\Omega} g_N \quad \forall \tilde{\sigma} \in S^n(\tilde{K}_k) \text{ dual of } \sigma \in \partial_N\Omega \cup (\Omega_0 \setminus \partial\Omega_0).
\end{aligned} \tag{5.5}$$

Notice that now there are two equations for each node in $\Omega_0 \setminus \partial\Omega_0$ but no equations for nodes in $\Omega_T \setminus \partial\Omega_T$. Therefore we require that these two sets contain the same number of mesh nodes, to obtain an equal number of variables and equations. This additional requirement on the mesh is imposed only in the hyperbolic case.

5.2 Time stepping for time-dependent problems

In principle, the systems (5.4) and (5.5) can be solved using any suitable means. For (5.4) the rest is indeed a matter of numerical linear algebra (which is outside the scope of the present paper), and we can use the LU decomposition to solve the system. However, for time-dependent problems it is possible to solve the system much more efficiently when the variables are ordered in chronological order. This leads to a time stepping method with two useful interpretations. On one hand, we can consider a mesh consisting of one time step only, solve (5.5) on this mesh using previously known values to determine initial conditions, and then move the mesh forward in time to repeat the process. On the other hand, this is equivalent to exploiting a special block structure of the system matrix to solve the large system one time step at a time. For the rest of this section, we assume that F is of the form $F(x, t)$ (so the system matrix is essentially $\mathrm{d}^t * \mathrm{d}$) and the mesh is structural in the time direction so that we can identify one time step that can be repeated to obtain the whole mesh. Two examples of such meshes are given in Figure 2.

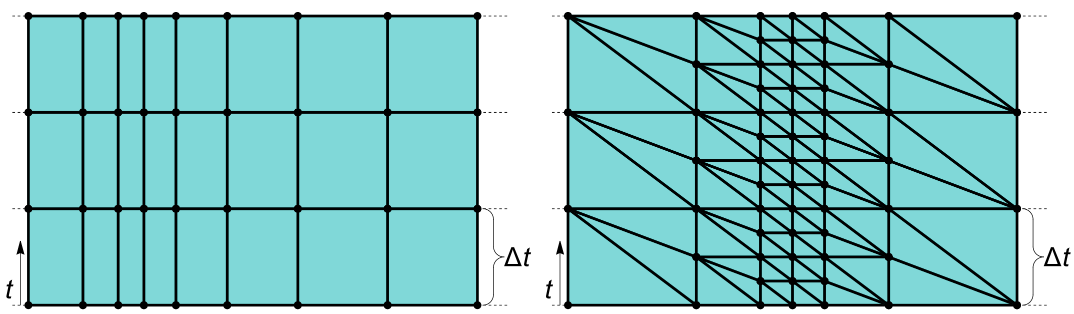

Figure 2: Two examples of meshes that are structural in the time direction.

In both cases in Figure 2, we have marked one time step (denoted by Δt) that has been repeated three times to obtain the whole mesh. Note that within the time step there is a lot of flexibility, but more complicated structures of course increase the computational cost of the time step.

We also assume that the mesh nodes are indexed in chronological order. Then the system matrix of (5.5) has the following special block structure:

$$L = \begin{bmatrix} A & & & & & & \\ B & A & & & & & \\ C & B & A & & & & \\ & C & B & A & & & \\ & & \ddots & \ddots & \ddots & & \\ & & & C & B & A & \\ & & & & C & B & A \end{bmatrix}.$$

The blocks A, B, and C are obtained by restricting the matrix $\mathrm{d}^t * \mathrm{d}$ as follows. We say that a row of $\mathrm{d}^t * \mathrm{d}$ corresponds to time step i if it corresponds to a node that is in time step i but not in time step $i+1$ (i.e. not in the back end of time step i). Contrarily, we say that a column of $\mathrm{d}^t * \mathrm{d}$ corresponds to time step i if it corresponds to a node that is in time step i but not in time step $i-1$ (i.e. not in the front end of time step i). Then

- A is the restriction to rows and columns corresponding to time step i.
- B is the restriction to rows corresponding to time step i and columns corresponding to time step $i-1$.
- C is the restriction to rows corresponding to time step i and columns corresponding to time step $i-2$.

By our assumption that the mesh is structural in the time direction, the blocks A, B, and C are the same for all time steps i. This enables an efficient solution process. If X_i denotes the solution in time step i and F_i the right-hand side, we get

$$X_1 = A^{-1}F_1,\ X_2 = A^{-1}(F_2 - BX_1),\ X_i = A^{-1}(F_i - BX_{i-1} - CX_{i-2}) \text{ for } i \geq 3. \quad (5.6)$$

In the absence of the source term, this scheme can also be written in the form

$$\tilde{X}_{i+1} = M\tilde{X}_i, \text{ where } \tilde{X}_i = \begin{pmatrix} X_i \\ X_{i-1} \end{pmatrix} \text{ and } M = \begin{bmatrix} -A^{-1}B & -A^{-1}C \\ I & \end{bmatrix}. \quad (5.7)$$

While this is simply linear algebra, the other interpretation is useful for implementation: A is the system matrix in a mesh consisting of one time step only, and B and C determine the initial condition for next time step based on previously known values. In implementation, it suffices to form only one time step of the mesh and compute the LU decomposition for A. The solution in time step i is obtained using (5.6), and then we can move the mesh one time step forward in time for the next time step. This time stepping process can be repeated as long as desired.

Remark 5.2. Notice that the inverse of L can be computed recursively as follows:

$$L^{-1} = \begin{bmatrix} A_1 & & & & & & \\ A_2 & A_1 & & & & & \\ A_3 & A_2 & A_1 & & & & \\ A_4 & A_3 & A_2 & A_1 & & & \\ \vdots & \vdots & \vdots & \vdots & \ddots & & \\ A_{m-1} & \cdots & A_4 & A_3 & A_2 & A_1 & \\ A_m & \cdots & A_5 & A_4 & A_3 & A_2 & A_1 \end{bmatrix},$$

where $A_1 = A^{-1}$, $A_2 = -A^{-1}BA^{-1}$, and $A_i = -A^{-1}(BA_{i-1} + CA_{i-2})$ for $i \geq 3$. We will use this recursive formula in stability analysis to compute the norm of L^{-1}.

5.3 Causalised schemes for time-dependent problems

The block lower triangular structure of L^{-1} reflects the fact that information from the future should not affect the solution in the past. However, for our finite-dimensional solution this holds only in the large scale: within a single time step there may be nodes on which the solution depends on source term integrals over future dual cells. Figure 3 provides a simple example with third order small cubes in 1+1 dimensions. This is rather understandable, since the finite-dimensional solution cannot satisfy all properties exactly. Nevertheless, it raises the question whether it is possible to derive higher order time stepping methods in which the solution is updated using previous values and source term integrals only over dual cells that are strictly in the past. We provide an example of such causalised schemes in this subsection.

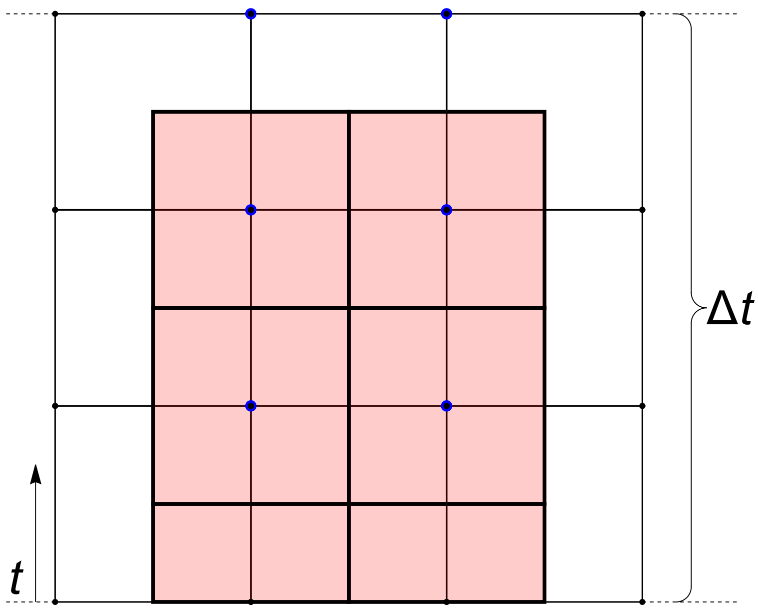

Figure 3: Instance of (5.5) with $\partial_N\Omega = \emptyset$: source term integrals over the six highlighted dual cells determine the values of the solution on the six highlighted nodes.

Suppose that we have a cubical mesh in some spatial domain and we take its tensor product with $[0, T]$ to obtain a mesh in spacetime with one time step of length T. Let

K_k be the division of this mesh into small cubes of order $k \geq 2$. Then K_k has nodes on $k+1$ different time levels, with time coordinates $0, T/k, 2T/k, \ldots, T$. Denote these sets of nodes by $Z_0, \ldots, Z_k$, and suppose that the values of the solution are known on nodes in $Z_0, \ldots, Z_{k-1}$. We can use the previous values, the boundary condition, and source term integrals over dual cells of nodes in Z_{k-1} to determine the values on nodes in Z_k. More precisely, we find $X \in C_0^*(K_k)$ such that its values match with the known values on nodes in $Z_0, \ldots, Z_{k-1}$ and it satisfies

$$
\begin{aligned}
&\mathrm{d}^t * \mathrm{d}\, X(\tilde{\sigma}) = -\int_{\tilde{\sigma}} F \quad \forall \tilde{\sigma} \in S^n(\tilde{K}_k) \text{ dual of } \sigma \in Z_{k-1} \setminus \partial\Omega, \\
&X(\sigma) = g_D(\sigma) \quad \text{for all } \sigma \in S^0(K_k) \text{ that are in } \partial_D\Omega \cap Z_k, \\
&\mathrm{d}^t * \mathrm{d}\, X(\tilde{\sigma}) = -\int_{\tilde{\sigma}} F - \int_{\partial\tilde{\sigma} \cap \partial\Omega} g_N \quad \forall \tilde{\sigma} \in S^n(\tilde{K}_k) \text{ dual of } \sigma \in \partial_N\Omega \cap Z_{k-1}.
\end{aligned}
\tag{5.8}
$$

The idea is elucidated in Figure 4. Here the initial 1-dimensional spatial mesh contained two 1-cells, and its tensor product with $[0, T]$ contains two 2-cells. This has then been divided into small cubes of order three. We have a Neumann boundary condition on the left and a Dirichlet boundary condition on the right. The values on nodes in Z_0, Z_1, and Z_2 are known. The values on the six highlighted nodes in Z_3 are determined by the right-hand side corresponding to the six highlighted dual cells. This right-hand side takes into account the source term integrals but also the contribution from the previously known values.

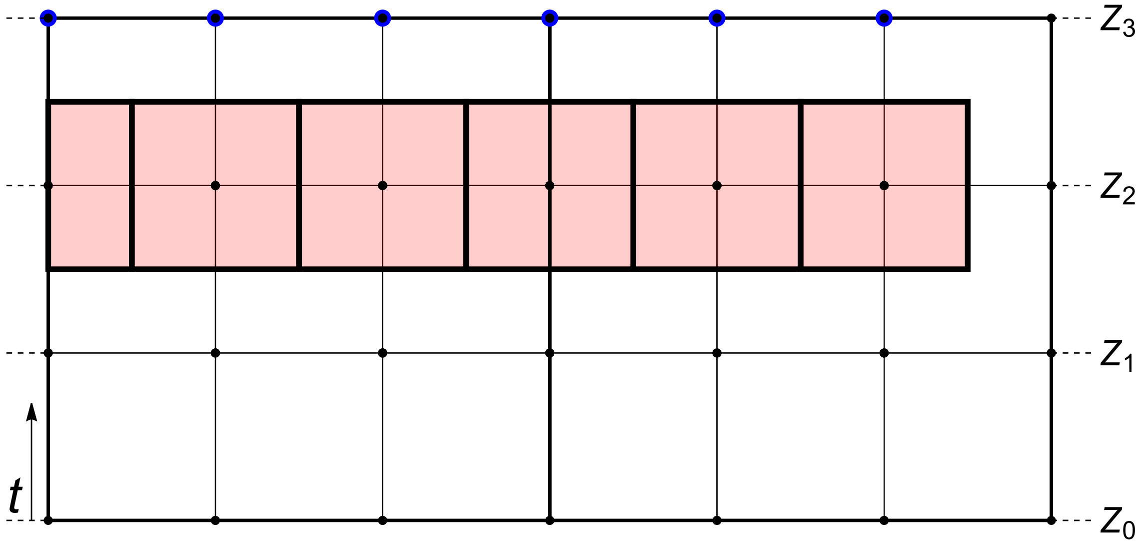

Figure 4: The right-hand side corresponding to the six highlighted dual cells determines the values of the solution on the six highlighted nodes.

When the solution is found on nodes in Z_k, we can move the mesh by T/k units in the time direction, replace Z_i with Z_{i+1}, and solve the next values similarly. Notice that now the steps are smaller than in the previous approach: previously we solved all values within one time step simultaneously, but now the different time levels within the time step are solved in chronological order. The scheme requires that previous values are known on multiple time levels, so it cannot be applied immediately with the initial condition. To initialise the scheme, we must first solve the values on k different time levels (e.g. by using the earlier approach).

This scheme can also be interpreted with a system matrix that has again a special block structure, but this time it is more complicated than before. For $0 \le i \le k$, let B_i denote the restriction of $\mathrm{d}^t * \mathrm{d}$ to rows corresponding to nodes in Z_{k-1} and columns corresponding to nodes in Z_i. Assuming we start with zero previous values (or adjust the right-hand side for the first step), we can interpret the matrix

$$\tilde{L} = \begin{bmatrix} B_k & & & & & & & & \\ B_{k-1} & B_k & & & & & & & \\ B_{k-2} & B_{k-1} & B_k & & & & & & \\ \vdots & \vdots & \vdots & \ddots & & & & & \\ B_1 & B_2 & \cdots & B_{k-1} & B_k & & & & \\ B_0 & B_1 & \cdots & B_{k-2} & B_{k-1} & B_k & & & \\ & B_0 & B_1 & \cdots & B_{k-2} & B_{k-1} & B_k & & \\ & & \ddots & \ddots & \ddots & \ddots & \ddots & \ddots & \\ & & & B_0 & B_1 & \cdots & B_{k-2} & B_{k-1} & B_k \end{bmatrix}.$$

as the system matrix of the scheme: the solution X satisfies $\tilde{L}X = F$, where F is determined by source term integrals over dual cells (and boundary conditions).

The number of block-rows in $\tilde{L}$ is equal to the number of steps we take. Now B_k is the system matrix for one step with zero previous values, and the blocks $B_0, \dots, B_{k-1}$ determine the initial condition for next step. On the first step, the solution is obtained from the right-hand side alone, since zero previous values were assumed. On the second step, the situation is otherwise the same, but now the values solved on the previous step affect the solution as described by the block B_{k-1}. On a general step, the solution is affected by previous values that were solved on k previous steps. If we denote by X_i the solution on nodes in time level i and by F_i the corresponding right-hand side, the scheme can be concisely summarised as

$$X_i = B_k^{-1}(F_i - B_{k-1}X_{i-1} - B_{k-2}X_{i-2} - \ldots - B_1 X_{i-k+1} - B_0 X_{i-k}). \tag{5.9}$$

Note that it suffices the compute the LU decomposition only for B_k. A reformulation similar to (5.7) is possible in the absence of the source term.

Remark 5.3. Again, it is possible to compute the inverse of $\tilde{L}$ recursively:

$$\tilde{L}^{-1} = \begin{bmatrix} A_1 & & & & & & \\ A_2 & A_1 & & & & & \\ A_3 & A_2 & A_1 & & & & \\ A_4 & A_3 & A_2 & A_1 & & & \\ \vdots & \vdots & \vdots & \vdots & \ddots & & \\ A_{m-1} & \cdots & A_4 & A_3 & A_2 & A_1 & \\ A_m & \cdots & A_5 & A_4 & A_3 & A_2 & A_1 \end{bmatrix},$$

where $A_1 = B_k^{-1}$ and $A_i = -B_k^{-1} \sum_{j=1}^{\min(k,i-1)} B_{k-j} A_{i-j}$ for $i \ge 2$.

6 Error bounds for Poisson's and the wave equation

Let us next consider the boundary value problem

$$\begin{aligned} \mathrm{d} \star \mathrm{d}\, \omega &= f \quad \text{in } \Omega, \\ \omega &= 0 \quad \text{on } \partial\Omega, \end{aligned} \tag{6.1}$$

where ω is an unknown 0-form, f is a given n-form, and the Hodge star is taken with respect to the Euclidean metric. This is simply Poisson's equation expressed in terms of differential forms. For clarity, we first consider Poisson's equation with homogenous boundary condition $\omega = 0$, but in Subsection 6.1 we elaborate how a combination of inhomogenous Dirichlet and Neumann boundary conditions (and the initial condition for the wave equation) does not produce any additional error.

Following the approach of Section 5, we approximate 0-forms with primal 0-cochains and n-forms with dual n-cochains, replacing the operators with their discrete counterparts. To handle boundary conditions, we make a distinction between active and inactive primal nodes and dual n-cells. At this point, the active nodes are simply the interior nodes (i.e. those that are not on the boundary), and their duals are the active dual cells. For a cochain X, let $I(X)$ denote its restriction to active nodes (if X is a primal 0-cochain) or to active dual n-cells (if X is a dual n-cochain). Similarly, let $B(X)$ denote the restriction to inactive nodes or dual cells. Let us also denote by L the matrix obtained by restricting the system matrix $\mathrm{d}^t * \mathrm{d}$ to rows and columns that correspond to active nodes and dual cells. Then the discrete version of (6.1) is to find $X \in C_0^*(K_k)$ such that

$$\begin{aligned} LI(X) &= I(\tilde{\mathcal{C}}_k f), \\ B(X) &= 0. \end{aligned} \tag{6.2}$$

Note that this is a special case of (5.4).

We assume without proof that the system matrix L is invertible. (This is the case in all of our examples but uncertain for more general instances of (5.4) and (5.5).) Then the values of X on interior nodes are given as $L^{-1} I(\tilde{\mathcal{C}}_k f)$, and the values on boundary nodes are set to zero. Let us study this discrete solution $L^{-1} I(\tilde{\mathcal{C}}_k f)$ next. The first observation is that if the actual solution ω is in the finite element space $\mathfrak{I}(C_0^*(K_k))$, the discrete solution is actually exact.

Proposition 6.1. *Suppose $\omega \in \mathfrak{I}(C_0^*(K_k))$ solves (6.1). Then $L^{-1} I(\tilde{\mathcal{C}}_k f) = I(\mathcal{C}_k \omega)$, that is, the discrete solution is exact.*

Proof. Since ω vanishes on boundary nodes and $\mathrm{d} \star \mathrm{d}\, \omega = f$, we have by Corollary 4.5

$$LI(\mathcal{C}_k \omega) = I(\mathrm{d}^t * \mathrm{d}\, \mathcal{C}_k \omega) = I(\tilde{\mathcal{C}}_k\, \mathrm{d} \star \mathrm{d}\, \omega) = I(\tilde{\mathcal{C}}_k f).$$

Hence $L^{-1} I(\tilde{\mathcal{C}}_k f) = I(\mathcal{C}_k \omega)$. □

Let us define the mesh grain h_K as

$$h_K = \max_{\sigma \in K} \operatorname{diam}(\sigma)$$

and define a norm $\|\cdot\|_{\underline{\infty}}$ for dual n-cochains by

$$\|\sum_{\tilde{\sigma}_i \in S^n(\tilde{K}_k)} a_i \tilde{\sigma}_i\|_{\underline{\infty}} = \max_{\tilde{\sigma}_i \in S^n(\tilde{K}_k)} \frac{|a_i|}{|\tilde{\sigma}_i|}.$$

In this norm, Corollary 4.10 gives the bound

$$\|I(\mathrm{d}^t * \mathrm{d}\,\mathcal{C}_k\omega) - I(\tilde{\mathcal{C}}_k\,\mathrm{d} \star \mathrm{d}\,\omega)\|_{\underline{\infty}} \leq Ch_K^{k-1} \tag{6.3}$$

for the consistency error $I(\mathrm{d}^t * \mathrm{d}\,\mathcal{C}_k\omega) - I(\tilde{\mathcal{C}}_k\,\mathrm{d} \star \mathrm{d}\,\omega)$. To prove convergence, we also need a bound for the norm of L^{-1} to ensure stability when the mesh is refined. For this, we will use the maximum norm $\|\cdot\|_\infty$ for primal 0-cochains and consider the resulting operator norm $\|\cdot\|$ of L^{-1} — that is, the operator norm induced by the norms $\|\cdot\|_{\underline{\infty}}$ and $\|\cdot\|_\infty$. We will return to the question of stability shortly, but let us first show how convergence follows from (6.3) if we can assume that $\|L^{-1}\|$ remains bounded when the mesh is refined.

Theorem 6.2. *Suppose ω is a smooth p-form in Ω that solves* (6.1)*. Then*

$$\|L^{-1}I(\tilde{\mathcal{C}}_k f) - I(\mathcal{C}_k\omega)\|_\infty \leq \|L^{-1}\| \cdot \|I(\mathrm{d}^t * \mathrm{d}\,\mathcal{C}_k\omega) - I(\tilde{\mathcal{C}}_k\,\mathrm{d} \star \mathrm{d}\,\omega)\|_{\underline{\infty}}.$$

Proof. Since $f = \mathrm{d} \star \mathrm{d}\,\omega$ and $I(\mathcal{C}_k\omega) = L^{-1}LI(\mathcal{C}_k\omega) = L^{-1}I(\mathrm{d}^t * \mathrm{d}\,\mathcal{C}_k\omega)$, we have

$$\begin{aligned}\|L^{-1}I(\tilde{\mathcal{C}}_k f) - I(\mathcal{C}_k\omega)\|_\infty &= \|L^{-1}\big(I(\tilde{\mathcal{C}}_k\,\mathrm{d} \star \mathrm{d}\,\omega) - I(\mathrm{d}^t * \mathrm{d}\,\mathcal{C}_k\omega)\big)\|_\infty \\ &\leq \|L^{-1}\| \cdot \|I(\mathrm{d}^t * \mathrm{d}\,\mathcal{C}_k\omega) - I(\tilde{\mathcal{C}}_k\,\mathrm{d} \star \mathrm{d}\,\omega)\|_{\underline{\infty}}.\end{aligned}$$

□

Combining (6.3) and Theorem 6.2, we see that the order of convergence is at least $k-1$ in the maximum norm if $\|L^{-1}\|$ remains bounded when the mesh is refined. This is only the worst-case estimate, and the numerical examples that will be exhibited in Section 7 indicate that in practice faster convergence is possible.

Unfortunately, a bound for $\|L^{-1}\|$ is elusive because we do not have an explicit expression for the elements of L. Eigenvalue analysis does not help for the same reason. It would suffice to prove that if the maximum of $\omega \in \mathfrak{I}(C_0^*(K_k))$ over primal nodes is equal to one, then the average $\int_{\tilde{\sigma}} \mathrm{d} \star \mathrm{d}\,\omega/|\tilde{\sigma}| \geq C$ over some dual cell $\tilde{\sigma}$, where $C \geq 0$ is independent of K and ω. Also this is difficult to prove, so we will study stability numerically by computing $\|L^{-1}\|$ in the test examples of Section 7. (In the time-dependent case without source term, we could alternatively (numerically) solve the eigenvalues of the matrix M in (5.7).) The norm of L^{-1} is obtained rather efficiently as the maximum row sum (of absolute values) after each column is scaled with the volume of the corresponding dual cell, and the recursive formula of Remark 5.2 can be used to analyse how the norm evolves during time stepping without having to store the whole matrix in memory.

6.1 Boundary and initial conditions

Above we assumed that $\omega = 0$ on the boundary, but a combination of (inhomogenous) Dirichlet and Neumann boundary conditions does not produce any additional error. To see why, let us briefly consider the problem

$$\begin{aligned}
\mathrm{d}\star\mathrm{d}\,\omega &= f \quad \text{in } \Omega,\\
\omega &= g_D \quad \text{on } \partial_D\Omega,\\
\star\,\mathrm{d}\,\omega &= g_N \quad \text{on } \partial_N\Omega.
\end{aligned} \tag{6.4}$$

This time the active nodes are those that are not on $\partial_D\Omega$, and their duals are the active dual cells. Again, we assume that the mesh pair is created such that $\partial\tilde{\sigma}\cap\partial\Omega\subset\partial_N\Omega$ if $\sigma\in S^0(K_k)$ is active and on the boundary — then the integral $\int_{\partial\tilde{\sigma}\cap\partial\Omega} g_N$ is well-defined.

We adjust the right-hand side of (6.2) by defining the following cochains $Y\in C_0^*(K_k)$ and $Z\in C_n^*(\tilde{K}_k)$:

$$\begin{aligned}
Y &= \sum_{\sigma_i\in S^0(K_k)} y_i\sigma_i, \quad y_i = g_D(\sigma_i) \text{ if } \sigma_i\in S^0(K_k) \text{ is inactive and } y_i = 0 \text{ otherwise,}\\
Z &= \sum_{\tilde{\sigma}_i\in S^n(\tilde{K}_k)} z_i\tilde{\sigma}_i, \quad z_i = \int_{\partial\tilde{\sigma}_i\cap\partial\Omega} g_N \text{ if } \sigma_i\in\partial\Omega \text{ is active and } z_i = 0 \text{ otherwise.}
\end{aligned}$$

The discrete version of (6.4) is then to find $X\in C_0^*(K_k)$ such that

$$\begin{aligned}
&LI(X) = I(\tilde{\mathcal{C}}_k f) - I(\mathrm{d}^t * \mathrm{d}\,Y) - Z,\\
&B(X) = B(Y).
\end{aligned} \tag{6.5}$$

The values of X are given as $L^{-1}\big(I(\tilde{\mathcal{C}}_k f) - I(\mathrm{d}^t * \mathrm{d}\,Y) - Z\big)$ on active nodes (and by the boundary condition on inactive nodes).

Thanks to our adjustments Y and Z, no additional error is produced. Z corrects the values the system matrix yields for dual cells with incomplete boundary (see Remark 4.9), and (6.3) is replaced with

$$\|I(\mathrm{d}^t * \mathrm{d}\,\mathcal{C}_k\omega) + Z - I(\tilde{\mathcal{C}}_k\,\mathrm{d}\star\mathrm{d}\,\omega)\|_{\underline{\infty}} \le Ch_K^{k-1}.$$

Y counts in nonzero boundary values, so we can write $LI(\mathcal{C}_k\omega) + I(\mathrm{d}^t * \mathrm{d}\,Y) = I(\mathrm{d}^t * \mathrm{d}\,\mathcal{C}_k\omega)$ and

$$\begin{aligned}
&\|L^{-1}\big(I(\tilde{\mathcal{C}}_k f) - I(\mathrm{d}^t * \mathrm{d}\,Y) - Z\big) - I(\mathcal{C}_k\omega)\|_\infty = \|L^{-1}\big(I(\tilde{\mathcal{C}}_k\,\mathrm{d}\star\mathrm{d}\,\omega) - Z - I(\mathrm{d}^t * \mathrm{d}\,\mathcal{C}_k\omega)\big)\|_\infty\\
&\le \|L^{-1}\|\cdot\|I(\mathrm{d}^t * \mathrm{d}\,\mathcal{C}_k\omega) + Z - I(\tilde{\mathcal{C}}_k\,\mathrm{d}\star\mathrm{d}\,\omega)\|_{\underline{\infty}}.
\end{aligned}$$

Hence Theorem 6.2 continues to hold in this corrected form.

The same bound holds for the wave equation

$$\begin{aligned}
\mathrm{d}\star\mathrm{d}\,\omega &= f \quad \text{in } \Omega,\\
\omega &= g_D \quad \text{on } \partial_D\Omega\cup\Omega_0,\\
\star\,\mathrm{d}\,\omega &= g_N \quad \text{on } \partial_N\Omega\cup\Omega_0,
\end{aligned}$$

where the only difference to (6.4) is that $\partial_D\Omega$ and $\partial_N\Omega$ have been replaced with $\partial_D\Omega\cup\Omega_0$ and $\partial_N\Omega\cup\Omega_0$ and the Hodge star is taken with respect to the Minkowski metric. We only have to alter the set of active cells. Now the active nodes are those that are not on $\partial_D\Omega\cup\Omega_0$, and the active dual cells are those that are dual to nodes in $\Omega\setminus(\partial_D\Omega\cup\Omega_T)$.

7 Numerical examples

In this section we test our higher order approach with numerical examples. The section is divided into two parts. In the first part we solve Poisson's equation, and in the second part we consider the wave equation.

7.1 Poisson's equation

We first illustrate the application of higher order discrete Hodge operators in the case of Poisson's equation (6.4). In this subsection we use only simplicial meshes, so the discrete Hodge operators are defined using higher order Whitney forms. The solution given by our approach is obtained by solving the system (6.5); let us call it "DEC solution" of order k. As a comparison, we can consider "FEM solution" with the same basis functions; it is defined to be the function $u \in \mathfrak{I}(C_0^*(K_k))$ that agrees with g_D on nodes on $\partial_D\Omega$ and satisfies

$$\int_\Omega \nabla u \cdot \nabla v = -\int_\Omega fv + \int_{\partial_N\Omega} g_N v$$

for all $v \in \mathfrak{I}(C_0^*(K_k))$ that vanish on nodes on $\partial_D\Omega$. FEM solutions are computed with the MFEM library [1], using integration rules of order 20 in the assembly.

In all of the examples, we specify the domain Ω and the parts $\partial_D\Omega$ and $\partial_N\Omega$ of the boundary $\partial\Omega$. To study accuracy and convergence, we choose a suitable test function ω and select the right-hand sides f, g_D, and g_N such that ω is the exact solution. This enables us to measure the errors of the solutions. H^1 norms of the errors are computed numerically using a sufficiently fine mesh and 11th order quadrature rules for tetrahedra. For this we interpolate the cochain X that solves (6.5) and its coboundary. We recall that the discrete Hodge operators (and hence the corresponding DEC solutions) depend on the choice of a dual mesh. In the following examples we have used barycentric duals, but the results with circumcentric duals are very similar.

Example 7.1. Let Ω be the quadrilateral with vertices $(\pm 2, -2)$ and $(\pm 4, 2)$, and set $\partial_D\Omega = [-2, 2] \times \{-2\}$ and $\partial_N\Omega = \partial\Omega \setminus \partial_D\Omega$. We consider a coarse mesh K consisting of three triangles (shown in Figure 5) and the three polynomial test functions

$$\omega_1(x, y) = 2.5x - y, \quad \omega_5(x, y) = \frac{1}{8}x^3y^2 - \frac{1}{2}y^4, \quad \omega_{10}(x, y) = \frac{1}{2048}x^7y^3 + \frac{1}{64}y^{10}.$$

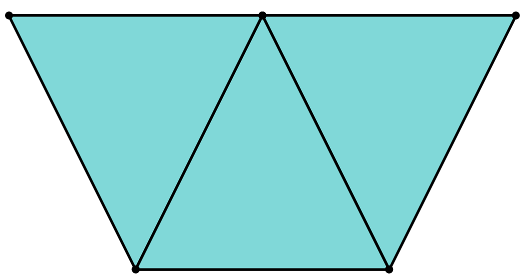

Figure 5: The coarse mesh used in Example 7.1.

For each test function, we compute DEC and FEM solutions of orders 1–10. Error H^1 norms are displayed in Table 2, illustrating that the solution obtained is exact as soon as the actual solution is in the space of kth order Whitney forms.

	DEC solution			FEM solution		
	ω_1	ω_5	ω_{10}	ω_1	ω_5	ω_{10}
$k=1$	9.02706e-15	5.50040e+01	1.28203e+02	6.62761e-15	6.31048e+01	1.45119e+02
$k=2$	9.40713e-15	3.17827e+01	1.20663e+02	1.38615e-14	2.10032e+01	8.05901e+01
$k=3$	2.06452e-14	1.70880e+01	1.05248e+02	6.54696e-14	1.29330e+01	6.97721e+01
$k=4$	3.44867e-14	9.88528e-01	7.70575e+01	1.49102e-13	7.27361e-01	3.28879e+01
$k=5$	5.01056e-14	6.44577e-14	6.05708e+01	1.31915e-13	2.59119e-13	2.79139e+01
$k=6$	8.27595e-14	7.16017e-14	3.32260e+01	1.56677e-12	3.28959e-12	8.21523e+00
$k=7$	2.23253e-13	1.86042e-13	2.47789e+01	8.06758e-13	7.48100e-13	7.02312e+00
$k=8$	3.11119e-13	2.57272e-13	7.67078e+00	1.24225e-12	1.60354e-12	9.57451e-01
$k=9$	7.64370e-13	9.08936e-13	5.34325e+00	6.27094e-12	1.03419e-11	8.00713e-01
$k=10$	2.12529e-12	1.91280e-12	3.05771e-12	3.04631e-11	2.67026e-11	5.42083e-11

Table 2: H^1 norms of the errors when solving (6.4) in Example 7.1.

Example 7.2. Let Ω be as in Example 7.1, $\partial_D\Omega = \partial\Omega$, $\partial_N\Omega = \emptyset$, and

$$\omega(x, y) = e^{x/4} \sin(x + y + 2) \cos(y).$$

In this example we study convergence when the mesh is consecutively refined. We have chosen to analyse orders 1, 2, 4, and 8 using four meshes. The first two meshes are shown in Figure 6, and the relevant information is given in Table 3. With these choices, we can build the initial mesh K such that the refined mesh K_k is always one of the meshes described in Table 3. In other words, the meshes of Table 3 are not further refined; the small simplices are contained in them already. This ensures a fair comparison in that the number of degrees of freedom is the same for all solutions on a given mesh. The results are displayed in Table 4 and illustrated in Figure 7.

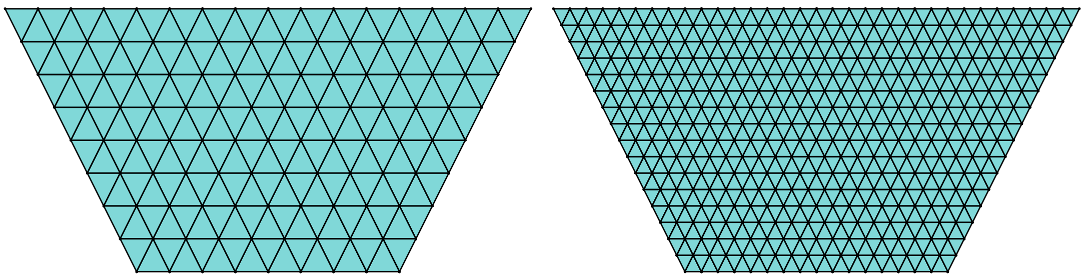

Figure 6: The first two of the four meshes used in Example 7.2.

	Mesh 1	Mesh 2	Mesh 3	Mesh 4
maximum edge length	$\sqrt{5}/4$	$\sqrt{5}/8$	$\sqrt{5}/16$	$\sqrt{5}/32$
number of triangles	192	768	3072	12288
number of vertices	117	425	1617	6305

Table 3: Information about the four meshes used in Example 7.2.

	Mesh 1	Mesh 2	Mesh 3	Mesh 4
$k=1$, DEC	1.55672e+00	7.81162e-01	3.90919e-01	1.95501e-01
$k=1$, FEM	1.55402e+00	7.80857e-01	3.90882e-01	1.95497e-01
$k=2$, DEC	8.06158e-01	2.08315e-01	5.25474e-02	1.31666e-02
$k=2$, FEM	7.68483e-01	2.01674e-01	5.11129e-02	1.28234e-02
$k=4$, DEC	3.50318e-01	2.62552e-02	1.70709e-03	1.07985e-04
$k=4$, FEM	2.61693e-01	1.94130e-02	1.25019e-03	7.86250e-05
$k=8$, DEC	1.48180e-01	1.11741e-03	4.96630e-06	2.00802e-08
$k=8$, FEM	7.15793e-02	4.21156e-04	1.67349e-06	6.05745e-09

Table 4: H^1 norms of the error when solving (6.4) in Example 7.2.

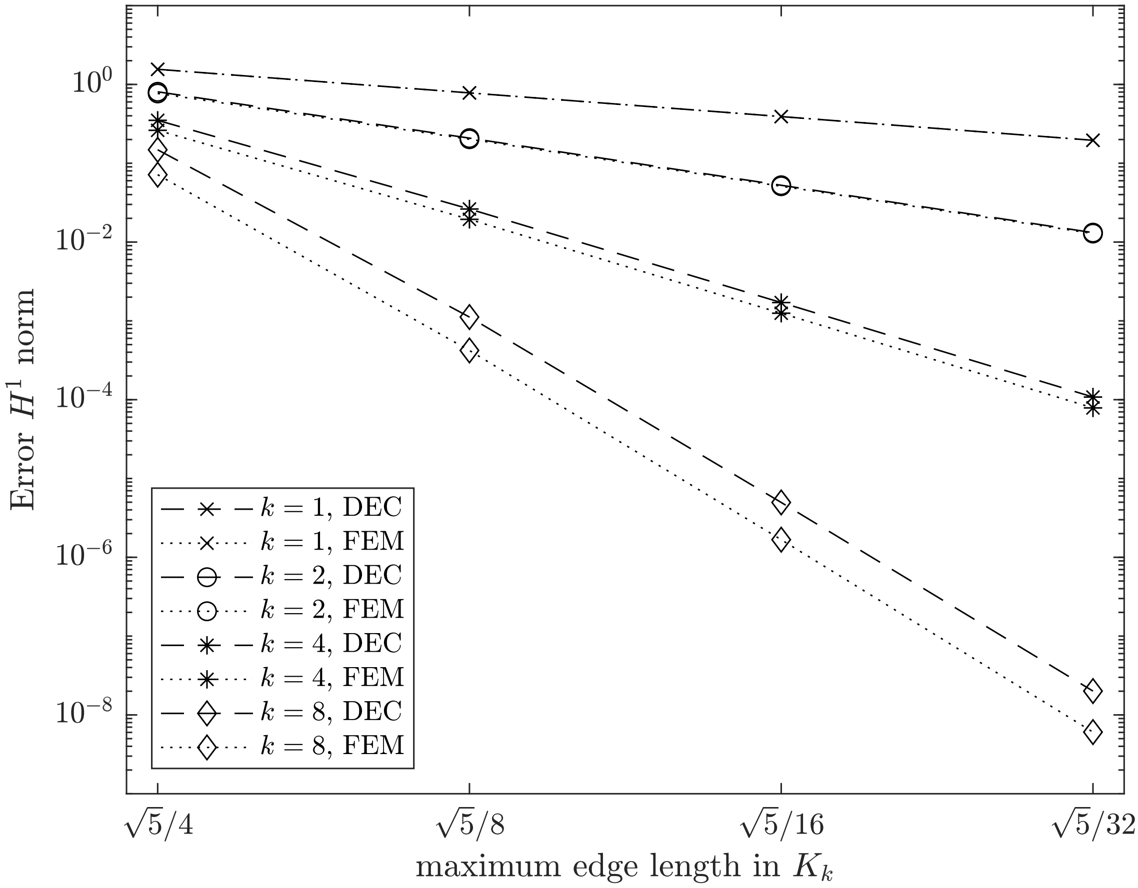

Figure 7: Illustration of the results displayed in Table 4.

Example 7.3. Let Ω be the octahedron with vertices $(\pm 1, -1, 0)$, $(\pm 1, 1, 0)$, and $(0, 0, \pm 1)$, $\partial_D\Omega = \{(x, y, z) \in \partial\Omega \mid z \geq 0\}$, and $\partial_N\Omega = \partial\Omega \setminus \partial_D\Omega$. We consider a coarse mesh K consisting of four tetrahedra (shown in Figure 8) and the three polynomial test functions

$$\omega_1(x,y,z) = 2.5x - y + 1.25z,\ \omega_5(x,y,z) = 10x^2y^3 - 40z^5,\ \omega_{10}(x,y,z) = 20x^{10} - 1000xy^6z^3.$$

For each test function, we compute DEC and FEM solutions of orders 1–10. Error H^1 norms are displayed in Table 5, illustrating that the solution obtained is exact as soon as the actual solution is in the space of kth order Whitney forms.

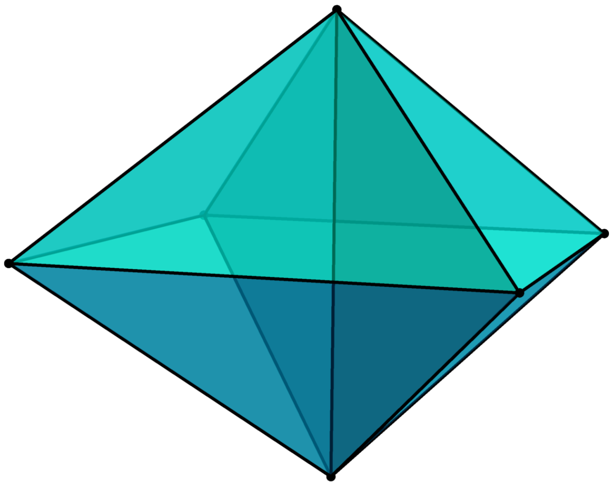

Figure 8: The coarse mesh used in Example 7.3.

	DEC solution			FEM solution		
	ω_1	ω_5	ω_{10}	ω_1	ω_5	ω_{10}
$k=1$	8.94886e-16	5.30595e+01	4.14278e+01	4.04750e-16	6.56341e+01	4.12532e+01
$k=2$	1.77604e-15	3.89600e+01	2.97825e+01	2.63562e-15	4.91586e+01	3.00148e+01
$k=3$	4.69410e-15	1.55684e+01	1.96751e+01	1.69378e-14	1.73549e+01	1.98591e+01
$k=4$	4.19878e-15	1.14529e+01	1.17294e+01	2.71790e-14	8.56964e+00	1.05661e+01
$k=5$	9.57713e-15	3.88413e-14	7.86926e+00	6.26691e-14	2.00562e-11	6.90483e+00
$k=6$	2.21892e-14	5.14741e-14	4.73297e+00	9.95346e-13	3.83621e-11	3.45919e+00
$k=7$	5.47779e-14	1.02590e-13	2.94603e+00	3.84930e-12	1.25911e-10	2.21506e+00
$k=8$	1.02314e-13	2.02383e-13	8.53239e-01	1.54633e-11	2.81736e-10	5.26278e-01
$k=9$	3.39112e-13	6.79238e-13	4.62951e-01	1.06899e-10	6.77012e-10	3.27912e-01
$k=10$	1.20902e-12	2.29335e-12	2.90757e-12	3.48505e-10	2.16836e-09	2.40078e-09

Table 5: H^1 norms of the errors when solving (6.4) in Example 7.3.

Example 7.4. Let Ω be as in Example 7.3, $\partial_D\Omega = \partial\Omega$, $\partial_N\Omega = \emptyset$, and

$$\omega(x, y, z) = e^{x+z} \sin(x + y + 2) \cos(yz).$$

To study convergence when the mesh is consecutively refined, we use again four meshes that enable us to compare discrete Hodge operators of orders 1, 2, 4, and 8 when the given mesh is taken as the refined mesh. The first two of the four meshes are shown in Figure 9, and the relevant information is given in Table 6. We emphasise that these meshes contain the small simplices already (and are not further refined), the only exception being that the first mesh does not contain 8th order small simplices, and hence the 8th order case is studied using meshes 2–4 only. This ensures the same number of degrees of freedom in all cases on a given mesh. The results are displayed in Table 7 and illustrated in Figure 10.

	Mesh 1	Mesh 2	Mesh 3	Mesh 4
maximum edge length	1/2	1/4	1/8	1/16
number of tetrahedra	256	2048	16384	131072
number of vertices	85	489	3281	23969

Table 6: Information about the four meshes used in Example 7.4.

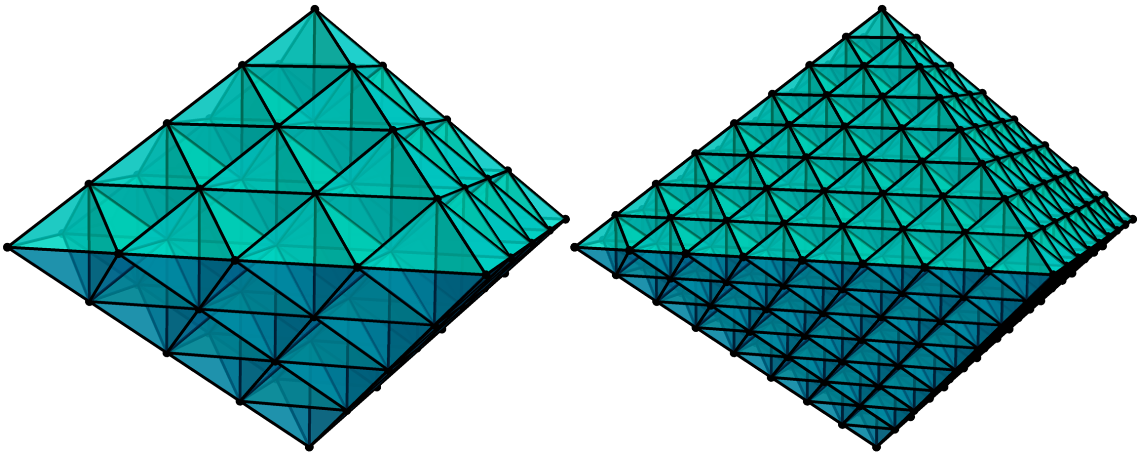

Figure 9: The first two of the four meshes used in Example 7.4.

	Mesh 1	Mesh 2	Mesh 3	Mesh 4
$k = 1$, DEC	6.73042e-01	3.38886e-01	1.69743e-01	8.49090e-02
$k = 1$, FEM	6.72936e-01	3.38870e-01	1.69741e-01	8.49087e-02
$k = 2$, DEC	2.23368e-01	5.97159e-02	1.51593e-02	3.80370e-03
$k = 2$, FEM	2.22407e-01	5.95299e-02	1.51350e-02	3.79999e-03
$k = 4$, DEC	5.02907e-02	4.63521e-03	3.15646e-04	2.01149e-05
$k = 4$, FEM	4.89353e-02	4.22144e-03	2.79932e-04	1.75908e-05
$k = 8$, DEC	-	9.60229e-05	7.77152e-07	3.70156e-09
$k = 8$, FEM	-	6.79247e-05	3.91215e-07	1.62228e-09

Table 7: H^1 norms of the error when solving (6.4) in Example 7.4.

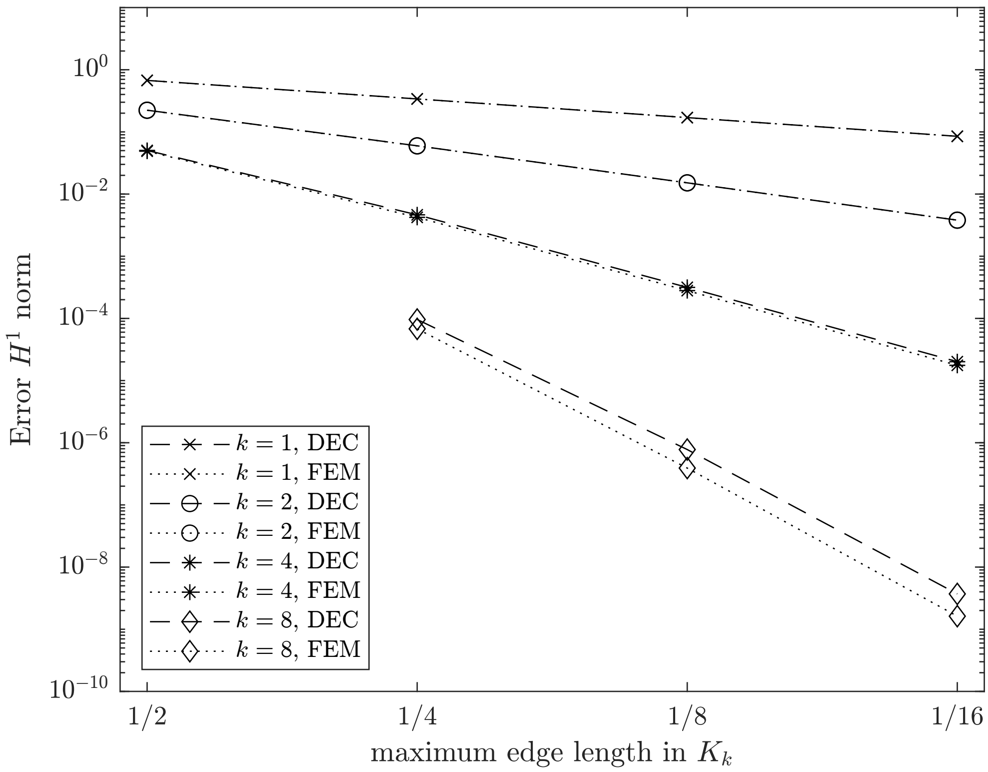

Figure 10: Illustration of the results displayed in Table 7.

Remark 7.5. Examples 7.2 and 7.4 indicate faster convergence than predicted theoretically in Section 6. Although higher order DEC does not outperform higher order FEM, the results are comparable and the order of convergence seems to be the same (i.e. optimal) in H^1 norm.

Example 7.6. We have examined $\|L^{-1}\|$ numerically, in the setting of Examples 7.2 and 7.4. The results are shown in Tables 8 and 9. Even though we do not have a proof, based on these examples we conjecture that $\|L^{-1}\|$ remains bounded when the mesh is suitably refined.

	Mesh 1	Mesh 2	Mesh 3	Mesh 4
$k = 1$	1.56258e+00	1.56306e+00	1.56324e+00	1.56330e+00
$k = 2$	1.56367e+00	1.56340e+00	1.56334e+00	1.56332e+00
$k = 4$	1.56429e+00	1.56343e+00	1.56333e+00	1.56332e+00
$k = 8$	1.89726e+00	1.61437e+00	1.56546e+00	1.56360e+00

Table 8: Values of $\|L^{-1}\|$ when the four meshes of Example 7.2 are taken as K_k.

	Mesh 1	Mesh 2	Mesh 3	Mesh 4
$k = 1$	1.08631e-01	1.07627e-01	1.07844e-01	1.07945e-01
$k = 2$	1.06740e-01	1.08048e-01	1.08018e-01	1.07995e-01
$k = 4$	1.08094e-01	1.11758e-01	1.08055e-01	1.07993e-01
$k = 8$	-	2.63535e-01	1.70704e-01	1.22657e-01

Table 9: Values of $\|L^{-1}\|$ when the four meshes of Example 7.4 are taken as K_k.

7.2 Wave equation

We next consider examples of the application of the discretisation (5.5) and the scheme (5.6) to the inhomogenous wave equation. For simplicity we assume Dirichlet boundary condition, so $\partial_D\Omega = \cup_{t\in[0,T]}\partial\Omega_t$ and $\partial_N\Omega = \emptyset$. The problem considered is hence

$$\begin{aligned} \mathrm{d}\star\mathrm{d}\,\omega &= f \quad \text{in } \Omega, \\ \omega &= g_D \quad \text{on } \cup_{t\in[0,T]}\partial\Omega_t \cup \Omega_0, \\ \star\,\mathrm{d}\,\omega &= g_N \quad \text{on } \Omega_0, \end{aligned} \tag{7.1}$$

where the Hodge star is taken with respect to the Minkowski metric.

The stability of the scheme seems to require a somewhat similar stability criterion as in the standard finite difference method. Informally, it states that steps in the time direction cannot be too large when compared to steps in the space direction. Unfortunately, with Whitney forms and simplices the higher order schemes suffer from late-time instabilities, which occur regardless of the time step length. In these cases the norm $\|L^{-1}\|$ grows exponentially with respect to time. (Linear growth is expected behaviour because the solution may grow linearly in time even with a bounded source term.) It seems that such late-time instabilities can be avoided with cubical forms. The following examples aim to illustrate these issues.

In each example, we specify the domain Ω and a test function ω which is chosen to be the exact solution; this determines the boundary conditions g_D and g_N and the source term f. We also explain what kind of meshes are used. It should be noted that with higher order elements the initial mesh is still refined into small simplices or cubes. For this reason, we consider the accuracy with respect to the maximum element diameter in the refined mesh K_k when comparing solutions of different orders.

Example 7.7. Let $\Omega = [0,2] \times [0,T]$ and $\omega(x,t) = e^{x/4}\sin(x+t+2)\cos(t)$. We solve the problem (7.1) using Whitney forms of orders 1–6 on triangular meshes of the type shown in Figure 11. The values of the parameter Δx are displayed in Table 10; note that the maximum element diameter in the refined mesh K_k is $\sqrt{(\Delta x)^2 + (\Delta t)^2}/k$. First we let $\Delta t = \Delta x$ and continue the simulation for 200 time units. This yields a solution for $t \in [0,200]$, and the results (shown in Table 11) suggest that the solution converges to the exact solution when the mesh is refined. Next we slightly increase the time step length so that $\Delta t = 1.0005\Delta x$. After 40.02 time units we can already see that the solution obtained for $t \in [0, 40.02]$ does not converge (see Table 12 for the results).

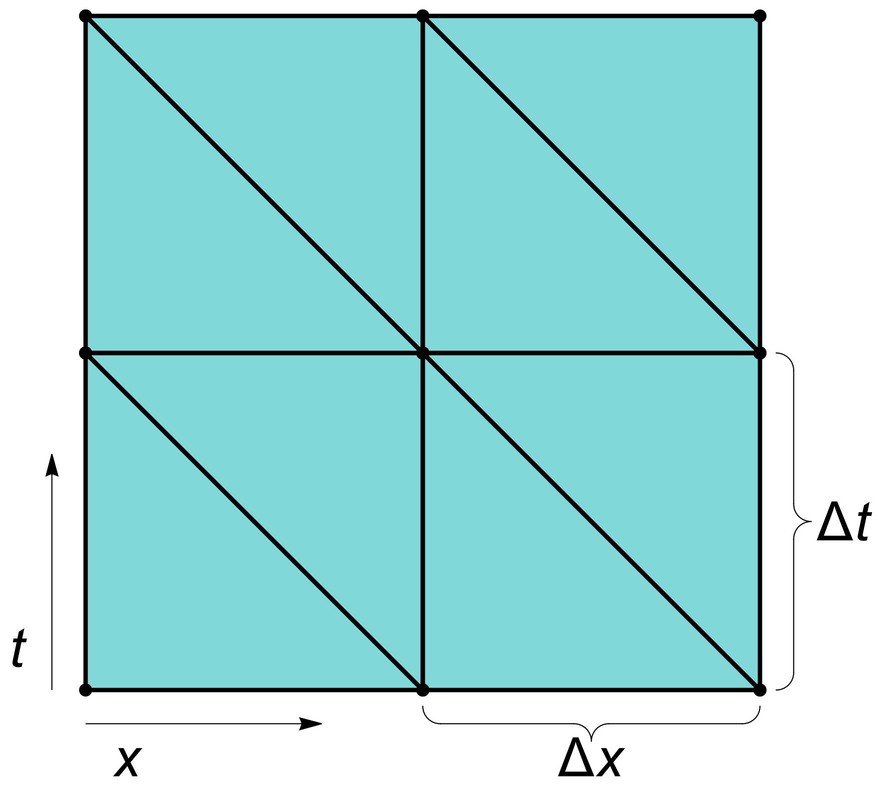

Figure 11: The type of the triangular meshes used in Example 7.7.

	Mesh 1	Mesh 2	Mesh 3	Mesh 4	Mesh 5
$k=1$	1/4	1/8	1/16	1/32	1/64
$k=2$	1/2	1/4	1/8	1/16	1/32
$k=3$	1	1/2	1/4	1/8	1/16
$k=4$	1	1/2	1/4	1/8	1/16
$k=5$	1	1/2	1/4	1/8	1/16
$k=6$	2	1	1/2	1/4	1/8

Table 10: Values of the parameter Δx for the meshes used in Example 7.7.

	Mesh 1	Mesh 2	Mesh 3	Mesh 4	Mesh 5
$k = 1$	4.33688e-02	1.08747e-02	2.71159e-03	6.78351e-04	1.69567e-04
$k = 2$	4.23952e-02	1.07308e-02	2.71159e-03	6.77823e-04	1.69560e-04
$k = 3$	3.08957e-02	1.91104e-03	2.50883e-04	4.07449e-05	8.12255e-06
$k = 4$	1.20904e-02	2.98952e-04	1.53769e-05	9.47519e-07	5.85806e-08
$k = 5$	3.03279e-03	1.67476e-04	1.01104e-05	6.25685e-07	3.91960e-08
$k = 6$	3.22629e-02	2.52014e-04	1.41281e-06	1.94040e-08	3.05841e-10

Table 11: Maximum norms of the error when $T = 200$ and $\Delta t = \Delta x$ in Example 7.7.

	Mesh 1	Mesh 2	Mesh 3	Mesh 4	Mesh 5
$k = 1$	4.35691e-02	1.08816e-02	2.71576e-03	1.00053e+15	9.30398e+55
$k = 2$	4.14201e-02	9.62690e-03	1.85463e-03	2.12047e+07	2.89982e+47
$k = 3$	2.64330e-02	2.03266e-03	2.51150e-04	4.44084e-05	1.84916e+17
$k = 4$	4.46329e-03	2.03903e-04	1.17623e-05	6.91967e-07	1.62325e+29
$k = 5$	8.81297e-04	6.95690e-05	2.10459e-05	6.87815e-05	5.37592e+31
$k = 6$	5.93816e-03	9.49624e-05	7.67003e-07	2.25720e-08	3.03107e+01

Table 12: Maximum norms of the error when $T = 40.02$ and $\Delta t = 1.0005\Delta x$ in Example 7.7.

Example 7.8. We have computed the norms of the inverses of the system matrices in the previous example. The results for $T = 200$ and $\Delta t = \Delta x$ are displayed in Table 13 and those for $T = 40.02$ and $\Delta t = 1.0005\Delta x$ in Table 14. Although the results suggest a stability limit $\Delta t \leq \Delta x$ that is the same for all orders, it should be noted that $\|L^{-1}\|$ grows exponentially with respect to time when $k > 2$; this can be seen by multiplying T by 100 and considering the results for $T = 20000$, which are shown in Table 15. The case $k = 2$ is stable when Δt equals exactly Δx but not e.g. when $\Delta t = \frac{5}{6}\Delta x$. We can conclude that higher order Whitney forms do not provide a stable scheme.

	Mesh 1	Mesh 2	Mesh 3	Mesh 4	Mesh 5
$k = 1$	1.00000e+02	1.00000e+02	1.00000e+02	1.00000e+02	1.00000e+02
$k = 2$	1.05483e+02	1.03209e+02	1.01721e+02	1.00890e+02	1.00452e+02
$k = 3$	1.80286e+02	1.85558e+02	1.84566e+02	1.83129e+02	1.82175e+02
$k = 4$	8.16034e+02	8.27430e+02	8.28864e+02	8.28515e+02	8.28074e+02
$k = 5$	8.85277e+02	8.91321e+02	8.90390e+02	8.88029e+02	8.86349e+02
$k = 6$	2.98432e+03	2.98137e+03	2.99361e+03	2.99390e+03	2.99295e+03

Table 13: Values of $\|L^{-1}\|$ when $T = 200$ and $\Delta t = \Delta x$ in Example 7.7.

	Mesh 1	Mesh 2	Mesh 3	Mesh 4	Mesh 5
$k = 1$	2.55849e+01	2.96637e+01	3.40954e+01	5.67562e+21	2.89042e+63
$k = 2$	2.42771e+01	2.93094e+01	3.20353e+01	3.03248e+11	1.70547e+51
$k = 3$	2.47382e+01	2.90469e+01	3.32893e+01	4.06869e+01	5.34394e+26
$k = 4$	4.88746e+01	5.54463e+01	6.88985e+01	1.64061e+02	5.11668e+36
$k = 5$	6.52733e+01	8.33101e+01	1.98038e+02	5.03649e+03	9.10906e+44
$k = 6$	1.46396e+02	1.56708e+02	2.15131e+02	1.00880e+03	3.32276e+12

Table 14: Values of $\|L^{-1}\|$ when $T = 40.02$ and $\Delta t = 1.0005\Delta x$ in Example 7.7.

	Mesh 1	Mesh 2	Mesh 3	Mesh 4	Mesh 5
$k=1$, $\Delta t=\Delta x$	1.00000e+04	1.00000e+04	1.00000e+04	1.00000e+04	1.00000e+04
$k=2$, $\Delta t=\Delta x$	1.05514e+04	1.03217e+04	1.01723e+04	1.00890e+04	1.00452e+04
$\Delta t=(5/6)\Delta x$, $T=200$	5.66276e+22	4.83997e+44	9.50793e+84	1.58994e+165	-
$k=3$, $\Delta t=\Delta x$	9.00273e+05	9.00247e+05	8.99866e+05	8.99584e+05	8.99420e+05
$k=4$, $\Delta t=\Delta x$	7.48659e+06	7.48761e+06	7.48772e+06	7.48768e+06	7.48763e+06
$k=5$, $\Delta t=\Delta x$	7.76172e+06	7.76242e+06	7.76223e+06	7.76200e+06	7.76182e+06
$k=6$, $\Delta t=\Delta x$	2.88729e+07	2.88728e+07	2.88740e+07	2.88739e+07	2.88738e+07

Table 15: Values of $\|L^{-1}\|$ when $T=20000$ in Example 7.7.

The stability issues can be remedied with cubical forms when the time step length is small enough. We will elaborate this in more detail in three dimensions below, but before that we briefly repeat Example 7.7 with cubical forms.

Example 7.9. We replace the triangles of Example 7.7 with squares (of width Δx and height Δt) and test cubical forms of orders 1–5. The values of Δx are as in Table 10, with the exception that the case $k=5$ obeys the last row (and the case $k=6$ is excluded because of instability). The results are displayed in Table 16 along with the (sufficiently small) choices of Δt. The results displayed in Tables 11 and 16 are also illustrated in Figure 12, which highlights the superior performance of cubical forms.

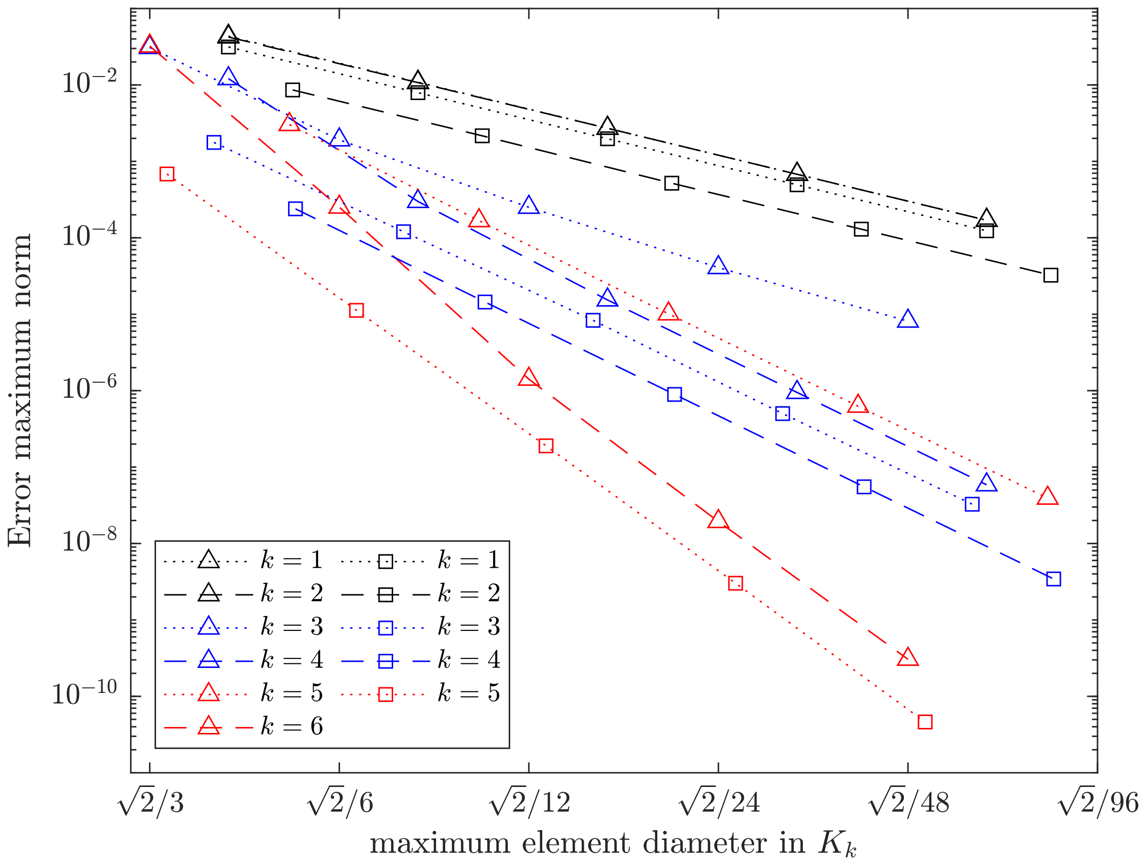

Figure 12: Illustration of the results displayed in Tables 11 and 16.

	Mesh 1	Mesh 2	Mesh 3	Mesh 4	Mesh 5
$k = 1$, $\Delta t = \Delta x$	3.14062e-02	7.92798e-03	1.97713e-03	4.94015e-04	1.23530e-04
$k = 2$, $\Delta t = 0.5\Delta x$	8.60180e-03	2.16105e-03	5.18099e-04	1.29699e-04	3.24255e-05
$k = 3$, $\Delta t = 0.5\Delta x$	1.76908e-03	1.20000e-04	8.32462e-06	5.01013e-07	3.26518e-08
$k = 4$, $\Delta t = (100/211)\Delta x$	2.39414e-04	1.44422e-05	8.92410e-07	5.51391e-08	3.43419e-09
$k = 5$, $\Delta t = (100/211)\Delta x$	6.84000e-04	1.12375e-05	1.89523e-07	3.02169e-09	4.61932e-11

Table 16: Maximum norms of the error when $T = 200$ in Example 7.9.

Example 7.10. Let $\Omega = [0, 2] \times [0, 2] \times [0, T]$ and consider tetrahedral meshes of the type shown in Figure 13 (left). We take $\Delta y = \Delta x$ and choose Δx as displayed in Table 17; note that the maximum element diameter in K_k is $\sqrt{2(\Delta x)^2 + (\Delta t)^2/k}$. First we attempt to find a stability limit for Δt. For order $k = 1$, we compute the norms of the inverses of the system matrices that result when $\Delta t = 0.705\Delta x$ and $T = 141$. Then we repeat the test with choices $\Delta t = 0.71\Delta x$ and $T = 28.4$. The results are shown in Table 18, suggesting that the limit is $\Delta t \leq \frac{1}{\sqrt{2}}\Delta x \approx 0.707\Delta x$ for order $k = 1$. For orders $k \geq 2$, it seems that the method is not stable; even for $\Delta t = 0.125\Delta x$, the norms of the inverses blow up already after 25 time units.

	Mesh 1	Mesh 2	Mesh 3	Mesh 4
$k = 1$	1/2	1/4	1/8	1/16
$k = 2$	1	1/2	1/4	1/8
$k = 3$	2	1	1/2	1/4
$k = 4$	2	1	1/2	1/4

Table 17: Values of the parameter Δx (and Δy) for the meshes used in Example 7.10.

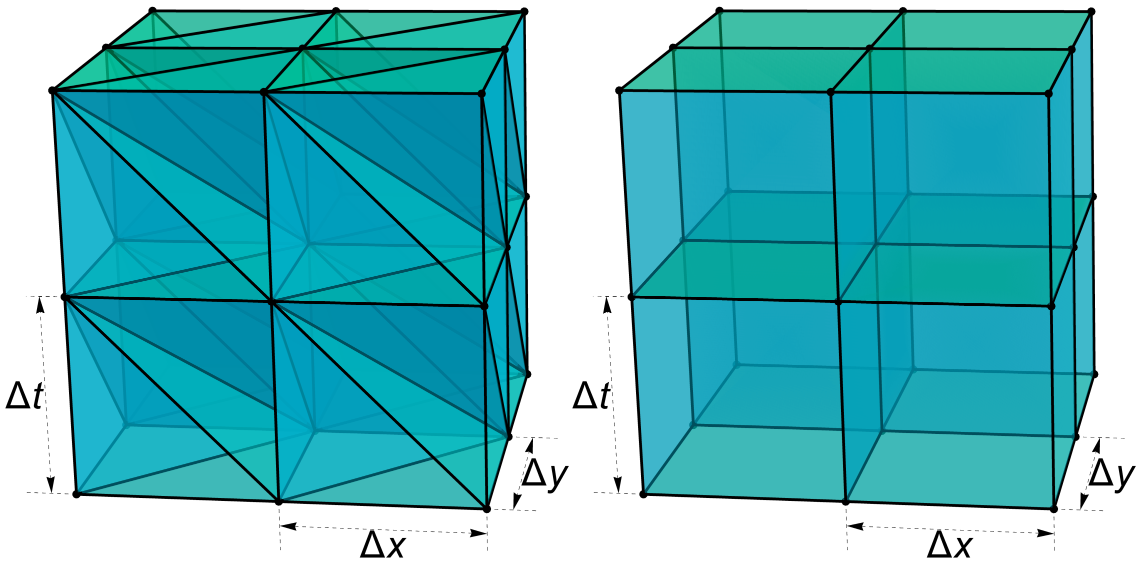

Figure 13: The type of the tetrahedral and cubical meshes used in Examples 7.10–7.11.

It seems that the same stability condition $\Delta t \leq (1/(\Delta x)^2 + 1/(\Delta y)^2)^{-1/2}$ as in the standard finite difference method is required for $k = 1$, but for $k \geq 2$ Whitney forms do not yield a stable scheme. We can remedy this by switching to cubical forms instead.

	Mesh 1	Mesh 2	Mesh 3	Mesh 4
$k = 1$, $\Delta t = 0.705\Delta x$, $T = 141$	9.85087e+01	1.30068e+02	1.52392e+02	1.67124e+02
$k = 1$, $\Delta t = 0.71\Delta x$, $T = 28.4$	1.90436e+01	2.74373e+01	4.40917e+01	1.08196e+41
$k = 2$, $\Delta t = 0.125\Delta x$, $T = 25$	1.65625e+01	2.23028e+01	4.25870e+01	6.57043e+02
$k = 3$, $\Delta t = 0.125\Delta x$, $T = 10$	5.10136e+00	1.17796e+01	4.74376e+01	1.36691e+04
$k = 4$, $\Delta t = 0.125\Delta x$, $T = 10$	7.78276e+00	1.45221e+02	7.79304e+04	6.77675e+12

Table 18: Values of $\|L^{-1}\|$ in Example 7.10.

Example 7.11. Let $\Omega = [0,2] \times [0,2] \times [0,T]$ and replace the tetrahedral meshes used in the previous example with cubical meshes (see Figure 13, right). The values of the parameters Δx and Δy are again as in Table 17. We perform a similar stability test with cubical forms. The choices for the relative time step length and the duration T are displayed with the results in Table 19.

	Mesh 1	Mesh 2	Mesh 3	Mesh 4
$k = 1$, $\Delta t = 0.705\Delta x$, $T = 141$	1.44533e+02	1.95811e+02	2.28832e+02	2.47293e+02
$k = 1$, $\Delta t = 0.71\Delta x$, $T = 28.4$	2.90634e+01	4.04550e+01	5.29431e+01	2.65088e+22
$k = 2$, $\Delta t = 0.355\Delta x$, $T = 142$	1.35038e+02	1.66944e+02	1.86032e+02	1.99260e+02
$k = 2$, $\Delta t = 0.375\Delta x$, $T = 37.5$	3.61421e+01	4.63148e+01	3.74518e+08	3.16672e+33
$k = 3$, $\Delta t = 0.25\Delta x$, $T = 500$	2.33128e+02	6.36183e+02	7.11727e+02	7.66676e+02
$k = 3$, $\Delta t = 0.265\Delta x$, $T = 106$	4.94310e+01	1.37435e+02	1.88688e+02	1.40144e+25
$k = 4$, $\Delta t = 0.2\Delta x$, $T = 40$	2.76939e+01	6.18803e+01	6.61323e+01	7.02919e+01
$k = 4$, $\Delta t = 0.21\Delta x$, $T = 42$	2.91784e+01	6.56954e+01	7.82796e+01	1.36919e+02

Table 19: Values of $\|L^{-1}\|$ in Example 7.11.

Again, it seems that for order $k = 1$ we have the usual limit $\Delta t \leq \frac{1}{\sqrt{2}}\Delta x \approx 0.707\Delta x$. For $k \geq 2$, the situation is more subtle, and there is no definite stability limit that we could identify. We can see that the choices $\Delta t = 0.375\Delta x$ for $k = 2$ and $\Delta t = 0.265\Delta x$ for $k = 3$ are unstable and decreasing the relative time step slightly seems to improve the situation. Of course, we can make no guarantee for the stability of the choices $\Delta t = 0.355\Delta x$ and $\Delta t = 0.25\Delta x$ either, but cubical forms clearly perform better than Whitney forms. For order $k = 4$ and mesh 4, Figure 14 illustrates the growth of the system matrix inverse norm with respect to time. The figure suggests that with $\Delta t = 0.2\Delta x$ the norm grows linearly in time, but after the relative time step length is slightly increased to $\Delta t = 0.21\Delta x$, the norm begins to grow exponentially.

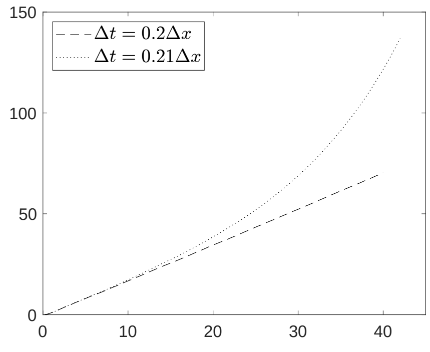

Figure 14: Values of $\|L^{-1}\|$ with respect to time for $k = 4$ and mesh 4 in Example 7.11.

For higher orders than those considered in Example 7.11, it seems that the results for $k = 5$ are similar than those for $k = 4$, but for $k \geq 6$ we could not find any time step that would yield a stable scheme. We will hence continue our convergence study with orders 1–5, choosing the relative time step length based on Example 7.11.

Example 7.12. Let $\Omega = [0, 2] \times [0, 2] \times [0, 100]$ and

$$\omega(x, y, t) = e^{x/4} \sin(x + y + t + 1) \cos(y)(2 - 0.003t - 0.00002t^2).$$

We solve the problem (7.1) using cubical forms of orders 1–5 on cubical meshes of the type shown in Figure 13 (right). For orders 1–4, we divide the values of Table 17 by two and use these for the parameters Δx and Δy; the case $k = 5$ obeys the last row of Table 17. Based on Example 7.11, the relative time step lengths are chosen as follows: $\Delta t = \frac{50}{71}\Delta x$ for $k = 1$, $\Delta t = \frac{50}{142}\Delta x$ for $k = 2$, $\Delta t = 0.25\Delta x$ for $k = 3$, and $\Delta t = 0.2\Delta x$ for $k = 4$ and $k = 5$. The results are shown in Table 20 and illustrated in Figure 15. It seems that in this case the order of convergence is two for $k = 1$ and $k = 2$, four for $k = 3$ and $k = 4$, and six for $k = 5$.

	Mesh 1	Mesh 2	Mesh 3	Mesh 4
$k = 1$	4.36612e-02	1.10626e-02	2.76855e-03	6.93555e-04
$k = 2$	2.34829e-02	6.02590e-03	1.52140e-03	3.81456e-04
$k = 3$	1.66525e-02	1.35834e-03	9.19698e-05	5.96036e-06
$k = 4$	3.46360e-03	1.93251e-04	1.12072e-05	6.83310e-07
$k = 5$	1.64667e-02	3.57679e-04	6.24342e-06	1.08734e-07

Table 20: Maximum norms of the error when $T = 100$ in Example 7.12.

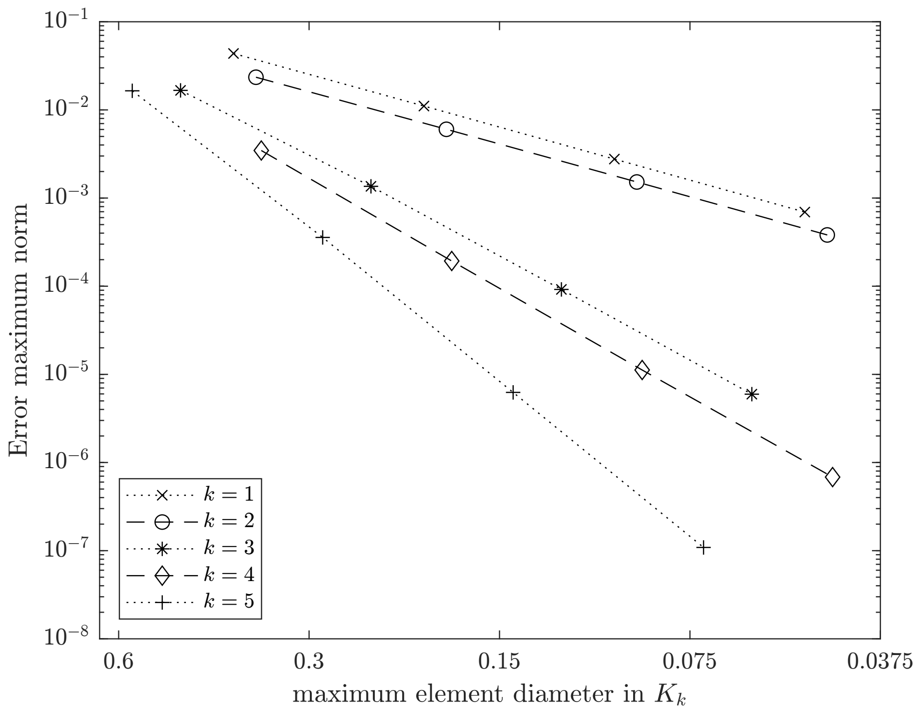

Figure 15: Illustration of the results displayed in Table 20.

8 Conclusions

We have shown that higher order methods based on discrete exterior calculus can be obtained using discrete Hodge operators of higher approximation order. These higher order discrete Hodge operators are defined using suitable finite element differential forms to interpolate cochains. In the present paper simplicial and cubical meshes were considered, but the same strategy applies whenever have an interpolation operator that satisfies the properties that are summarised in Section 3 and used in the proofs. We have shown that higher discrete Hodge operators yield higher order methods for Poisson's equation and the wave equation, both of which follow from the unifying approach for elliptic and hyperbolic boundary value problems presented in Section 5. Since the approach is formulated for 0-forms, we only used discrete Hodge operators acting on 1-cochains ($p = 1$); however, the definition and properties in Section 4 were considered for all p. The application of other cases than $p = 1$ is left for future work.

The methods resulting from higher order discrete Hodge operators yield exact solutions when the actual solution is in the finite element space used to define the discrete Hodge operator. We have provided a bound for the consistency error, which ensures that the order of consistency is at least $k-1$ in the maximum norm. Numerical results indicate that in practice faster convergence is possible. However, our convergence proof is incomplete because the stability of the methods has been studied only numerically. Based on the numerical studies, it seems that the method is stable for Poisson's equation, but for the wave equation stability requires additional conditions that the spacetime mesh must satisfy. Altogether, the numerical examples in three dimensions indicate that our approach is highly viable and higher order convergence can be attained with cochain-based methods.

References

[1] Robert Anderson, Julian Andrej, Andrew Barker, Jamie Bramwell, Jean-Sylvain Camier, Jakub Cerveny, Veselin Dobrev, Yohann Dudouit, Aaron Fisher, Tzanio Kolev, Will Pazner, Mark Stowell, Vladimir Tomov, Ido Akkerman, Johann Dahm, David Medina, and Stefano Zampini. MFEM: A modular finite element methods library. *Computers and Mathematics with Applications*, 81:42–74, 2021.

[2] Douglas N. Arnold, Richard S. Falk, and Ragnar Winther. Finite element exterior calculus, homological techniques, and applications. *Acta Numerica*, 15:1–155, 2006.

[3] Alain Bossavit. On the geometry of electromagnetism. (1): Affine space. *Journal of the Japan Society of Applied Electromagnetics and Mechanics*, 6(1):17–28, 1998.

[4] Alain Bossavit. On the geometry of electromagnetism. (2): Geometrical objects. *Journal of the Japan Society of Applied Electromagnetics and Mechanics*, 6(2):114–123, 1998.

[5] Alain Bossavit. On the geometry of electromagnetism. (3): Integration, Stokes, Faraday's law. *Journal of the Japan Society of Applied Electromagnetics and Mechanics*, 6(3):233–240, 1998.

[6] Alain Bossavit. On the geometry of electromagnetism. (4): Maxwell's house. *Journal of the Japan Society of Applied Electromagnetics and Mechanics*, 6(4):318–326, 1998.

[7] Alain Bossavit. Computational electromagnetism and geometry. (1): Network equations. *Journal of the Japan Society of Applied Electromagnetics and Mechanics*, 7(2):150–159, 1999.

[8] Alain Bossavit. Computational electromagnetism and geometry. (2): Network constitutive laws. *Journal of the Japan Society of Applied Electromagnetics and Mechanics*, 7(3):294–301, 1999.

[9] Alain Bossavit. Computational electromagnetism and geometry. (3): Convergence. *Journal of the Japan Society of Applied Electromagnetics and Mechanics*, 7(4):401–408, 1999.

[10] Alain Bossavit. Computational electromagnetism and geometry. (4): From degrees of freedom to fields. *Journal of the Japan Society of Applied Electromagnetics and Mechanics*, 8(1):102–109, 2000.

[11] Alain Bossavit. 'Generalized finite differences' in computational electromagnetics. *Progress In Electromagnetics Research*, 32:45–64, 2001.

[12] Alain Bossavit. Discretization of electromagnetic problems: The "generalized finite differences" approach. In *Numerical Methods in Electromagnetics*, volume 13 of *Handbook of Numerical Analysis*, pages 105–197. Elsevier, 2005.

[13] Alain Bossavit and Lauri Kettunen. Yee-like schemes on a tetrahedral mesh, with diagonal lumping. *International Journal of Numerical Modelling: Electronic Networks, Devices and Fields*, 12(1-2):129–142, 1999.

[14] Alain Bossavit and Lauri Kettunen. Yee-like schemes on staggered cellular grids: A synthesis between FIT and FEM approaches. *IEEE Transactions on Magnetics*, 36(4):861–867, 2000.

[15] Markus Clemens and Thomas Weiland. Discrete electromagnetism with the finite integration technique. *Progress In Electromagnetics Research*, 32:65–87, 2001.

[16] Mathieu Desbrun, Anil N. Hirani, Melvin Leok, and Jerrold E. Marsden. Discrete exterior calculus. *arXiv preprint math/0508341*, 2005.

[17] R. Hiptmair. Discrete Hodge-operators: An algebraic perspective. *Progress In Electromagnetics Research*, 32:247–269, 2001.

[18] Lauri Kettunen, Jonni Lohi, Jukka Räbinä, Sanna Mönkölä, and Tuomo Rossi. Generalized finite difference schemes with higher order Whitney forms. *ESAIM: Mathematical Modelling and Numerical Analysis*, 55(4):1439–1460, 2021.

[19] Jonni Lohi. Discrete exterior calculus and higher order Whitney forms. Master's thesis, University of Jyväskylä, 2019.

[20] Jonni Lohi. New degrees of freedom for differential forms on cubical meshes. *Advances in Computational Mathematics*, Accepted for publication, 2022.

[21] Jonni Lohi. Systematic implementation of higher order Whitney forms in methods based on discrete exterior calculus. *Numerical Algorithms*, 91(3):1261–1285, 2022.

[22] Jonni Lohi and Lauri Kettunen. Whitney forms and their extensions. *Journal of Computational and Applied Mathematics*, 393:113520, 2021.

[23] Francesca Rapetti and Alain Bossavit. Whitney forms of higher degree. *SIAM Journal on Numerical Analysis*, 47(3):2369–2386, 2009.

[24] Timo Tarhasaari, Lauri Kettunen, and Alain Bossavit. Some realizations of a discrete Hodge operator: A reinterpretation of finite element techniques. *IEEE Transactions on Magnetics*, 35(3):1494–1497, 1999.

[25] Hassler Whitney. *Geometric Integration Theory.* Princeton University Press, 1957.